Is the Epidermal Growth Factor Receptor involved in visual system regenerative failure?

By

Kevin Carlo Morrison

A thesis submitted to the University of Birmingham for the degree of DOCTOR OF PHILOSOPHY

School of Clinical and Experimental Medicine

College of Medical and Dental Sciences

Medical School

The University of Birmingham

September 2010

Dedication

This thesis is dedicated to my girlfriend

…….

If only she existed.

Acknowledgements

This thesis doesn't just represent 4 years of my work. Its successful completion owes almost entirely to 4 years of continued love, support and tolerance from everyone I love. This PhD and its day to day connotations and ramifications have permeated every aspect of my life for the last 40% of a decade, and at times, there has been a distance between myself some of you, both physically and emotionally. I have sometimes treated those I adore less well than they deserve, or have been short-tempered, or selfish, partly due to the stress associated with any such large undertaking. And, wonderfully, the reciprocal has rarely, if ever been true. Over these four years, the faith and patience of my family and closest friends has been tested and never found wanting. It is not an exaggeration to say that for the following people, for the following reasons, my success is largely *their* success. And insofar as an affirmed atheist can be such, I am eternally grateful. I love you all.

Mum, Dad

You were at all times supportive. Omnipresent. Unfailingly there for me, as you have been my whole life. I don't tell you enough how much you mean to me and how proud I am to be your son.

My sister jade

I was impatient with you often, and could have been there for you more than I was. You on the other hand always made the effort. Thank you.

(the rest are in alphabetical order so nobody starts a blood feud)

Cherry Alexander

You told me what I needed to hear. Not what I wanted to hear. Time and again you put up with more in a week than most friends would in a lifetime. Thank you for all that you've done, and for having unending faith in me. Ive said and done things that would have driven most people away but not you. You make me smile. You are wonderful and you always will be.

Richard Cochrane

Perhaps the funniest, kindest man I have ever met – has made me laugh and feel good about myself as much as anyone else alive, pretty much from the day we met. Gave me a roof over my head and managed to be brilliant company, considerate and generous, even in the immediate aftermath of a terrible personal loss. One of the best human beings I will ever meet.

Barry Gibson

My adoptive big brother. You've been there for me; constantly, unfailingly, unflinchingly loyal. Even when I didn't deserve you to be. Youre also one of the funniest human beings on the planet. You cant make up people like you, and I am forever grateful.

Benjamin Heywood

Weirdly, you and I have helped each other out a lot. Ill never forget all the battlefield moments… and the mentals weve seen. Cheers bud.

Steven Jacques

Arguably the finest scientist i have met so far. Immensely knowledgeable without a trace of arrogance. Hugely funny and witty, and absolutely unflappable. Along with Sohaib Mir and Samantha Prince, made working a joy, not a chore.

Georgina Merrick

The only person ive ever met who can destroy my panic, my neuroses, my doubt, over a 5 minute cup of coffee. The most quietly self assured person ive ever known – and immensely good at conferring that quality to those around her.

Sohaib Mir

A living embodiment of how a person should be: hugely witty, funny and supportive, hardworking kind and generous. Gave me encouragement and guidance when I badly needed it.

Samantha Prince

Has the unique ability to make me cry with laughter then somehow make me feel like IVE helped her. You have helped to keep me sane, and made me smile each and every day you were at work. Thank you.

Katie Ramm

Where to start? Camping trips, pubbing, clubbing, boxing, galavanting, exploring and fire-building. Has more enthusiasm and get up and go than anyone I know. You have given me so many of my favourite memories from the last 4 years, as well as arguably the best home-made presents ive ever had. You, maybe more than anyone else in Birmingham, have picked me up and forced me to do fun things.

Mikela Rochford

Weve only been friends for less than a year Mik and in that time you've been my counsellor, jester, gluttony-buddy and Kung-Fu Associate (white belt). Youre an amazing person and, like everyone on this page, I am constantly delighted to have someone like you in my life. You made me laugh (and cry) for almost my entire time in Aberdeen. If it hadn't been for you I would have felt, at times, utterly alone. You are truly unique.

And of course…

All else at the MNG:

Ann Logan and Martin Berry, Zubair Ahmed and Michael Douglas for persevering and for always doing their level best to help me.

Ana-Maria Gonzalez for endless patience and kindness.

Ruth seabright, Rachel Spice, Jenna Car, Wendy Leadbeater for making lab work bearable and for making me grin. (Jenna and Ruth deserve a special mention for using one certain curse word more than anyone I know, in pleasant English accents. This never gets old).

Andy Thewles for support, advice, hilarity, ridiculous noises and generally being himself. A man surely destined for sketch show caricature.

Deborah Gordon for being absolutely (superbly) disgraceful 90% of the time, for incalculable help with the final version of this thesis, and for that ridiculous bag of meat you gave me that time your freezer broke down. Ive never regretting breaking into someones' kitchen the night before with a pair of scissors less.

ABSTRACT

Introduction: A study in 2005 found that Epidermal Growth Factor Kinase Inhibitors (EGFRki) could promote Retinal Ganglion Cell (RGC) axonal regeneration *in vivo* when delivered to the crushed Optic Nerve (ON). The axon regenerative effects of these EGFRki were attributed to their blockade of the Epidermal Growth Factor Receptor (EGFR), and EGFR activation was hence suggested to lead to growth cone collapse and failed RGC axon regeneration.

Aims: To investigate the role of EGFR in RGC axonal regenerative failure, and to elucidate the mechanisms of action by which EGFRki promote RGC axonal regeneration.

Methods: Immunohistochemistry and immunocytochemistry to visualize activated EGFR (pEGFR) Primary retinal cultures to examine the actions of EGFRki such as AG1478 on RGC *in vitro*. ELISA to examine the conditioned media from these cultures for NeuroTrophic Factors (NTF). *Intravitreal (ivit)* injections of EGFRki (PD168393) into Optic Nerve Crush (ONC) recipient rats to attempt to elicit *in vivo* regeneration. The implantation of PD168393-impregnated collagen matrices into ONC recipient rats to attempt to elicit *in vivo* regeneration. PCR on retinal lysates to detect NTF mRNA.

Results: No pEGFR was detected on RGC axons, either in the retina or in the ON of any treatment or control group. pEGFR was detected on almost all ON and retinal glial types prior to injury and almost all glial types exhibited increased pEGFR levels post-ONC. A sub population (~30%) of RGC cell bodies were $pEGFR^{+}$ but this proportion did not change between control and treatment groups. AG1478 was shown to disinhibit RGC in Nogo-P4 inhibited primary retinal cultures but ELISA on conditioned media for various NTF detected none, however PCR detected mRNA for several of these NTF in retinal lysates. *Ivit* PD168393 failed to elicit RGC survival or axonal regeneration *in vivo*. Intra ON implantation of PD168393-impregnated collagen matrices appeared to promote significant RGC axonal regeneration post-ONC, but did not affect RGC survival.

Discussion: Several models explaining the *in vitro* regenerative and *in vivo* neuritogenic actions of EGFRki were developed. These included the abrogation of various harmful glially mediated processes, the stimulation of NTF release by local glia and the stimulation or blockade of several other non-EGFR dependent signalling cascades by EGFRki.

Conclusions: The axogenic and neuritogenic actions of EGFRki *in vitro* and *in vivo* were confirmed. The identification of numerous other means by which EGFRki could indirectly promote RGC axonal regeneration, including by acting on targets other than EGFR allowed the construction of a combinatorial model of how EGFRki effect axonal regeneration, and the original hypothesis positing EGFR as an intra-axonal component of a growth cone collapsing signalling cascade was disgarded.

Table of Contents

List of Figures and Tables

List of Common Abbreviations

A2A – Adenosine A2A receptor

AGIM – Axon Growth Inhibitory Molecules

Akt – Protein Kinase B

A.U. – Arbitrary Units (pixel brightness)

BBB – Blood Brain Barrier

C – (Degrees) Celcius

CA-II – Carbonic Anhydrase II

cAMP- Cyclic Adenosine MonoPhosphate

CME – Central Myelin Extract

CNS – Central Nervous System

BDNF – Brain Derived Neurotrophic Factor

CaR – Calcium Sensing Receptor

CNTF – Cilliary NeuroTrophic Factor

CSPG – Chondrotin Sulphate ProteoGlycan

DNA – DeoxyriboseNucleic Acid

EGFR – Epidermal Growth Factor Receptor

EGFRki – Epidermal Growth Factor Receptor kinase inhibitor

ELISA – Enzyme Linked ImmunoSorbent Assay

ERK – Mitogen Activated Protein Kinase 3

FGF – Fibroblast Growth Factor

FL – Fibre Layer

GAP-43 – Growth Associated Protein 43

GCL - Ganglion Cell Layer

GDNF – Glially Derived Neurotrophic Factor

GFAP – Glial Fibrilliary Acidic Protein

H & E - Haemotoxilin and Eosin (staining)

IPL - Inner plexiform Layer

INL - Inner Nuclear Layer

Ivit – Intravitreal

MAG – Myelin Associated Glycoprotein

MAPK – Mitogen Activated Protein Kinase

mRNA – Messenger RiboNucleicAcid

NgR – Nogo Receptor

NGF – Nerve Growth Factor

NF – NeuroFilament

NRM - Non Regenerating Model

NT – NeurotTrophin

NTF – NeuroTrophic Factor

NT-3/4 – Neurotrophin 3/4

OPL - Outer Plexiform Layer

OMgp – Oligodendrocyte Myelin GlycoProtein

ON -Optic Nerve

ONC - Optic Nerve Crush

ONL - Outer Nuclear Layer

$P75^{NTR}$ – Low affinity Neurotrophin Receptor

PCR – Polymerase Chain Reaction

PDL – Poly-D-Lysine

pEGFR – activated (phosphorylated) EGFR

PKA – Protein Kinase A

PKC – Protein Kinase C

PNS – Peripheral Nervous System

PN - Peripheral Nerve

RhoA – Ras homolog gene family, member A

RGC – Retinal Ganglion Cell

ROCK – Rho Kinase

RPM – Revolutions Per Minute

RM - Regenerating Model

RT- PCT – Reverse Transcription Polymerase Chain Reaction

siRNA – Short Interfereing RNA

TNF-α – Tumour Necrosis Factor Alpha

Trk - Tropomyosin receptor kinase (receptor)

Chapter 1

General Introduction

1.1 The Central Nervous System

The vertebrate Central Nervous System (CNS) consists of the brain and the spinal cord. The brain, comprising tens of billions of neurons and glial cells, and many times that number of axons and dendrites, is responsible for decoding, analysing and sorting sensory information, as well as generating appropriate motor, endocrine and physiological responses. The brain also forms, stores and recalls associations between events - memories - and, in higher organisms, performs complex cognition and generates emotion and consciousness. The spinal cord contains the axons and some of the cell bodies of the neurons responsible for relaying sensory information to, and motor and endocrine responses from, the brain. The CNS also includes, as part of the brain, the retinae and the optic nerves (ON). The retina is the neural tissue of the eye responsible for the initial detection of light, its subsequent conversion into electrical action potentials (APs), and finally the conduction of these APs along axons projected by retinal neurons to the relevant areas of the brain. Collectively, these retinofugal ('retina-fleeing') axons form the ON. The CNS is enveloped by the cranial meninges, surrounded by cerebro-spinal fluid (CSF) and isolated from the rest of the body by the blood brain barrier (BBB). The BBB is a system of endothelial cell tight-junctions in the capillaries supplying the brain, abutted on the CNS side by the end feet of astrocytes. These astrocytes form the glia limitans, a network of astrocytic processes which separate CNS tissue from the overlying layer of the meninges.

Unlike our peripheral nervous system (PNS), or even the CNS of fish or reptiles, the mammalian CNS does not regenerate after injury, with the result that severed CNS tracts do not reinnervate their targets and any neurons lost are not replaced.

1.2 Why does the CNS fail to regenerate?

The catastrophic and permanent functional consequences of human CNS injury, including paralysis, loss of sensation, and loss of bowel and bladder continence, have been recognised and described since at least 3500 B.C (Edwin Smith papyrus, 1930). In the 5,510 years since then it is only in the last century or so that the CNS has been studied at the cellular level, with the pioneering work of Cajal at the beginning of 20th century. Cajal showed that some axons did in fact regenerate from the severed end of an ON into a sutured-on segment of peripheral nerve, critical evidence that the CNS was not utterly incapable of regeneration. It was not until the late 1970s that further steps were taken towards successful CNS regeneration with the work of Aguayo and David (1981, 1985) and Richardson et al. (1980) confirming that the severed axons of the damaged adult CNS are not intrinsically incapable of regrowth, as had previously been thought. By impanting living peripheral nerve grafts or 'bridges' into the brain (Richardson *et al.* 1980) or between the undamaged spinal cord and brain stem of adult rats and mice, so as to connect the brain stem and upper thoracic spinal cord, it was shown that, axons from CNS neurons would grow several cm into and across these grafts and that these axons were at least partially myelinated by Schwann cells (Aguayo *et al* 1981, David and Agauyo 1981). This robust CNS axon growth in a PNS environment suggested that the environment of the CNS itself played a large part in the CNS regenerative failure. Further evidence for the difference in regenerative permissiveness when a subsequent study showed that these invading CNS axons will readily regenerate significant distances after being crushed (David and Aguayo 1985), and that ON fibres regenerated up to 2cm into grafted peripheral nerve sections (So and Aguayo, 1985). The extremely important discovery that

proteins within CNS myelin are strongly inhibitory to axon growth led to the production of an antibody which significantly dinsihibted CNS neurite outgrowth *in vitro* (Caroni and Schwab 1988a, b) and promoted modest regeneration in the spinal cord *in vivo* (Schnell and Schwab 1990). However, the discovery that embryonic CNS neurons exhibited substantial growth when implanted into the adult CNS (Wictorin and Bjorklund, 1992) strongly suggested that there was also an intrinsic reduction in inherent regenerative capacity in adult CNS neurons. By the year 2000 3 separate myelin derived proteins had been identified: myelin associated glycoprotein (MAG) (McKerracher *et al.* 1994), oligodendrocyte-myelin glycoprotein (OMgp) (Wang *et al.* 2002) and Nogo-A and –C (Caroni and Schwab 1988a, Chen *et al.* 2000, GrandPre *et al.* 2000, Prinjha *et al.* 2000). It was subsequently discovered that each of these proteins bind to and signal through the the Nogo receptor (NgR) (Fournier *et al.* 2001) and that this receptor signalled through its coreceptors Lingo (Mi *et al.* 2004) and either $p75^{NTR}$ (Wang *et al.* 2002) or TROY (Park *et al.* 2005). Surprisingly, it became apparent that inactivating either the individual proteins, or the NGR receptor itself yielded modest *in vivo* regeneration at best, and that even inactivating the downstream signalling molecules RhoA or ROCK, did not promote extensive *in vivo* axogenesis (Fischer *et al.* 2004a,b, Benowitz and Yin, 2007). Other studies showed that certain growth antagonistic molecules such as Netrin-1 and MAG were actually growth promoting *in utero/*immediately post natal, demonstrating that adult CNS neurons respond to the environment differently to PNS and even embryonic CNS neurons (Cai *et al* 2001, Shewan *et al* 2002). The discovery that such switches from growth promotion to growh retardation are in fact triggered by changes in levels of intraneuronal cAMP (Cai *et al.* 2001) showed that the internal growth state of the CNS neuron was potentially at least as important as the surrounding environment, confirming

the early findings of Wictorin and Bjorklund (1992).

In less than a third of a century, the previously non-existent field of CNS repair has expanded to become a major branch of neuroscience and medicine, with millions of pounds being spent yearly on researching potential therapies. Alongside the landmark studies mentioned above, thousands of others have investigated and uncovered the events, tissues, cells, proteins, genes, factors and signalling pathways which underlie the failure of CNS axons to regenerate, resulting in the identification of several major barriers to CNS regeneration. These include the death of damaged neurons, the growth-hostile nature of the injured CNS and the tendency for many injured CNS neurons to rapidly abort any attempts at regeneration.

1.2.1 Many neurons die in response to CNS injury and are not replaced

Between 2 and 3 days after CNS injury, many mammalian CNS neurons begin to die. Contributing factors include mechanical cellular damage caused by the initial injury, infection, secondary cellular damage by invading macrophages (Danton and Dietrich 2003), myelin stripping by lymphocytes (Crocker *et al.* 2006), glutamate excitotoxicity as a hypoxic response (Sasaki *et al.* 2005) and damage from Reactive Oxygen Species (ROS) released by activated microglia/macrophages during phagocytosis (Smith *et al.* 1998). Cell death has traditionally been described as either of two processes: a passive, cell damage-mediated process termed necrosis and an active program of cell-suicide known as apoptosis. Necrosis is characterised by cell swelling, organelle destruction and, eventually, cell lysis and fragmentation, provoking an inflammatory response (Yakovlev and Faden 2004). Conversely, cells undergoing apoptosis disassemble their cytoskeleton

and organelles whilst maintaining membrane integrity, and disintegrate into apoptotic bodies which are phagocytosed by neighbouring cells and thus do not instigate an inflammatory response (Yakovlev and Faden 2004). The extent to which each of these two processes mediate neuronal death is dependent on the nature and location of the CNS insult. Damage to primarily neuronal areas, as seen in penetrating brain injuries, tend to cause local neuronal death through necrosis brought about by ischaemia, oxidative stress and glutamate excitotoxicity (Faden, 1996), whereas when the damage is primarily limited to axotomy (amputation of axon from neuron), and occurs remote to the neuron itself, as in the case of ON transection, subsequent neuronal death primarily results from apoptosis. Until relatively recently it was assumed that necrosis was an uncontrolled process, purely resulting from disrupted cell function, but a Ca^{2+} mediated cysteine protease-dependent pathway has been identified which appears to account for much of the intracellular disintegration which characterises neuronal necrosis (Syntichaki *et al.,* 2002, Yamashima, 2000). Apoptosis has been extensively studied and there are now several known apoptotic signalling pathways, each of which ultimately culminates in the activation of one or more families of proteases which efficiently disassemble the cell from within (Yakovlev and Faden 2004, Leist and Jaattela, 2001). First identified and best understood of these protease families are the caspases. For brevity, and due to the extensive nature of associated literature, only caspase-dependent neuronal apoptosis will be described here, but for a broader picture of apoptosis see Yakovlev and Faden (2004) and Leist and Jaattela (2001). The caspases (Cysteine-dependent Aspartate-directed proteases) mediate apoptosis through two separate but interconnected pathways. The first pathway is initiated by the binding of extracellular ligands to membrane bound receptors, whereas the second is mediated by mitochondrial protein release. These are

respectively termed the 'extrinsic' and 'intrinsic' signalling cascades/pathways (figure 1). The extrinsic signalling pathway begins with ligand activation of death receptors such as TNF-αR and $p75^{NTR}$/Sortilin receptor complex, whereas the intrinsic cascade is initiated in response to mitochondrial damage. Both pathways culminate in the conversion of an inactive pro-caspase to an active caspase (caspases 8 and 9 respectively) which then goes on to activate the executioner caspases, 3, 6 and 7 (Yakovlev and Faden 2004). These executioner caspases then go on to initiate cell-wide mass proteolysis, resulting in the disassembly of the cytoskeleton and intracellular organelles and the cessation of cellular metabolism (Raff, 1998). Caspase 3 appears to be the primary executioner caspase in neuronal apoptosis (Yakovlev and Faden 2004, Leist and Jaattela 2001) and as such is the only executioner caspase shown in Figure 1.1.

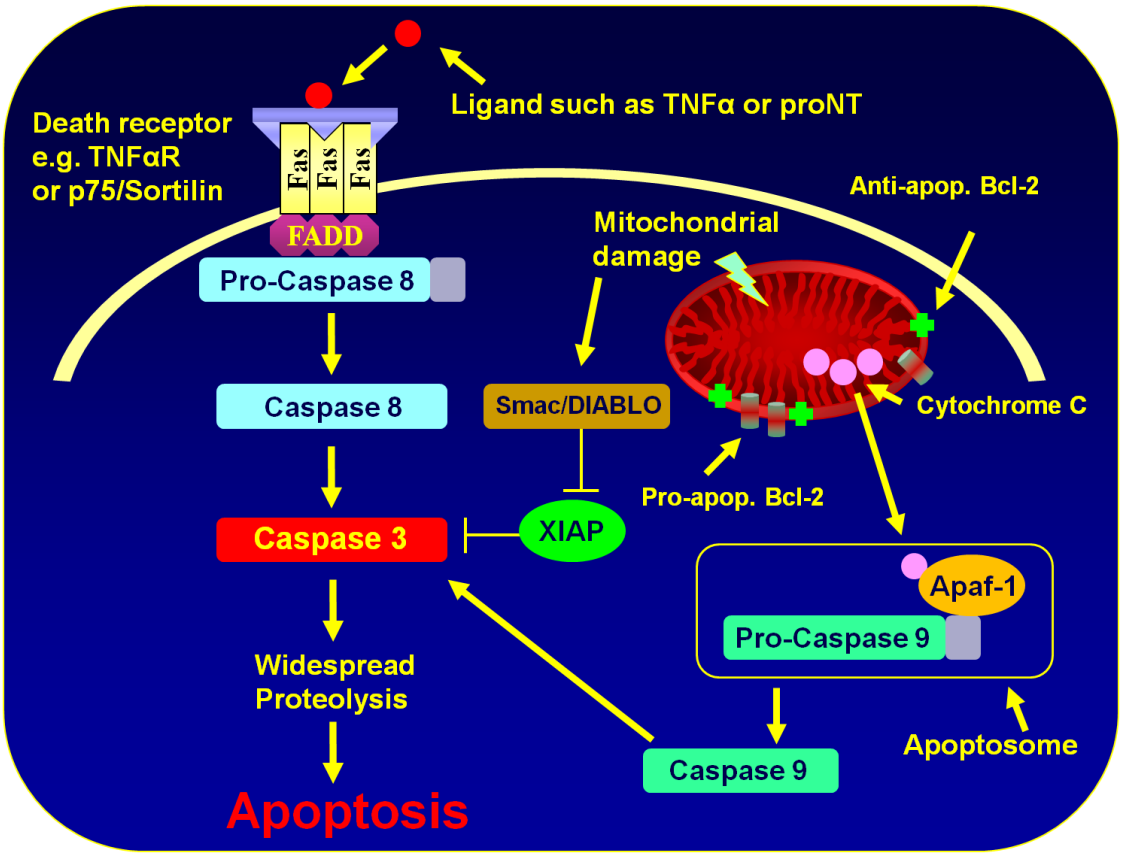

Figure 1.1. Caspase mediated apoptosis. The extrinsic pathway begins with ligand binding to a death receptor which cleaves pro-caspase 8 to form active caspase 8. Caspase 8 activates the executor caspase 3, leading to intracellular organelle and cytoskeletal proteolysis and cell death. The intrinsic pathway begins with mitochondrial damage, which leads to the release of cytochrome c. Cytochrome C in turn leads to the formation of the apoptosome, a structure which allosterically cleaves procaspase 9 to form active caspase 9. Caspase 9 then activates caspase 3, leading to cell death. Inhibitos of apoptotic proteins including XIAP block the activation of caspase 3, preventing apoptosis. Mitochondrial damage also leads to the release of Smac/DIABLO, which inhibits XIAP, indirectly causing caspase 3 activation and subsequent cell death. Pro-apoptotic Bcl-2 family members form channels in the mitochondrial membrane, allowing the exit of Cytochrome C. Anti-apoptotic Bcl-2 proteins prevent the formation of these channels.

The pro-survival inhibitors of apoptosis proteins (IAP), such as XIAP, blockade executioner caspase activation, preventing cell death, but the IAP are themselves inactivated by factors such as Smac/DIABLO which are released from mitochondria in response to mitochondrial damage. Anti apoptotic members of the Bcl-2 family such as Bcl-2, Bcl-x and Mcl-1 are located on the surface of mitochondria and prevent the release of

cytochrome C (Raff, 1998), blocking the intrinsic pathway and allowing IAP such as XIAP to prevent executioner caspase activation.

Although the various secondary insults to the injured CNS mentioned above undoubtedly cause neuronal loss through both necrotic and apoptotic processes, perhaps the most likely reason for neuronal apoptosis after axotomy is the resultant loss of target-derived survival signals (Majdan and Miller, 1999, Chao *et al.* 2006). During the formation of the embryonic nervous system many more axons are produced than are needed to innervate distant targets. Only the neurons whose axons successfully contact and connect with their targets survive, the others undergo apoptosis – a process referred to as 'pruning'. The neurons whose axons have successfully connected to their targets survive because the target cell (often another neuron) supplies the newly connected neuron with survival factors, which prevent the onset of apoptosis by activating the anti-apoptotic members of the Bcl-2 family described above, and by preventing the release of cytochrome C which would otherwise initiate the intrinsic apoptotic pathway (Chao *et al.* 2006, Yakovlev and Faden 2004).

These neuronal survival factors are known as neurotrophic factors (NTF) and include the four classical neurotrophins (NT) NGF, BDNF NT-3 and NT-4, as well as basic fibroblast growth factor (FGF2) and ciliary neurotrophic factor (CNTF) (figure 2).

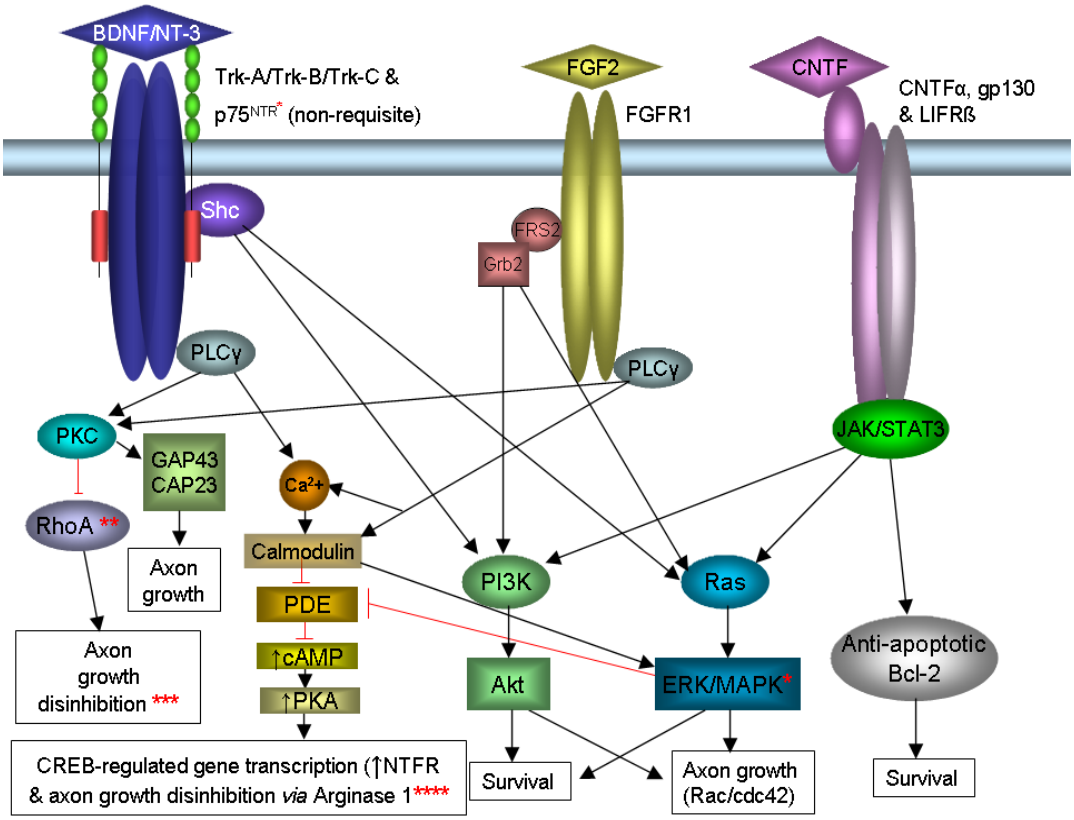

Figure 1.2. Neuronal neurotrophic factor (NTF) signalling. The neurotrophins (NT) NGF, BDNF, NT-3 and NT-4 can individually bind to and activate both their cognate Trk receptors Trk A, Trk B and Trk C, as well as $p75^{NTR}$, a member of the TNF receptor superfamily, but signal for survival most effectively through complexes of Trk+$p75^{NTR}$. Basic fibroblast growth factor (FGF2) binds to FGFR1 and ciliary neurotrophic factor (CNTF) binds to a heterotrimeric receptor complex composed of CNTFα, GP130 and LIFRβ sub-units. All receptors signal for survival through the activation of ERK/MAPK and AKT which ultimately maintain the presence of anti-apoptotic Bcl-2 family members on mitochondrial membranes while blocking the activity of pro-apopototic Bcl-2 family members such as Bax (see figure 1.1). Simultaneously, activation of ERK/MAPK and PKC pathways promote axonal outgrowth by modulating the activity of the Rho family of small GTPases; inhibiting the growth cone collapse-inducing RhoA and activating the filopodial and lamellipodial outgrowth inducing cdc42 and Rac (see figure 1.4 for details). Figure taken with permission from Berry *et al.* 2008.

The NTs are first synthesised and released as pro-neurotrohphins, and the attached pro-domain must be cleaved for NTs to function as survival factors. The individual NTs and pro-NTs each preferentially bind to and activate one or more of the tropomyosin receptor kinase (Trk) receptors Trk A, Trk B and Trk C. While each NT has a weak affinity for at least one other Trk, it is broadly the case that NGF interacts chiefly with Trk A, BDNF and NT-4 with Trk B and NT-3 with Trk C (Chao 2003, 2006, Berry *et al.* 2008). All

NTs and pro-NTs also bind to $p75^{NTR}$, a member of the tumour necrosis factor (TNF) receptor superfamily, with proNTs exhibiting a greater affinity for $p75^{NTR}$ than Trks and mature NTs preferentially binding to Trks over $p75^{NTR}$. The $p75^{NTR}$ is unusual in that it plays multiple roles simultaneously. As a standalone receptor $p75^{NTR}$ can signal for both survival and apoptosis, depending on the nature of the ligands, coreceptors and intracellular signalling proteins involved (Chao 2003, Schecterson and Bothwell 2010), although sortilin is required as a coreceptor for the binding of pro-NTs which leads to apoptotic signalling (Chao 2006, Schechterson and Bothwell 2010). The $p75^{NTR}$ also forms part of a complex with individual Trk receptors, resulting in significant increases in both the affinity and the specificity of the Trk-NT interaction, (Chao 2003, Schechterson and Bothwell 2010), e.g. both NGF and NT-3 will bind to TrkA receptors but the TrkA-$p75^{NTR}$ complex binds only NGF (Chao, 2003, 2006). The net effect of this is that proNTs tend to activate $p75^{NTR}$ over Trk, leading to apoptotic signalling, whereas mature NTs tend to signal through Trk and the Trk-$p75^{NTR}$ complex leading to survival and axonal growth (see figure 1.2). The $p75^{NTR}$ also acts as a coreceptor for various other ligands, including myelin derived growth antagonistic proteins (see figure 1.3 and accompanying text).

Basic fibroblast growth factor (FGF2) binds to FGFR1 and ciliary neurotrophic factor (CNTF) binds to a heterotrimeric receptor complex composed of the CNTFα, GP^{130} and LIFRβ sub-units. Each of these receptors signal for survival through the activation of ERK/MAPK and AKT which ultimately maintain the presence of anti-apoptotic Bcl-2 family members on mitochondrial membranes while blocking the activity of pro-apopototic Bcl-2 family members (see figure 1.1). Interestingly, CNTF has been identified as the most potent promoter of long tract regeneration in the ON, whilst having little or no discernable effect on RGC survival (Cui *et al.* (1999) and Cho *et al.* (1999)), whereas Li *et*

al. (2009) showed certain synthetic FGF analogues differentially promote either *in vitro* neurite outgrowth or neuronal survival but not both. BDNF has also been reported to have the opposite effect; increasing RGC survival without affecting regeneration (Pernet and Dipollo, 2003).

The death of CNS neurons after injury is therefore attributable to both apoptosis and necrosis; the former due to the loss of target-derived NTF survival signals, and the latter both as a result of the initial physical injury and in response to the secondary insults caused by infection and the actions of inflammatory and immune cells.

1.2.2 The adult CNS contains many axon growth antagonistic factors and a dearth of growth permissive molecules

During *in utero* development and regeneration, axons grow and navigate through the actions of a specialised structure at their tip – the growth cone. Axon growth inhibitory molecules (AGIM) are molecules which, when encountered by growth cones, cause them to stop, retract and even collapse completely. These AGIM include 3 proteins derived from CNS myelin: myelin associated glycoprotein (MAG) (McKerracher *et al.* 1994 (but see Cai *et al.* 2001)), oligodendrocyte-myelin glycoprotein (OMgp) (Wang *et al.* 2002) and Nogo-A and –C (Caroni and Schwab 1988a, Chen *et al.* 2000, GrandPre *et al.* 2000, Prinjha *et al.* 2000) as well as sempaphorins, netrins, ephrins and chondroitin sulphate proteoglycans (CSPG) such as versican, brevican, neurocan, aggrecan, phosphacan and NG2 (Berry *et al.* 2008). Secreted by fibroblasts, the semaphorins (especially sema-3a) along with the ephrins are important chemorepulsive axonal guidance cues during development but also contribute to abortive axonal regeneration (Kaneko *et al.* 2006 and

Goldshmit *et al.* 2006 respectively). CSPGs are produced and secreted by reactive astrocytes post injury (Sandvig *et al.* 2004).

The reason for much of this CNS inhospitability, especially the prevalence of myelin derived AGIM in the CNS, is the incomplete Wallerian degeneration that follows CNS axotomy. Wallerian degeneration is the active processes whereby the distal sections of severed axons (ie those sections no longer connected to the neuronal cell body), including their myelin sheathes, are actively degraded, and removed from the injury site (Vargas and Baress, 2007). In the PNS, which readily regenerates after injury, distal sections of axons degenerate within hours-days and both Schwann cells and invading haematogenous macrophages phagocytose and destroy all PNS myelin – a process which is largely complete in mammals within 7-14 days post injury (Vargas and Baress, 2007). In stark contrast to this CNS axonal debris, including myelin, is cleared over the space of months or years, if at all and the injury site remains full of axona debris, (see figure 1.7, lower panel) growth inhibitory CNS myelin and its derivative AGIM proteins (Vargas and Baress, 2007, Berry *et al.* 2008). Schwann cells which are not in contact with intact axons also proliferate in response to PNS injury and release NTFs which strongly enhance neuronal survival and regeneration (Fawcett &Keynes, 1990). CNS oligodendrocytes do not take part in myelin clearance, do not secrete significant levels of NTFs and not only do not proliferate in response to injury, they often die in large numbers – a process linked to oligodendrocytes dual need for multiple neurotrophic support and the electrical activity of adjacent axons (Barres *et al.* 1993, Vargas and Baress, 2007). Along with the phagocytic role played by Schwann cells, the other primary reason for the difference in debris clearance rates is the difference in immune response to PNS and CNS insult. Unlike the CNS which is mostly isolated from the immune system by the BBB and is thus

accessible only at and around the injury site, the injured blood nerve barrier (BNB) of the PNS is open to the immune system along the entire length of degenerating axons, allowing rapid influx of huge numbers of phagocytic macrophages to clear debris which has been marked for destruction with opsins or with the complement system (Vargas and Baress , 2007). One final consequence of successfully Wallerian degeneration is the sparing of the basal lamina tubes of Schwann cells. Unlike the CNS, where a single oligodendrocyte will myelinate multiple axons, each segement of PNS axons are myelinated by a single Schwann cell which wraps around the axon in its entirety, like a bandage around a limb, and once consolidated, constructs a basal laminal tube around itself. These tubes surround the Schwann cells and the axons around which they are wrapped and, following Wallerian degeneration, serve as a highly permissive axon growth substrate, through which regenerating axons readily advance (Vargas and Baress, 2007). Additionally, these structures allow regenerating axons to navigate back to their targets unerringly as the tubes continue uninterrupted to the axons' original target (Nguyen *et al*. 2002). Taken together, astrocytic secretion of growth inhibitory factors such as CSPG, the failure to clear CNS myelin and axonal debris and the lack of any equivalent to the ready-made Schwann cell derived growth substrate and NTF supply found in the PNS equates to an enormous difference in the respective environments surrounding axotomised PNS and CNS axons.

To understand the mechanisms by which AGIM prevent growth cone advancement, and so prevent axonal regeneration in the CNS, the structure and function of the growth cone itself must first be described. The neuronal growth cone consists of rod like structures (filopodia) interspersed with 'veils' (lamellipodia) projecting out from a central area, which abuts the end of the axon-shaft. Once memorably referred to as 'a

leukocyte on a leash', the classical model of the growth cone, illustrated in figure 1.3, somewhat resembles a human hand, with the fingers as filopodia, the skin between the fingers as lamellipodia, the palm as the main body of the growth cone and the wrist as consolidated axon shaft. The microtubules, which strengthen and stabilise the axon-shaft, the growth cone proper and individual filopodia, can similarly be thought of as the 'bones' of the wrist, hand and fingers. Both filopodia and lamellipodia are primarily constructed from the small protein actin, which is polymerised in huge numbers into filaments termed F-actin, but whereas filopodia are organised into long slender columns, lamellipodia are a sheet of interconnected, meshwork-like actin filaments of varying length (see Figure 1.3) (Lowery and Van Vactor 2009). Both filopodia and lamellipodia are situated at the outermost part of the growth cone, and extend and push outwards by being continually elongated at their juxtamembranous ends through the ongoing addition of actin monomers. Simultaneously, polymerised sections of F-actin are removed at the proximal end of filopodia/lamellipodia and recycled as monomers back to the growing, juxtamembraneous end of the structure (Lowery and Van Vactor 2009).

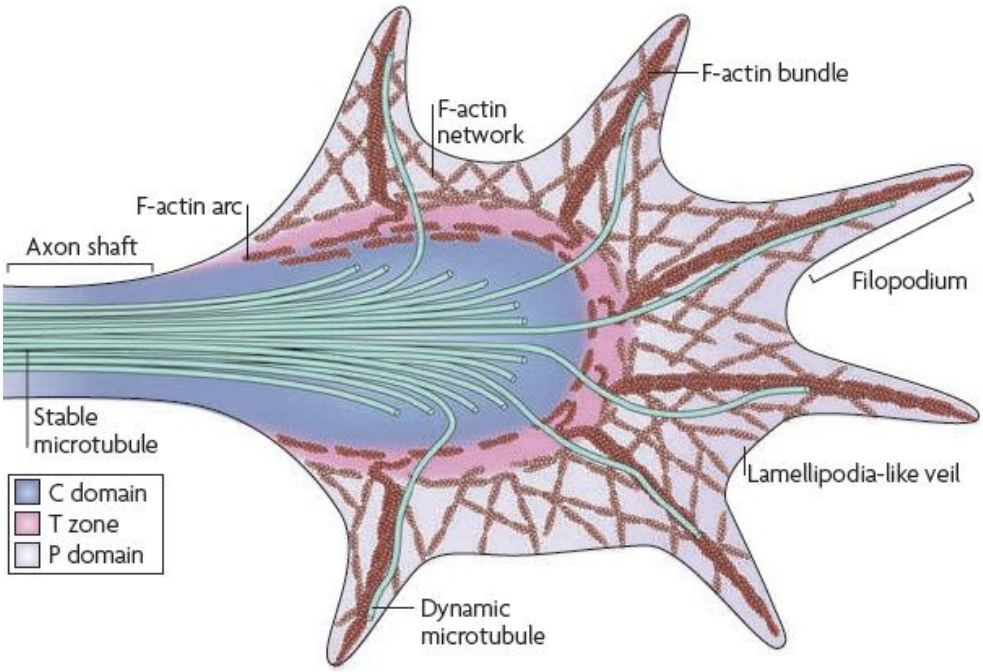

Figure 1.3. The growth cone. Filopodia consisting of F-actin bundles project outwards, extending due to ongoing F-actin polymerisation at their tips, and the mesh-like network of F-actin which make up lamellipodia, follow. Microtubules extend from the soma through the consolidated axon shaft, and stabilise the entire structure of the growth cone, as well as extending into and reinforcing filopodia. The Central (C) and Peripheral (P) domains and the Transition (T) zone are respectively characterised by a stabilised, relatively fixed cytoskeleton and an accumulation of vesicles, proteins and mRNAs required by the growth cone (C), the anchor-points and beginnings of the lamellipodia and filopodia (p) and a ring of contractile actomyosin rings which are involved in growth cone retraction and collapse. Proteins governing the rates of actin polymerisation and depolymerisation are closely associated with actin throughout the growth cone and almost all factors affecting the course of growth cones ultimately impinge on these proteins. Taken from Lowery and Van Vactor, 2009.

The relative rates of these two opposing processes determine the length/size of the respective structure. If the rate of actin polymerisation outstrips that of depolymerisation, the individual filopodium or lamellipodium will lengthen, resulting in local membrane expansion. Conversely, if the rate of actin depolymerisation outpaces that of actin polymerisation, filopodial and lamellipodial retraction occurs, leading to local membrane retraction. When polymerisation and depolymerisation rates are identical the growth cone can be said to be “arrested”. When filopodial and lamellipodial retraction is global the result is growth cone shrinkage. When growth cone expansion takes place

primarily along the forward edge of the growth cone (i.e. to the right in figure 1.3), it will advance forwards in a straight line. When filopodially and lamellipodially mediated expansion or contraction dominates one side of the growth cone the result is extension in one specific direction – the growth cone turns.

A further process exists, known as growth cone collapse. Growth cone collapse and contraction are separate processes, the latter occurring, as described above, largely as a result of filopodial and lamellipodial shortening, whereas the former is characterised by filopodial and lamellipodial disassembly as well as the activation of contractile actomyosin fibres which actively pull the outermost parts of the growth cone towards its centre (Gallo and Letourneau 2004).

Crucially, the rates of actin polymerisation and depolymerisation are controlled by a vast array of actin-associated proteins which act as final convergence points for multiple, interconnected signalling networks. Many of these networks are connected to membrane-bound receptors and ion channels, meaning that local actin polymerisation and depolymerisation, and thus the extent to which the growth cone grows, shrinks, turns or collapses, is strongly influenced by factors in the extra-neuronal environment. But how do these cytoskeletal changes relate to AGIM and the antagonism of CNS axonal regeneration?

While all known CNS myelin-derived AGIM bind to and signal through the Nogo receptor (NgR) (Fournier *et al.* 2001) and its coreceptors Lingo (Mi *et al.* 2004) and either $p75^{NTR}$ (Wang *et al.* 2002) or TROY (Park *et al.* 2005), and while CSPGs, semaphorins and ephrins all signal through separate, specific receptors, each of these AGIM can only instigate growth cone collapse by first interacting with downstream intracellular proteins

such as RhoA (Sandvig *et al.* 2004, Berry *et al.* 2008) which in turn activate specific actin-associated proteins including Myosin II and ADF/Cofilin (see Figure 1.4).

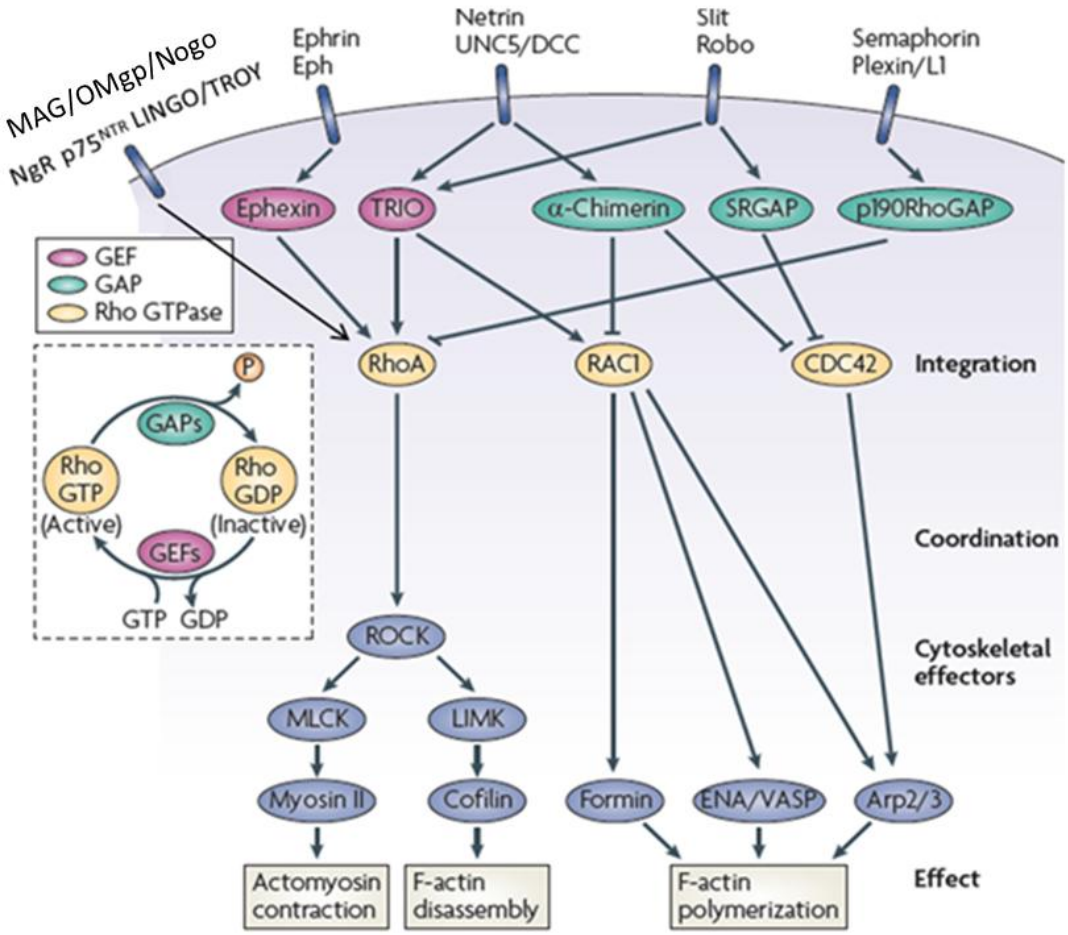

Figure 1.4. The Rho family of small GTPases mediate growth cone extension, retraction, arrest, collapse and turning. Rho proteins are activated by guanidine exchange factos (GEFs) which convert Rho+GDP to Rho+GTP, and inactivated by the confusingly named GTPase activating proteins (GAPs). RhoA, signalling, through Rho Kinase (ROCK) leads to F-actin disassembly (retraction) and the formation of contractile actomyosin fibres (collapse). Rac and CDC42 signalling lead to lamellipodial and filopodial extension respectively (extension). Activation of RhoA plus Rac/CDC42 causes growth cone arrest if co-activated globally, whereas asymmetrical, focal activation of either/both will result in RhoA localised retraction and Rac/CDC42 localised extension, resulting in growth cone turning. Modified from Lowery and Van Vactor, 2009.

RhoA is a member of the Rho family of small GTPases, which play key roles in growth cone extension, retraction, arrest, turning and collapse (see figure 1.4). The Rho family members RhoA, Rac and CDC42 are profoundly important regulators of the cytoskeletal events underlying growth cone behaviour, their activation variously leading to localised growth cone collapse (RhoA), and the formation and extension of lamellipodia (Rac) and filopodia (CDC42) (see (Fischer *et al.* 2004), (Jain *et al.* 2004), and (Scott *et al.* 2003) respectively for examples and (Koh, 2006) or (Gallo and Retourneau 2004) for review). Of these three Rho family members, RhoA has been the most intensively studied, its role in growth cone retraction and collapse making it an obvious target for therapies aimed at enhancing axonal regeneration, and the knockout/inhibition/silencing of both RhoA, or its downstream effector kinase ROCK, has formed the basis of numerous studies seeking to enhance CNS regeneration (examples include Fournier *et al.* 2003, Kreibich *et al.* 2004, Bertrand *et al.* 2005, 2007 and McKerracher *et al.* 2006). The results of such studies have themselves been the subject of multiple reviews (e.g. Kubo *et al.* 2007, Gross *et al.* 2007). The advantage of inactivating Rho family members such as RhoA, or their respective downstream signalling effector proteins such as ROCK, is that all signalling pathways converging on that protein are blocked simultaneously. In the case of RhoA, this renders multiple AGIM largely impotent.

As the growth cone extends its filopodia and lamellipodia within the CNS, they encounter factors present on, and bound to, the substrate over which the axon is attempting to grow. These factors can be either conducive or antagonistic to growth cone adhesion. Substrate bound anti-adhesion factors such as slits, ephrins, CSPG and semaphorins, signalling through RhoA/ROCK, elicit localised growth cone shrinkage or collapse. In this way they prevent the growth of axons towards inappropriate targets *in*

utero by forcing the growth cone to turn away – a process known as chemorepulsion. If the growth cone is surrounded on all sides by such growth antagonistic factors, as occurs within the injured adult CNS, the growth cone collapses as described above. Growth cone adhesion-permissive factors, more commonly known as cell adhesion molecules (CAMs) consist primarily of constituents of the extracellular matrix (ECM) such as laminin, fibronectin and collagen, members of the Ig (immunoglobulin) superfamily (IgSF) of CAMs), and the Cadherins.

ECM constituents include laminins, collagens and fibronectins, each of which activates specific members of the Integrin receptor family present on the surface of lamellipodia and filopodia. Integrin receptors are heterodimers formed of one α and one β subunit. There are numerous subtypes of both, and ligand selectivity is determined by the extracellular binding site formed by the specific combination of particular α and β subunits (Lemons and Condic 2007, Hynes 2002). RGC are known to express α1β1 and α1β2 integrins which function as receptors for laminin-1 and laminin-2 (merosin) (Cohen and Johnson, 1991). Increased expression of integrins containing the β-1 subunit is associated with increased RGC neurite outgrowth (Lilienabum *et al* 1995, Clegg *et al* 2000) and survival (Leu *et al.* 2004). Increased integrin expression has also been linked to both *in vitro* and *in vivo* regeneration of many neuronal phenotypes, from sensory neurons to Dorsal Root Ganglion Neurons (DRGN) (Lemons and Condic, 2007), whereas decreased integrin activation correlates with reduced regenerative potential in CNS neurons (Ivins *et al* 2000).

The IgSF of CAMS includes Neural Cell Adhesion Molecule (NCAM)/CD56, L1 and TAG-1. Many of these proteins bind homophilically, forming attachments primarily with copies of themselves, whereas others bind to members of the aforementioned integrin

receptor family or to other IgSF CAMs (Maness and Scachner, 2007, Sakisaka and Takai, 2005). RGC are known to express L1 and TAG-1 (Jung *et al* 1997, Klöcker *et al* 2001), and NCAM (Murphy *et al* 2007a, b, 2009) RGC axonal regeneration after ON transection has been reported to be drastically reduced in NCAM deficient mice, and NCAM expression has been strongly linked to RGC survival following axotomy (Murphy *et al* 2007b, 2009). Both L1 and NCAM can promote adhesion and neurite outgrowth through interactions with integrin receptors, but can also signal through through the semaphorin receptor neuropilin-1 for growth cone collapse (Maness and Schachner, 2007). TAG-1 is reportedly downregulated post axotomy by CNS but not PNS axons and is upregulated in RGC axons following the addition of extraneous BDNF (Klöcker *et al* 2001), and studies in goldfish (Lang *et al.* 2001) and zebrafish (Wolman *et al.* 2008) have provided evidence that TAG-1 plays an important role in growth cone guidance, growth and even correct retinotopic reconnection in the tectum (the structure analgous to the superior and inferior colliculi in lower vertebrates).

Cadherins are calcium dependent CAMs which primarily function to bind cells together. The predominant neuronal cadherin is N-cadherin, which is which is known to be upregulated in regenerating zebrafish RGC (Liu *et al.* 2002), to increase *in vitro* survival of cultured RGC by signalling through the FGF receptor (Skaper *et al.* 2004), and to promote axonal regeneration in the embryonic spinal cord (Blackmore and Letourneau, 2006, Skaper, 2005). Cadherins, like many of the other CAMs described above, interact homophilically, meaning that filopodial and lamellipodial CAMs form homodimers with other CAMs present on adjacent cells, allowing axons to 'piggyback' across other cells/processes (Sakisaka and Takai, 2005).

Each of these CAMs then forms complexes with intra-filopodial and intra-

lamellipodial actin bundles, anchoring the growth cone to the external surface (Lowery and Van Vactor, 2009). The initial effect of this is an immediate attenuation of local actin depolymerisation, enhancing the rate at which the filopodium or lamellipodium is elongated. With the growth cone now firmly attached to the underlying substrate, filopidal and lamellipodial extension continues distal to the attachment site, and the entire growth cone is gradually pulled forward by contractile actomyosin bundles, which connect the fixed substrate-receptor-F-actin complexes to F-actin arcs and microtubules (Lowery and Van Vactor 2009). This growth is consolidated by subsequent microtubule stabilisation, and the rearmost portion of the growth cone narrows, and the microtubules within are compressed by F-actin arcs, forming another segment of axon shaft. Once this is complete, the entire process can begin again, allowing the growth cone to crawl forwards incrementally, leaving consolidated axon-shaft behind and gradually elongating the axon. In the absence of such adhesion molecules growth cone advance is impossible. It is worth noting that in addition to their other growth inhibitory effects, CSPG also bind laminin and neuronal cell adhesion molecule (N-CAM) (Prag *et al.* 2001), obstructing their ability to facilitate axonal growth. In this way AGIM in the injured adult CNS prevent axonal regeneration by causing growth cone collapse through RhoA/ROCK signalling, and the lack of permissive growth-substrate molecules inhibits any regeneration which does occur.

1.2.3 Surviving neurons fail to switch to an active growth state

After axotomy the segment of the axon still attached to the neuron retracts from the injury site, the resulting slight shrinkage allowing the plasma membrane to seal the newly created gap (Spira *et al.* 1996), whereas the distal axon, disconnected from the soma, gradually degrades, a process termed 'Wallerian degeneration'. At this point most axotomised PNS neurons, such as dorsal root ganglia (DRG), tend to readily form growth cones, whereas CNS neurons, such as Retinal Ganglion Cells (RGC) sometimes do not (Verma *et al.*, 2005). Most CNS neurons do form growth cones and enter a relatively well characterized phase of attempted outgrowth for between 1 and 3 days post injury. If CNS axons have not begun to regenerate by this timepoint, the vast majority become quiescent - a process termed 'abortive regeneration' (Berry *et al.* 1996, 2008). It is shortly after this abortion of regeneration that many CNS neurons begin to die (Berry *et al.* 2008). The initial failure of some CNS neurons to even form a growth cone has been interpreted as indicating the differential regenerative responses inherent to CNS and PNS neurons (Gumy *et al.* 2010), particularly as the PNS contains the full complement of AGIM found within the CNS (Berry *et al.* 2008) and yet exhibits spontaneous and often successful regeneration.

The concept of inherent differential responses between CNS and non-CNS neurons has important connotations, making it apparent that, in addition to neuronal death and the innate inhospitability of the injured adult CNS, the internal growth state of the neuron is equally critical in promoting and maintaining axonal regeneration. Many studies have shown that while certain therapies can result in the majority of a CNS neuronal population successfully staving off cell-death, only a tiny proportion of these will typically

regenerate their axons, and that conversely, certain factors can stimulate axonal regeneration whilst having no effect on survival (Cui *et al.* 1999, Cho *et al.* 1999, Li *et al.* 2009, Pernet and Dipollo, 2003). This suggests that in addition to keeping neurons alive, an active-growth program, such as is present *in utero*, must also be initiated in order for CNS axons to actively regenerate. Further support for this hypothesis comes from studies showing that embryonic, prenatal and even immediately postnatal mammalian CNS neurons exhibit considerable regenerative capability, which declines sharply and disappears completely by the first few days postnatal (Goldberg *et al.* 2004). At least one of the events underlying this change was elucidated following the triple discovery that at least two molecules present in the CNS switch from being axon-growth promoting in the embryo to being strongly growth antagonistic immediately postnatally, that this shift is mediated by intracellular cAMP levels, and that these intracellular cAMP levels rapidly decline in postnatal neurons. Both netrin-1 (Shewan *et al.* 2002) and MAG (Cai *et al.* 2001) function chiefly as chemoattractants in the developing CNS but by the first week postnatal (in the rat) both are strongly chemorepellent and if present in sufficient quantities can lead to growth cone collapse. This switch from growth promotion to growth antagonism has been shown to be in response to cAMP levels falling below a certain critical threshold concentration (Shewan *et al.* 2000, Cai *et al.* 2001) and coincides closely with the fall in postnatal intraneuronal cAMP levels and concomitant loss of regenerative capacity (Filbin 2003). In addition to rendering netrin-1 and MAG growth promoting, elevated levels of cAMP, signalling through the cAMP response binding element binding protein (CREB) can lead to increased expression of NTF receptors and the transcription of several genes related to growth and survival (Gao *et al.* 2004) (see Figure 1.2). Such an active growth state is likely to be characterised by other intra-neuronal/ -

axonal changes which recapitulate to a certain extent the intracellular environment in the embryonic neuron. These include the increased expression of growth permitting genes, such as those encoding the growth associated protein GAP-43 (expressed by regenerating but not non-regenerating RGC (Berry et al. 1996, Lorber et al. 2008, Fischer et al. 2004b)), the closely related CAP-23 (Bomze et al. 2001), the cytoskeletal associated protein SPRR-1A (Bonilla et al. 2002) and many of the genes activated by the ERK/MAPK pathway, including genes responsible for activating protein synthesis and increased cytoskeletal reorganisation/growth (Rossi *et al.* 2007). There is also evidence to suggest that upregulation of protein synthesis is another prerequisite for axonal regeneration both within the axon and within the growth cone itself (Chierzi and Fawcett 2001); inactivation of PTEN, a negative regulator of the protein synthesis controlling protein mTOR promotes significant axonal regeneration in the ON (Park *et al.* 2008), whereas the application of protein synthesis inhibitors prevent the elongation of severed segments of peripheral nerve *in vitro* (Gaete *et al.* 1998).

It is then apparent that for CNS neurons to switch from quiescence to an active growth phenotype requires a) the upregulation of growth promoting genes, b) increased intraneuronal cAMP levels and c) increased intra-neuronal and intra-axonal protein synthesis, and that the failure to instigate these changes plays a large part in abortive axonal regeneration in the adult CNS.

1.2.4. The injured CNS is further damaged by inflammatory and immune cells

The inflammatory and immune responses which follow tissue damage are critical to survival; clearing the injury site of pathogens and foreign bodies and killing damaged or infected cells before they can become cancerous or further spread infection. Unfortunately these actions tend to exacerbate CNS injury, damaging axons and killing neurons, which are not replaced, as well as secreting factors inhibitory to axonal regeneration. The primary instigators of the inflammatory and immune responses are the only immune cells normally present in the CNS, the microglia. Microglia reside in the CNS, interspersed with astrocytes and oligodendrocytes, and are constantly extending processes into their surrounding area, probing for pathogens. CNS injury and the influx of foreign bodies and pathogens activate resident microglia, and this microglial activation is largely responsible for initiating and maintaining the immune response to CNS injury (see Garden and Moller 2006 for review).

The majority of subsequent microglia mediated influenced events are antagonistic to neuronal survival and axonal regeneration. Within minutes of CNS injury the pro-inflammatory cytokines IL-1, IL-6 and TNF-α are released by microglia (Allan and Rothwell 2001) in response to raised ATP levels (Tanaka and Koike 2002, Inoue 2006). These cytokines (cytokines are hormone-like factors which communicate with other cells, usually immune/inflammatory cells, often causing them to migrate) trigger widespread microglial activation away from the immediate injury site and cause upregulation of cell adhesion factors on nearby endothelial cells, allowing lymphocytes to “roll” along the endothelium of blood vessels and enter the compromised CNS area (Dinarello 1994).

Activated microglia, along with macrophages, also release IL-8, which summons neutrophils into the injury site (Knall *et al.* 1996). Microglia, macrophages, neutrophils then cooperatively express and/or release numerous molecules which exacerbate CNS injury. These include the highly destructive reactive oxygen species' peroxynitrite ($OONO^-$), superoxide (O_2^-) and nitric oxide (NO) all of which irreversibly damage lipids, proteins, DNA and organelles, killing bacteria and host cells alike (Profyris *et al.* 2004), excitotoxic neurotransmitters such as glutatmate which trigger neuronal apoptosis (Sattler and Tymianski 2001) and the cyclooxygenases, enzymes which convert free arachidonic acid to various prostanoids such as prostaglandins and prostacyclins which amplify inflammation (Lucas *et al.* 2006) and cause vasodilatation, which can lead to harmful local microhaemorrhages (Profyris *et al.* 2004). Perhaps more harmful than any of these processes is the auto-immune actions of the aforementioned lymphocytes in the injured CNS. The presence of endogenous self-reactive lymphocytes (i.e. responsive to self-antigens, not reactive to other lymphocytes) is at first surprising but at least one study has suggested that such auto-immunity is necessary in some way to "calibrate" naive cells (Stefanova *et al.* 2002). These cells include sub-populations which will recognise myelin basic protein (MBP) as foreign (Ankeny and Popovich 2009). These self-recognising lymphocytes are normally kept in check by regulatory T-cells (Ankeny and Popovich 2009) and by the fact that an intact BBB prevents lymphocyte contact with MBP. After CNS injury the BBB is compromised, allowing these anti-MBP lymphocytes to "see" large quantities of MBP for the first time. The result, following the largely microglia-mediatedmediated, cytokine induced lymphocyte recruitment into the injured CNS described above, is a swathe of secondary damage to myelinated axons (Popovich *et al.* 1997) and oligodendrocytes (Crowe *et al.* 1997), which results in the demyelination of

previously viable axons and substantial neuronal and oligodendrocytic cell death.

Complicating the picture somewhat is the evidence that the inflammatory and immune responses can have neuroprotective effects. Activated microglia are known to secrete various neurotrophic and gliotrophic proteins including NGF, BDNF, NT-3, and GDNF (Garden and Moller 2006, Presta *et al.* 1995, Elkabes *et al.* 1996 and Honda *et al.* 1999) which support neuronal and glial survival, whereas several studies using the ONC model have shown that macrophage influx, induced by lens injury or zymosan injection, yields significantly increased post-injury RGC survival and axonal regeneration (Ahmed *et al.* 2010, Lorber *et al.* 2005, 2009), a process directly attributed to the release of the protein oncomodulin by macrophages (Benowitz and Yin 2006, Yin *et al.* 2006, but see Muller *et al.* 2007 and Cui *et al.* 2009).

Despite these potentially benevolent actions, inflammatory and immune responses make up a large part of the series of secondary insults which compound CNS injury and further hinder axonal regeneration.

1.2.5 A regeneration-antagonistic glial scar develops at the injury site

From around 4-5 days post injury, reactive CNS astrocytes and invading meningeal fibroblasts begin the formation of a scar in and around the lesion site (Berry *et al.* 1999a). This scar serves to 'wall off' the injured CNS areas from their surrounds, and this process, which takes place in all mammals as well as in many lower vertebrates, almost certainly evolved as a barrier to infection (Tanaka and Ferretti, 2010). The glial scar is composed of extracellular matrix (ECM) components such as collagen, laminin, fibronectin and chondrotin sulphate proteoglycans (CSPG) as well as living astrocytes and fibroblasts

(Berry *et al.* 1999a, 2008) and is normally functionally complete by 10-14 days after most CNS injuries, although in some CNS tissues the scar may continue to mature and contract for months. Regenerating axons were often observed to halt at the boundary of the glial scar and to proceed no further, and it was assumed that the scar presented an impassable barrier to axons, physically preventing their progress. Instead it has been shown that the axon growth inhibitory properties of the scar are in fact caused by the large amounts of AGIM present within and around the scar, including semaphorins, ephrins and CSPG (see Sandvig *et al.* 2004 and Berry *et al.* 2008 for review), and not due to any physical barrier effect. Evidence for this includes the observation that regenerating RGC axons will successfully dissolve the scar as they progress through it *via* the production and secretion of matrix metalloproteases (MMPs) (Ahmed *et al.* 2005), that axons will display arrested growth at the boundary of the lesion site even in the absence of the glial scar (Berry *et al.* 2008, Sandvig *et al.* 2004) and that various lower vertebrates exhibit robust axonal regeneration through the fully formed glial scar, resulting in functional recovery (Tanaka and Ferretti, 2010). Crucially, robust axonal regeneration appears to prevent formation of the glial scar at all (Berry *et al.*, 1996, 1999b, Logan *et al.* 2006), and axonal regeneration through the glial scar leads to its dissolution (Ahmed *et al.* 2005).

Accordingly, axon regeneration either pre or post scarring does not appear to be impeded by the scar itself, providing the influences of AGIM throughout the CNS can be overcome e.g. by direct or indirect combinatorial NTF application (Logan *et al.* 2006, Berry *et al.* 1996, 1999b respectively), thus the actual growth inhibitory actions of the glial scar is largely a further example of the importance of overcoming the AGIM in the CNS.

1.3 Current CNS axon regenerative therapies

It is apparent then that any therapy hoping to elicit function CNS regeneration must simultaneously prevent neuronal loss by inhibiting necrosis and apoptosis, switch neurons and axons into an active growth state, overcome the growth-cone collapsing effects of AGIM and provide the growth cone with factors encouraging its adhesion and advance. This fact is reinforced by the absence of regeneration in response to the inactivation of individual AGIM, AGIM receptors or even the downstream signalling molecules RhoA or ROCK (Fischer *et al.* 2004a,b, Benowitz and Yin, 2007), and the inefficacy of the application of most single NTFs (Logan *et al.* 2006, Benowitz and Yin, 2007). To this end many, but not all, current therapies are combinatorial, seeking to simultaneously drive axonal growth, neutralise/limit the effectiveness of AGIM and maintain neuronal survival, often through multiple sub-therapies, each aimed at achieving one or more of these sub-goals.

Thanks to the generally benign influence of NTFs on neuronal survival, growth-state and growth cone advancement, many such combinatorial therapies revolve around multiple-NTF application, often in combination with other sub-therapies. The application of multiple NTF has been shown to enhance neuronal survival whilst encouraging active growth (Logan *et al.* 2006, Ahmed *et al.* 2006a) and can even enhance the axons' ability to ignore AGIM by initiating regulated intramembraneous proteolysis (RIP) of its sometime-coreceptor $p75^{NTR}$, rendering many NgR unable to signal, and effectively blinding the axon to a swathe of AGIM (Ahmed *et al.* 2006a, b). More commonly, exogenous NTF therapy is combined with some means of combating the effects of AGIM, including neutralisation of AGIM e.g. by degrading CSPG with the enzyme Chondroitinase (Chi, 2010, Tom *et al.*

2009) or by blockading RhoA/ROCK signalling (Fischer *et al.* 2004a, b, Ahmed *et al.* 2009). One problem associated with exogenous NTF application is the formation of a neurotrophic 'sink' when NTF are applied to the lesion site. This is an area of highly concentrated NTF into which axons will readily regenerate (growing 'up' an NTF chemotropic gradient which mimics *in utero* axonal pathfinding), but from which they subsequently do not exit. To overcome this, many NTF based therapies involve either delivering NTF to the neuronal cell body (Logan *et al.* 2006) or, increasingly commonly, delivering the genes encoding NTF to either the cell body or to the lesion site (Berry *et al.* 2001, Gonzalez *et al.* 2009) where the genes are retrogradely transported to the neuronal cell body enclosed within a plasmid or viral construct. Studies have also combined one or more of the above therapies with anti-apoptotic sub-therapies such as forced over-expression of mitochondrial anti-apoptotic Bcl-2 family members such as Bcl -2 itself (Goldberg *et al.* 2002b), and agents that elevate and maintain intraneuronal cAMP levels (Nikulina *et al.* 2004), provoking significant axonal regeneration in various models of CNS injury (see Hanilla and Filbin 2008 for review).

It should be noted that several types of therapy shown to yield significant axonal regeneration and/or neuronal survival are not combinatorial, although closer inspection of their mechanisms of action almost always reveal multiple contemporaneous effects which could be considered combinatorial. These include the two therapies which arguably promote among the most robust and successful CNS axonal regeneration; intravitreal (*ivit*) peripheral nerve (PN) grafts and macrophage recruitment by lens injury/*ivit* zymosan injection. Surgical insertion of a section of living sciatic nerve into the vitreous immediately prior to optic nerve crush (ONC) has been shown repeatedly to significantly prolong the lifespan of RGC post-axotomy and to promote significant levels

of axonal regeneration: up to 10% of the total RGC population have been reported to regenerate up to 3-4 mm in the adult (Berry *et al.* 1996), with greatly increased neuronal survival and axonal regeneration lasting up to around 20-30 days post injury. This significantly enhanced RGC survival and robust regeneration has been attributed to multiple-NTF secretion by Schwann cells within the PN graft (Berry *et al.* 1996, 2008). Lens injury and/or *ivit* injection of the yeast extract zymosan has also been shown to lead to significant RGC survival and regeneration after ONC (Leon *et al.*, 2000, Fischer *et al.*, 2001, Yin *et al.*, 2003, Lorber *et al.*, 2005), a process which has now been identified as requiring the macrophage derived factor oncomodulin and the sugar mannose (Yin *et al.* 2003, 2006, Benowitz and Yin, 2007). It is also worth noting that the authors of the lattermost study suggest that this macrophage derived effect may also partially underlie the beneficial effects on *ivit* PN grafts.

1.4 The discovery of EGFRki mediated RGC axonal regeneration

The partial success of these various CNS regenerative studies demonstrates that, in order to promote extensive axonal regeneration, any putative CNS regenerative therapy must combat several, if not all, of the phenomena responsible for CNS regenerative failure discussed above. In apparent contradiction of this, a recent study found that the Epidermal Growth Factor Receptor kinase inhibitors (EGFRki) PD168393 and AG1478 promoted neurite outgrowth on CNS myelin substrates, in the absence of exogenous neurotrophic support, and provoked considerable *in vivo* regeneration of RGC axons in the mouse optic nerve (Koprivica *et al.* 2005). For a single, known, exogenously applied

factor to elicit significant *in vivo* axonal regeneration was completely unprecedented. This study went on to show that EGFRki elicited neurite outgrowth on CNS myelin, two myelin derivatives, Nogo-66 and MAG, and CSPG. The authors suggested that NgR ligands such as Nogo-66 and MAG elicited EGFR activation in a calcium dependent manner, although neither the NgR ligands nor NgR itself were seen to interact directly with EGFR.

From this it was surmised by the authors that a Ca^{2+} influx caused by NgR-$p75^{NTR}$ activation trans-phosphorylates the tyrosine kinase domains of the EGFR, which then activates Rho-activated kinase (ROCK) mediated cytoskeletal collapse *via* as yet unknown signalling intermediaries. It was hypothesised that EGFRki thus exert their CNS axon regenerative effects via the blockade of EGFR phosphorylation, thereby inactivating the putative signalling pathways downstream from the NgR which ultimately result in cytoskeletal rearrangement and growth cone collapse via interactions with Rho-A (Koprivica *et al.* 2005, Erschbamer *et al.* 2007).

The authors speculated that EGFR-transactivation by other, as yet unidentified, signalling partners may explain why EGFR ligand binding and subsequent EGFR activation (e.g. in response to EGF) does not result in axonal growth inhibition. Other data showed that while Nogo-66-elicited EGFR activation could be blocked with calcium chelators. EGF-mediated EGFR activation could not, suggesting distinct and separate signalling pathways for different EGFR activating events. Several subsequent studies have also investigated this unexpected axogenic effect of EGFRki, lending evidence to the idea that EGFR activation plays a crucial role in the inhibitory signalling cascade. Western blot analysis of retinal lysates from rats with regenerating ON shows a significant reduction in pEGFR levels compared with animals from a non regenerating group (Ahmed *et al.* 2006), EGFRki were shown to disinhibit CGN neurite outgrowth on CSPG and various myelin derived

inhibitory proteins (Schachtrup *et al.* 2007) and intra-lesion site application of EGFRki led to significant recovery of rat locomotor function following spinal cord injury (SCI) (Erschbamer *et al.* 2007).

1.5 Investigating EGFR and EGFRki in the visual system

Being that the epidermal growth factor receptor (EFGR) had never before been directly implicated in CNS axonal growth cone collapse, or indeed in axonal signalling at all, and that never before had any single agent led to such significant *in vivo* CNS axon regeneration, it was decided to further investigate these phenomena. As the original study was based on the ONC model which our laboratory had extensive experience of (Berry *et al.* 1996, 1999, 2001, Ahmed *et al.* 2006, Logan *et al.* 2006) it was decided to investigate the role of EGFR and EGFRki in the injured rat visual system, using regenerating (ONC+PN graft) and non regenerating (ONC) models.

1.6 The visual system

The adult mammalian visual system consists of the eyes, containing the neural retinae which translate incoming light signals into outgoing action potentials, and the optic nerves (ON) which contain the axons of the RGC which transmit these action potentials to the lateral geniculate nucleus (LGN) and superior colliculus (SC). The two ON meet at the optic chiasm where they split into the optic tracts which then proceed on to these brain areas. The axons within the mammalian ON decussate (cross over) at the optic chiasm to

varying degrees, in rats 95-99% of all axons decussate (Thuen *et al.* 2005). The retina is a complex neural structure which has earned the nickname 'mini-brain' due to its exceptional level of autonomous signal integration and anatomical complexity. The mammalian retina as shown in Figure 1.5, (note that all retinal figures are from/of rat retinae) is comprised of two types of photoreceptors, rods which are sensitive enough to detect a single photon but which only supply monochrome (black and white) visual information, and cones, which are less sensitive to light but, by existing in several subtypes, each of which is responsive to only specific wavelengths of light, allow colour vision. These photoreceptors, the cell bodies of which make up the outer nuclear layer (ONL) hyperpolarize in response to appropriate levels and wavelengths of light, leading to hyperpolarisation of their partner bipolar cells, the primary interneuron of the retina. The bipolar cell in turn stimulates RGC, and if a certain signalling threshold is exceeded, an action potential is generated which propagates along the RGC axon to the brain. Horizontal and amacrine cells, whose cell bodies (along with those of bipolar cells and resident microglia) make up the inner nuclear layer (INL), play complex roles in integrating and sorting visual information including the detection of edges and boundaries between objects and the detection of moving stimuli. Müller glia extend longitudinally throughout the retina, extending from the fibre layer overlying the ganglion cell layer (GCL) down through each successive layer of the retina. Astrocytes also reside in the innermost fibre layer. The axons of RGC converge at the optic foramen where they pass through the optic disc and become the ON proper as they exit the eye.

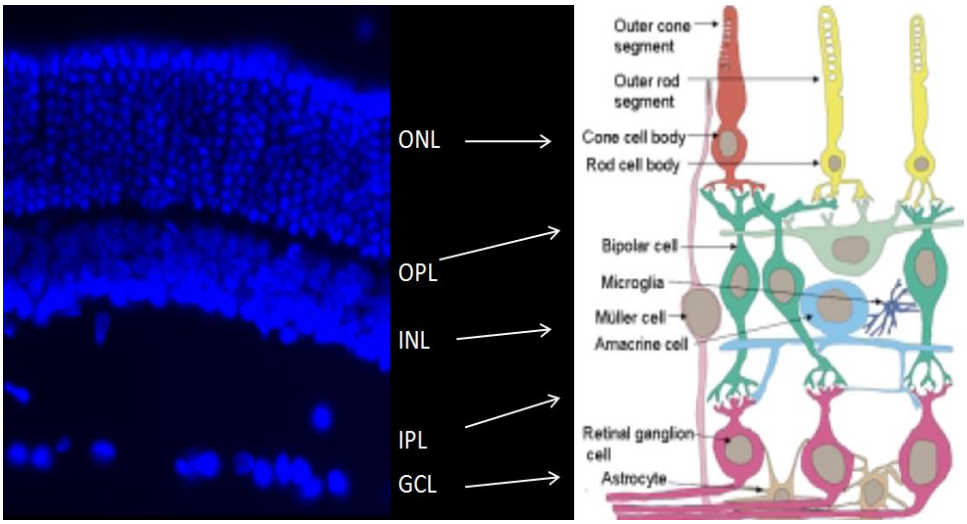

Figure 1.5. The layers and cells of the rat retina, stained with DAPI to show nuclei (left) and represented diagrammatically (right). The cell bodies of photoreceptors, bipolar and amacrine cells and RGC are located in the outer nuclear layer (ONL), Inner nuclear layer (INL) and ganglion cell layer (GCL) respectively. Inner and outer plexiform layers (IPL) and (OPL) are composed of the axons and dendrites passing between bipolar cells and RGC (IPL) and photoreceptors and bipolar cells (OPL). Hyperpolarisation of rods/cones leads to hyperpolarisation of bipolar cells, which in turn excite RGC to threshold, resulting in an action potentials being sent along the RGC axons of the ON to the brain. Horizontal and amacrine cells play complex roles in integrating and sorting visual information including the detection of edges and the detection of moving stimuli. Adapted from Berry *et al.* 2008.

The ON is composed of the axons of RGC, and is populated by the full complement of CNS glia, including the axon-myelinating oligodendrocytes, astrocytes, microglia and synantocytes (Figure1.6) (Berry *et al.* 2008).

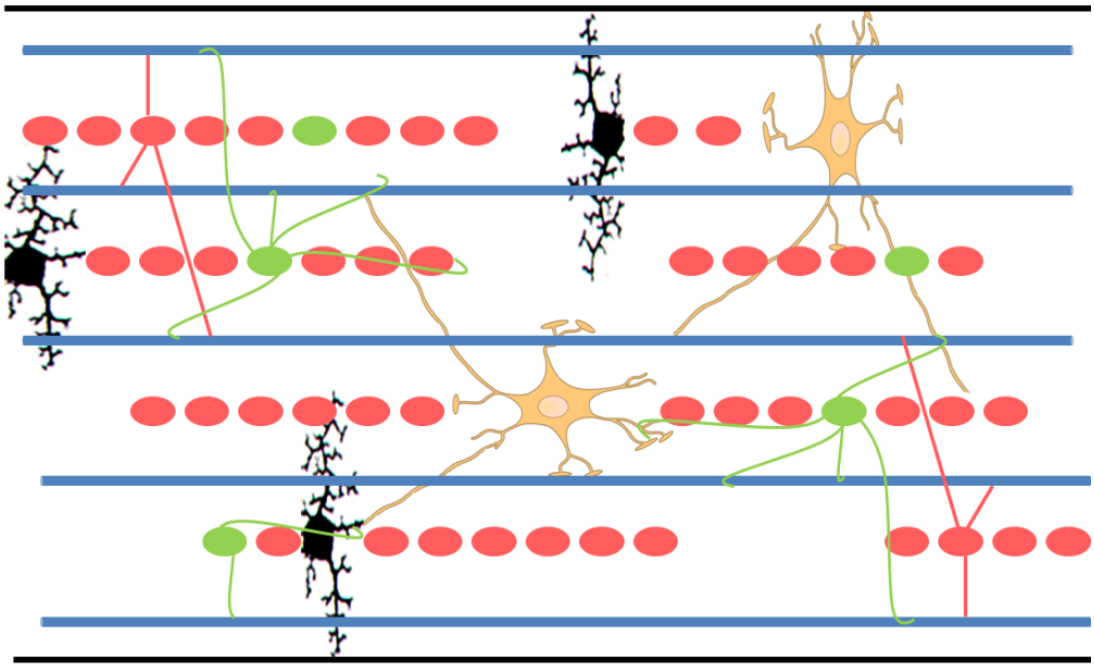

Figure 1.6. Simplified schematic representation of the uninjured optic nerve. RGC axons (blue) are interspersed between orderly lines of oligodendrocytes (pink) and the intermittently spaced astrocytes (yellow-ochre), microglia (black) and synantocytes (green). For clarity most of the cellular processes are not shown, but the examples illustrated demonstrate the pattern of interconnection exhibited by each glial type. Synantocytes are included for completeness but are not studied elsewhere in this study, as the extant literature is very sparse, and no studies focussing on synantocytic EGFR or its blockade have been published.

Crush or transection divides the axons of the ON into proximal segments, which are still attached to the RGC cell bodies in the retina, and distal segments which are not. The distal segments undergo Wallerian degeneration and decay into bulbous and fragmentary debris. Figure 1.7 shows axons in a healthy, uninjured ON contrasted with an ON which has been crushed 14 days previously.

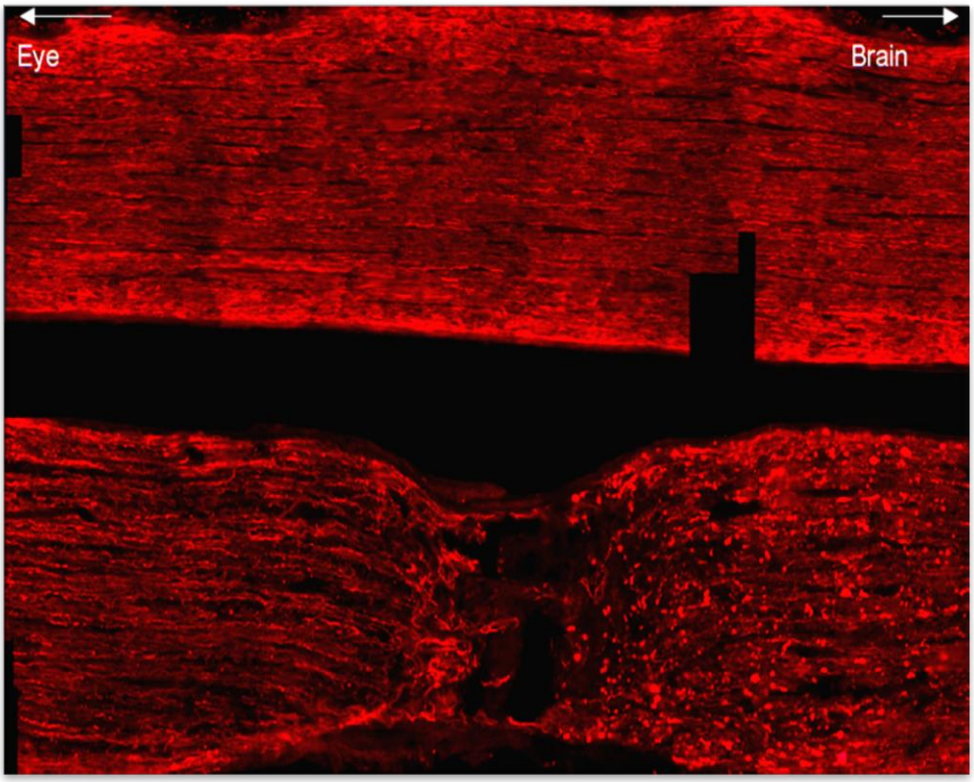

Figure 1.7. A comparison of an uninjured (top) and 14 day post injury (bottom) ON. RGC axons were visualised through immunostaining for the cytoskeletal intermediate filament and axon marker neurofilament 200 (NF 200). Note the proximal segments of ON axons on the left of the injured nerve, which are still attached to their neurons in the retina and the swollen, bulb like and fragmentary sections of axons in the distal (right hand side) segment of the injured ON. P= Proximal segment D= Distal segment. * denotes centre of the lesion site. Image is a composite of multiple x 200 magnification pictures.

1.7 The Optic Nerve Crush + Peripheral Nerve graft model

The ONC+PN model (Berry *et al.* 1996) involves the crushing of the rat ON within its sheath, such that all RGC axons are severed approximately 2mm distal to the optic disc, followed by the grafting of a piece of teased but living peripheral (specifically, sciatic) nerve into the vitreal body of the eye, through a small incision in the eyes' caudal surface.

The PN is held in place by a small piece of implanted sterispan sponge ((figure 1.8), and see materials and methods for detailed description).

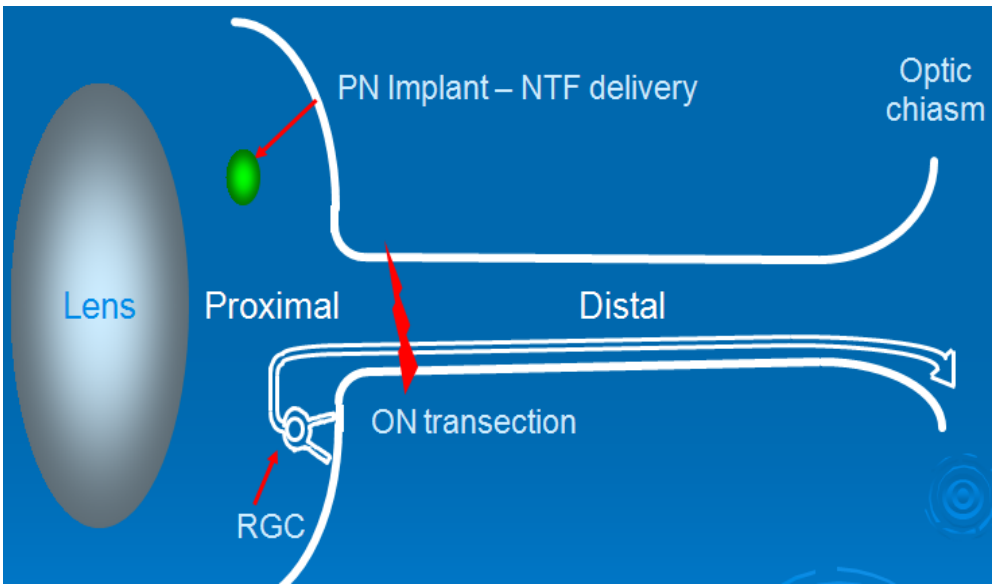

Figure 1.8. The ONC+PN model. The ON is transected 2mm distal to the optic disc, axotomizing all RGC. Immediately afterwards a piece of living peripheral nerve (PN) is implanted into the vitreous through an incision in the caudal surface of the eye. This PN is held in place by a piece of sterispon sponge. NTF secreted by Schwann cells in the PN graft lead to prolonged RGC survival and significant RGC axonal regeneration (Berry *et al.* 1996).

In animals which have received a PN graft, Schwann cell-derived NTFs promote RGC survival and axonal regeneration into and beyond the lesion site, whereas animals receiving ONC alone exhibit little to no RGC axonal regenration at all (Berry *et al.* 1996) as can be confirmed by immunohistochemical staining for growth associated protein 43 (GAP-43), a protein which is only expressed by growing axons (figure 1.9).

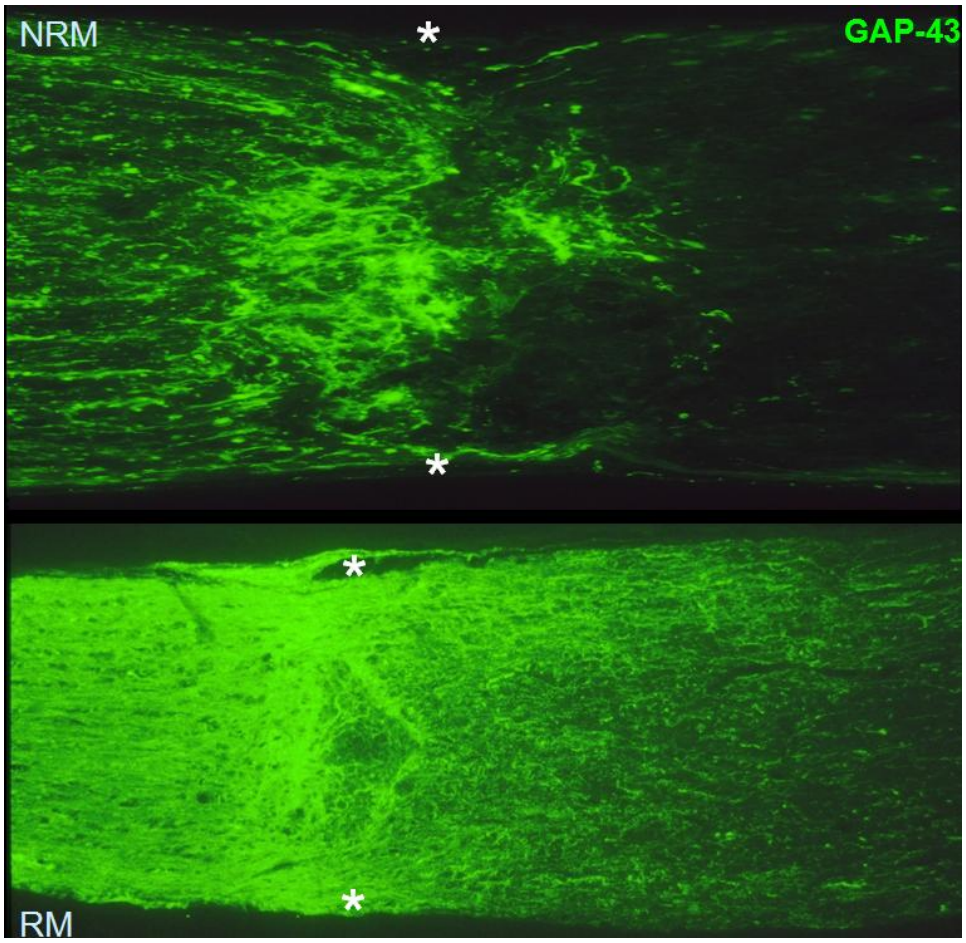

Figure 1.9. GAP-43 immunostaining (green) shows the regeneration of RGC axons in the ON in response to *ivit* PN graft. Animals which received ONC alone (NRM) show little or no axonal regeneration beyond the crush site,whereas PN graft recipient animals (RM) exhibit robust axonal regeneration into and beyond the lesion site.* denotes crush site. NRM = non regenerating model. RM = regenerating model.

1.8 General Aims

To elucidate:

1) The role of EGFR in RGC regenerative failure

2) The mechanism of action by which EGFRki mediate RGC axonal regeneration

1.9 Initial Hypothesis

Levels of activated EGFR (pEGFR) on RGC axons within the retina and ON will be elevated in non regenerating RGC axons (ONC treatment group) and decreased/absent in regenerating RGC axons (ONC+PN graft treatment group).

Chapter 2

Materials and Methods

Unless specifically stated otherwise all reagents used were purchased from Sigma-Aldrich, Poole, UK.

*2.1 In Vivo M*ethods

2.1.1 Animals and Surgical Procedures

All animal procedures were evaluated and licensed by the UK Home Office. Adult, female inbred Fischer f344 rats of 200 – 250 g (Charles River) were used for Optic Nerve Crush (ONC) experiments. All animal surgery was performed by Professor Martin Berry whilst I observed and assisted. Animals were anaesthetized with 4% isofluorane at the beginning of the procedure, dropping to 2.5% prior to first incision and 2% mid way through procedure. 5% EMLA anaesthetic cream (Astra Zeneca, Loughborough, UK) was applied topically to the inside of animals' ears prior to head immobilization with surgical head support. Additionally, subcutaneous injections of Buprenorphine analgesic (0.03mg/kg) were administered twice on the day of procedure and twice per day for the following two days if deemed necessary. To avoid corneal dehydration whilst sedated, animals' eyes were lubricated with Lacri-Lube (Allegan, High Wycombe, UK).

2.1.1.1 Optic Nerve Crush Procedure

The ON was accessed intraorbitally as described by Berry *et al.* (Berry *et al.* 1988a). Briefly; after a midline cutaneous incision over the skull, the skin was reflected up over the upper lid, exposing the orbital margin. Following removal of the superficial fascia, a vertical incision was made through temporalis fascia and muscle. This incision was extended rostrally over the orbital margin without damaging the supraorbital vessels. The supraorbital neurovascular bundle, comprising of the supraorbital nerve, vein and artery, were clamped and incised between the clamped sites so as to expose the Harderian gland. The gland was excised from its capsule and reflected rostrally, exposing the superior rectus muscle. Retractors were inserted between the medial rectus and superior rectus muscles to expose the ON within its dural sheath. In order to avoid retinal ischaemia and subsequent retinal necrosis, care was taken not to damage the retinal artery which also runs inside the Dural sheath. To this end the retractor bulbi muscle and dural sheath were incised, exposing the ON. The ON was crushed with blunt forceps transecting all axons 2mm caudal to the lamina cribrosa whilst leaving the pia mater intact. After ONC the retractor bulbi and rectus muscles and the Harderian gland were returned to their preoperative positions and the skin margins sutured using 4-0 Ethicon™ absorbable suture (Johnson and Johnson International, New Jersey, USA). All animals receiving ONC were killed 14 days post injury (DPI) by CO_2 narcosis.

2.1.1.2 Intravitreal (*ivit)* Peripheral Nerve (PN) implant procedure

Adult, female Fischer rats were used as donors for *ivit* PN implants. After ONC the sclera was incised over the caudal surface and the vitreous body accessed through the choroid and retina. 2mm sections of teased sciatic nerve were implanted through this incision into the vitreous and retained with a plug of absorbable gelatin foam (Sterispon, Allen and Hanbury, London, UK). For efficacy of PN graft see Berry *et al.* 1996.

2.1.1.3 Intravitreal (*ivit)* injection procedure

All injections were performed with glass micropipettes, piercing the sclera immediately posterior to the corneal limbus - the border between the cornea and the sclera.

2.1.2 Tissue block preparation and sectioning

Rats were killed by CO_2 narcosis and tissue was lightly fixed *in situ* by cardiac perfusion with 4% paraformaldehyde (TAAB Laboratories, Berkshire, UK). Following excision, ON and eye tissue was cryoprotected by immersion in increasing sucrose gradients (10%, 20%, 30% in PBS) until tissue was observed to sink, before embedding in OCT mounting medium (R.A. Lamb Laboratory supplies, Eastborne, UK), and frozen rapidly using dry ice. Blocked tissue was stored at -80^0 C. Parasaggital retinal sections and longitudinal ON sections were cut at a thickness of 15 µm using a Bright 5030 Cryostat (Bright,

Cambridgeshire, England), mounted onto charged slides (Surgipath, Peterborough, England) and stored at - 20^0C.

2.1.3 Collagen Matrices

Collagen matrices are 3-dimensional net like structures, created by the polymerisation of liquid collagen, which can act as growth substrates for cells and cellular processes. Collagen matrices have been implanted into injury sites where they encourage healing by providing a permissive growth substrate, and more recently, they have been used to deliver genes, proteins and pharmacological agents. This is achieved by either impregnating the matrix with mRNA, proteins or drugs, or by having the matrix contain replication deficient viral particles containing the genes for desired proteins. The net result is a scaffold like structure that is conducive to cellular and cellular process invasion, which can provide an immobilised repository of drugs, proteins, mRNA, DNA, or vectors, allowing uptake only by structures invading the matrix. This both minimises inappropriate uptake of materials by cells or structures outside the implant and allows a long term, slow release of any drug or protein without the normal problems of diffusion and active clearance.

2.1.4 Specific protocol for creation of collagen matrices

All reagents were kept on ice throughout. 28µl of Na_2HPO_4 were added to 1 ml of 3mg/ml bovine type II collagen (NutaCon, Leimuiden, Netherlands), mixed well and

allowed to stand (on ice) for 5 min. 140µl of collagen were added to 200µl PBS or PBS containing pharmacological agent and mixed well. For each matrix required, 17µl of this solution were pipetted into the very bottom of a 0.5ml tube, with care taken not to form bubbles. Tubes were placed, uncapped, into foam tube racks, which were placed into a sterile bag, which was in turn placed into a glass freezedrying jar. The jar was placed in -80°C freezer for a minimum of 2 hours. After this time the jar was taken from -80°C freezer, placed immediately onto a bed of dry ice, and connected to a lyophilizer. The jar was left overnight (~ 16 hours) and tubes, once removed, were immediate capped and placed into -80°C freezer.

2.1.5 Collagen matrix implantation

The ON was accessed intraorbitally as described previously. After making a careful incision into the superior aspect of the dural sheath the ON was transected within the sheath. The sheath was kept intact to ensure the matrix remained in place. The dry collagen matrix was then placed into the space between the cut ends of the nerve. As the matrix absorbed moisture from the wound it swelled, filling the potential space such that it was in direct contact with both ends of the transected nerve. Care was taken to ensure the matrix was conveyed directly from sealed tube to the nerve, so as to both maintain sterility and to minimize pre-implantation swelling.

2.2 In Vitro methods

2.2.1 Retinal dissection and cell culture

Adult male Sprague Dawley rats (200-300g) were killed by CO_2 narcosis followed by cervical dislocation. Both eyes were removed and placed in ice cold, sterile, phosphate buffered saline (PBS; Gibco, Paisley, UK). Retinae were removed from eyes under sterile conditions and dissociated with a Papain Dissociation System kit (Worthington Biolabs, New Jersey, USA). This kit included the following reagents: Earle's Balanced Salt Solution (EBSS) - which also contained phenol red and bicarbonate, papain, Deoxyribonuclease (DNAse), and albumin ovomucoid inhibitor. Retinae were dissociated for 90 minutes (min) in 5ml of EBSS containing 20 units/ml papain and 100 units/ml DNAse 1, at 37°C within a humidified incubator at 95% air 5% CO_2. Before incubation, retinae were minced slightly in the above solution using ultra-fine surgical scissors in order to increase surface area and aid dissociation. After 90 min, retinae were triturated in a 10 ml pipette to break up any remaining tissue fragments, and the mixture centrifuged at 300 g for 5 min at room temperature (rt). The supernatant was discarded and the pellet resuspended in EBSS containing 1mg/ml ovomucoid inhibitor, 1 mg/ml albumin and 100 units/ml DNAse 1. This cell suspension was then carefully layered on top of 2.5 ml of albumin ovomucoid inhibitor, with care taken to create and maintain two separate layers, and the resulting double layered solution centrifuged at RT for 6 min at 70g. Albumin ovomucoid inhibitor served as a density gradient; intact cells, being larger and heavier than cellular and extracellular matrix debris, experienced greater centrifugal forces,

resulting in cells being forced through the viscous lower layer whilst smaller debris remained above or within the albumin ovomucoid inhibitor. The resulting pellet was thus almost entirely composed of intact cells and largely debris-free. The supernatant was discarded and the cellular pellet resuspended in 1 ml of supplemented Neurobasal A (sNBA; for 25ml, 24.2 ml Neurobasal-A, 500µl B27 supplement, 62.5 µl 200mM L-Glutamine, 125 µl Gentimycin – all from Gibco).

2.2.2 Retinal culture, cell counts and plating

Of the final 1ml cell suspension in sNBA (see above), 25µl was added to 25 µl Trypan Blue dye (Gibco), mixed, and 25µl of this mixture injected into one side of a haemocytometer. The number of cells observed (using a light microscope at x 40 magnification) to be within the 25 small divisions in the centre of the haemocytometer were counted and this number doubled (to account for x 2 dilution in cell number due to addition of Trypan Blue) and this number multiplied by 1×10^4 to yield the total number of cells in the 1ml cell suspension. Cells were plated onto chamber slides (BD Biosciences,) pre coated with poly-D-Lysine (100µg/ml) and Laminin (10µg/ml) at 125,000 per well, in 300µl sNBA. As retinal ganglion cells (RGC) account for 1-3% of all cells in the rat retina, 125,000 cells per well equated to approximately 1500 RGC per well. Cells were allowed 24h to attach to the well floor and test reagents were added to the wells after this time. Unless stated otherwise, all cultures were maintained for 72h in the above incubatory conditions before being fixed and processed further.

2.2.3 Immunohistochemistry and Immunocytochemistry

The mammalian adaptive immune system has the ability to raise antibodies to almost any molecule or antigen (ANTIbody GENerator). When a laboratory animal such as a rabbit is co-injected with an adjuvant (a chemical designed to elicit an immune response) and a specific protein, the immune system manufactures antibodies specific to this protein. If a B cell responsible for generating this antibody is subsequently isolated and successfully hybridized with an immortalized cell, a mono-clonal antibody can be repeatedly collected and purified. This antibody will recognize a single epitope on the target molecule (almost always a protein). When a mixture of antibodies is taken and purified from the host animals' serum, the result is a poly-clonal antibody; a variety of antibodies to different epitopes on the same protein.

Using these antibodies, thin sections of tissue (immunohistochemistry, IHC) or cells in culture (immunocytochemistry, ICC) can be probed for the protein of interest. This is achieved by coating the tissue/cells in a solution containing these antibodies, which then recognize and bind specifically to the target proteins. In order to prevent these antibodies binding aberrantly and non-specifically to other proteins, a blocking agent is used immediately before antibody application, typically consisting of a solution containing non-specific proteins such as BSA. The proteins in solution will bind weakly to all proteins in the tissue/cell sample and will only be outcompeted by the primary antibody at their specific epitope. In this way, the antibody will bind strongly only to its target allowing subsequent washes with relevant buffer to remove all non-bound protein. As a result visualization of the remaining antibody specifically labels only the protein of interest. To this end, some antibodies are conjugated to either fluorescent, enzymatic or

radioactive compounds which allow for direct or indirect visualization. More commonly, antibodies raised against the first (primary) antibody are themselves conjugated as above. These secondary antibodies are raised against the species specific, conserved region of all antibodies, such that a secondary antibody raised against an animal will recognize all antibodies created by that species, regardless of the primary antibody's' target.

Antibodies used in this study are shown below in Table 2.1.

Epitope	Manufacturer	Catalogue No.	Species	Initial Conc.	Dilution Factor	Marker For
CAII	UCL	n/a	Rabbit	21mg/ml	1 : 400	Oligo-Dendrocytes
OX-42	Serotech	MCA 275R	Mouse	n/a (ascites)	1 : 200	Microglia
CD-68	Serotech	MCA 341 R	Mouse	n/a (ascites)	1 : 200	Macrophage
GAP-43	n/a	n/a	Sheep	n/a (ascites)	1 : 2500	Regen-erating Axons
EGFR – Phosphorylated	ABCAM	Ab5652	Rabbit	0.125 mg/ml	1:200	pEGFR
EGFR - Phosphorylated	Santa Cruz	SC-12351	Goat	200µg/ml	1 : 50	Activated EGFR
B-III-Tubulin	Sigma	T8660	Mouse	n/a (ascites)	1 : 400	Retinal Ganglion Cells
Neurofilament 200 (Heavy Chain)	Sigma	N0142	Mouse	n/a (ascites)	1 : 400	Axons
Glial Fibrilliary Acidic Protein (GFAP)	Sigma	G3893	Mouse	n/a (ascites)	1 : 500	Astrocytes, Müller Cells
Goat Ig - tagged with Alexa Fluor 488	Molecular Probes	A11055	Donkey	2mg/ml	1 : 500	Goat Ig
Rabbit Ig - tagged with Alexa Fluor 488	Molecular Probes	A11034	Goat	2mg/ml	1 : 500	Rabbit Ig
Mouse Ig - tagged with Alexa Fluor 594	Molecular Probes	A11032	Goat	2mg/ml	1 : 500	Mouse Ig
Rabbit Ig - tagged with Alexa Fluor 594	Molecular Probes	A11037	Goat	2mg/ml	1 : 500	Rabbit Ig

Table 2.1. Antibodies used in immunohistochemical and immunocytochemical analyses.

2.2.3.1 Immunofluorescence

Antibodies can be linked to a variety of functional groups designed to aid their visualization, including enzymes, radioisotopes and fluorophores. Of these, flurophore-linked antibodies are arguably the most common. Fluorophores are molecules which absorb light of a specific wavelength and emit light of a specific, longer wavelength. Fluorescence microscopes differ from conventional light microscopes only in that they have two sets of special light filters. The first set filters the light projected onto the sample, ensuring that only light of the wavelength absorbed by the fluorophore reaches it. The second set of filters ensures only light of the wavelength emitted by the fluorophore reaches the eyepiece and camera. As a result, fluorescent labelled antibodies can provide very accurate, high resolution protein imagery.

2.2.3.2 Primary IHC protocol for immunofluorescence

Sections were warmed to RT, fixed in 100% ethanol for 1 min, and washed in tris buffered saline (TBS, 50ml 1M Tris pH'd to 7.4 with HCl, 30 ml 5M NaCl in 1 L H_2o), 2 x 5 min followed by 1 x 10 min wash in TBS with 0.1% Triton - X – 100 to permeate the tissue. Sections were isolated using a hydrophobic pap-pen (Vector Labs, Peterborough, UK). Blocking solution/Antibody Diluting Buffer (ADB); (1% Bovine Serum Albumin, 0.1% Triton - X – 100, 5% (various) Serum in TBS) were applied at 95µl per section and slides were incubated at RT in an enclosed metal chamber for 30 min. Sections were incubated overnight (16 h) at 4^0C in ADB containing relevant antibody dilutions within a humidified

metal chamber. Following 5 x TBS washes, Secondary antibody solutions were added at 95µl per section and slides were incubated at RT in a humidified metal chamber for 60 min. Secondary antibody solutions were removed and sections underwent 3 x 5 min TBS washes. Sections were drained of excess TBS and mounted with Vectamount containing DAPI (Vector Labs). Sections were stored at 4^0C in cardboard slide containers wrapped with aluminium foil.

2.2.3.3 Protocol for immunofluorescence IHC using anti-GAP-43 antibody

All washes and blocking steps were carried out in plastic 14ml 5-slide-containers. Slide-containers were rocked within larger cylindrical containers, padded with tissue paper on a motorized roller. Sections were washed and rocked for 5 min in TBS**,** followed by 10 min standing at RT in 100% methanol, incubated and rocked in blocking solution (10% NDS in TBS) for 1h at RT, isolated using a hydrophobic pap-pen, incubated in 1/2500 dilution of primary GAP-43 AB in ADB (5% NDS, 2% BSA in TBS_2T) overnight (16h) at 4^0C in a humidified metal chamber, washed and rocked in TBS_2T for 1h, followed by washing and rocking for 1 hour in ADB and a further wash and finally rocked for 1 hour in TBS_2T, all at RT (TBS_2T, 50ml Tris pH 7.4, 60ml NaCl, 0.5% Tween 20). Sections were then incubated in 1 to 500 dilution of secondary AB in ADB overnight (16 h) at 4^0C in a humidified metal chamber, washed and rocked for 2 x 30 min in TBS_2T, followed by 1 x 30 min in TBS and 1 x 5 min in purified H_20 (Millicue, Millipore, Watford, UK) all at RT. Sections were then mounted using Vectamount containing DAPI and covered with glass cover slips. All sections were stored at 4^0C in cardboard slide containers wrapped with aluminium foil to avoid signal quenching.

2.2.3.4 Specific protocol for immunofluorescence ICC

In order to avoid the use of pipettes which could aspirate and dislodge cells from the well surface, chamber slides were quickly and gently inverted to remove solutions. Similarly, Pasteur pipettes were used for the addition of all non-antibody solutions and reagents were carefully dripped down one corner of the well. For antibody solutions which required the addition of exact volumes of solution, large diameter pipettes were used. When adjacent wells required different antibodies, antibody solutions were removed carefully by large diameter pipette as inverting the entire slide could have resulted in small quantities of inappropriate antibodies entering wells. Cells were fixed for 10 min in 4% PFA and washed 3 x 10 min in TBS. Following 10 min at RT in blocking solution (3% BSA, 5% relevant serum, 0.1% Triton-X-100) within humidified metal container, cells were incubated at RT for 1h, then at 4°C overnight in a blocking solution containing relevant concentrations of primary antibodies, within a humidified metal container. Following 3 x 10 min wash in TBS, cells were incubated for 1 hour at RT in a blocking solution containing relevant concentrations of secondary antibodies, within a humidified metal container. Following 3 x 10 min TBS washes, chambers were removed from slides using the special tool provided by the manufacturer and glass cover slips were mounted over the cells with Vectamount containing DAPI.

2.2.4 Photography

Images were captured using an AxioCam HRC Camera, an Axioplan 2 microscope with Zeiss Neofluar lenses and Axiovision software, (all from Carl Zeiss, Hertfordshire, England). Care was taken to ensure that exposure times for all channels were kept constant across all sections including controls. Image processing was performed using Adobe Photoshop (including creation of composite ON images) after contrast and brightness level adjustment. In order to keep such adjustments standard, macros were recorded which applied identical values to all images including controls.

2.2.5 RGC counts

Ten fields of view of retinal sections encompassing the RGC layer of the retina were randomly selected for each sample from each treatment group. RGC were classified as clearly β-III-tubulin positive cells with round somata, in the ganglion cell layer (GCL) of the retina. The total number of observable RGC was calculate for each of the ten fields of view and summed to obtain an overall count for the 10 fields. The number of RGC which co-expressed β-III-Tubulin and pEGFR were counted and summed simultaneously. The % of all RGC expressing pEGFR per treatment group = [Total number of pEGFR positive RGC/Total number of RGC] x 100. These counts were repeated for a minimum of three animals per treatment group.

2.2.6 *In Vitro* RGC quantification

RGC were identified as those cells which both expressed β-III-tubulin and possessed large, round somata. Neurites were defined as processes which emerge from RGC somata and were at least the diameter of that cell body in length. Sampling was achieved by dividing the well into 9 sectors as shown below (Figure 2.1).

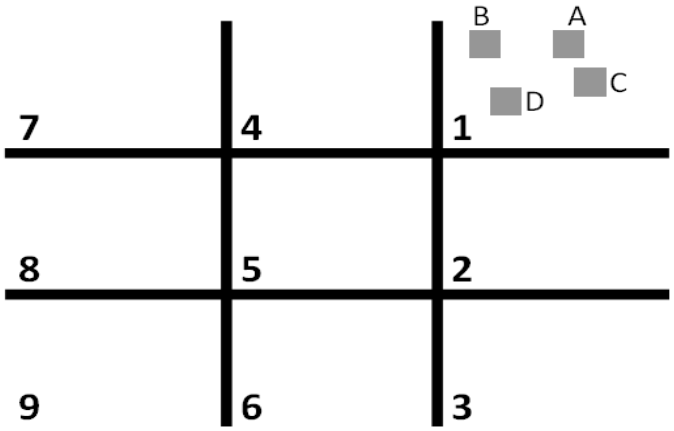

Figure 2.1. Sampling method. Subdivision of well into 9 sectors.
A-D: examples of 4 pictures from random fields of view within a sector.

A pilot study (included in Chapter 4, introduction) was performed on one entire well in which the actual mean RGC neurite length was calculated after measuring the longest neurite length for every RGC. Next, sample sizes of 10, 20, 50, 100 and 200 individual measurements were taken and the standard error of the mean (SEM) in these sample sizes compared, using the actual mean neurite length obtained previously as a baseline. A graph of SEM vs sample size was constructed and an optimum number of 36 samples per well was obtained (defined as the point at which further increasing sample numbers no longer significantly decreased error levels). This equated to 4 pictures taken at random in each of the 9 well sectors. For each experimental condition 3 wells were used, resulting in 108 pictures per treatment group per experiment being sampled.

2.3 Statistical analyses

All statistical analyses and post hoc tests were performed using Graphpad Prism 4 (San Diego, CA, USA).

2.3.1 One way ANOVAs and t-tests

Unpaired t tests were used to determine if differences in the data from two groups were real or coincidental. When more than two groups were compared a One way Analysis Of Variation (ANOVA) test was used. Bonferronis and Dunnetts post hoc tests were used when comparing groups with one another or with controls respectively. P values, which estimate probability that differences observed between groups are coincidental, were denoted as * for $p < 0.05$, ** $p < 0.01$ and *** $p < 0.001$, which indicate the confidence values that are considered to be increasingly statistically significant. NS denotes no significant difference between groups.

2.4 Protein assays

Many techniques require the confirmation of sample protein levels in order to return accurate results. Colorimetric protein assays measure protein concentrations by using the protein within a sample to catalyse a colour-change reaction such that opacity increases linearly with concentration. The opacity of samples is then compared with that of pre-prepared samples of known protein concentration (standards) and sample protein concentrations are extrapolated. Protein assays were performed according to the protocol supplied with the BioRad DC Protein Assay (BioRad, Hemel Hempstead, UK) and, unless stated otherwise, all reagents were supplied with this kit. This assay consists of two consecutive reactions; a reaction between protein and copper in an alkaline medium and a subsequent reduction of the reagent Folin by the protein-copper solution, producing a blue solution with maximum and minimum absorbencies of 750 and 405 nm respectively.

2.4.1 Specific protein assay protocol

Reagent A' was formed by adding 20µl reagent S to each ml of reagent A. A standard curve of increasing bovine serum albumen (BSA) in PBS was plotted with values of 0.2mg/ml to 1.5 mg/ml. 100µl samples or BSA standards were mixed with 500µl reagent A', vortexed, 4ml of reagent B added and this mixture vortexed. After 15 min incubation in a darkroom at RT, absorbencies were read at 750nm using a Victor spectrophotometer.

The slope of a concentration vs absorbance graph using BSA standards was used to extrapolate sample protein levels from their absorbance values.

2.5 SDS-PAGE and Western blot

Polyacrylamide gel electrophoresis (PAGE) is a technique which separates mixtures of proteins by weight for subsequent detection with antibodies. By passing an electrical current through a gel of defined density the negatively charged proteins move towards a positively charged anode at a constant rate. Individual proteins progress through the gel at a rate proportional to their molecular weight; larger, heavier proteins move slower than smaller, lighter proteins. In order to make sure that proteins are separated purely by size and not by any differences in charge, all proteins must be of equivalent electronegativity/weight ratio. To this end, β-mercaptoethanol and the anionic detergent sodium dodecyl sulphate (SDS) are used to respectively a) destroy tertiary structures by reducing disulphide bridges, and b) denature and bind to the resulting unrolled, rod-like string of amino acids. The negatively charged SDS binds approximately one molecule to every two amino acids, resulting in each protein being maximally negatively charged. The gel in which this migration takes place is known as the resolving gel. As proteins sizes are measured as a function of the distance travelled through this resolving gel, it is vital that all proteins enter the gel simultaneously. To this end a second gel, the stacking gel, is poured onto the resolving gel so that the two are continuous. The stacking gel is made using buffers at a considerably lower pH than the surrounding buffers and is of a much lower density than the resolving gel. At the stacking gel-resolving gel interface all proteins irrespective of size are concentrated into a band of approximately 20μm, and

enter the resolving gel simultaneously. To create individual wells in which each sample can run, a comb is placed in the stacking gel mixture before polymerization. The forks of this comb occupy fixed, rectangular spaces within the gel, forming regularly spaced wells at the top of the stacking gel. Samples are then pipetted into the bottom of these wells. Immediately prior to electrophoresis each sample is at the same vertical level within the gel and sufficiently dispersed horizontally to facilitate detection in separate wells.

Following SDS PAGE, a Western blot can be performed. The gel containing the separated proteins is placed next to a membrane of nitrocellulose or polvinylidine fluoride (PVDF) and application of electrical current transfers the proteins onto the membrane. This membrane can then be probed with relevant primary antibodies followed by secondary antibodies conjugated to various enzymatic, fluorescent or radioactive detector compounds. Commonly, a horse radish peroxidase (HRP) enzyme is conjugated to the secondary antibody and used to catalyse a chemiluminescent reaction. The photons emitted develop photographic film placed directly above the membrane, resulting in a dark band corresponding to the specific protein. A premade protein ladder consisting of prestained proteins of specific sizes is run through the gel and the approximate sizes of bands detected are compared to these standards, allowing accurate estimation of molecular weight.

To accurately measure changes in levels of a specific protein between treatment groups the same amount of total protein must be added to each well. This ensures that changes in protein titres are a result of a real, biological effect and not a consequence of unequal sample volumes. This is achieved by probing membranes with an antibody to the ubiquitious cytoskeltal component β-actin; ratio of β-actin levels between samples will indicate relative levels of total protein.

2.5.1 Tissue preparation and homogenization for SDS-PAGE and Western blot

ON and retinal tissues were homogenized in homogenization buffer (20mM Tris Hal, pH 7.4, 150mM NaCl, 1mM EDTA, 0,5mM EGTA, 1% NP-40, 1.5% protease inhibitor, all in milliQ H_2O, ON in 100µl and retinae in 200µl. Tissue was homogenized, on ice, with homogenizer (IKA, Staufen, Germany) for 2 min starting at low speed and then increased to maximum rpm. After 30 min on ice, the homogenate was centrifuged at 13, 000 RPM for 30 min at 4°C. The supernatant was removed and pellet stored at -80°C.

2.5.2 Specific SDS PAGE and Western blot protocol

Resolving gel (12 %, 2.75ml Protogel (IBR stores, University of Birmingham) 1.65ml 1.5 M Tris, 2.2ml milliQ H_2O, 66µl 10% SDS, 23.1µl 10% APS, 9.9µl TEMED) was poured into a single use gel cassette such that the cassette was 3/5ths full. To prevent air bubble formation, (which would inhibit polymerization) 100% ethanol was poured on top of the gel. After the resolving gel had set, the ethanol was removed, the cassette washed with milliQ H_2O and stacking gel (0.4ml Protogel, 1.85ml 0.5M Tris, 0.75 ml milliQ H_2O, 30µl 10% SDS, 15µl 10% APS, 7.5 µl TEMED) was poured on top of the resolving gel. A gel comb was placed carefully into the top of the stacking gel, the gel was checked to make sure no bubbles of air remained, and the gel was allowed to polymerise. Prepared gel cassettes were wrapped in Clingfilm and damp tissue and stored at 4°C until needed (typically less than 3 h). Although resolving gel was normally set at 12% polyaccrylamide,

for molecules larger than ~100 kDa an 8% polyaccrylimide gel was used and the remaining volume replaced with milliQ H_2O. Stacking gels remained unchanged.

Pre-calculated volumes of samples were diluted 1:1 with a sample buffer (125mM Tris containing 2% SDS, 10% glycerol, 2.5% Mercaptoethanol) in Eppendorf tubes with pre-pierced lids, centrifuged at 12,000 G for 1 min and boiled for 4 min at 90°C. Samples were centrifuged as before and loaded into the wells using long, ultra-fine pipette tips. Empty wells were loaded with sample buffer alone. First and last wells were loaded with 10µl of protein ladder (Benchmark, Invitrogen)

Running buffer (3.03g Tris base, 14.4g glycine, 20 ml methanol, 980 ml milliQ H_2O, 5 ml 20% SDS) was added until wells were submerged. The powerpack (Powerease 500, Invitrogen) was set at 125V, 18mA, 2.1W and gel run for 90 min. Times were reduced or increased when probing for low or high molecular weight proteins respectively. During this time, filter paper and foam blotting pads were soaked in chilled transfer buffer (3.03g Tris Base, 14.4g Glycine, 200ml Methanol, 1 ml 20% SDS in 800 ml milliQ H_2O). Following SDS PAGE, a PVDF membrane (Immobilon, Millipore) was activated by 1 min immersion in methanol followed by 5 min in milliQ H_2O and finally for 5 min in chilled transfer buffer.

The gel was removed from the case, immersed in transfer buffer for 15 min and placed within the Western blotting module (X-cell 2, Novex, San Diego, CA, USA) with foam pads, membrane and filter paper in the following order, bottom to top: 3 foam pads, filter paper, membrane, gel, filter paper, 2 foam pads. Care was taken to handle gel and membrane only with tweezers, so as to avoid contamination with extraneous protein. The Western blotting module, containing gel and membrane, was immersed in chilled transfer buffer and the outer compartments of the tank were filled with transfer buffer. The western blot option was selected on the powerpack and the transfer time set to 2h.

Following transfer the membrane was washed 3 x 5 min in TTBS (1.21g Tris, 8.77g NaCl, 500µl tween, in 1 litre milliQ H_2O) and then immersed in blocking solution (5% Marvel powdered milk (Premium International Foods, Lincs, UK) in TTBS) for 1 h. The membrane was immersed in the relevant concentration of primary antibody diluted in blocking solution within a heat sealed bag then incubated on a rocker overnight at 4°C. Following 3 x 10 min washes in TTBS, the membrane was immersed in its relevant concentration of HRP-conjugated secondary antibody, diluted in blocking solution within a heat sealed bag, then incubated on a rocker for 1 hour at RT. After 3 x 10 min washes in TTBS, an Enhanced Chemi-Luminescence Kit (Amersham Biosciences, Buckinghamshire, UK) was used as follows. 1ml of ECL reagent 1 was mixed with 1ml of ECL reagent 2 and pipetted evenly over the membrane which was flipped upside down after 30 s so as to coat each side evenly and after a further 30 s (1 min in total) blotted gently with filter paper and placed within an unsealed translucent bag. After transfer to the darkroom, the bag containing the membrane was secured inside a lightproof metal container and a similar sized piece of photosensitive film (Kodak, Hemel Hempstead, UK) placed directly on top of the bag. After relevant exposure time (typically 1, 5 or 15 min) the film was removed and placed into an autodeveloper machine (SRX-101A, Konica Minolta, Banbury, UK). After ECL, membranes were washed 3 x in TTBS and placed into TTBS within a heat sealed bag to be stored at 4°C. If required, the membrane was stripped in stripping buffer (25µM glycine-Hal, pH 2, 1% SDS) for 1h, washed 3 x 10 min in TTBS, blocked in blocking solution and underwent another primary antibody incubation and detection cycle as detailed above.

2.6 Enzyme Linked ImmunoSorbent Assay (ELISA)

The ELISA yields an accurate measurement of the concentration of a specific compound within a solution. In its simplest form, an ELISA consists of a procedure where an antibody is added to an unknown concentration of immobilized antigen. This antibody is pre-linked to an enzyme or a fluorescent compound, which is used to catalyse a colorometric reaction, giving a linear relationship between concentration of initial substrate and final light absorbance levels. Fluorescent antibodies are used to identify initial concentration of substrate in terms of light emitted. Commonly, for mammalian *in vitro* studies, an enzymatic antibody-sandwich approach is used. In this case the initial solution containing the substrate is applied to a surface (usually a 96 well plate) which has been precoated with an antibody specific to the compound of interest. After incubation the solution containing unbound substrate is removed and a second antibody specific to a different epitope on the same compound is applied. The result is a 'sandwich' in which the compound of interest is trapped between two antibodies. The second antibody, attached to HRP, is used to catalyse a chromogenic (colour creating) reaction with, for example, 3, 3, 5, 5' –tetramethylbenzidine (TMB). The amount of compound present is directly proportional to the amount of TMB catalysed. Solutions containing a range of concentrations of the compound of interest are processed simultaneously. The concentration of compound in each sample is derived by first plotting a standard curve of light absorbance versus concentration, using known conventrations of protein standards, on a logarithmic scale and then noting the concentration value on this curve which corresponds to the absorbance value gleaned from the sample in question.

2.6.1 Specific ELISA protocol for NT-3

The NT-3 Emax ELISA system (Promega, Southhampton, UK) was used to assay NT-3 concentration in conditioned media. Both protocol and reagents used were supplied with this kit. Briefly: the wells of sterile, 96 well plates (Nunc, Loughborough, UK) were coated with polyclonal anti-human NT-3 (20µl antibody + 10 ml carbonate coating buffer (p.H. 9.7)), 100µl per well, covered with Parafilm and incubated at 4°C overnight (16 hours). Following a single wash with TBST (p.H.7.6, 0.05% Tween), 200µl of 1x block and sample buffer were added to each well and the plate was incubated without shaking for 1 hour (1x block and sample buffer: 34.4ml deionised water, 8.6 ml block and sample 5X Buffer). The plate was set up as indicated in figure 2.2.

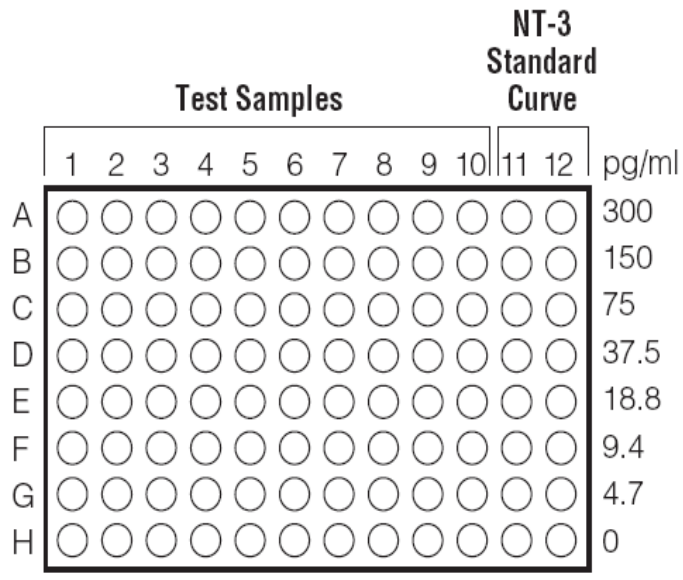

Figure 2.2. NT-3 ELISA Plate set-up. Diagram modified from NT-3 Emax instruction manual (Promega)

The initial NT-3 standard solution was diluted 1:2000 with block and Sample buffer and subsequently diluted 1:2 serially from 300pg/ml (11A + 12A) to 4.7pg/ml (11G + 12G). The bottom-most well (H) contained only block and sample buffer. Following an initial dilution of sample (see specific figure in results) in the topmost lane, e.g. A1, samples were subsequently serially diluted 1:2 or 1:5 with block and sample buffer, with the bottom-most well containing buffer only. The plate was then sealed with Parafilm and shaken on a plate shaker for 6 hours at RT. After 5 washes in TBST, 2.5µl NT-3 antibody was added to 10mls block and sample buffer, mixed well, and 100µl of this solution was added to each well. The plate was then sealed with Parafilm and incubated overnight at 4°C. Following 5 washes in TBST, 100µl of HRP conjugated anti-mouse IgG were added to 9.9 ml Block and Sample buffer, mixed well, and 100µl of this solution added to each well. The plate was sealed with Parafilm and incubated with shaking at RT for 2.5 hours. During this time TMB-1 (3,3 ‘, 5,5’ –tetramethylbenzidine) solution was allowed to warm to room temperature. 100µl of TMB-1 was then added to each well and the plate was sealed with Parafilm and shaken at RT for 15 minutes. After this time 100µl of 1N HCL was added to each well, halting the chromogenic reaction, and absorbencies were read on plate-reader at 450nm. Using Microsoft Excel, a standard curve of absorbance *vs* NT-3 concentration was prepared for the NT-3 standards. This graph then allowed the correlation of sample absorbencies to relative NT-3 levels.

2.6.2 Specific ELISA protocol for GDNF

The GDNF Emax ELISA system (Promega, Southhampton, UK) was used to assay GDNF concentration in conditioned media. Both protocol and reagents used were supplied with this kit. Briefly: the wells of sterile, 96 well plates (Nunc, Loughborough, UK) were coated with monoclonal anti-GDNF antibody (10µl antibody + 10mls carbonate coating buffer (p.H. 8.2), 100µl per well), covered with Parafilm and incubated at 4°C overnight (16 hours). Buffer was emptied from wells and 200µl of 1x block and sample buffer was added to each well and the plate was incubated without shaking for 1 hour (1x block and sample buffer: 34.4ml deionised water, 8.6 ml Block and Sample 5X Buffer).

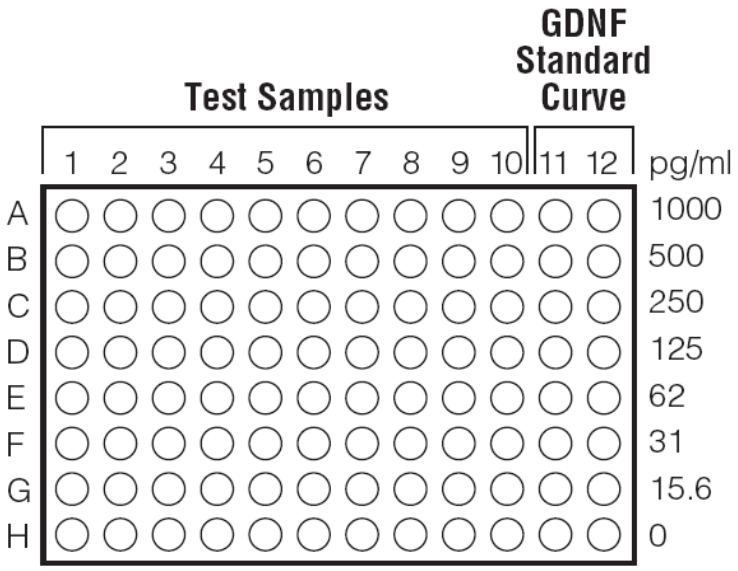

Figure 2.3. GDNF ELISA plate set-up. Diagram modified from GDNF Emax instruction manual (Promega)

Plate was set up as indicated in Figure 2.3. The initial GDNF standard solution was diluted 1:2000 with block and sample buffer and subsequently diluted 1:2 serially from

1000pg/ml (11A + 12A) to 15.6pg/ml (11G + 12G). The bottom-most well (H) contained only block and sample buffer. Following an initial dilution of sample (see specific figure in results) in the topmost lane, e.g. A1, samples were subsequently serially diluted 1:2 or 1:5 with block and sample buffer, with the bottom-most well containing buffer only. The plate was then sealed with Parafilm and placed on a plate shaker for 6 hours at RT. Following 5 washes in TBST, 20µl anti-human GDNF polyclonal antibody was added to 10mls block and sample buffer, mixed well, and 100µl of this solution were added to each well. The plate was then sealed with Parafilm and incubated at 4°C overnight. Following 5 washes in TBST, 40µl of anti-chicken IgY HRP conjugate were added to 9.96 ml 1x block and sample buffer, mixed well, and 100µl of this solution added to each well. The plate was sealed with Parafilm and incubated with shaking at RT for 2 hours. During this time TMB-1 (3,3 ‘, 5,5’ –tetramethylbenzidine) solution was allowed to warm to rt. 100µl of TMB-1 were then added to each well and the plate was sealed with Parafilm and shaken at rt for 10 minutes. After this time 100µl of 1N HCL were added to each well, halting the chromogenic reaction, and absorbencies were read on plate-reader at 450nm. Using Microsoft Excel, a standard curve of absorbance *vs* GDNF concentration was prepared using the supplied GDNF protein standards. This graph then allowed the correlation of sample absorbencies to relative GDNF levels.

2.6.3 Specific ELISA protocol for CNTF

The Duoset Rat CNTF ELISA kit (R and D systems, Inc, MN, USA) was used to assay CNTF concentration in conditioned media. Both protocol and all reagents were supplied with this kit. Briefly: the wells of sterile, 96 well plates (Nunc, Loughborough, UK) were coated with 2µg/mL mouse monoclonal anti-CNTF antibody in sterile PBS, (100µl per well), covered with Parafilm and incubated at RT, overnight (16 hours). Following 3 washes with PBST (referred to in protocol as "Wash Buffer") wells were blocked with reagent diluent (1% BSA in PBS, pH 7.2. – 7.4, 0.2µm filtered), 300µl per well, incubated for 1.5 hours at RT. Following 3 washes in PBST, 100 µL of sample or standard were added to each well. Plate was set up as indicated as in figure 2.4. The initial CNTF standard solution was diluted with reagent diluent such that the topmost wells (11A and 12A) contained 2000pg/mL, with subsequent solutions being diluted 1:2 serially from 2000pg/ml (11A + 12A) to 31 pg/ml (11G + 12G) in sequential wells. The bottom-most well (H) contained only reagent diluent. Following an initial dilution of sample (see specific figure in results) in the topmost lane, (A1), samples were subsequently serially diluted 1:2 or 1:5 with reagent diluent, with the bottom-most well containing diluent only.

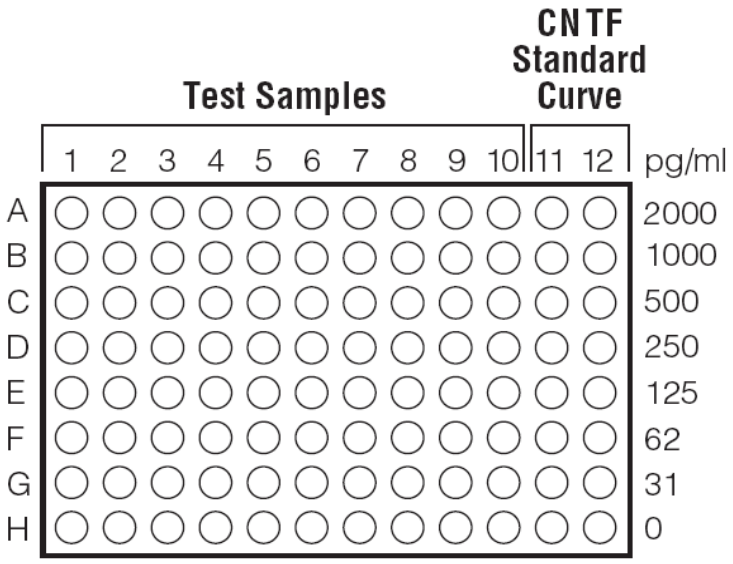

Figure 2.4. CNTF ELISA plate set up. Diagram modified from GDNF Emax instruction manual (Promega)

The plate was then covered with Parafilm and incubated for 2 hours at RT. After 2 washes in PBST, 100µL of detection antibody (biotinylated goat anti-rat CNTF, 200ng/mL, diluted from 36µg/mL in reagent diluent) were added to each well, before the plate was covered in Parafilm and incubated for 2 hours at RT. After 3 washes in PBST, 100µl of Streptavidin-HRP (diluted 1 to 200 from original stock concentration in reagent diluent) were added to each well, the plate covered in Parafilm, and incubated for 20 min at RT. After this 20 minutes 50µl stop solution (2N H_2SO_4) was added to each well, the plate gently agitated, and absorbencies read at 450nm. Using Microsoft Excel, a standard curve of absorbance *vs* CNTF concentration was prepared using the supplied CNTF protein standards. This graph then allowed the correlation of sample absorbencies to relative CNTF levels.

2.7 RNA extraction, cDNA synthesis and polymerase chain reaction

If protein levels are sufficiently small, such that they cannot be detected directly, it is sometimes possible to infer protein expression from the presence of relevant intracellular RNA. RNA encoding a specific protein is normally present only when protein synthesis is to follow. After isolating and removing the RNA from one or more cells, it is then possible to convert each of the single stranded RNA molecules into single stranded complementary DNA (cDNA) using the enzyme Reverse Transcriptase. This is the DNA sequence which would have originally served as the template for the RNA molecule *in vivo*, assuming the RNA sequence would not have undergone post-translational modifications. The single stranded cDNA corresponding to the protein of interest must then be isolated. This is achieved using a technique known as Polymerase Chain Reaction (PCR). After being treated with an enzyme to degrade any remaining RNA, the cDNA mixture is mixed with an excess of primers, which are oligonucleotides specific and complementary to the beginning of the cDNA sequence of interest. These primers attach (anneal) to the beginning of the relevant cDNA molecule via normal base pairings. There are forward and reverse primers, each complementary to and binding at the beginning (3' end) of each single strand. For example, if the entire double stranded DNA sequence were to read "GGCCAATT" on one strand and, correspondingly, "CCGGTTAA" on the other, the forward primer for the first strand would be complementary to "GGCCAATT" so "CCGG...". The primer for the second strand, binding at the 3' end, would be complementary to "CCGGTTAA" but reading in the opposite direction, so this primer, the reverse primer, would read "TTAACCGG" – see figure 2.5 below.

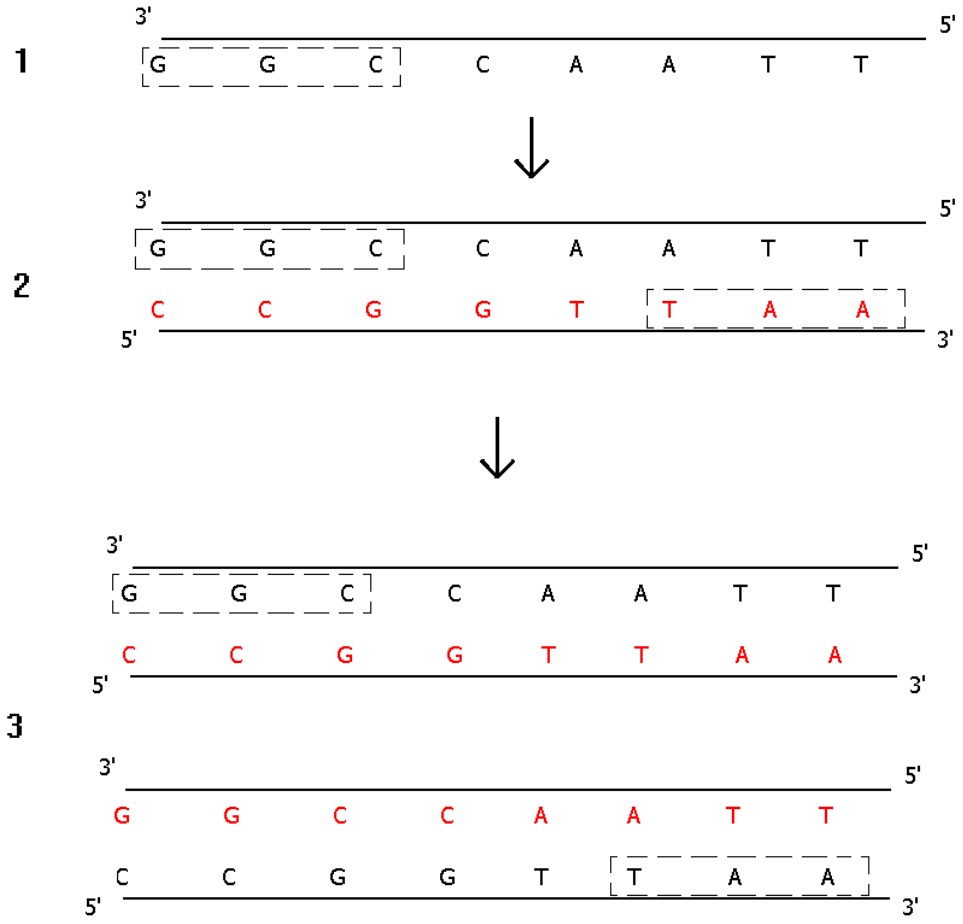

Figure 2.5 cDNA amplification. 1) Primer binds at relevant sequence on cDNA molecule of interest (broken box). 2) Polymerases then incorporate supplied free nucleotides (shown in red), generating the complementary strand. 3) Subsequent cycles of heating, cooling and annealing repeat this process allowing exponential increases in amounts of desired DNA**.**

The enzyme DNA polymerase and an excess of single nucleotides with triphosphate groups (DNA Nucleotide Tri Phosphates - DNTPs) are added. The polymerase catalyses base pairing between the original cDNA strand and the single nucleotides, resulting in the formation of the full length double stranded DNA molecule coding for the appropriate protein. Once the double stranded DNA molecule has been synthesized, the mixture is heated until the DNA denatures into two separate single strands, and then allowed to cool. Each of the two strands then acts as a template for the other, as in normal DNA

replication, and together with the polymerase and free nucleotides, rapidly produce two complete double stranded DNA molecules. Once all the above reagents are mixed together, the heating and cooling steps can be easily automated, allowing dozens of duplications in a single day. The power of exponential growth is such that 15 cycles will turn one strand of DNA into 16,000. Using PCR it is thus possible to take tiny samples of DNA and quickly produce samples large enough to analyse with other techniques, such as gel electrophoresis. DNA (or RNA) samples are electrophoresed through a gel of appropriate material and density, commonly 0.7-1% agarose. The buffer used will contain a reporter compound such as ethidium bromide, which will intercalate between the bases of nucleic acid and function as a fluorescent marker, emitting visible light which is excited by ultraviolet radiation.

2.7.1 Specific protocol for RNA extraction

All reagents and protocols used were supplied with the RNAeasy kit (Qiagen Crawley, UK). Primary retinal cultures, consisting of 1.5 x10^6 cells plated onto small petri dishes, were drained of media and washed once with PBS. Cultures had PBS removed, 1ml 0.1% trypsin added and, after gentle manual shaking, were incubated at 37°C for 5 min. 1 ml of media was added (to neutralise trypsin) and the cell suspension was centrifuged at 300g for 5 min in supplied 1.5ml sample tube. The supernatant was discarded and 600µl of supplied RLT buffer were added (to disrupt cells) and the mixture was vortexed. Following 30 seconds homogenization by a rotoshredder at medium speed, 600µl of 70% ethanol was added to the cell suspension and the resulting solution was mixed well by pipette. 700µl of solution were added to RNAeasy spin columns, set inside sterile 2ml

collection tubes and spun at 8000g for 15 seconds. After discarding flow through, 700µl of supplied RW1 buffer was added to spin column, and column + 2 ml collection tube were centrifuged at 8000g for 15 seconds. Flow through was discarded and column + tube were centrifuged at 8000g for 2 minutes. Spin column was placed within a new, sterile 2ml collection tube and 50µl of RNAse free H_2O pippetted carefully onto centre of spin column. Following a final 2 minute centrifugation at 8000g, the resulting RNA-H_2O solution was stored in a sealed, sterile, RNAase free 2 ml Eppendorf at -80°C. Prior to freezing, 1-2µl of RNA solution were removed and assayed for concentration using a NanoDrop machine (Thermo Scientific, DE, USA).

2.7.2 Specific protocol for cDNA synthesis and PCR

cDNA was synthesized using the reagents and protocol from a High Capacity cDNA Reverse Transcription kit (Applied Biosystems, CA, USA). The following reagents were added to a sterile, RNAse free PCR tube and mixed well: 3.2µl of 10 x supplied RT Buffer, 0.8µl dntps (free nucleotide-bases), 2µl primers (1 µl forward, 1µl reverse), 1µl Reverse Transcriptase, 1µl RNAse inhibitor and 24µl RNA. After centrifugation to ensure no liquid remained in the PCR tube cap, the tube was placed in a thermal cycler and a reverse transcription program run. Following testing for concentration on a Nanodrop machine, cDNA was stored in a sealed PCR tube at -80°C. Each 40µl PCR reaction mixture consisted of 2µl forward and 2µl reverse primers, 18µl cDNA and 18µl ReddyMix PCR multimix (Thermo Scientific, DE, USA), a mixture containing all enzymes and nucleotides required. A PCR tube containing each reaction mixture was placed in the thermal cycler and the default PCR program run (96^{o}C for 30 sec, 50^{o}C for 30 sec, 72^{o}C for 45 sec, 30 repetitions).

In order to visualise PCR products, PCR tube contents underwent gel electrophoresis (0.7% agarose gel in Tris/Borate/EDTA (TBE) buffer, with 10mg/mL Ethidium Bromide) for 30 minutes at 50v. Gels were photographed with a Multigenius machine (Geneflow, Fradly, UK). For tissue control, rat brain lysate was used and primers for the house keeping gene GAPdh were also used to confirm that RNA extraction, cDNA synthesis and subsequent PCR had been successfully performed. NTF primer sequences were as follows.

(F=Forward, R= Reverse)

BDNF-F: AGA GTG ATG ACC ATC CTT TTC

BDNF-R: CTA TCT TCC CCT TTT AAT GGT

CNTF-F: TAG GGG ATG GCT TTC GCA GAG

CNTF-R: CTA CAT CTG CTT ATC TTT GGC

NGF-F: ATG TCC ATG TTG TTC TAC ACT

NGF-R: TCA GCC TCT TCT TGC AGC CTT

NT3-F: ATG TCC ATC TTG TTT TAT GTG

NT3-R: TCA TGT TCT TCC GAT TTT TCT

NT4-F: ATG CTC CCT CGC CAC TCC TGC

NT4-R: TCA GGC ACG GCC TGT TCG GCT

Chapter 3

The cellular distribution of pEGFR in the retina and optic nerve

3.0 Introduction

3.1 The Epidermal Growth Factor Receptor

While the NgR and the PTP receptors for myelin derived proteins and CSPG respectively were elucidated by identifying the ligands and then searching for relevant receptors, the EGFR was well characterised and had been studied extensively in, for example, cancer research, for decades prior to its currently implied role in CNS regenerative failure. The 170KD EGFR/ErbB-1 (Figure 3.1) is a member of the ERb family of receptors, a sub-family of the receptor tyrosine kinase super family of receptors, the functioning of which require the phosphorylation of specific sites on their intracellular domains.

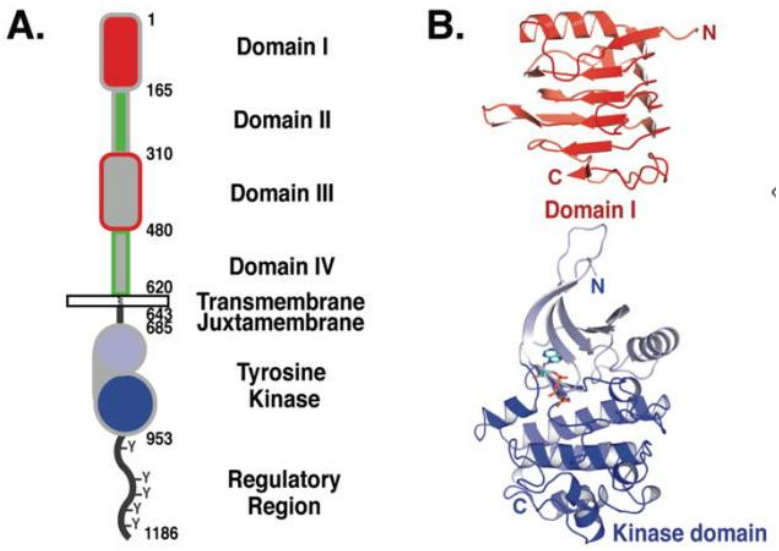

Figure 3.1. The Epidermal Growth Factor Receptor (monomer).
A. Diagrammatical representation showing all domains and regions.
B. Alternative, ribbon-like diagram of EGFR structure. Adapted from Ferguson, 2008.

The 4 known members of the ERB family are Erb-B-1 (EGFR), Erb-B-2, Erb-B-3 and Erb-B-4. To date 7 EGFR-specific ligands have been identified: EGF, Transforming Growth Factor (TGF) – α, Heparin-Binding EGF-like-factor (HP-EGF), betacellulin, amphiregulin, epiregulin, and epigen (Wells, 1999). EGFR activation promotes cell survival, mitosis and migration, although it is also associated with apoptosis and cytoskeletal reorganization (Bazley and Gullick 2005, Oda *et al.* 2005, Appleton *et al.* 2010). When activated by ligand, EGFR dimerises and undergoes autosphosphorylation , i.e. each monomer phosphorylates the tyrosine kinase domains of the other, before being internalized in clathrin-coated vesicles. The mechanisms underlying EGFR activation and signaling are complex and the EGFR signaling network is vast; a paper entitled "A comprehensive pathway map of epidermal growth factor receptor signaling" (Oda *et al.* 2005) lists several hundred species and interactions as well as 6 distinct G-protein-coupled transactivatory-pathways. The huge variety in ligand dependent signaling pathways stems from three main sources. Firstly, EGFR can form heterodimers with each of the other ErbB family members (Shankaran *et al.* 2006). Secondly, following activation and internalization, the fate of the receptor-ligand complex is determined by both the ligand and by the nature of the receptor hetero/homodimer. Thirdly, this specific species of receptor-ligand complex determines which of the numerous intracellular signaling proteins are interacted with, which determines the downstream signaling partners and, ultimately, the final intracellular effect, e.g. activation of transcription factors, effecting Ca^{2+} realease, initiating the cell cycle etc. (Jorissen *et al.* 2003, Oda *et al.* 2005). The intracellular portion of the EGFR has three main signaling domains. The first, juxtamembraneous, domain provides an activation site for protein kinase C (PKC), the second, central tyrosine kinase domain, contains the SH1 domain which is required for transphosphorylation of the 6

tyrosine residues in the carboxy terminal and the third, the carboxy terminal tail, contains the SH2 domain, with the tyrosine residues required for docking of adaptor/effector proteins such as SHC, Grb 2 or Phospholipase C-γ, which then link the EGFR to a variety of signaling pathways. The second of the three, the central tyrosine domain, also contains the signaling motifs required for receptor internalization and degradation.

Following internalization and the initial interaction with intracellular adaptor/effector proteins, either the entire EGFR-ligand complex is directed to lyzosomes for degradation, or the ligand and receptor dissociate within early endosomes, the receptor being recycled to the cell surface whilst the ligand is lysosomally degraded (Wiley,2003, Shankaran *et al.* 2006,Jorrisen *et al.* 2003). Figure 3.2 shows the dimerisation and conformational changes which take place when an inactive EGFR monomer is activated by EGF.

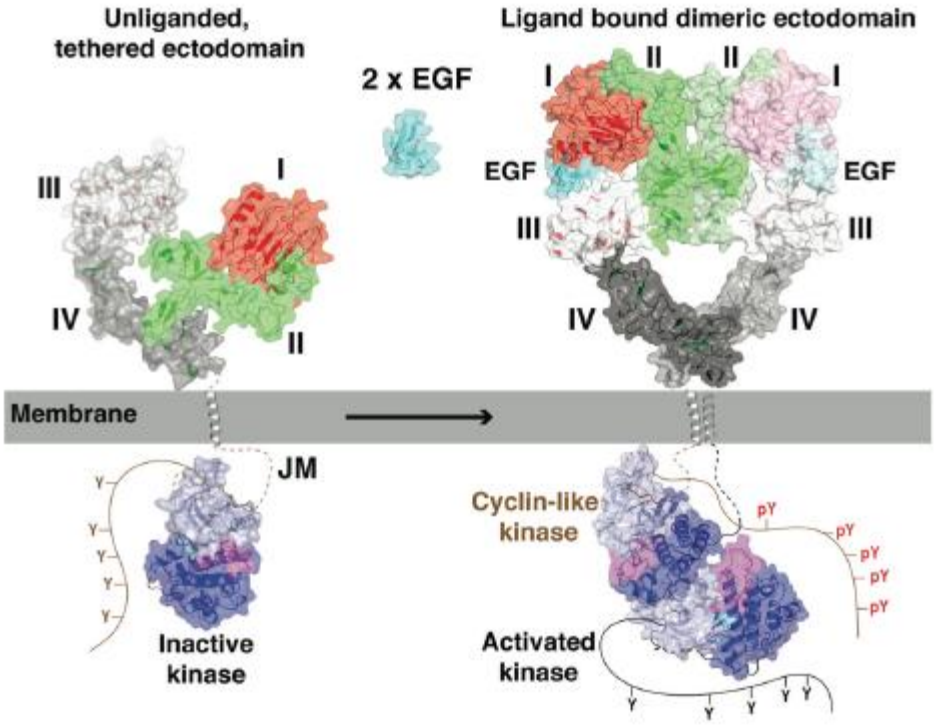

Figure 3.2. Non activated and activated EGFR. Inactive, non phosphorylated monomeric EGFR (left) binds EGF and dimerises (right) causing the tyrosine kinase domains on each EGFR monomer to autophosphorylate its partner. Adapted from Ferguson 2008.

In addition to ligand binding, EGFR can also be transactivated, that is activated intramembraneously or intracellularly, by non ErbB receptors and/or other signalling intermediaries. Known transactivators of EGFR include the integrins (Yamada and Even-Ram 2002, Cabodi *et al.* 2004), rapamycin (Chaturvedi *et al.* 2009), fibrinogen (Schachtrup *et al.* 2005), and G-protein coupled receptors (Rosengurt 2007,Oda *et al.* 2005). Most commonly the signaling mechanisms by which EGFR is transactivated involve Ca^{2+} influx, PLC-γ activation or PKC activation, often as downstream consequences of ligand binding to non-ErbB-family receptors such as GPCR (Gschwind *et al.* 2001, Rosengurt 2007).

EGFR can be transactivated in the absence of ligand binding by co-clustering with other receptors that sequester adaptor/effector proteins which then bind to and initiate

phosphorylation of the tyrosine kinase domains of EGFR (Gschwind *et al.* 2002, Cabodi *et al.* 2004). Reported interactions include the integrin receptors (Cabodi *et al.* 2004) and members of the cadherin family (Andl and Rustgi 2005). See figure 3.3 for diagram.

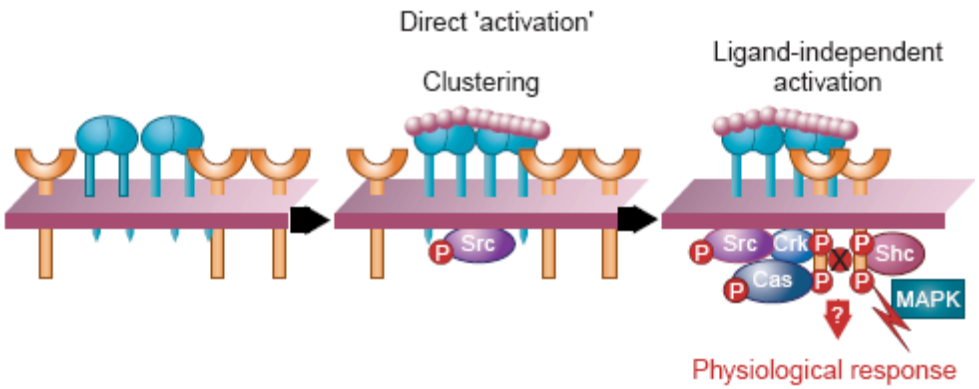

Figure3.3. Non ErbB receptors (Blue) clustered near EGFR (orange) sequester adaptor\effector proteins including Src and Shc which transphosphorylate and thus activate the adjacent EGFR. Adapted from Yamada and Even-Ram, 2002.

EGFR can also be transactivated following the shedding of membrane bound pro- forms of EGFR ligands which activate the EGFR in an autocrine manner (Higashiyama *et al.* 2008, Schneider and Wolf 2009). This EGFR ligand shedding is mediated by the ADAM (A Disintegrin And Metalloprotease) family of metalloproteases including ADAM 17, also known as TACE (Tumour necrosis factor-α Converting Enzyme) (Higashiyama *et al.* 2008, Schneider and Wolf 2009). At least two EGFR ligands, epigen and amphiregulin, have been shown to be released from the membrane in an ADAM-dependent manner (Sahin and Blobel 2007, Kasina *et al.* 2009, respectively).

The ADAM-mediated EGFR ligand shedding which leads to EGFR transactivation is often initiated by the binding and internalization of ligand to a receptor such as a GPCR. This “outside-inside -outside” signaling cascade has been termed “triple-membrane-passing-signalling” and is illustrated in figure 3.4.

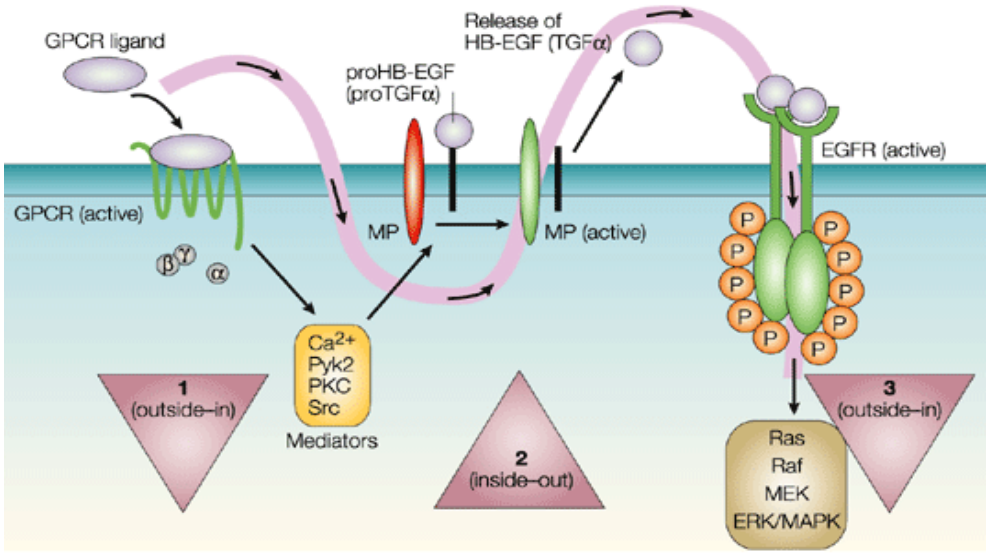

Figure 3.4. The "triple-membrane-passing-signalling" model of EGFR transactivation. Ligand binding to receptor (which does not have to be a GPCR) initiates the recruitment of intracellular second messengers, including Ca^{2+}, proteins such as Src and PKC (1) This results in the activation of one or more of the ADAM family of metalloproteases, which cleave membrane bound pro- forms of EGFR ligands, resulting in the release of the mature protein which can act juxtacrinally, paracrinally, or, as shown, autocrinally (2) to activate EGFR in the normal manner (3) Adapted from Wetzker and Boëmer 2003.

Although the term transactivation is taken to mean "the activation of a receptor by any means other than direct ligand binding", there is a final means of EGFR transactivation which is transactivation in the truest sense. In this model (figure 3.5) GPCR sequester adaptor/effector proteins such as Src and cause them to be recruited to the cytoplasmic domain of nearby EGFR, phosphorylating the tyrosine residues responsible for EGFR activation and subsequent downstream signaling (Wetzker and Boëhmer 2003, Keely *et al.* 2000). In this case there is no vertical transfer of signal through the EGFR at all and potentially even EGFR lacking an extracellular domain could be activated in this way.

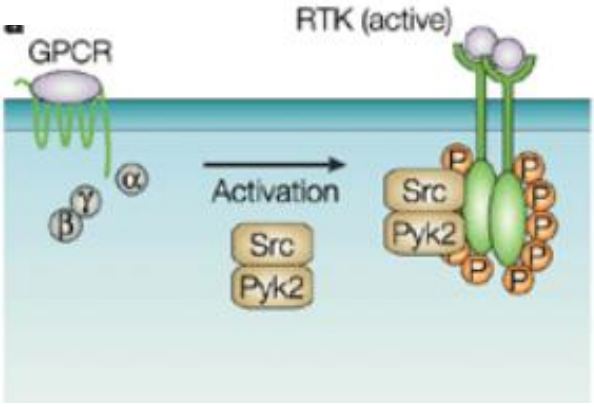

Figure 3.5. The recruitment of SRC proteins by GPCR adjacent to EGFR result in the phosphorylation of tyrosine residues responsible for EGFR activation. Adapted from Wetzker and Boëmer 2003.

While many of the aforementioned phenomena which make up the huge EGFR activation and signalling network are not specific to neurons (mitogenic signalling pathways for example), there have been several studies concerned purely with the distribution and function of neuronal EGFR, including studies of EGFR distribution in the mammalian CNS (Erschbamer *et al.* 2007, see Wong and Guilliaud 2004 for review) and more specifically within the visual system (Liu *et al.* 2006, Chen *et al.* 2007).

As the EGFRki mediated axon-regeneration reported by Koprivica *et al.*(2005) was obtained using a visual system *in vivo* model, and as many of their corroborative *in vitro* results were gleaned from retinal cultures, the visual system is probably the most relevant area of the CNS for examining the role of neuronal EGFR.

EGFR plays a critical role in much of the developing visual system; EGF and TGF-α each cause retinal progenitor cells to generate neurons and glia (Anchan *et al.* 1991), heparin binding EGF-like growth factor (hb-EGF) causes mitosis in both astrocytic and multipotent progenitor cells (Kornblum 1999), and EGFR signalling is required for the differentiation of many post mitotic neurons and glia from pluripotent precursors (Lillien

1995). In the normal adult mammalian retina EGFR is largely absent from glia (Gomez-pinilla et al., 1988, Chen *et al.* 2007, Liu *et al.* 2006) but is present on a variety of retinal neurons (Kramer *et al.* 2001) including RGC and amacrine cells (Chen *et al.* 2007). EGFR ligands are spread throughout the adult retina, including TGF-α in the processes of Müller glia (Kramer *et al.* 2001), RGC and in amacrine cells (Chen *et al.* 2007) and EGF in RGC (Kramer *et al.* 2001, Chen *et al.* 2007) and in horizontal cells (Chen *et al.* 2007). EGFR has been suggested to play a role in RGC physiological homeostasis and possibly even in assisting the processing of visual information (Chen *et al.* 2007), but most studies on neuronal EGFR have concluded that the EGFR signalling impinges on neurons via glia, primarily astrocytes (Liu *et al.* 2006, Yamada *et al.*1997, Wagner *et al.* 2006, Liu and Neufeld 2007), but in the retina, also *via* Müller glia (Bringmann et al. 2009). Each of these studies concerned with the neuronal effects of glial EGFR signalling has concluded that this signalling is usually to the detriment of nearby neurons, primarily because neither astrocytes nor Müller glia express significant levels of EGFR prior to CNS insult/pathology whereupon EGFR is strongly upregulated and activated (Liu and Neufeld 2003, Liu *et al.* 2006, Jin *et al.* 2002). Thus retinal glial EGFR is associated with, and perhaps necessary for, astrogliosis and Müller gliosis, processes known to be strongly antagonistic to axonal regeneration and potentially potently neurotoxic (for review see Berry *et al.* 2008).

It has previously been shown in ONC models that retinal and ON pEGFR levels are significantly lower in those animals with regenerating ON than in those of non-regenerating ON (Ahmed *et al.* 2006). While this study confirmed pEGFR reduction via western blot, correlated with GAP-43 staining of ON sections to confirm regeneration, the actual cellular distribution of pEGFR was not investigated. Hence, although it was

confirmed that pEGFR levels were modulated by injury and subsequent surgical intervention, it was not confirmed whether neurons, axons, glia or all three were the predominant source of pEGFR. At the time of writing it does not appear that any paper has published definitive proof of axonal pEGFR or even EGFR, anywhere in the adult CNS. Schachtrup *et al.* (2007) immunostained spinal cord sections for pEGFR and obtained what appeared to be axonal staining, but did not perform coimmunostaining using any axonal marker so it is possible that this pEGFR is in fact on the processes of glia such as oligodendrocytes or astrocytes.

In an attempt to further investigate this novel association between well characterised receptor and CNS regenerative failure, it was decided to immunohistochemically examine the distribution of pEGFR, the activated form of EGFR, in the rat visual system, with particular emphasis on axonal pEGFR. The decision to study distribution of the activated from alone was based on both the proposed necessity of EGFR phosphorylation for axonal growth antagonism, and the existence of at least one previous paper investigating (non-activated) EGFR distribution within the rodent visual system (Liu *et al.* 2006). The rat visual system itself was chosen due to its relative simple cytoarchitecture, ease of access for surgical procedures, and, crucially, because many of the results obtained by Koprivica *et al.* (2005) were obtained from rat retinal cultures and the rodent ONC *in vivo* model. Similarly, all treatment group animals were to be killed at 14 days post injury, as this was the timepoint used by that group.

If EGFR activation is in fact critical for axonal growth cone collapse, then axons regenerating into or beyond a CNS lesion would be expected to have lower levels of activated EGFR (pEGFR) compared to non regenerating axons, or possibly no pEGFR at all.

Additionally, many previous studies have reported glial EGFR to be nearly absent in the uninjured visual system but to be strong upregulated following CNS injury.

3.1.2 Specific Aims

- To confirm immunohistochemically that regenerating RGC axons exhibit reduced pEGFR levels compared to non regenerating RGC axons

- To determine the distribution of pEGFR in neurons, axons and glia in uninjured, regenerating and non regenerating retinae and ON

3.1.3 Specific Hypotheses

1) Levels of RGC axonal pEGFR will increase after injury and regenerating axons within ON and retinae will exhibit attenuated pEGFR levels compared to non regenerating axons

2) Glia in uninjured ON and retinae will express little if any pEGFR, but following injury, glia will become strongly $pEGFR^{+}$

3.2 Results

3.2.1 Antibody to pEGFR was specific and detected a protein of the correct weight

Figure 3.6 shows the results of immunostaining for pEGFR using the goat polyclonal anti-pEGFR antibody SC-12351 at a concentration of 4µg/ml with (A) and without (B) 80µg/ml blocking peptide. This was performed on consecutive 15µm sections of uninjured rat retina, using a standard IHC protocol (described in materials and methods section) and produced clear and specific staining, whilst sc12351+ blocking peptide yielded no staining.

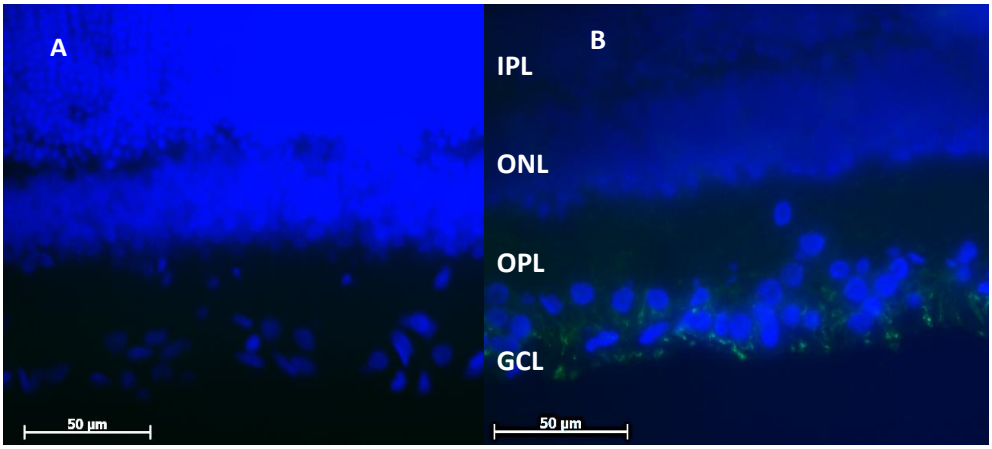

Figure 3.6. Consecutive 15µm sections of uninjured rat retina, stained with 4µg/ml Goat anti pEGFR antibody (sc12351, green staining) with (A) and without (B) 80µg/ml blocking peptide. Complete absence of staining in the presence of blocking peptide confirmed antibody specificity.

Antibody specificity was further confirmed by SDS-PAGE and Western blot on retinal lysates (Figure 3.7). Lysates consisted of homogenized retinae from animals which had undergone ONC 14 days prior to death. A clear protein band was obtained at the correct weight of ~170kDa.

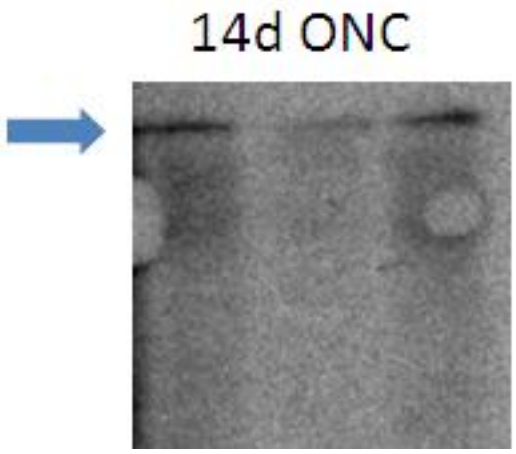

Figure 3.7. Western blot confirmed specificity of antibody SC12351. 3 Retinal lysates from 14dpi ONC animals were subjected to SDS-PAGE and Western blotting, using polyclonal anti pEGFR Antibody SC-12351. A clear band was obtained from all lysates at the predicted weight of 170kDa (arrow).

3.2.2 RGC axons in the optic nerve did not contain pEGFR

Figure 3.8 shows double immunohistochemical staining for pEGFR and the cytoskeletal protein Neurofilament 200 (NF), an axonal marker, on 15µm thick uninjured control, post injury non-regenerating (NRM), and post injury regenerating (RM) rat optic nerve sections. pEGFR was found not to colocalise with NF in any experimental or control group, neither constitutively nor post injury, in any part on the optic nerve. This strongly suggests that all axons in the rat optic nerve are $pEGFR^{-}$. Confocal microscopy (Figure 3.9) confirms this absence of axonal pEGFR.

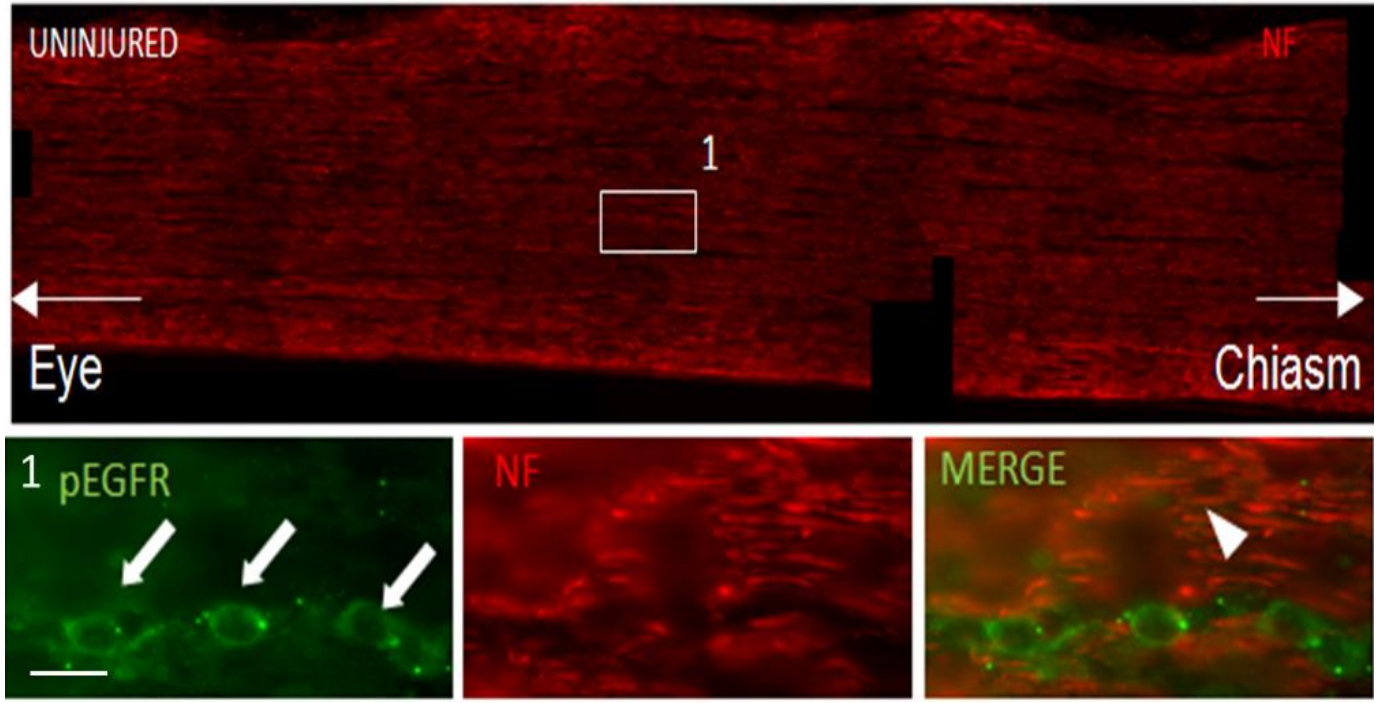
UNINJURED
NF
1
Eye
Chiasm
1 pEGFR
NF
MERGE

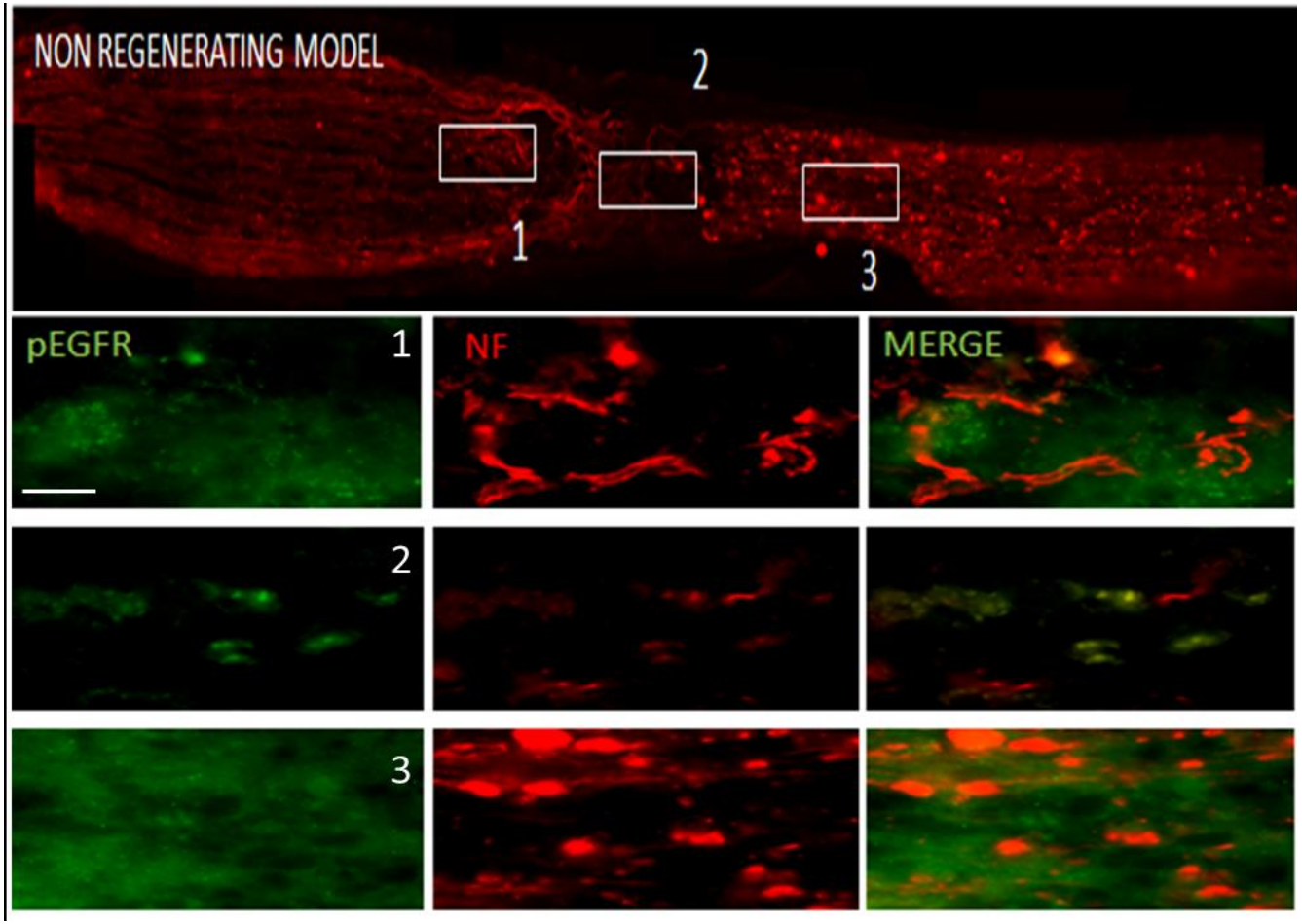
NON REGENERATING MODEL
2
1
3
pEGFR
1
NF
MERGE
2
3

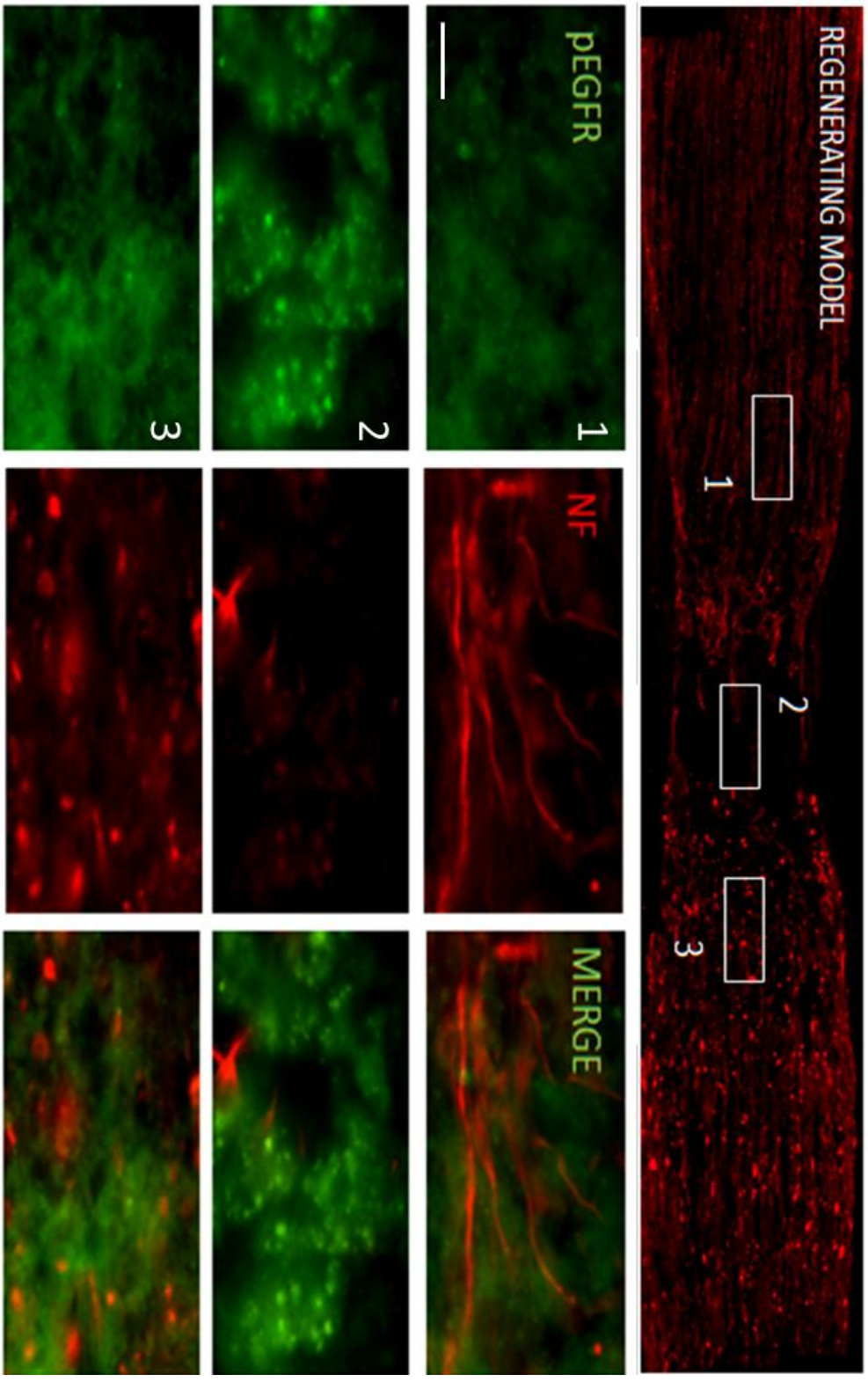

Figure 3.8 Axons did not contain pEGFR. First panel: Uninjured control ON. The boxed region (1) is reproduced at high power to show that NF $^{+}$ axons (arrow head) were not pEGFR^{+} (green). Note rows of pEGFR^{+} glia (arrows). Similarly, boxed regions within NRM and RM (second and third panels respectively) show in high power that NF^{+} axonal debris (red) was also pEGFR^{-}. (NRM – non regenerating model, RM – regenerating model, NF – Neurofilament 200, axonal marker).

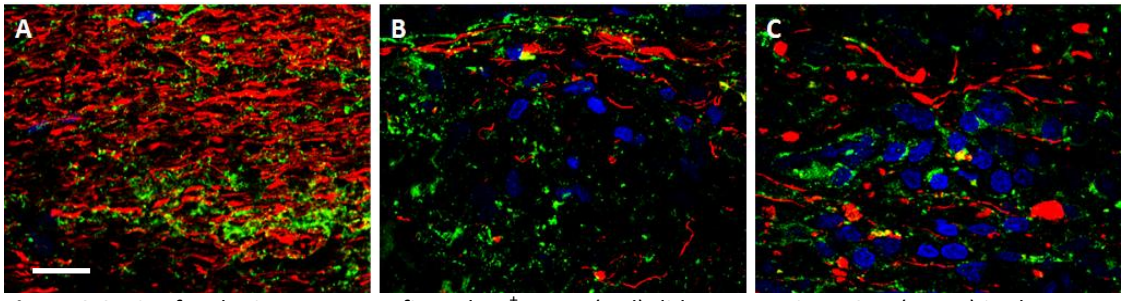

Figure 3.9. Confocal microscopy confirmed NF^+ axons (red) did not contain pEGFR (green) in the uninjured (A), NRM (B), RM (C) groups. Images were taken at proximal boundary of lesion site (B, C) or equivalent area of uninjured nerve (A). Scale bar = 10µm. DAPI stained nuclei are blue.

3.2.3 Astrocytes in the optic nerve were constitutively $pEGFR^+$, and levels of pEGFR along with GFAP, increased after injury

Figures 3.10 and 3.11 show immunohistochemical staining for the astrocyte marker GFAP (red) and pEGFR (green). Colocalisation of GFAP/pEGFR staining (orange/yellow) can be observed in uninjured, non regenerating and regenerating groups, indicating $pEGFR^+$ astrocytes. Note increase in both pEGFR and GFAP staining in all post injury images. Post injury astrocyte hypertrophy and upregulated GFAP are consistent with the reactive astrogliosis known to occur following CNS injury.

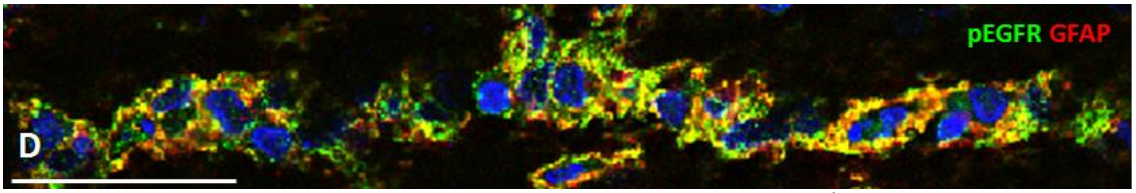

Figure 3.10. Confocal imagery confirms that astrocytes were strongly $pEGFR^+$ after ONC (NRM shown). pEGFR (green) and GFAP (red) colocalised extensively in these astrocytic cells and processes. DAPI stained nuclei are blue. Scale bar = 50µm

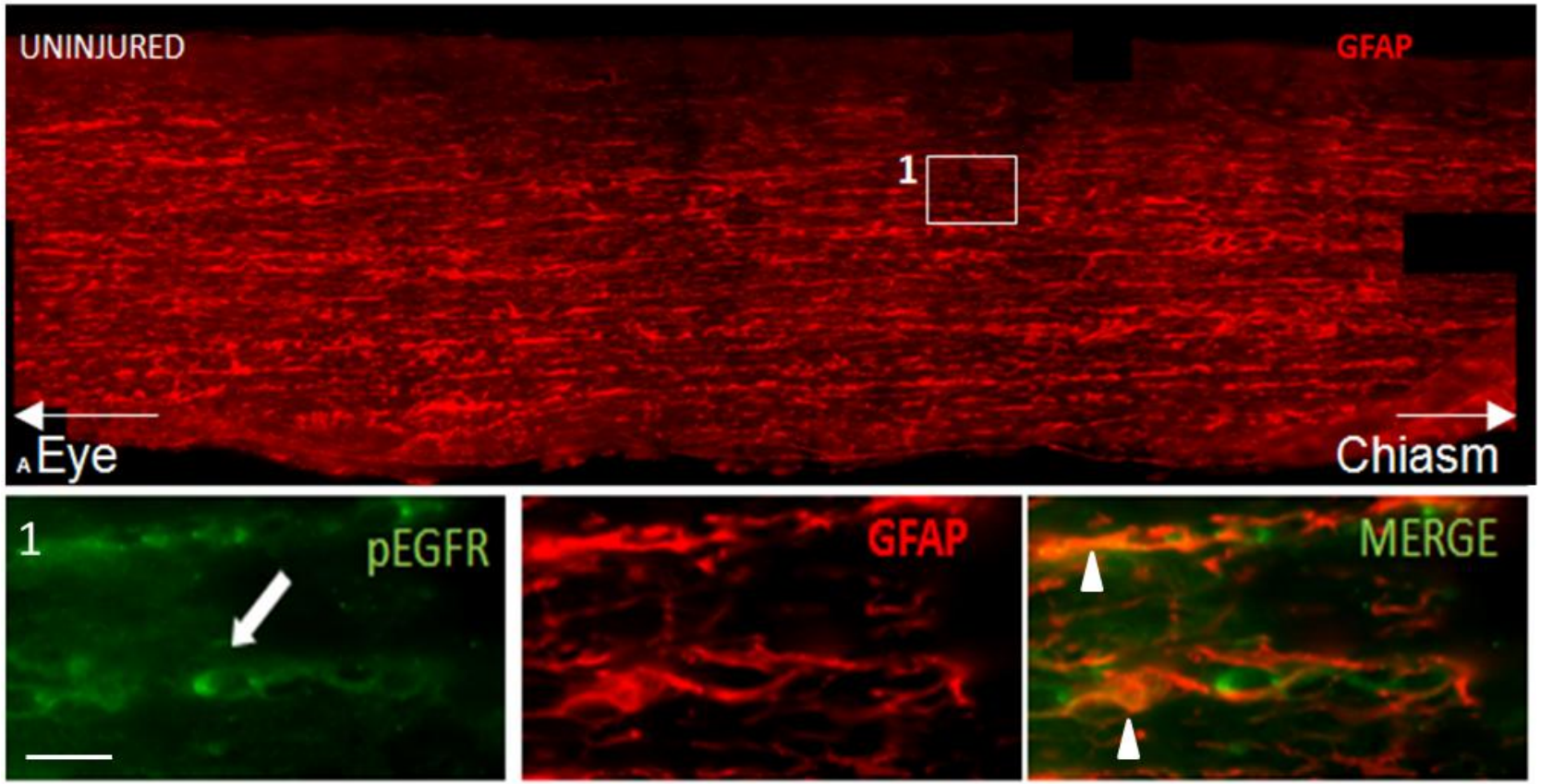
UNINJURED
GFAP
1
A Eye
Chiasm
1
pEGFR
GFAP
MERGE

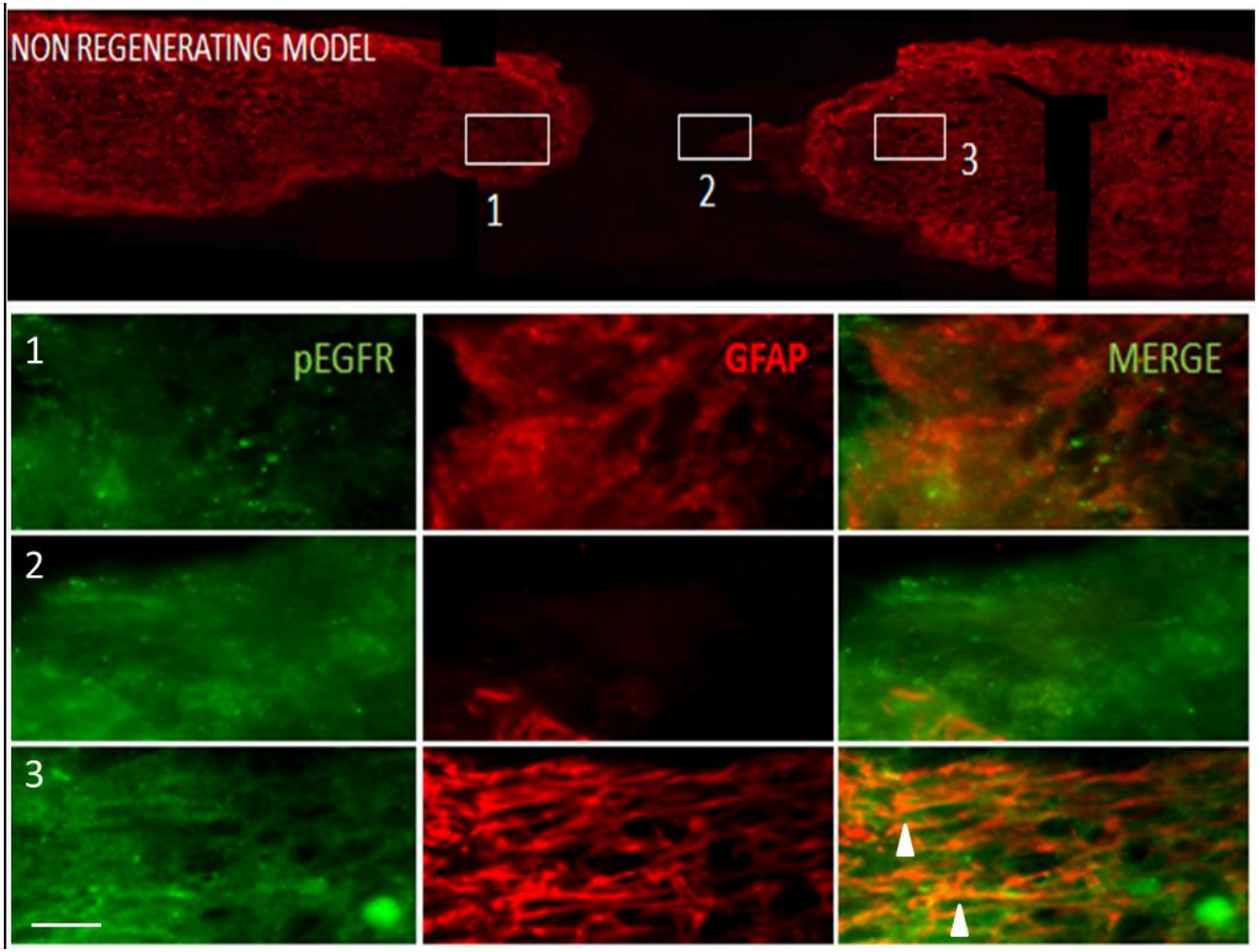
NON REGENERATING MODEL
1
2
3
1
pEGFR
GFAP
MERGE
2
3

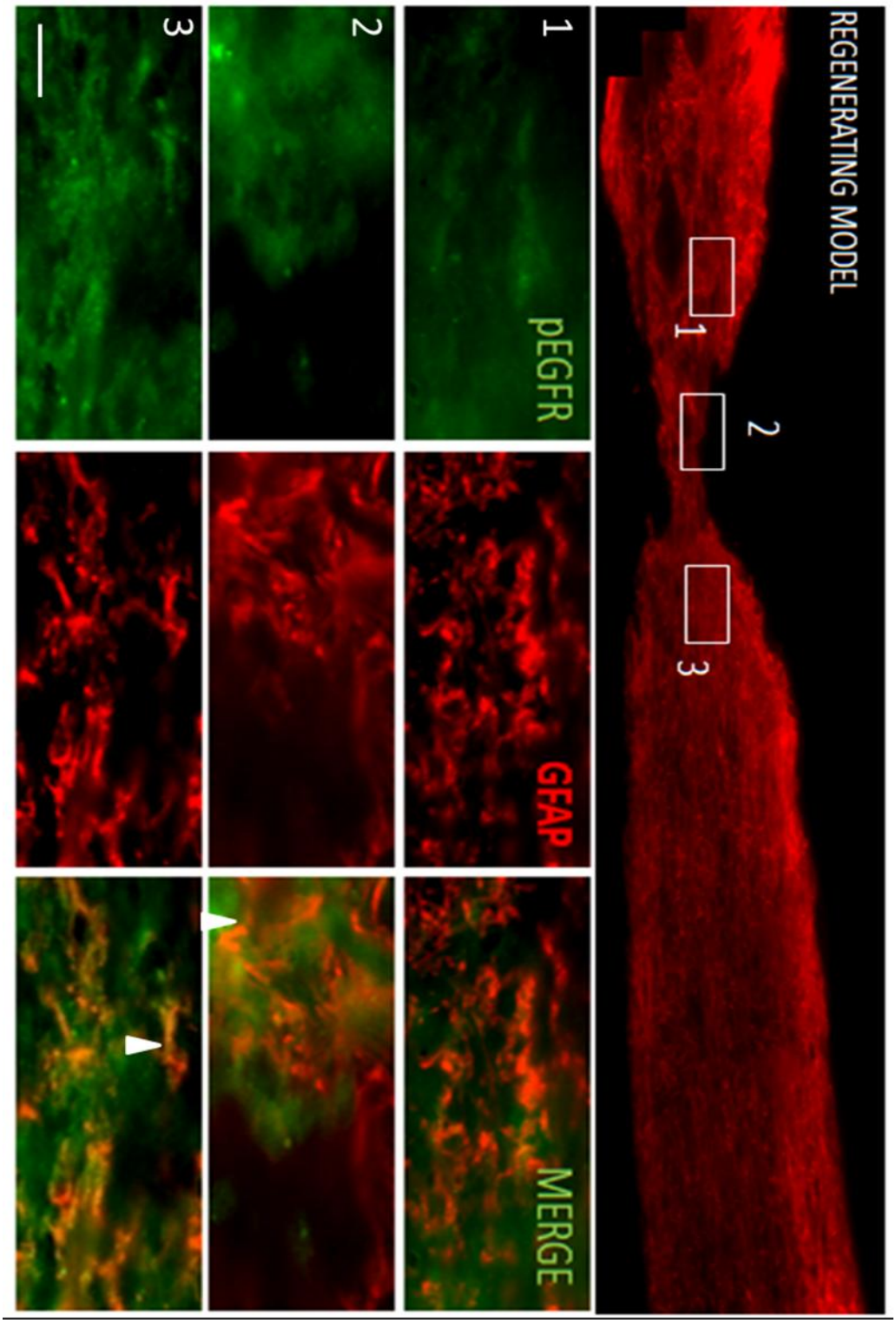

Figure 3.11. GFAP^{+} astrocytes showed higher pEGFR levels after injury. First panel: Representative image of an uninjured control ON (top). The boxed region (1) is reproduced at high power to show GFAP^{+} (red) and pEGFR^{+} (green) astrocytes in the longitudinal rows of ON glia. Second and third panels: NRM and RM in which boxed regions proximal (1) and distal (3) to the lesion show high power views of reactive astrocytes with upregulated GFAP co-localising with increased levels pEGFR (yellow-orange, arrowheads). (NRM – non regenerating model, RM – regenerating model, GFAP - astrocytic marker).

3.2.4 Oligodendrocytes in the optic nerve were constitutively pEGFR$^+$ but levels did not appear to increase after injury

Figures 3.12 and 3.13 show immunohistochemical staining for the oligodendrocyte marker Carbonic Anhydrase II (CAII) (red) and pEGFR (green). Colocalisation (orange/yellow) can be observed in uninjured, non regenerating and regenerating groups. No increase in oligodendrocytic pEGFR staining was observed after injury. Lesion sites were devoid of oligodendrocytes and the faintly CAII$^+$ and pEGFR$^+$ cells observed there were later shown to be phagocytic haematogeneous macrophages which had consumed both antigens. The large scale degeneration of the distal stump, subsequent flooding of the area with previously-contained CAII, and the apparent death of many oligodendrocytes made identifying individual oligodendrocytes more difficult but enough were observed to confirm that while many oligodendrocytes were pEGFR+, pEGFR levels did not seem to have increased.

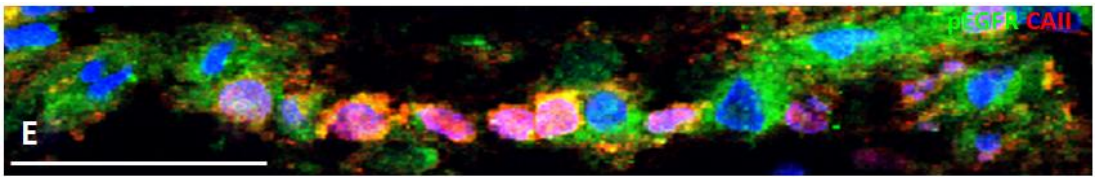

Figure 3.12. Confocal imagery confirmed that oligodendrocytes were strongly pEGFR$^+$ after ONC (NRM shown). pEGFR (green) and CA-II (red) colocalised extensively in ON oligodendrocytes. DAPI stained nuclei are blue. Scale bar = 50µm

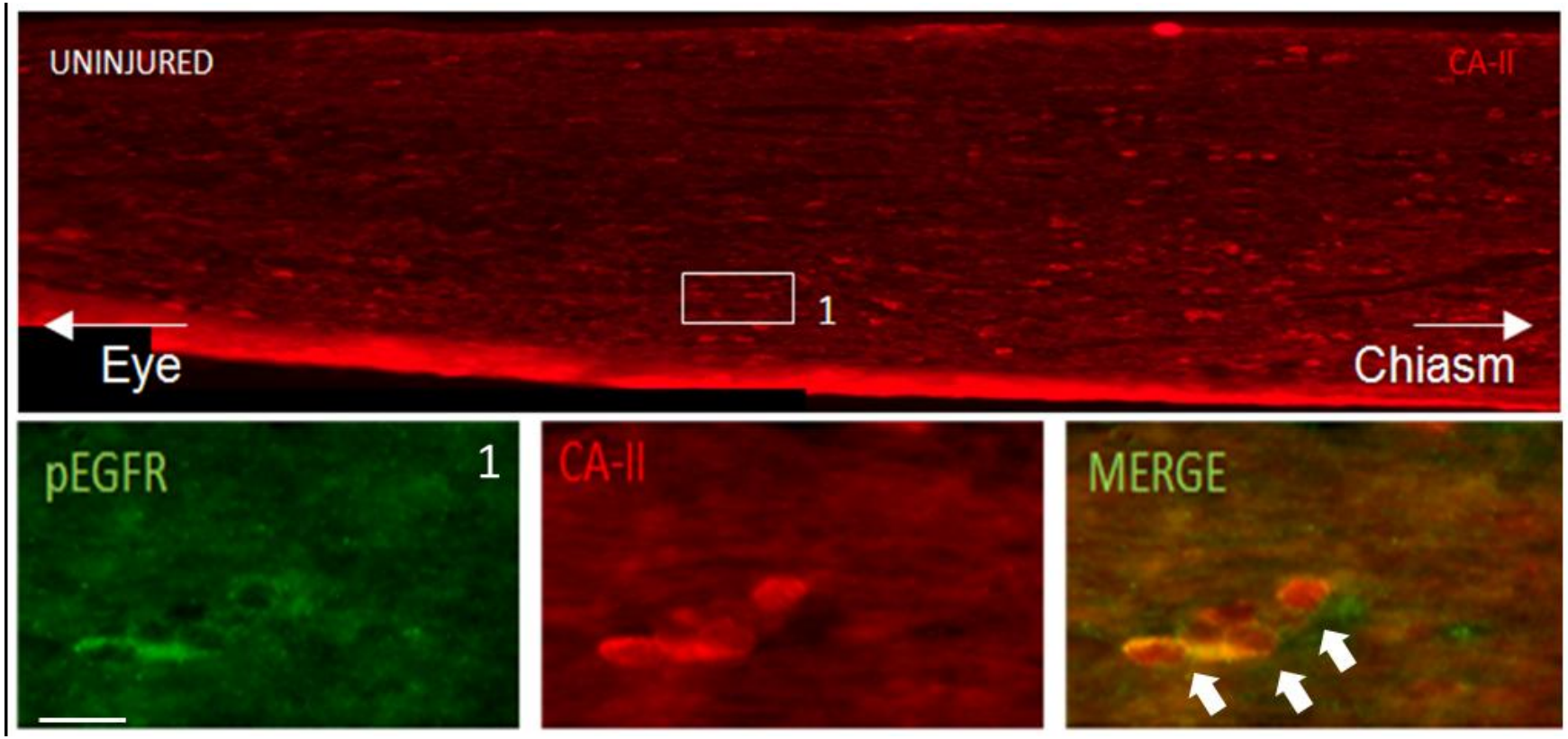
UNINJURED
CA-II
1
Eye
Chiasm
pEGFR
1
CA-II
MERGE

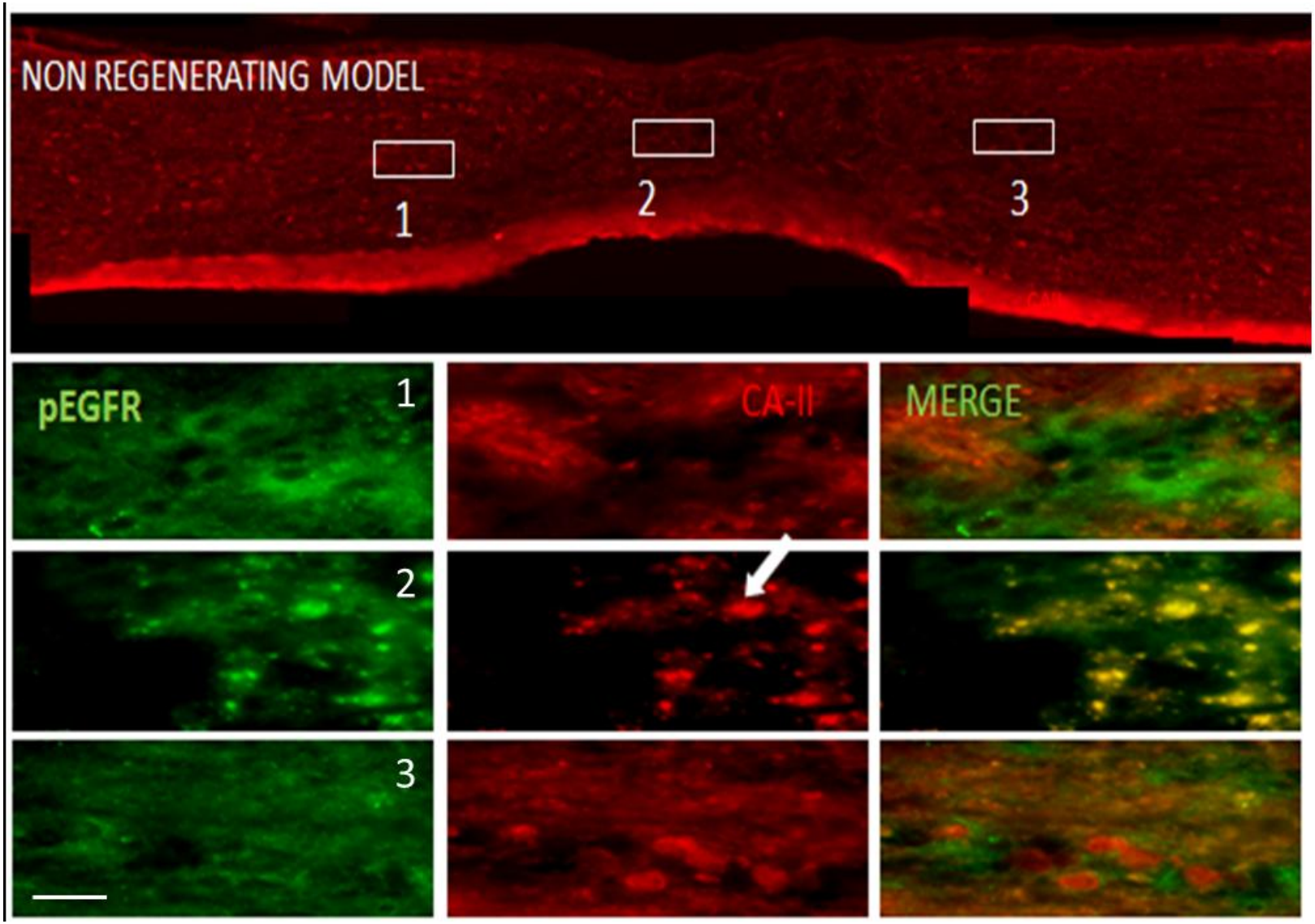
NON REGENERATING MODEL
1
2
3
pEGFR
1
CA-II
MERGE
2
3

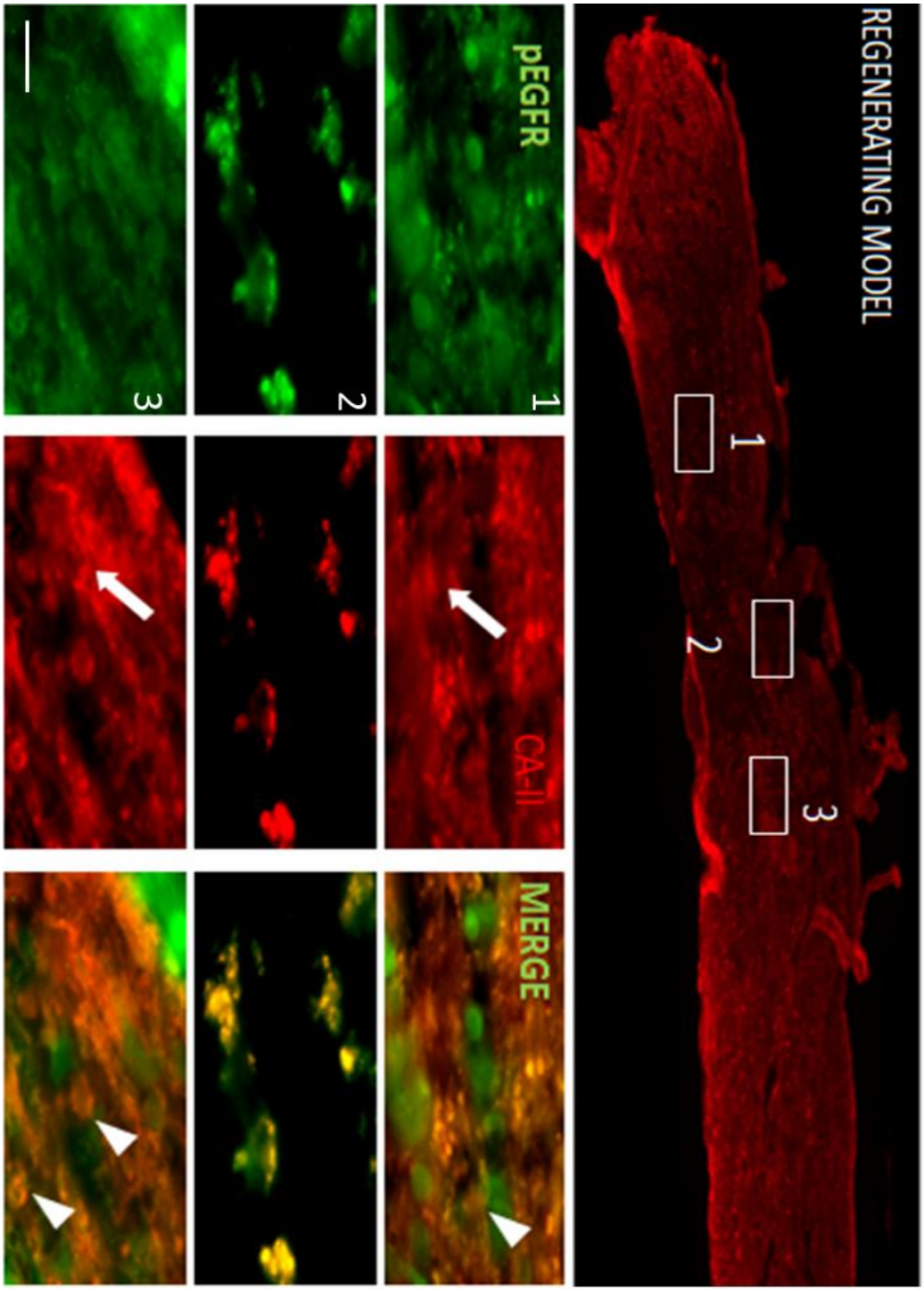

Figure 3.13. Oligodendrocytes were pEGFR^{+}. First panel: Representative image of an uninjured control ON. The boxed region (1) is reproduced at high power to show CAII^{+} (red) oligodendrocytes which are constitutively pEGFR+ (green) visible as longitudinal lines of ON glia (arrows). Second and third panels respectively show NRM and RM ON. There is no discernable increase in pEGFR levels in oligodendrocytes (arrowheads) in NRM and RM proximal (1) and distal (3) to the lesion. The lesion (2) was devoid of oligodendrocytes but contained pEGFR^{+} haematogenous macrophages (arrows). (NRM – non regenerating model, RM – regenerating model, CA-II – Carbonic Anhydrase II, oligodendrocytic marker).

3.2.5. Quiescent microglia in the optic nerve were constitutively weakly pEGFR^{+} or were pEGFR^{-} but levels increased significantly upon microglial activation

Figure 3.14 shows immunohistochemical staining for the microglial marker OX42 (red) and pEGFR (green). In the uninjured optic nerve, microglia were either very weakly pEGFR^{+} or were pEGFR^{-} and were spindle shaped and uniformly distributed. After injury (NRM, RM) microglia became activated, assuming a rounded, macrophage like phenotype and became strongly pEGFR^{+}. Although activated microglia are phagocytic, and thus could potentially become pEGFR^{+} by consuming cellular debris, much of the pEGFR staining is juxtamembraneous, and not just contained within vesicles, suggesting membrane bound pEGFR. pEGFR and OX42 colocalisation appeared most strongly and most commonly near the lesion site and in the distal stump, areas containing larger amounts of degenerating myelin sheaths and cellular debris (both NRM and RM, panels 2 and 3).

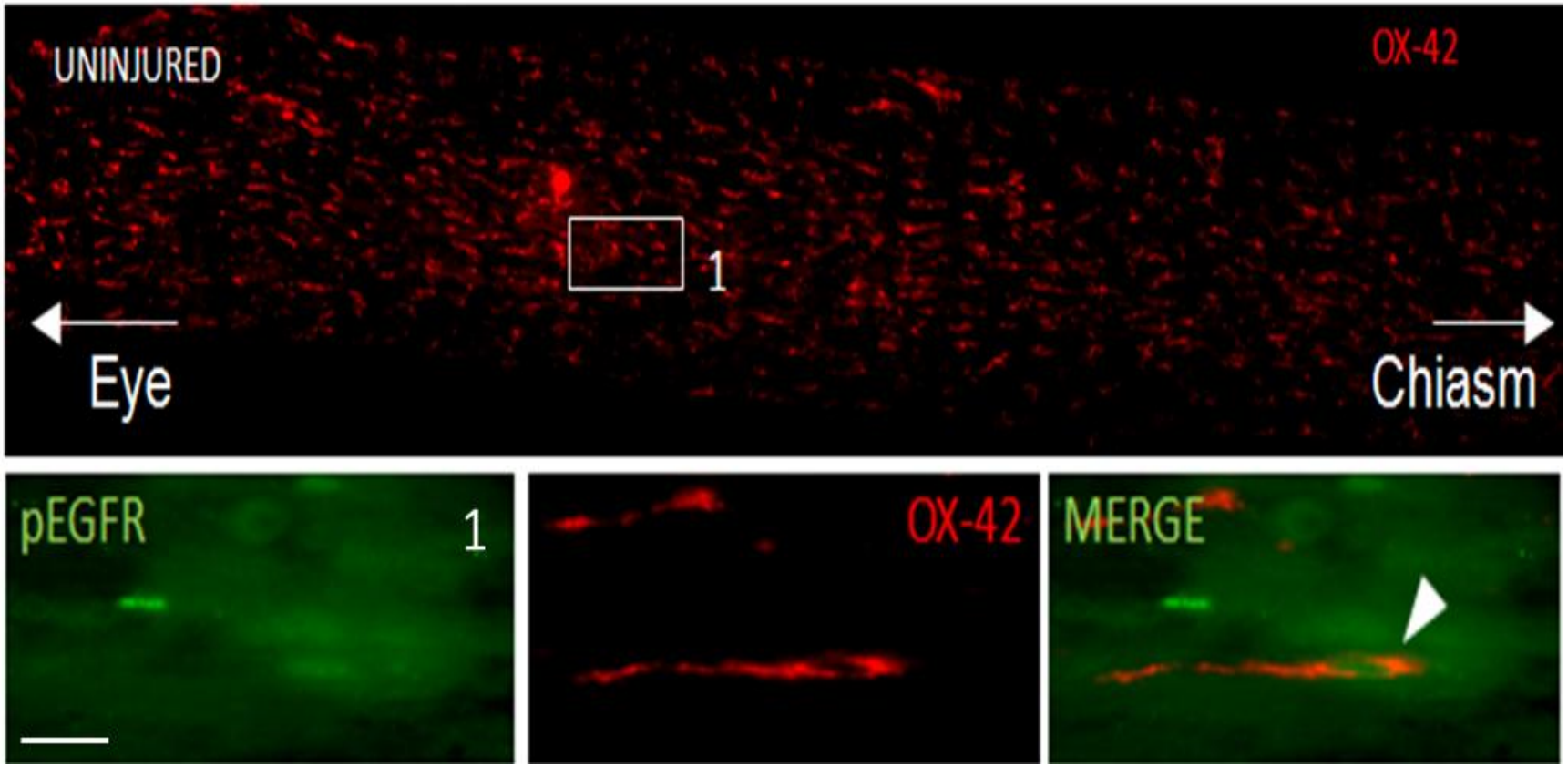
UNINJURED
OX-42
1
Eye
Chiasm
pEGFR
1
OX-42
MERGE

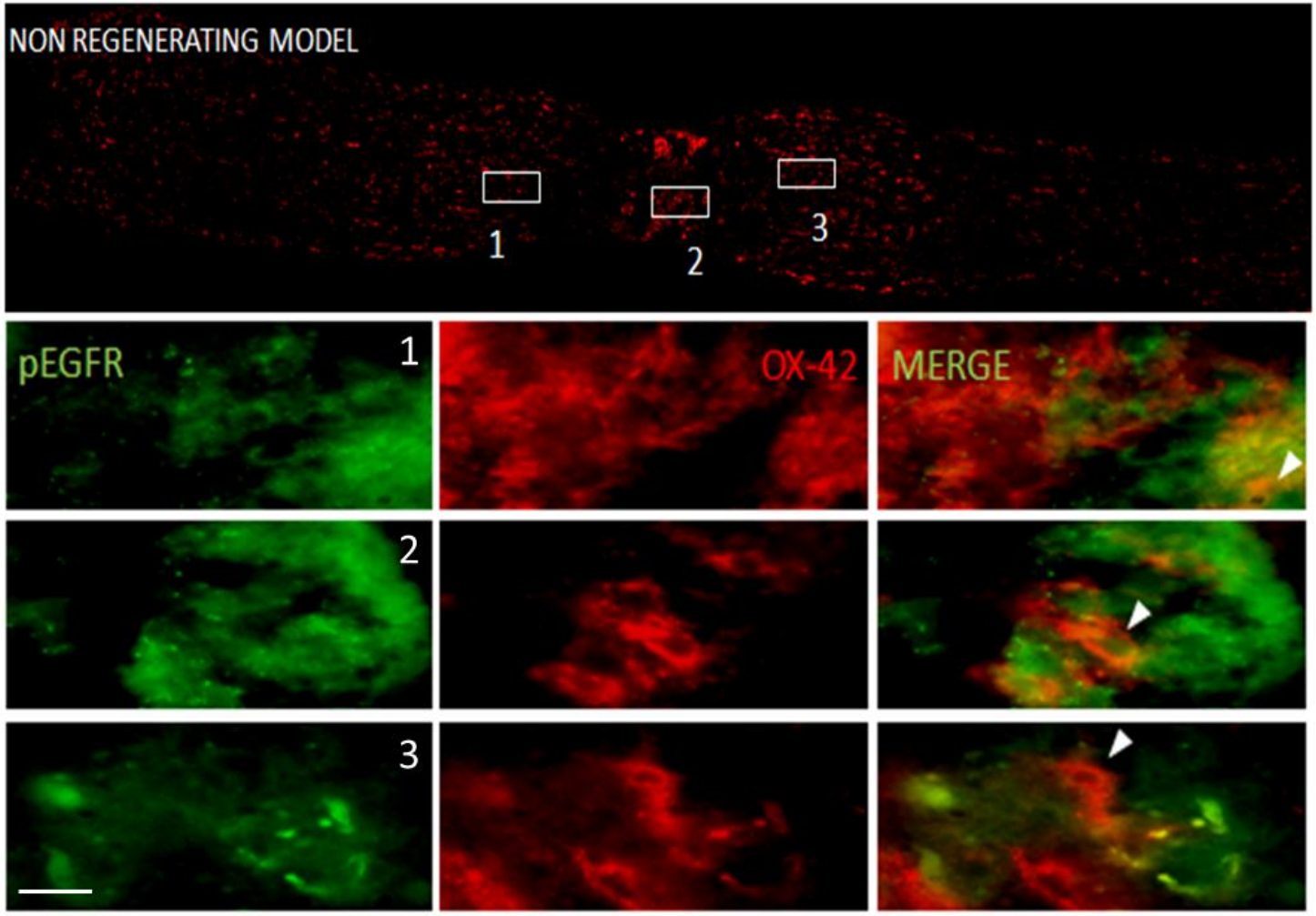
NON REGENERATING MODEL
1
2
3
pEGFR
1
OX-42
MERGE
2
3

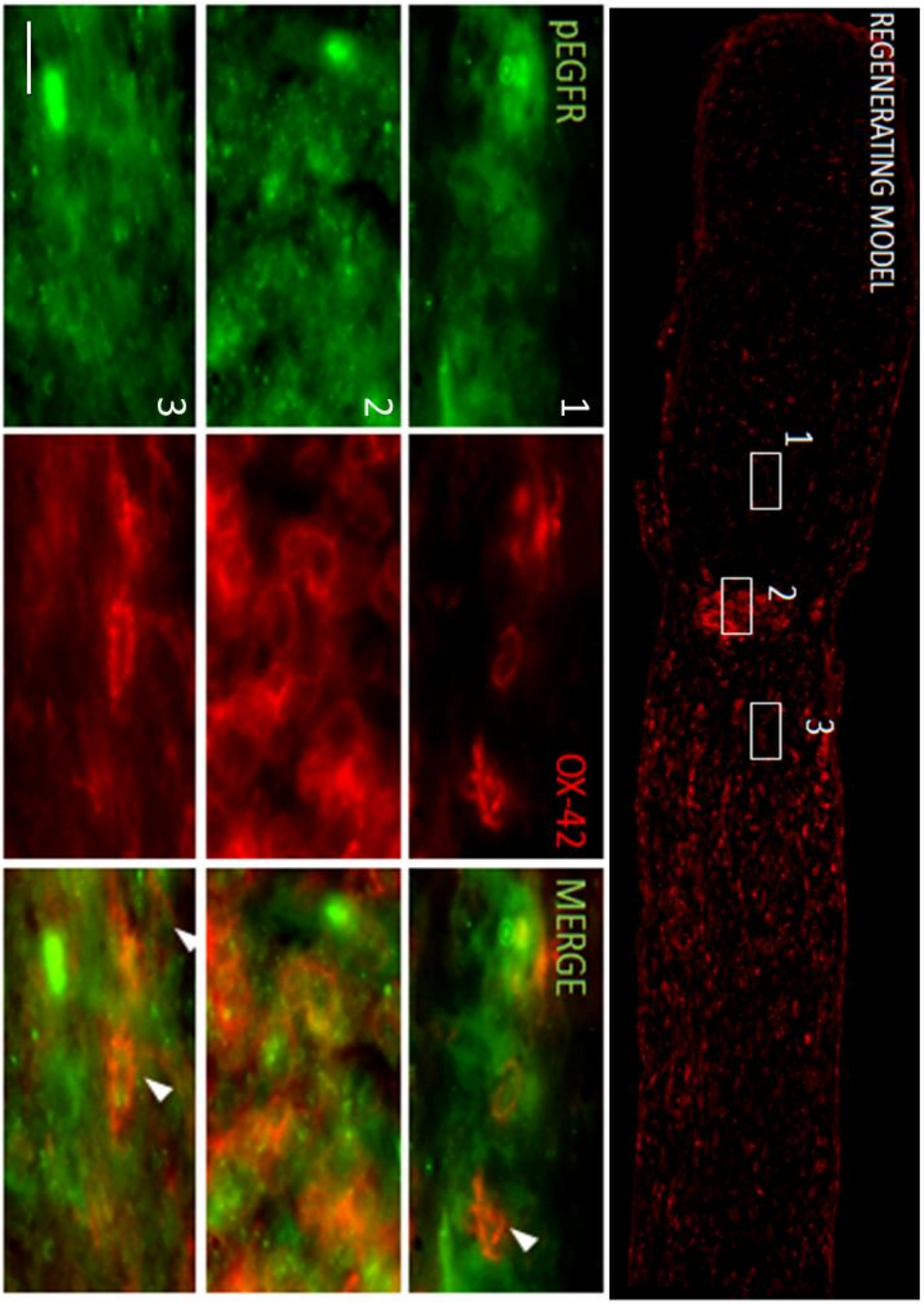

Figure 3.14. Activated microglia were pEGFR^{+}. First panel: Representative image of an uninjured control ON. The boxed region (1) is reproduced at high power to show that non-activated OX 42^{+} (red; arrowhead) microglia were constitutively weakly pEGFR^{+} (green) in the longitudinal rows of ON glia. Second and third panels respectively: NRM and RM ON microglia became activated and showed increased levels of pEGFR (arrow heads) proximal (1) and distal (3) to the lesion. The lesion (2) was full of activated microglia and large numbers of pEGFR^{+} haematogenous macrophages. (NRM – non regenerating model, RM – regenerating model, OX-42, microglial marker).

3.2.6 Haematogeneous macrophages entering the optic nerve after injury were constitutively pEGFR^{+}

Figure 3.15 shows immunohistochemical staining for the macrophage/activated microglia marker ED1 (red) and pEGFR (green). In the uninjured optic nerve macrophages are almost completely absent due to the immunoprivileged nature of the CNS, however the occasional macrophage may be found on the very boundary of the dural sheath, presumably not quite within the blood brain barrier (uninjured, arrow). After injury and subsequent disruption of the blood brain barrier, hameatogeneous macrophages flood the lesion site (NRM, 2 and RM, 2) and phagocytose the detritus. All macrophages observed were seen to be pEGFR^{+}. Although this may be partly due to the consumption of pEGFR^{+} debris, juxtamembraneous staining can be seen, strongly suggesting the presence of pEGFR on the cell membrane itself.

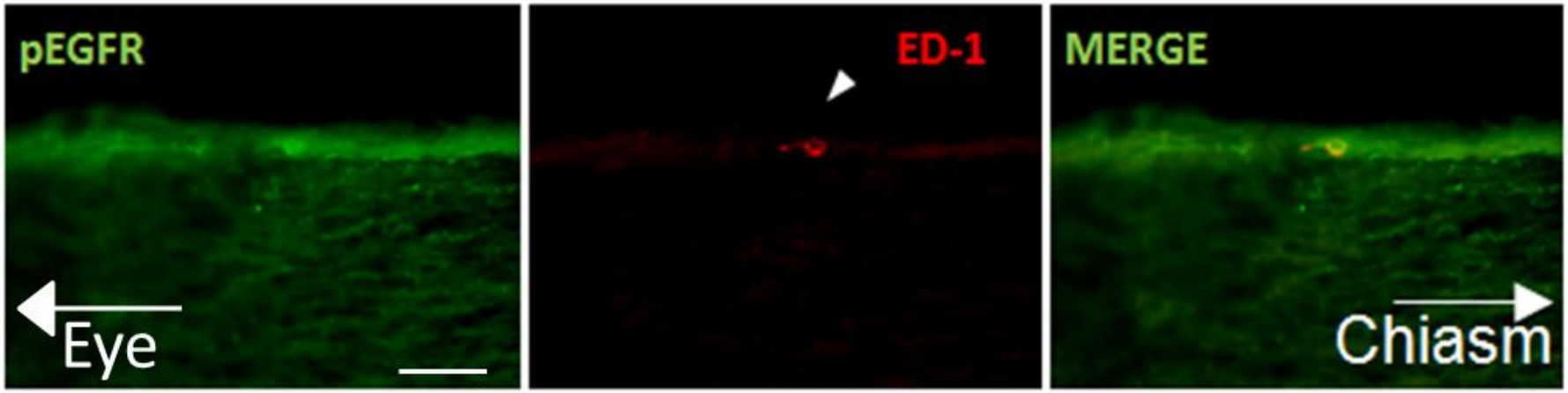
pEGFR
ED-1
MERGE
Eye
Chiasm

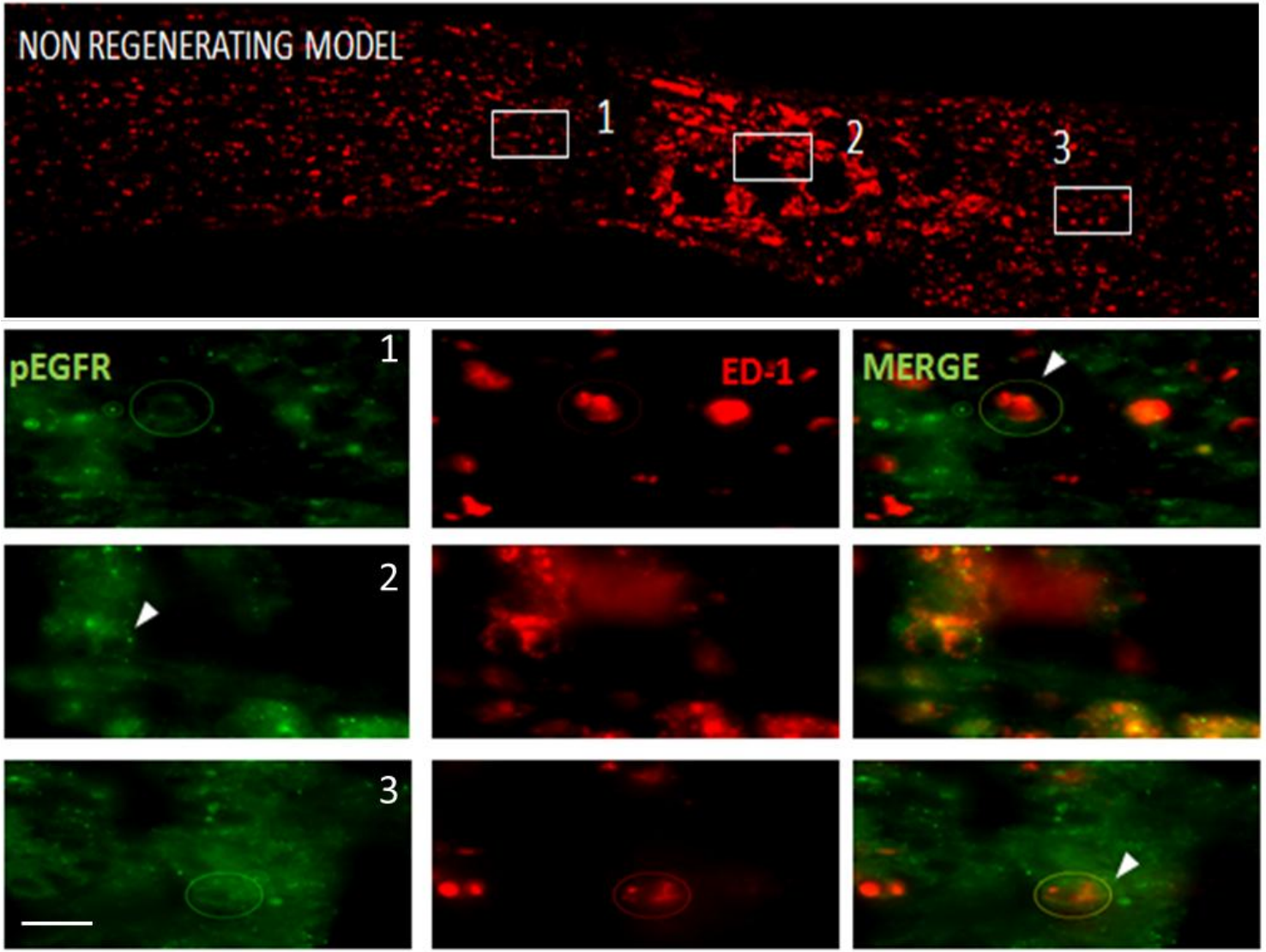
NON REGENERATING MODEL
1
2
3
pEGFR
1
ED-1
MERGE
2
3

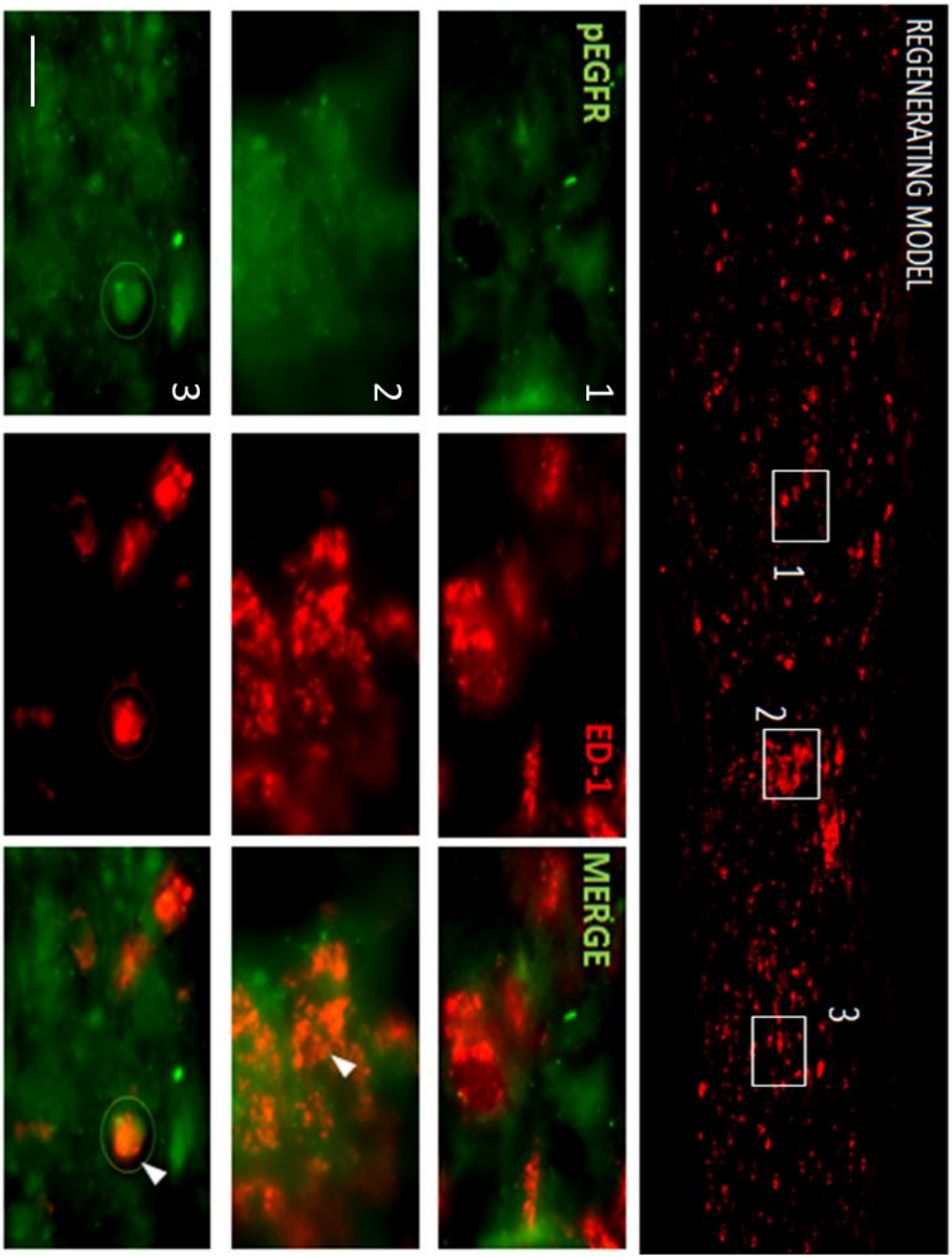

Figure 3.15. Invading haematogenous macrophages were pEGFR^{+}. First panel: Representative image of uninjured control ON (top) in which ED1^{+} (red; arrowhead) haematogenous macrophages were confined to the pia and were constitutively pEGFR^{+} (green). In NRM and RM (second and third panels respectively), macrophages and activated microglia (arrow head) showed increased levels of pEGFR and accumulated in the lesion (2), and were also present to a lesser extent in the proximal (1) and distal ON segments (3). (NRM – non regenerating model, RM – regenerating model, ED-1, Macrophage marker). Note that this marker also detects activated microglia, so many ED-1^{+} cells outside the lesion site (2) were likely activated CNS-resident microglia.

3.2.7 Axons within the retina were exclusively pEGFR^{-}

Figure 3.16 shows double immunohistochemical staining for pEGFR (green) and NF (red), on 15µm thick uninjured control (u/c), post injury non-regenerating (NRM), and post injury regenerating (RM) rat retinal sections. pEGFR was found not to colocalise with NF in any experimental or control group, neither constitutively nor post injury, in any part of the retina. This strongly suggests that all RGC axons in the FL of the rat retina are pEGFR^{-}.

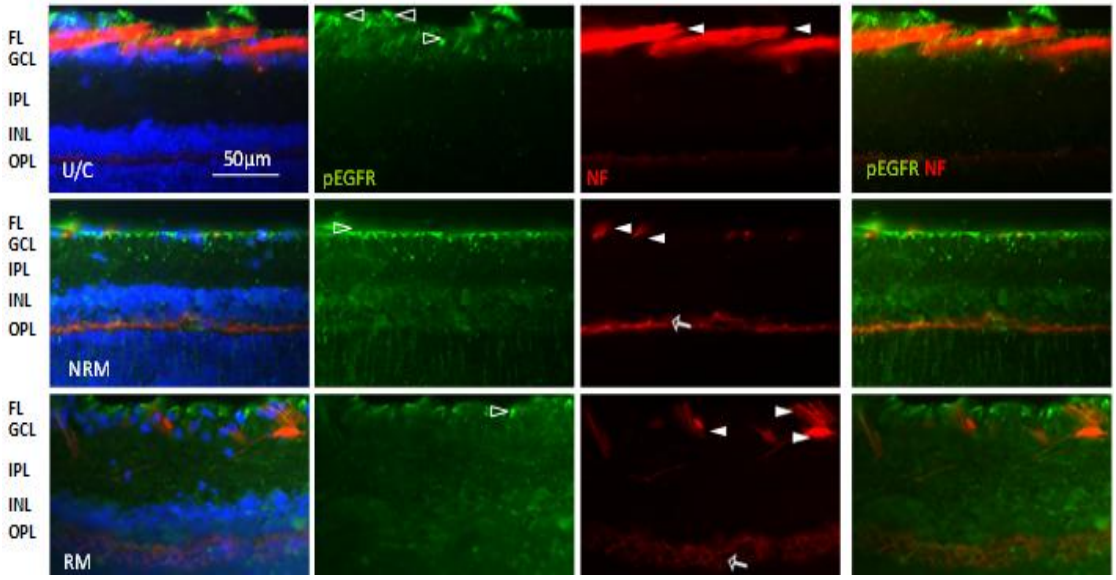

Figure 3.16. RGC axons did not contain pEGFR. Representative images of parasagittal sections of uninjured, NRM and RM retinae stained for pEGFR and NF. NF^{+} (red, closed arrow) axons in the FL were pEGFR (green) negative across all groups (DAPI stained nuclei are blue), as evidenced by complete lack of yellow-orange staining. The number of NF^{+} axons (red ,closed arrowhead) in the FL of NRM and RM retinae was reduced compared to U/C due to RGC death (See table 3.1). There was up-regulation of NF in the OPL in both NRM and RM retinae (open arrows).

3.2.8 A sub-population of retinal ganglion cells within the retina were constitutively pEGFR^{+} but this proportion remained the same in all treatment groups

Figure 3.17 shows double immunohistochemical staining for pEGFR (green) and the RGC marker β-III tubulin (red), on 15µm thick u/c, (top) NRM (middle), and RM (bottom) rat retinal sections. Confocal imagery (Figure 3.18) confirms β-III tubulin^{+} and pEGFR^{+} RGC somata. pEGFR was found to colocalise with β-III tubulin in approximately 30% of RGC, across all experimental and control groups, both constitutively and post injury (see Figure 3.19).

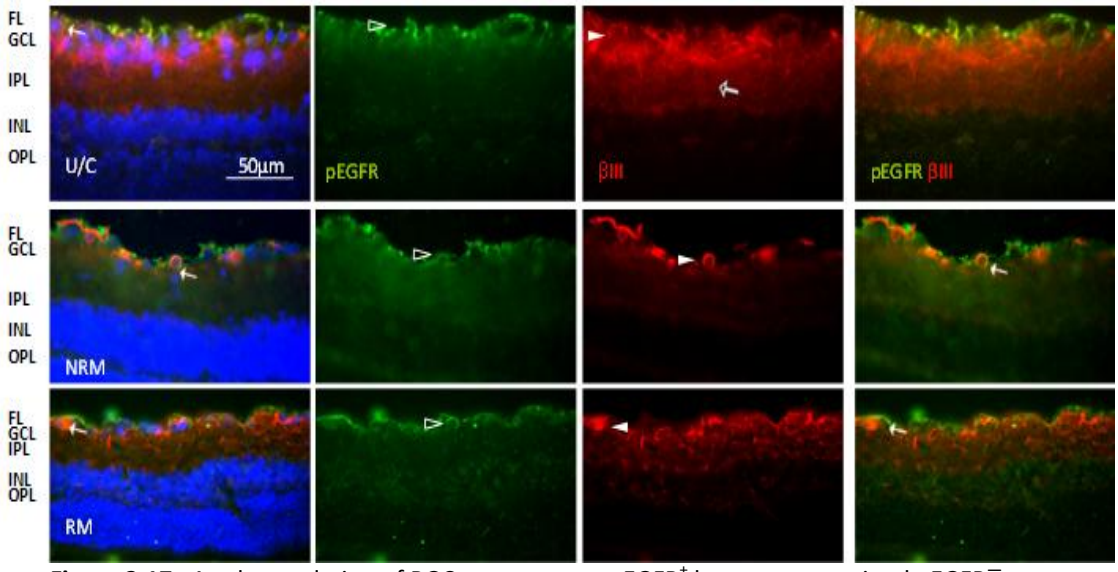

Figure 3.17. A sub population of RGC somata were pEGFR^{+} but axons remained pEGFR^{-}. Representative images of parasagittal sections of uninjured, NRM and RM retinae. A sub-population of RGC costained for both β-III-tubulin (red, closed arrowhead) and for pEGFR (green) in all groups, at approximately the same frequency. β-III-tubulin^{+} RGC dendritic arborisations ramified the IPL (red, open arrows). DAPI stained nuclei are blue.

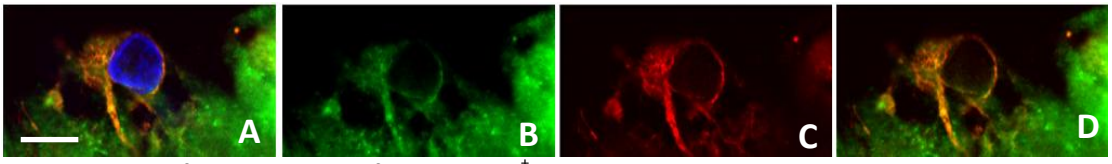

Figure 3.18. Confocal imagery confirmed pEGFR^{+} retinal ganglion cells. Double immunohistochemical staining for pEGFR (green, (B)) and the RGC marker β-III tubulin (red, (C)) shows colocalisation (orange-yellow, (D)). Scale bar = 10µm. DAPI stained nuclei are blue (A)

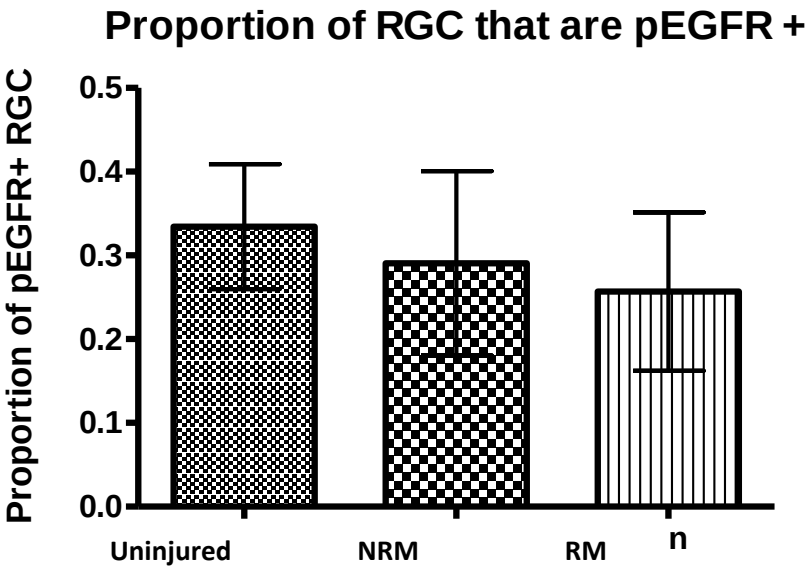

Figure 3.19. Proportion of all retinal ganglion cells which are pEGFR^{+}. Uninjured, NRM and RM retinae contain approximately the same proportion of pEGFR^{+} RGC. Proportions are expressed as:(number of pEGFR^{+} RGC) / (total number of RGC) Error bars represent 95% confidence intervals.

3.2.9 Retinal astrocytes and Müller glia were constitutively pEGFR$^+$ and levels increased after injury

Figure 3.20 shows double immunohistochemical staining for pEGFR (green) and the astrocyte and Müller cell marker GFAP (red), on 15µm thick uninjured control (u/c), post injury non-regenerating (NRM), and post injury regenerating (RM) rat retinal sections. In the uninjured retina pEGFR staining is limited to the FL, with the end feet of Müller glia and the cell bodies of astrocytes being predominantly pEGFR$^+$ (U/C, open arrowheads). Both astrocytes and the end feet of Müller glia are constitutively GFAP$^+$ but upregulate GFAP and exhibit increased pEGFR levels after injury (NRM and RM). Müller glial processes also become pEGFR$^+$ and GFAP$^+$ after injury, (NRM and RM).

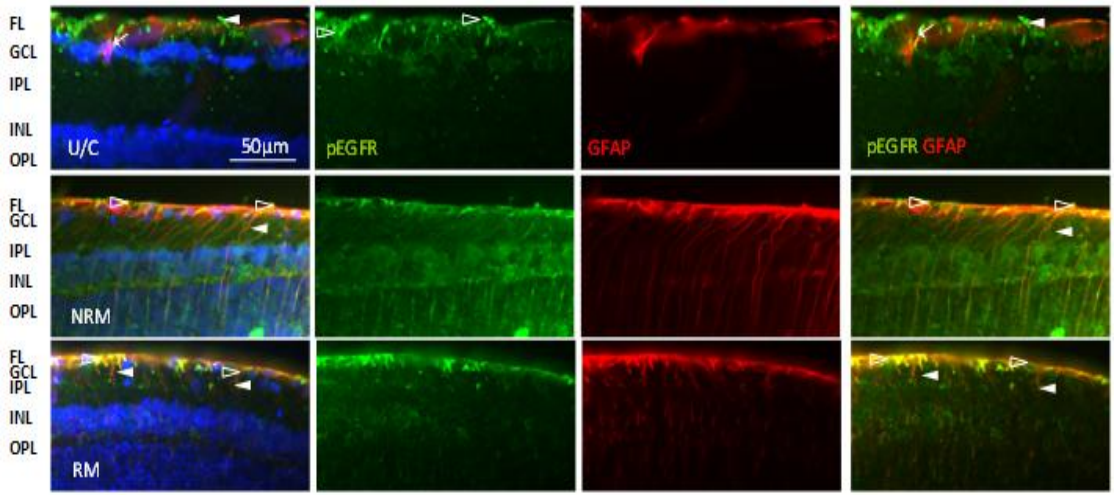

Figure 3.20. Representative images of parasagittal sections of U/C, NRM and RM retinae. GFAP (red,open/closed arrowhead) and pEGFR (green) are weakly and constitutively co-localised in retinal astrocytes (open arrow heads) and Müller cells (closed arrowheads) in uninjured retinae. Levels of both epitopes increase in Müller cell radial processes (closed arrowheads) Müller cell/astrocyte -feet (open arrow heads) in the FL of NRM and RM retinae.

3.3 Discussion

3.3.1 All retinal ganglion cell axons, in both the optic nerve and in the retina, were pEGFR^{-}

In light of the original hypothesis that intra-axonal EGFR transactivation is causal in CNS axon growth cone collapse, the total absence of pEGFR in RGC axons and growth cones is surprising. While several studies have provided evidence that EGFR is somehow involved in the AGIM signalling cascade (Koprivica *et al.* 2005, Erschbamer *et al.* 2007, Liu *et al.* 2006, Chen *et al.* 2007) no study to date has demonstrated pEGFR on RGC axons. Previous studies (Liu et al. 2006, Chen et al. 2007) have described EGFR on RGC somata but these studies did not examine retinal or ON pEGFR. The consensus of opinion is that transactivation of EGFR is required in order to transduce the AGIM signalling cascade (Koprivica et al. 2005, Liu et al. 2006, Chen et al. 2007, Schachtrup et al. 2007), as distinct to the pEGFR which results following EGFR ligand binding and would result in receptor internalisation. The putative NgR and fibrinogen interactions with EGFR, described in the papers by Koprivica et al. (2005) and Schachtrup et al. (2007) respectively, would require physical approximation of these molecules and/or signalling intermediaries and EGFR. The absence of pEGFR on RGC axons demonstrated here suggests that this interaction cannot be taking place intra-axonally, although this does not rule out the possibilities that a) EGFR interactions take place in some RGC somata or b) that pEGFR is present only in RGC axonal growth cones – which could not be directly visualised with the techniques used.

Although it is possible that pEGFR— mediated growth cone collapse could occur through intermediaries originating from the somata then being anterogradely transported to the axon, it is difficult to explain how such a system could limit its effects to the growth cone while avoiding cytoskeletal rearrangement at the somata and throughout the axon.

Conversely, growth cones are now known to synthesise certain proteins directly, rather than depend on anterograde transport from the somata (Zheng et al. 2001, Verma et al. 2005), so it is possible that EGFR could be synthesised and inserted into the membrane within the growth cone itself. One difficulty in directly observing such an event *in vivo* is the prevalence of $pEGFR^{+}$ cellular debris and the enormous increase in EGFR/pEGFR levels which occurs after CNS injury, primarily as observed in astrocytes and their processes (Liu and Neufeld 2007), but also in microglia (Planas *et al.* 1998), and invading macrophages (this study).

Nevertheless, the lack of observable axonal pEGFR makes a purely intra-axonal role for pEGFR difficult to accept. The axon regenerative actions of EGFRki are thus unlikely to be due to their abrogation of RhoA/ROCK mediated growth cone collapse through direct blockade of RGC axonal pEGFR.

3.3.2 A sub-population of retinal ganglion cell somata within the retina were constitutively pEGFR$^+$ but this proportion remained the same in all treatment groups

While RGC are known to express EGFR constitutively (Chen *et al.* 2006), no study to date has published observations on RGC pEGFR levels. In light of the complete absence of RGC- axonal pEGFR and considering the putative role of EGFR in the growth cone collapse signalling cascade, the near-identical proportions of pEGFR$^+$ RGC in all groups, including uninjured control, is surprising. The significance of this pEGFR$^+$ subpopulation, consisting of approximately 30% of total RGC, is unclear. What is certain is that this ~30% does not represent the population of axons which responded to intra-optic nerve EGFRki therapy: the proportion of regenerating RGC fibres were estimated by the authors to be around 0.5% of the total population (Koprivica *et al.* 2005). Among the best reported axon regeneration rates, in terms of total percentage of all RGC axons regenerating beyond the lesion site, are 0.6-10% 3 weeks after intravitreal peripheral nerve graft implant (Berry *et al.* 1996) and 7.5% 4 weeks after a triple combination of C3-transferase-mediated RhoA inactivation, application of exogenous, cell-permeable cAMP and simultaneous peripheral nerve autografting onto the cut end of the optic nerve (Hu *et al.* 2007). It is thus unlikely that the ~30% of pEGFR$^+$ RGC represents a specific population with any significantly different regenerative potential.

While EGFR activation has been linked to enhanced neurite outgrowth and neuronal survival of cerebellar granular neurons (CGN) *in vitro* (Yamada *et al.* 1997), its primary role in the adult CNS appears to be that of a neuromodulator, activating NMDA receptors and enhancing long term potentiation in the rat hippocampal neurons (Yamada *et al.* 1997, Abe and Saito, 1992). Importantly, both these neuronal-specific effects of

EGFR signalling are mediated by standard ligand-receptor interactions, EGF binding to and directly activating the EGFR. The mechanism behind EFGR-mediated growth cone collapse posited by Koprivica *et al* (2005). relies on EGFR-transactivation, a completely different process, potentially involving different signalling partners, impinging on different signalling pathways and thus capable of having distinct effects on neurons and axons. It is known that EGFR signalling in response to ligand binding involves receptor dimerisation and internalization, and that the fate of the ligand-receptor complex is dictated by the nature of both the dimer (EGFR can hetero-dimerise with other members of the ErbB family) and the specific ligand (Shankaran *et al.* 2006, Bazley and Gullick 2005, Wiley 2002, Wong and Guilliard 2004). Different ligand-receptor complexes can be variously degraded in endosomes or dissociate, with the EGFR returning to the membrane (Bazley and Gullick 2005, Wiley 2002). It has also been reported that EGFR can be internalised without receptor kinase activation (Wang *et al.* 2005) and, conversely, that EGFR tyrosine kinase domains can in turn be transactivated without receptor dimerisation or internalisation, by fibrinogen *via* β3-Integrin (Schachtrup *et al.* 2007) and by GPCRs (Gschwind *et al.* 2001).

Taking into account this multitude of potential mechanisms and outcomes of EGFR signalling, the presence of pEGFR on an unchanging size of subpopulation of RGC somata cannot reliably be construed to have any definite relevance to axonal regeneration.

3.3.3 Astrocytes in the optic nerve were constitutively pEGFR^{+} and levels appeared to increase after injury

In response to CNS injury local astrocytes undergo astrogliosis, a series of radical phenotypic changes characterised by GFAP upregulation, hypertrophy, mitosis, and, critically, increased secretion of various factors inhibitory to axonal regeneration, including Semaphorin 3 (Pasterkamp *et al.* 2001), ephrin-B2 (Bundesen *et al.* 2003), slit proteins (Hagino *et al.* 2003), and chondroitin sulfate proteoglycans (Rhodes and Fawcett 2004, Smith and Strunz 2005). It should be noted that reactive astrocytes also secrete fibronectin (Liu and Neufeld 2004a) and laminin (Martinez and Gomes, 2002), two components of the ECM which actually facilitate axonal regeneration by providing a positive growth substrate but also form part of the post injury glial scar. EGFR activation has been shown to increase astrocytic production of CSPG (Smith and Strunz 2005) and EGFR is known to regulate the release of several factors which attract and/or activate various other cell types associated with formation of the glial scar. These molecules include monocyte chemoattractant protein (MCP) 1, which encourages monocyte influx into the lesion site where they can transform into macrophages (Tanuma *et al.* 2006), monocyte to macrophage differentiation factor, which would enhance this process (Liu 2006), and cyclooxygenase 2 which attracts and activates microglia (Zhang and Neufeld 2005) allowing these cells to then take on a macrophage-like role. Although macrophages and microglia clearly have some neuroprotective roles, secreting NTFs, growth factors and phagocytosing any infectious agents within the injury site, these cells also contribute to axonal damage and death by stripping myelin from injured axons (for review see Donnelly and Popovich 2008). EGFR activation in astrocytes has also been shown to

provoke release of damaging reactive oxygen species such as nitric oxide which can directly damage and even kill adjacent neurons (Liu and Neufeld 2003).

It is then immediately apparent that EGFRki could potentially enhance axonal regeneration purely by ameliorating some or all of the above astrocyte-governed processes; rendering the lesion site less hostile by limiting the amount of growth antagonistic molecules and harmful cellular events, without necessarily having any direct effect on axonal or neuronal EGFR.

3.3.4 Müller glia and retinal astrocytes were both mostly constitutively pEGFR^{-} but became strongly pEGFR^{+} after injury

Müller glia in the healthy adult CNS express negligible or no GFAP, and when visible, GFAP is only seen in the cells' endfeet (Jadhav *et al.* 2009). The rapid activation of Müller glia in response to almost every type of retinal insult is well documented, as is the rapid upregulation of GFAP which accompanies this (see Bringmann *et al.* 2009 for review). Upon activation, GFAP becomes visible along the length of the Müller cell (Douglas *et al.* 2009, Liu *et al.* 2006). Interestingly, antibodies to EGFR (Close *et al.* 2006) and pEGFR (Douglas and Morrison *et al.* 2009) reveal very similar phenomenology; both forms being almost absent from normal adult Müller glia but clearly visible after injury along the full extent of the cell as it traverses the various layers of the retina (Close *et al.* 2006, Douglas and Morrison *et al.* 2009). At least three studies have linked EGFR activity to Müller cell gliosis (Milenkovic *et al.* 2003, Scherer and Schnitzer 1994, Roque *et al.* 1992) while another has shown that overexpression of EGFR by retinal progenitor cells consistently yields Müller glia instead of photoreceptors, interneurons or RGC (Lillien 1995). It appears then, that EGFR activation can elicit or at the very least facilitate Müller gliosis; a process linked to neuronal death *via* processes as diverse as neurotransmitter removal deficiency (leading to or aggravating neuronal excitotoxicity), K^{+} and H_2O dysregulation and the formation and release of cytotoxic reactive oxygen species (Bringmann *et al.* 2009). It has long been known that activated Müller glia, along with retinal astrocytes, hypertrophy and multiply after intra-orbital optic nerve crush, extending into and filling the spaces left by dead neurons and axons (Barron *et al.* 1986) and that these activated Müller glia can help form a glial scar within the ganglion cell fibre layer of the retina,

preventing axonal growth (Burke and Smith 1981). In short, it would seem that the appearance of pEGFR^{+} Müller glia heralds various processes antagonistic to axonal regeneration. One potential means of investigating intra-retinal Müller Glial (and astrocytic) pEGFR function might be to directly inject or implant a bolus of EGFRki directly into the vitreous body immediately following optic nerve crush injury and to observe what effects, if any, this had on RGC survival and axonal regeneration (see Chapter 3). It should be noted that the original study applying EGFRki to crushed optic nerves (Koprivica *et al.* 2005) did so at a considerable distance from the retina, thus it is likely that the RGC axon regeneration observed was elicited in spite of any retinal pEGFR involvement. Despite this, there remains the possibility that intra optic nerve EGFRki could have retrograde effects on retinal cells. EGFRki, or other molecules released in response to EGFRki, could be retrogradely transported by axons, from the optic nerve to RGC cell bodies in the retina, and from there local paracrine effects on surrounding glia and neurons are possible. Another possibility is astrocyte-astrocyte signalling *via* juxtacrine interactions, as an unbroken chain of astrocytes exists from the optic nerve to the retina.

3.3.5 Oligodendrocytes in the optic nerve were constitutively pEGFR^{+} and levels did not appear to increase after injury

A search of the literature yields only one paper directly concerned with oligodendrocytic EGFR. This study (Aguirre *et al.* 2007) provides strong evidence that EGFR signalling is required for both myelination and remyelination after injury, showing how overexpression of EGFR yields higher levels of myelin basic protein in focally demyelinated areas of the mouse brain. Myelin production after CNS injury can be both

beneficial and detrimental. In many CNS pathologies and injuries a sizeable percentage of long tract axons escape transection. Studies in cat SCI models showed that locomotion could still be achieved with only 5-10% axonal survival in the relevant tracts (Blight 1983, Blight and Decrescito 1986). Oligodendrocyte death and axonal debridement by invading lymphocytes often results in these surviving axons being completely demyelinated (Crowe *et al.* 1997) and unable to conduct action potentials effectively over any distance. Thus remyelination of these surviving tracts is highly desireable as this could avoid the need for the long tract axonal regeneration, pathfinding and reconnection that has so far been almost universally elusive in treating CNS pathologies. Conversely, myelin provides arguably the greatest source of axon growth-cone collapsing molecules: Nogo (Chen *et al.* 2000, Grandpre *et al.* 2000, Prinjha *et al.* 2000), OMgp (Kottis *et al.* 2002) and MAG (McKerracher *et al.* 1994) are all present in CNS myelin. Each of these has been shown to elicit growth cone collapse, leading to axonal regenerative failure and subsequent neuronal loss. Neutralising Nogo with the antibody IN-1 has been shown to enhance functional recovery and significantly increase axonal regeneration at the lesion site (Thallmair *et al.* 1998) and similar experiments with antibodies conjugated to MAG greatly enhanced neurite outgrowth in cerebral granular neurons plated in the presence of MAG (Irving *et al.* 2005). The large amounts of fragmented myelin in the distal stumps of both the RM and NRM ON are testament to the fact that Wallerian degeneration in the CNS is immensely slow or absent, as by the equivalent time point in PNS injuries (14 dpi) almost all axonal and myelin debris has normally been cleared (Vargas and Barres, 2007) – see general introduction for more detail. That oligodendrocytic pEGFR levels do not appear to change following injury implies that oligodendrocytic pEGFR is, on balance, not particularly relevant to axonal regeneration. Additionally, this may indicate that

oligodendrocytes require ongoing EGFR activity in order to maintain myelin production or other, unidentified, cellular processes.

3.3.6 Quiescent microglia in the optic nerve were constitutively weakly pEGFR^{+} or were pEGFR^{-} but became strongly pEGFR^{+} upon activation

Non-activated microglia being largely pEGFR^{-} and activated, post injury microglia becoming strongly pEGFR^{+} agrees with the results of at least one previous study of microglial EGFR expression (Planas *et al.* 1998). This group found that while quiescent microglia in the uninjured rat brain express very low levels of, or do not express EGFR, all microglia observed 4 days post ischaemic brain injury were strongly EGFR^{+} and suggested that EGFR signalling is required for microglial activation. Being that activated microglia are largely responsible for initiating and maintain the immune response to CNS injury (see Garden and Moller 2006 for review), this ties EGFR directly into the ongoing conundrum of whether the inflammatory and immune responses are beneficial or detrimental overall to CNS axonal regeneration (see general introduction for details). Thus both microglial activation and macrophage activity can be either conducive to, or inhibit neuronal survival and axonal regeneration, depending on the exact nature of the CNS injury.

Despite the potentially beneficial actions of activated microglia, putatively requiring or at least facilitated by pEGFR, numerous studies prior to and separate from those involving EGFRki have shown another EGFR antagonist, Decorin, to be profoundly conducive to axogenesis both *in vitro* and *in vivo*, and that these effects are at least partially mediated by microglia (Davies *et al.* 2006). Decorin is a small leucine rich proteoglycan, abundant in ECM, which is a natural antagonist of scar formation (see

Hocking *et al.* 1998 for review). Tumour suppression studies describe how Decorin binds to EGFR, causing it to be internalised and degraded (Csordas *et al.* 2000, Zhu *et al.* 2005) and, more importantly, abolishing the activation of remaining EGFR (Csordas *et al.* 2000). Within the CNS Decorin has been shown to degrade, and/or suppress the production of, various axon growth inhibitory molecules, including the CSPGs versican, neurocan, NG2 and brevican, reduce astrogliosis, prevent or attenuate glial scar deposition, significantly reduce post injury macrophage influx and massively increase cultured PNS dorsal root ganglia neuron (DRGN) neurite outgrowth on CSPG and CNS myelin substrates (Tang *et al.* 2003, Davies *et al.*, 2004, Logan *et al.* 1999, Minor *et al.* 2008). As Decorin potently inactivates EGFR, this is strong circumstantial evidence that microglial (and astrocytic) pEGFR plays an important role in many processes antagonistic to CNS repair. A recent study has also provided evidence that one member of the CSPG family, versican, actually signals directly through EGFR as a ligand (Xiang *et al.* 2006), suggesting another mechanism by which blocking pEGFR could potentially benefit the regenerating CNS. It should be noted however that this study actually found a specific domain of versican (the G3 region) to signal through the EGFR, and also found the results of this signaling to be neuritogenic for cultured hippocampal neurons, although the authors point out that two different isoforms of versican, V1 and V2 have different axon growth inhibitory properties, and thus much depends on the specific isoform/version of versican. Nevertheless, the direct activation of EGFR by a CSPG should not be overlooked as a potentially novel source of axonal growth inhibition, nor discounted when considering the actions of broad-spectrum EGFR antagonists such as Decorin or EGFRki.

3.3.7 Haematogenous macrophages entering the optic nerve after injury were constitutively pEGFR^{+}

The literature for EGFR signalling in macrophages/monocytes appears remarkably sparse. A PubMed search for either 'EGFR macrophage' or 'EGFR monocyte' yields only two directly relevant papers. The first confirms macrophage EGFR expression and posits EGFR signalling to be involved in macrophage chemotaxis and mitosis (Lamb *et al.* 2004) and the second simply confirmed the presence of EGFR^{+} macrophages in a melanoma model (Scholes *et al.* 2001). Nevertheless, this supports the present study's findings that macrophages express EGFR, and if EGFR is required for/involved in macrophage migration then invading macrophages would be expected to exhibit pEGFR. If attenuation of EGFR activation by EGFRki could limit macrophage numbers and reduce their influx into the injured CNS then this could potentially lead to a reduction in the secondary damage to axons associated with phagocytic leukocytes in SCI models of CNS injury. How such an attenuation of macrophage ingress would affect ONC models of CNS injury and regeneration is another matter, considering the proven beneficial effects of intravitreal macrophage recruitment described above.

3.4 Interim Conclusions

That all RGC axons observed in both the optic nerve and the retina were found to be pEGFR^{-} implies that the axonal regenerative effects of EGFRki are unlikely to be a result of direct interaction with neuronal/axonal EGFR. It is possible that pEGFR could be present in axonal growth cones alone, as the antibody used to identify axons was raised

against the heavy chain Neurofilament, NF-200, which is only present in the consolidated axon and therefore does not allow visualisation of the newly grown axon or the growth cone itself. Endogenous EGFR signalling would presumably result in detectable levels of axonal pEGFR as ligand-receptor complexes are endocytosed and travel to either the nucleus or endosomes. That this was not observed suggests an absence of pEGFR within RGC growth cones. The near ubiquity of glial pEGFR and the abundance of literature describing various glial EGFR-mediated, regeneration-antagonistic processes strongly suggest that the primary means by which EGFRki effect axonal regeneration is to partially neutralise the inhibitory impact of the CNS lesion itself. By reducing astrogliosis EGFRki could attenuate CSPG deposition, prevent or reduce the interaction between astrocytes and fibroblasts crucial to the formation of the glial scar in the ON. Suppressing Müller glial activation via EGFR blockade could prevent the neuronal death associated with Müller cell dysfunction following activation. Preventing or abrogating EGFR-mediated microglial activation, as shown prominently in studies involving decorin, can have wide reaching benefits including abrogated production of ROS, reduced recruitment of MBP-sensitised lymphocytes (and hence reduced axonal and neuronal myelin debridement) and lower levels of excitotoxic glutamate. If the migration and mitosis of macrophages is in fact primarily EGFR mediated then EGFRki could also potentially directly reduce macrophage numbers recruited. That one therapeutic target could attenuate or abolish so many potentially noxious processes appears promising but this is tempered somewhat by the fact that in the original study using EGFRki in an ONC model (Koprivica *et al.* 2005) no effect on RGC survival was found and, crucially, only 0.5% of the total RGC population regenerated axons across the lesion site and into the distal segment of the ON *in vivo*. Compared with the ~10% of the total RGC population which has been reported to

regenerate > 4 mm into the distal section of the crushed ON following intravitreal PN graft (Berry *et al.* 1996) this is not particularly impressive. However, the the mitosing Schwann cells contained within the intravitreal PN graft, which is undergoing Wallerian degeneration, supply a wealth of neurotrophic factors which strongly support RGC survival for weeks after axotomy (Berry *et al.* 1988, 2008, Logan *et al.* 2006), whereas, as mentioned, EGFRki do not appear to enhance RGC survival. That a subpopulation of RGC will regenerate in the (apparent) absence of exogenous NTF support is both unusual and potentially important, possibly pointing to a novel mechanism by which at least some RGC can be disinhibited. More importantly, if EGFRki are actually capable of rendering the CNS environment significantly less hostile to axonal growth, there is much potential for future combinatorial therapies involving EGFR blockade along with exogenous growth stimuli.

That no difference was observed in pEGFR levels between the RM and NRM does not necessarily reflect a real equivalence in pEGFR levels, rather it highlights that at best, semi-quantitative nature of immunohistochemical studies. SDS-page and Western blotting would establish whether or not any real differences in pEGFR levels existed but animal numbers and the need for mutually exclusive tissue preparation (fixation versus non fixation) prohibited these extra experiments in this case. Previously our laboratory has published studies involving larger scale experiments and included groups of RM and NRM animals to be used as tissue donors for SDS-PAGE and Western blot, and obtained results showing that pEGFR levels <u>are</u> in fact significantly lower in the RM compared to the NRM (see Ahmed *et al.* 2006, Figure 3A). It is also likely that such a clear discrepancy could not come about from merely differences in any extant axonal pEGFR, such a clear difference would very likely reflect differences in glial expression of EGFR. This is also

circumstantial evidence that suppressing pEGFR may be conducive to axonal regeneration.

As the *in vivo* immunohistochemical results obtained in this Chapter have highlighted a discrepancy between the proposed mechanism of action of EGFRki-mediated axonal regeneration as suggested by Koprivica *et al.* and the actual distribution of pEGFR in the rat visual system, namely the complete absence of axonal pEGFR, it was decided to examine the actions of one of the EGFRki used by Koprivica *et al.*, AG1478, in primary retinal cultures, to attempt to ascertain whether or not EGFRki can elicit RGC neurite outgrowth in an inhibitory environment and, if so, to attempt to elucidate the mechanisms underlying this effect.

Finally it should be noted that while this study is the first to examine pEGFR distribution in the visual system, Chen *et al.* (2007) studied the distribution of EGFR, not discerning between EGFR and pEGFR, and that the main findings of that study confirm those of the present study; namely that EGFR is not present on RGC axons, is present on at most a subpopulation of RGC somata and is weakly present on/absent from astrocytes and Müller glia pre-injury but strongly present after ONC.

Chapter 4

An investigation of the *In Vitro* effects of the EGFRki AG1478 on primary retinal cultures and the RGC-5 cell line

4.0 Introduction

Having shown all RGC axons and the majority of RGC somata to be pEGFR^{-}, the question arose of exactly how EGFRki elicited the *in vitro* neurite outgrowth and *in vivo* axonal regeneration reported by Koprivica *et a*(2005). The original mechanism suggested by these authors implicated the EGFR as a critical part of the intraneuronal/axonal inhibitory signalling cascade initiated by the NgR, based on the evidence that preventing the activation of (or more specifically the phosphorylation of) EGFR disinhibited neurite outgrowth *in vitro.* In light of the lack of axonal pEGFR this explanation was considered unsatisfactory; it was difficult to see how EGFR signalling could play such a direct intra-axonal role. While previous studies have shown that blocking single receptors for AGIM can elicit significant axonal regeneration and functional recovery (e.g. Grandpre *et al.* 2002, Fabes *et al.* 2007), these studies use spinal hemisection injury models, usually severing a dorsal tract and leaving its ventral counterpart intact. At least one study has shown that, without any therapeutic intervention whatsoever, considerable functional recovery can result from spontaneous 'rewiring' of injured dorsal corticospinal (CST) tracts *via* collateral sprouting from uninjured ventral CST tracts (Weidner *et al.* 2001). Conversely, the literature does not contain any reports of functional recovery-level RGC axonal regeneration in response to antagonism of any single receptor. As such, the significant regeneration associated with neutralisation of specific receptors in each of the aforementioned studies is likely to represent an enhancement of existing neural plasticity. As such, it is unlikely that the neutralisation of any one single receptor, including EGFR in its putative axon growth inhibitory role, would actively drive RGC axonal regeneration following complete ON transection – there being no other population of axons to which

RGC axons could laterally connect. Previous studies have shown the neutralisation of NgR alone to be largely insufficient for RGC regeneration *in vivo* (Fischer *et al.* 2004a, but see Chen *et al.* 2009) whereas similar neutralisation of the small GTPase Rho A (Fischer *et al.* 2004b), which transduces signals from multiple receptors, yields greater, if still marginal, levels of axonal regeneration. However, when NgR inactivation is combined with any growth promoting therapy such as NTF support, significant regeneration is often reported (Fischer *et al.* 2004b, Chen *et al.* 2009, Ahmed *et al.* 2005). It is thus likely that the growth promoting effects of EGFRki such as AG1478, as reported by Koprivica *et al*(2005), result from more than just the indirect intraneuronal blockade of NgR signalling *via* EGFR antagonism, and the purpose of this study was to determine the nature of this proposed stimulus to RGC neuritogenesis/axogenesis.

The previous Chapter showed that, while all RGC axons and most RGC somata were $pEGFR^{-}$, many retinal and ON glia were $pEGFR^{+}$, and pEGFR levels increased after ONC. This implied that the effects of EGFRki such as AG1478 could be significantly or even primarily glially mediated. Considering the numerous, neurite outgrowth antagonistic, glially mediated processes linked to EGFR signalling (see discussion, previous Chapter), this was considered a promising line of investigation. However, contemporaneous with this work, it was found by others in our laboratory that 90% siRNA knockdown of EGFR failed to disinhibit RGC neurite outgrowth in primary retinal cultures exposed to CNS Myelin Extract (CME) (then-unpublished findings of Dr M. Douglas and Dr Z. Ahmed, since published in Douglas *et al.* 2009), and that subsequently treating these EGFR knockdown cultures with AG1478 still resulted in disinhibited neurite outgrowth. This was strong evidence that the neuritogenesis elicited by AG1478 was <u>not</u> primarily due to its blockade of EGFR. These developments warranted further investigation of the

in vitro effects of AG1478. To this end, it was decided to confirm first hand that AG1478 could in fact disinhibit primary culture-RGC neurite outgrowth in a growth inhibitory environment. Ideally, this required an effective, replicable, non neurotoxic neurite outgrowth inhibition assay. Many research groups have used CSPG and CME in outgrowth inhibition assays, but the former is difficult to purify and expensive to purchase, whereas it is difficult to accurately assess relative protein levels in the latter. The synthetic recombinant Nogo-P4 peptide was selected as a potential candidate inhibitory ligand due to both its soluble nature - which allows the titration of specific and easily replicable concentrations of the compound into culture media - and its well understood NgR-dependent signalling properties. If a concentration of Nogo-P4 could be found which significantly inhibited RGC neuritogenesis without causing neuronal death, it could then be ascertained whether this inhibition could subsequently be neutralised by AG1478. As primary retinal cultures require the sacrifice of an animal and can be prone to relatively large inter-experimental variation, it was decided to also model Nogo-P4-inhibited and AG1478-disinhibited primary retinal culture experiments using the immortalised neuronal RGC-5 cell line. If successful, this would provide an inexpensive, highly replicable, neurite outgrowth-inhibitory assay. It is also worth noting that the literature does not appear to contain any studies having made use of Nogo-P4 peptide in such an assay; so successful inhibition of RGC neurite outgrowth with Nogo-P4 would represent a potentially novel neurite outgrowth inhibition assay.

Having confirmed the efficacy of AG1478 in disinhibiting neurite outgrowth, the next step would be to establish the nature of the hypothesised off target effect(s). The most obvious candidates for driving neurite outgrowth are NTFs, including the NTs, and/or any compound which could mimic their effects. If AG1478 could elicit NTF

release, autocrinally from RGC or paracrinally from retinal glia, these factors could be detected by ELISA analysis of collected conditioned culture media. Additionally, if both primary retinal cultures and the RGC-5 cell line were found to respond to AG1478, and if subsequent ELISAs on conditioned media detected NTF release, this would point to AG1478-stimulated autocrine NTF release as a primary drive of neuritogenesis, as RGC-5 cultures contain no glia. As mentioned, some effects of NTF can be elicited in the absence of NTF, normally by receptor crosstalk. Accordingly, it was decided to investigate reports that the adenosine A2A receptor could, in the absence of any exogenous NTF, transactivate Trk receptors, effectively enabling A2A agonists, including adenosine, to function as NTFs (Jeanneteau and Chao, 2006). To ascertain whether this A2A-dependent event contributed to the putative disinhibitory effects of AG1478, it would be investigated whether the potent and specific A2A receptor antagonist ZM21385 could neutralise or diminish the AG1478-stimulated effects.

Attention was then turned to the experimental end-point measurement criteria, in terms of discerning and measuring the effects of Nogo-P4 and AG1478 on neurite outgrowth. The mean number of neurites produced per neuron were considered to be a separate factor from that of actual mean neurite length, as each of these values are more or less significant for different types of neuron. For neurons normally possessed of a single long axon, including RGC, longest neurite length is arguably a more relevant indicator of regenerative success than neurite number. Following axotomy by ONC, RGC must regenerate their single axon (ignoring any axonal branching closer to the target area) to the relevant brain region. For other neurons such as bipolar cells, which connect intricately with several relatively nearby targets, neurite number becomes more relevant as a regenerative correlate. Also, whilst both neurite outgrowth and elongation both

require the parent neuron to enter an active growth state, exogenous signalling molecules local to the growth cone can elicit axonal elongation without necessarily involving or even travelling to the somata (Twiss and Van Minnen, 2006) thus probably not affecting the formation of new neurites. Conversely while neurons can enter an active growth state, and attempt to create several neurites, a potently growth antagonistic extracellular environment can attenuate growth cone advance to the extent where these new neurites barely extend away from the cell body at all and may collapse back to the somata completely. This is commonly seen in the ON *in vivo* - during the first 12 – 96 hours after axotomy; RGC sprout multiple neurites which generally extend very little distance through the growth-antagonistic CNS environment. For these reasons it was decided to measure and analyse both mean longest neurite length and mean neurite number. In order to detect any effects on neuronal survival, one further measurement criteria was included: the mean number of RGC. The number of RGC in each treatment group was standardised as much as possible initially (see methods) and monitored during data analysis.

In order to accurately measure RGC neurite outgrowth *in vitro* it was first necessary to ascertain the sample size required for accurate representation of the neuronal population. Equating this to the number of photographs taken per culture-slide well, a pilot study was performed which compared the standard error of the mean (SEM) of the entire population (i.e. every RGC in that well, as measured by photographing the entire well - 209 pictures) with SEMs from samples of 10, 20, 50, 100 and 200 pictures. SEMs were calculated for the "longest neurite" parameter (see figure 4.1). The optimum number of pictures to be taken per well was deemed to be around 40, as an ideal compromise between time-effectiveness and an acceptably low SEM, and as wells were

subdivided into 9 quadrants for quantification (see methods for details) it was decided to take 36 pictures per well, as this number allows 4 pictures per quadrant. It should be noted that 3 wells were used per condition, per experiment, so the actual number of pictures taken per treatment group would in fact be at least 108, further minimising any sampling error.

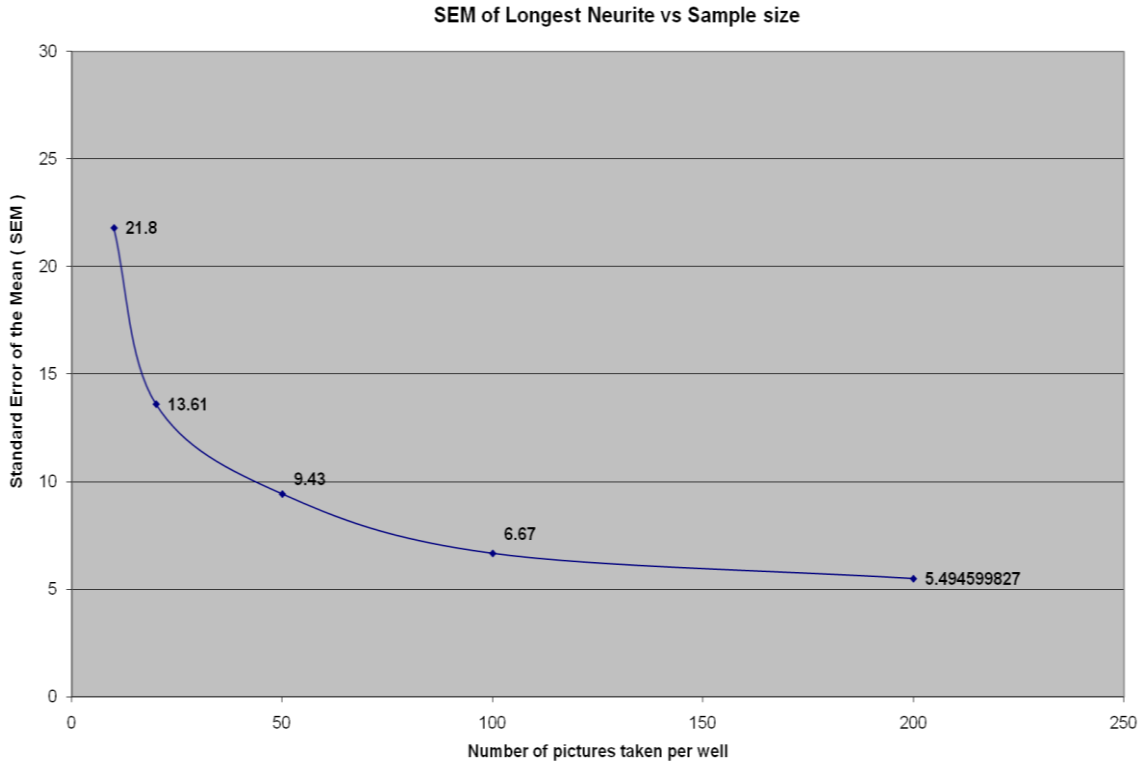

Figure 4.1. Standard Error of the Mean (SEM) of Longest Neurite parameter vs sample size (number of pictures taken) taken from a randomly chosen PDL/Laminin coated chamber slide well. One entire well was photographed such that every RGC was photographed and the SEM for the "longest neurite" parameter was calculated for the entire RGC population. This SEM was compared with those obtained from sampling 10, 20, 50, 100 and 200 pictures. The optimum number of pictures to be taken was deemed to be around 40, as an ideal compromise between time-effectiveness and an acceptably low SEM.

In this way, the specific experimental conditions, parameters, sample number and treatment groups were selected and investigations begun into the *in vitro* mechanisms of action of AG1478.

4.1 Specific Aims

- To establish an assay which would inhibit neuritogenesis in the RGC-5 cell line and in primary retinal cultures without causing significant neuronal death, using the recombinant Nogo-P4 peptide

- To attempt to rescue RGC-5 and RGC neurite outgrowth from the above Nogo-P4 assay using the EGFRki AG1478, and so confirm that EGFRki can disinhibit RGC neurite outgrowth *in vitro*

- If possible, to establish whether or not the Adenosine A2A receptor mediates any of the putative EGFRki disinhibitory effects by attempting to disrupt above rescue experiments with the concomitant addition of the A2A receptor antagonist ZM21385

4.2 Results

To establish the effects of AG1478 on RGC neurite outgrowth it was necessary to have an assay which simulated the growth antagonistic environment of the CNS. To this end the recombinant Nogo-P4 peptide was used to create a RGC neurite outgrowth inhibition assay. A dose-response pilot experiment was performed using primary retinal and RGC-5 cultures. These cultures were exposed to media containing Nogo-P4 at concentrations of 4-40μM. The number of neurons (specifically β-III-tubulin^{+}RGC in the case of primary retinal cultures), longest neurite length per neuron and number of neurites per neuron were measured, averaged and analysed. It is of paramount importance in a neurite outgrowth inhibition assay to inhibit neuritogeneis without cytotoxicity, primarily because neurons undergoing necrosis and apoptosis would not extend neurites, thus neurons in the early stages of necrosis or apoptosis could be mistakenly counted as merely possessing no neurites. As such, an appropriate concentration of Nogo-P4 would be one at which neurite outgrowth was maximally inhibited whilst avoiding any significant neurocytotoxicity.

4.2.1 Nogo-P4 inhibited RGC neuritogenesis at concentrations above 25μM

Primary adult rat retinal cultures were exposed to 25, 30 and 35μM concentrations of recombinant Nogo-P4. Each of these concentrations dramatically reduced the mean number of neurites per RGC (Figure 4.2). The mean number of neurites per RGC for the PDL – laminin control was 0.63± 0.08 whereas RGC in the 25, 30 and 35μM treatment groups had mean neurite numbers of 0.08± 0.04, 0.16± 0.08 and 0.12 ± 0.05 respectively.

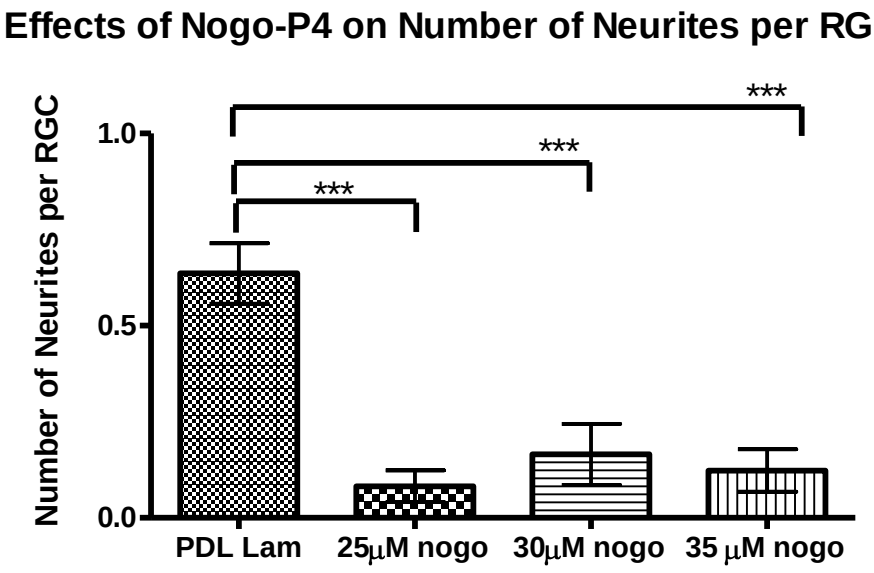

Figure 4.2. Nogo P4 peptide significantly reduced RGC neuritogenesis. Nogo P4 peptide inhibited RGC neurite number at concentrations of 25, 30 and 35μM. Error bars represent 95% confidence intervals. n = 4 for all groups.
*** = p value of <0.001.

4.2.2 Nogo-P4 attenuated RGC neurite length

Primary adult rat retinal cultures were exposed to 25, 30 and 35μM concentrations of recombinant Nogo-P4. Each of these concentrations dramatically reduced the mean longest neurite length per RGC (Figure 4.3). The mean length of the longest neurite per RGC for the PDL – laminin control was 28.1± 5.4 μm whereas RGC in the 25, 30 and 35μM Nogo-P4 treatment groups had mean longest neurites of 2.2 ± 2.1 μm, 4.2 ± 2.4 μm and 4.2± 2.3 μm respectively.

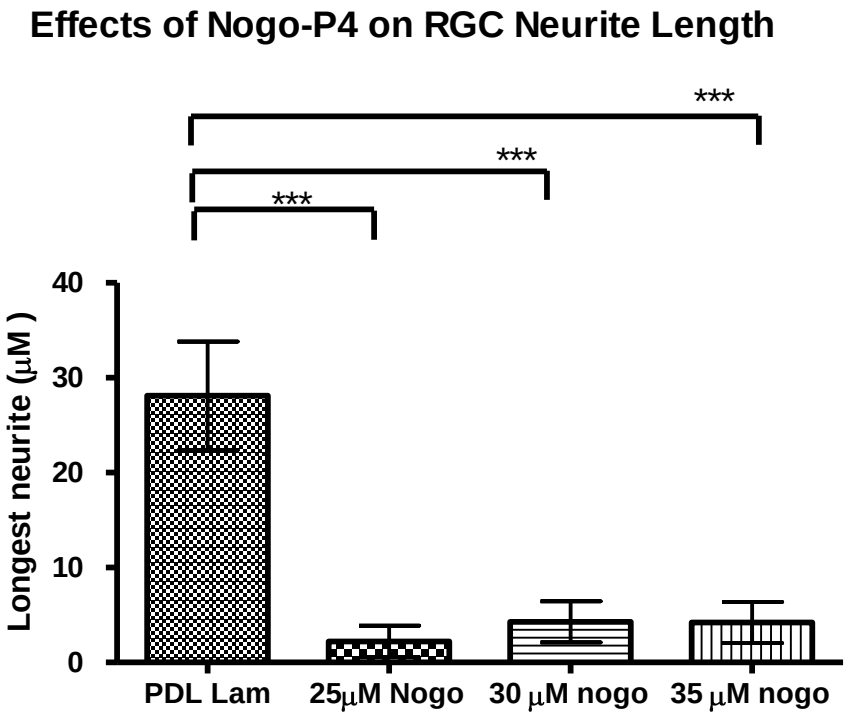

Figure 4.3. Nogo P4 peptide significantly reduces RGC longest-neurite length. Nogo P4 peptide inhibited RGC neurite outgrowth at concentrations of 25, 30 and 35μM. Error bars represent 95% confidence intervals.
n = 4 for all groups. *** = p value of <0.001.

4.2.3 Nogo-P4 was cytotoxic to RGC at 30µM and 35µM but not at 25µM

Primary adult rat retinal cultures were exposed to 25, 30 and 35µM concentrations of recombinant Nogo-P4. 30 and 35 µM concentrations of Nogo-P4 significantly reduced RGC numbers compared to PDL – laminin only controls whereas 25µM Nogo-P4 did not (figure 4.4). The mean number of RGC per field of view was 2.23± 0.3 for the PDL-laminin control group and 1.88± 0.28, 1.58± 0.28 and 1.70± 0.26 for the 25µM, 30µM and 35µM groups respectively. As 25µM Nogo-P4 was non-cytotoxic yet still significantly inhibited neurite number and neurite length (figures 4.5 and 4.6 respectively), it was decided that all future neurite outgrowth inhibition assays would use Nogo-P4 at a maximum concentration of 25µM.

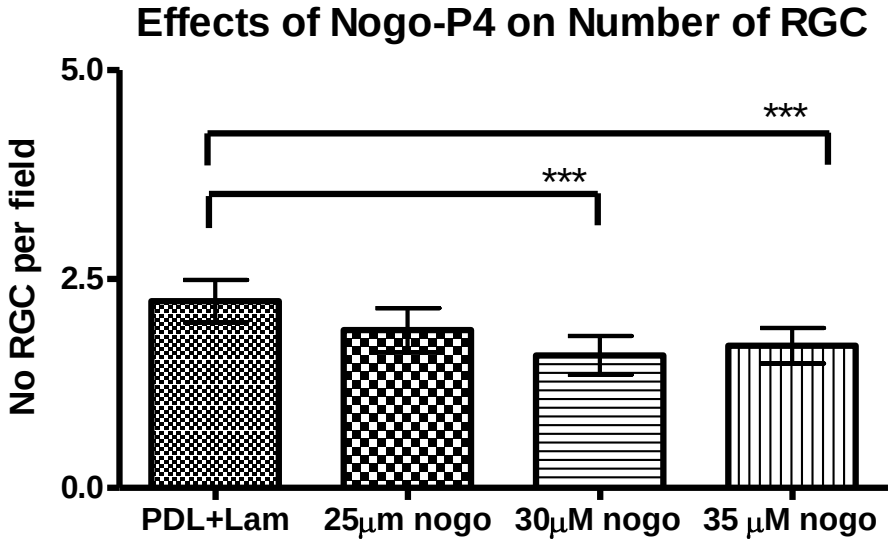

Figure 4.4. Effects of NogoP4 peptide on RGC survival *in vitro*. Nogo P4 peptide was toxic to RGC at 35 and 30µM but not at 25µM. Error bars represent 95% confidence intervals. n = 4 for all groups.
*** = p value of <0.001.

4.2.4 Nogo-P4 peptide did not affect RGC-5 cell survival

The RGC-5 cell line has been used to replicate primary cultured RGC *in vitro.* Here, it was shown that concentrations of Nogo-P4 up to and including 40μM had no effect of RGC-5 cell number (figure 4.5). Concentrations of 4, 10, 20 and 40μM Nogo-P4 peptide did not significantly affect the mean number of RGC-5, indicating that Nogo-P4 peptide at up to 40μM was not cytotoxic to RGC-5 cells. Mean number of RGC-5 per field of view for PDL – Laminin control was 3.4 ± 1.2 and no treatment group significantly differed from this.

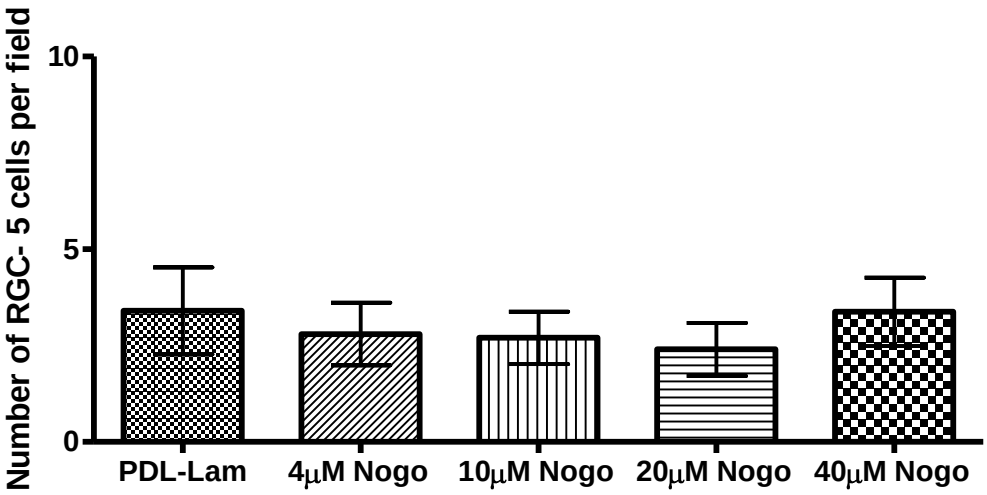

Figure 4.5. Nogo P4 peptide had no effect on survival of the RGC-5 cell line. Concentrations of Nogo P4 up to and including 40μM did not alter RGC-5 number. Error bars represent 95% confidence intervals. n = 5 for all groups.

4.2.5 Nogo-P4 peptide did not affect the mean number of RGC-5 neurites

Mean RGC-5 neurite number (i.e. mean number of neurites per cell) was not affected by concentrations of Nogo-P4 up to and including 40μM (figure 4.6). Mean number of neurites per RGC-5 for the control PDL – laminin group was found to be 3.12 ± 0.4. No treatment group exhibited a mean significantly different to this value.

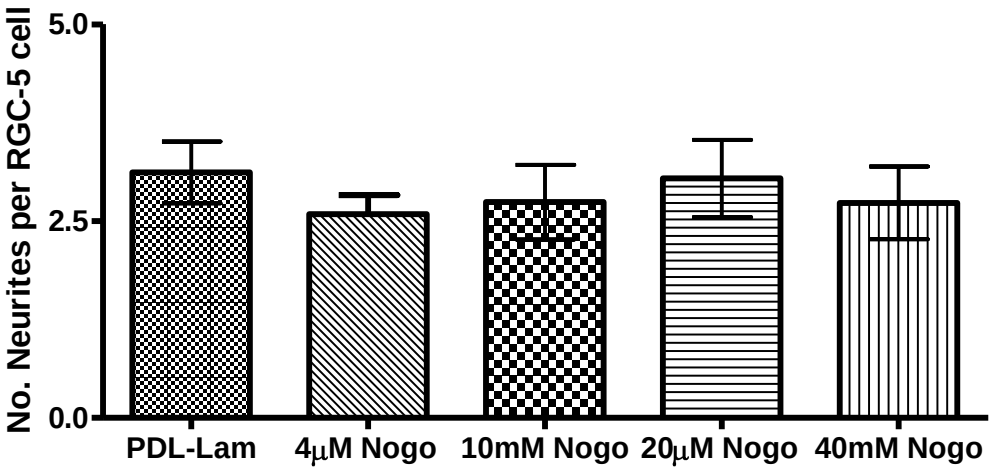

Figure 4.6. Nogo-P4 peptide had no effect on RGC-5 neuritogenesis. Concentrations of Nogo-P4 up to and including 40μM did not alter the number of neurites per RGC-5 cell. Error bars represent 95% confidence intervals. n = 5 for all groups.

4.2.6 Nogo-P4 peptide did not affect RGC-5 longest neurite length

Concentrations of Nogo-P4 up to 40μM did not affect the mean length of RGC-5 longest neurite. Mean longest neurite per cell was 100 ± 17 μm for the PDL – laminin control group and none of the treatment groups' neurite outgrowth deviated significantly from this value (Figure 4.7). This result combined with the lack of effect on neurite number

(Figure 4.8) indicated that Nogo-P4, in concentrations up to 40µM, had no significant effect on RGC-5 neuritogenesis. Almost all RGC-5 cells were observed to possess multiple, extensive neurites, irrespective of treatment group.

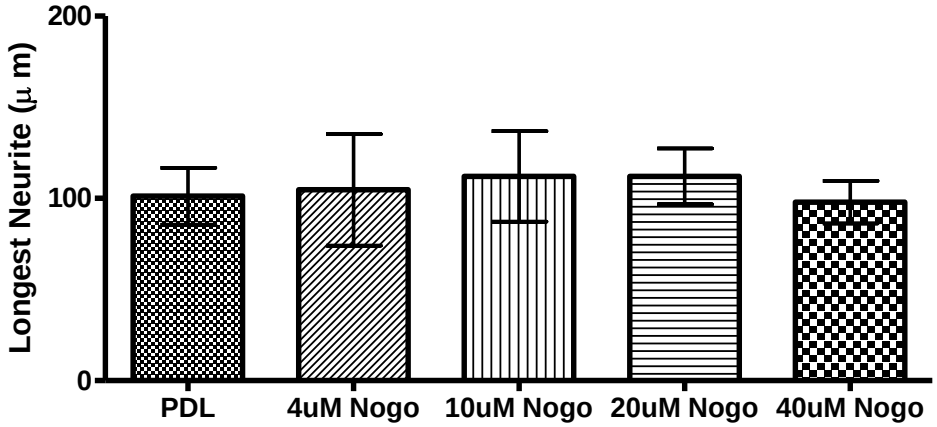

Figure 4.7. Nogo P4 peptide had no effect on RGC-5 neurite length. Concentrations of Nogo-P4 up to and including 40µM did not alter the length of RGC-5 cell neurites. Error bars represent 95% confidence intervals. n = 5 for all groups.

4.2.7 100nM AG1478 abolished the neurite number inhibitory effects of Nogo-P4 in primary retinal cultures and this effect was partially attenuated by the Adenosine A2A receptor antagonist ZM21385

Mean number of neurites per RGC for PDL – laminin control was 0.497± 0.05, mean number of neurites per RGC for Nogo, AG1478, Nogo+AG and Nogo+AG+ZM groups were 0.23 ± 0.04, 0.61 ± 0.09, 0.53 ± 0.07 and 0.36 ± 0.09 respectively (Figure 4.8). 25µM Nogo-P4 significantly inhibited RGC neuritogenesis (red column) whereas 100nM AG1478 elicited a modest but statistically significant increase in RGC neurite number (blue column). Nogo+AG treated RGC (red and black column) exhibited similar neurite

outgrowth to PDL-laminin control, indicating that AG1478 completely abolished the growth inhibitory effects of Nogo-P4. Interestingly 50nM ZM21385 significantly abrogated the disinhibitory effects of AG1478 on Nogo-P4 mediated neurite outgrowth inhibition (green column).

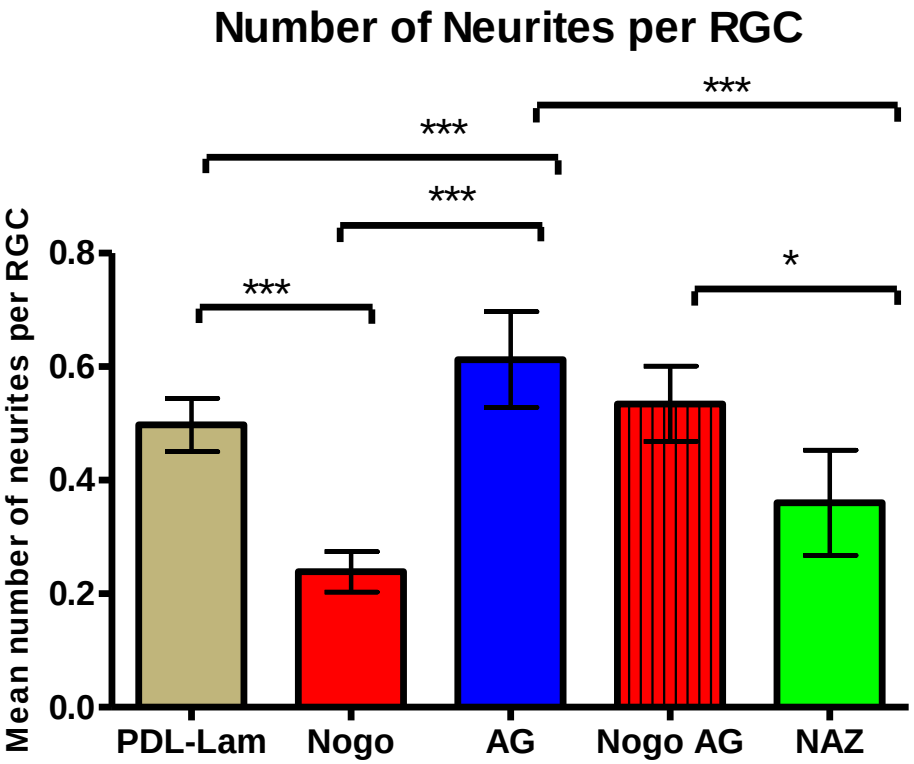

Figure 4.8. Effects of treatments on mean RGC neurite number. 25µM Nogo P4 peptide significantly reduced RGC neurite number (red column), whereas 100nM AG1478 promoted a slight but significant increase in neurite number (blue column). Nogo-P4mediated neuritogenic inhibition was abolished by AG1478 (red striped column), and this abrogation was itself partially attenuated by the addition of 50nM of the adenosine A2A receptor antagonist ZM21385 (green column). Error bars represent 95% confidence intervals. n = 4 for all groups except NAZ, wherein n = 3. * = p value of <0.05, ** = p value of <0.01, ***= p value of less than 0.001

4.2.8 100nM AG1478 abolished the RGC neurite outgrowth inhibitory effects of Nogo-P4 and significantly enhanced mean longest neurite length

Mean longest neurite length per RGC for PDL – laminin control was 19.11 ± 2.5µm, mean longest neurite length per RGC for Nogo, AG1478, Nogo+AG and Nogo+AG+ZM groups were 8.01 ± 1.6µm, 28.92 ± 6.6µm, 21.21 ± 3.6µm and 15.14 ± 5.1µm respectively (Figure 4.9). 25µM Nogo-P4 significantly inhibited RGC longest neurite length (red column) whereas 100nM AG1478 elicited a modest but statistically significant increase (blue column) compared to PDL – laminin control. Nogo+AG treated RGC (red and black column) exhibited similar mean neurite length to PDL-laminin control, showing that AG1478 completely abolished the growth inhibitory effects of Nogo-P4. ZM21385 did not significantly abrogate the ability of AG1478 to rescue Nogo-P4 mediated neurite outgrowth inhibition (green column), a result at odds with the inhibitory effect of ZM on "mean neurite number" parameter (see Figure 4.8). Figure 4.9b shows representative images of RGC neurite outgrowth in each treatment group.

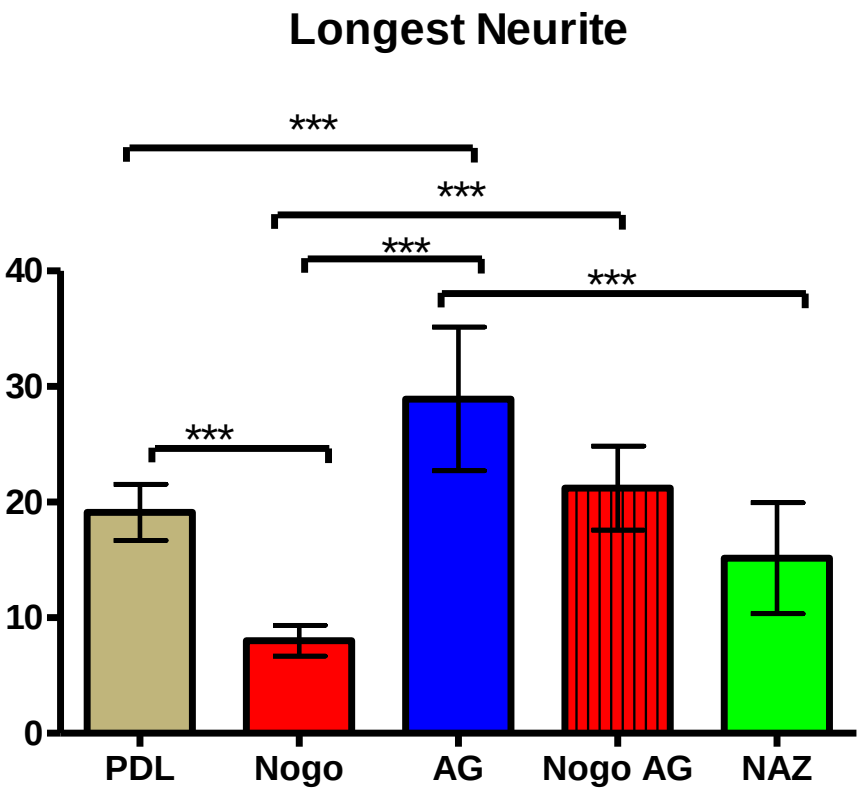

Figure 4.9. Effects of various treatments on RGC neurite length. 25µM Nogo P4 peptide significantly reduced RGC neurite outgrowth (red column), whereas 100nM AG1478 promoted a significant increase in neurite length (blue column). Nogo-P4 mediated neuritogenic inhibition was abolished by AG1478 (red striped column). 50nM ZM21385 (green column) did not prevent AG1478 from disinhibiting RGC in the presence of Nogo-P4. Error bars represent 95% confidence intervals. n = 4 for all groups except NAZ, wherein n = 3. ***= p value of less than 0.001.

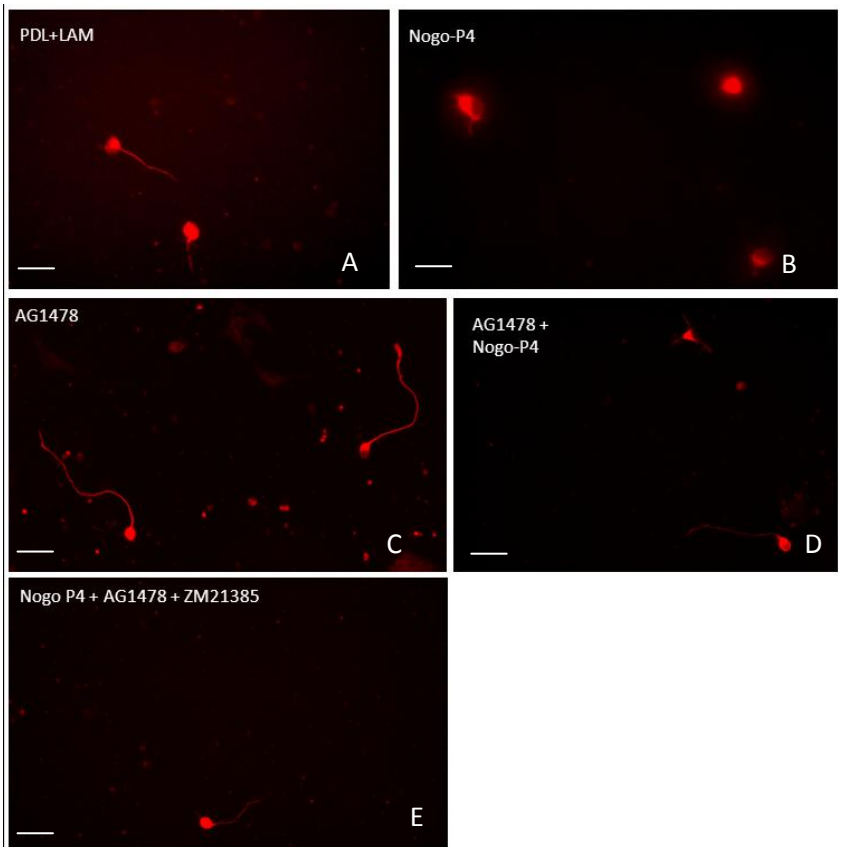

Figure 4.9b. Representative images of RGC neurite outgrowth. B-III^{+}RGC (red) in primary retinal cultures exhibit inhibited neurite outgrowth in the presence of Nogo-P4 (B) compared to untreated control cultures (A). AG1478 elcits modestly increased neurite outgrowth (C) compared to control (A) and abrogates the outgrowth inhibitory effects of Nogo-P4 (D). The adenosine A2A receptor antagonist ZM21385 may partially reduce the extent of this AG1478-mediated rescue of Nogo-P4 inhibition (E) (see figures 4.8 and 4.9 and accompanying text for details). Scale bar = 40µm apart from (B) where scale bar = 20µm.

4.2.9 RGC survival was not affected by 25µMNogo-P4, 100nM AG1478 nor 50 nM ZM21385

Mean number of RGC per field of view for PDL – laminin control was 2.86 ± 0.3. Mean number of RGC for AG1478, Nogo-P4, AG+Nogo and AG+Nogo+ZM treatment groups were 3.07 ± 0.33, 2.58 ± 0.36, 2.37 ± 0.25 and 2.72 ± 0.44 respectively. None of these values were significantly different from control (figure 4.10). From this it can be seen that no treatment group caused RGC cell death.

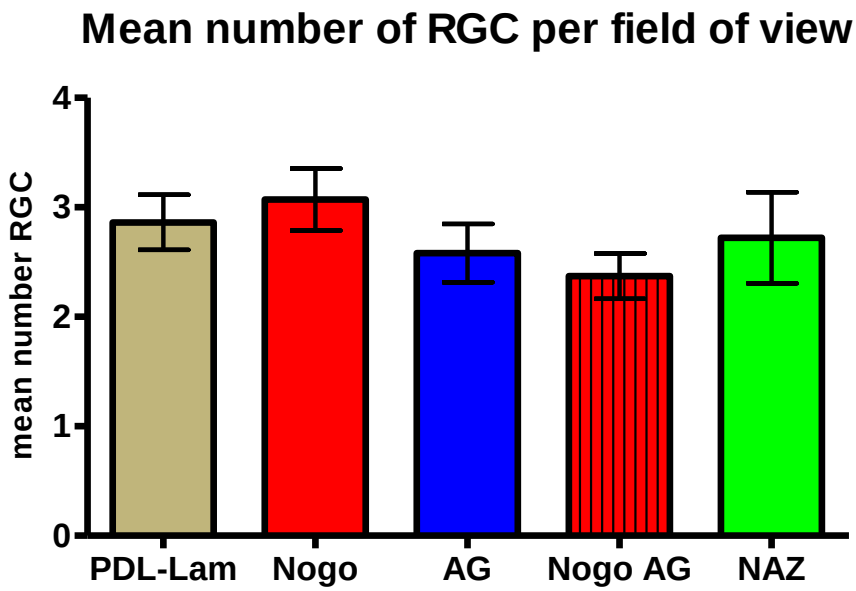

Figure 4.10. Effects of various treatments on RGC survival. RGC survival was not affected by any of the treatment groups. No treatment group exhibited any significant difference in RGC number compared to PDL Laminin control. Error bars represent 95% confidence intervals. n = 4 for all groups except NAZ, wherein n = 3.

4.2.10 Conditioned media collected from primary retinal cultures did not contain detectable amounts of CNTF, NT-3 or GDNF

Conditioned media were taken from all primary retinal cultures used to generate figures 4.8 – 4.10. This media was concentrated (see Chapter 2 for details) and these samples were used in ELISAs for CNTF, NT-3 and GDNF (Figure 4.11). No CNTF, NT-3 or GDNF was detected in the conditioned media of any of the treatment groups. Relevant NTF standards supplied with ELISAs confirmed that the assays were performed correctly; ensuring that absence of signal did in fact reflect absence of NTF.

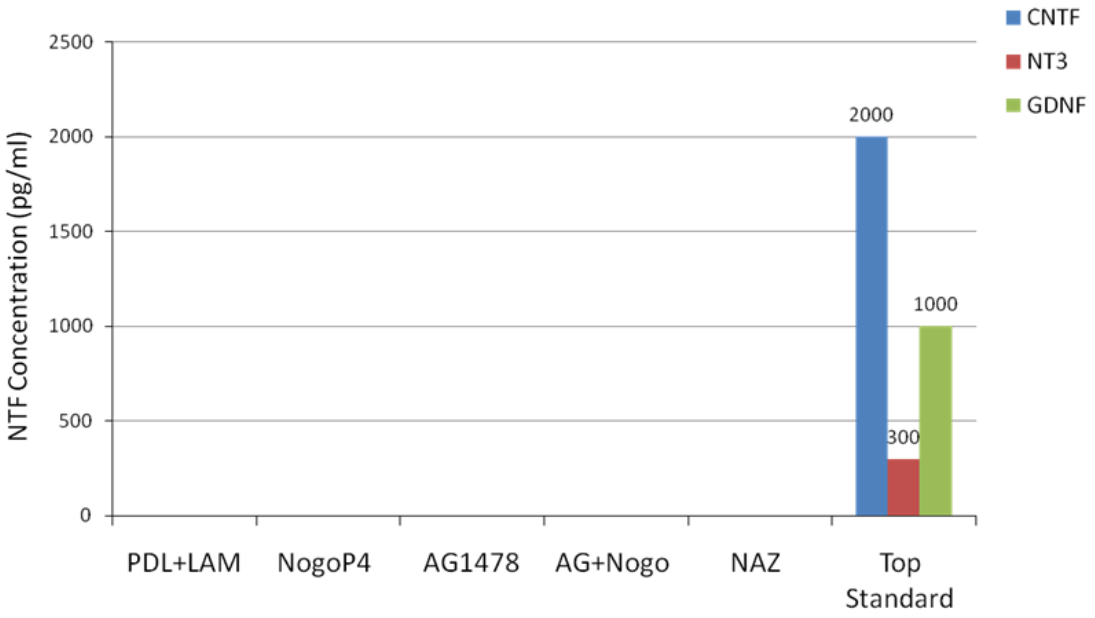

Figure 4.11. Combined results of ELISAs for CNTF (blue column), NT3 (red column) and GDNF (green column) on concentrated conditioned media from primary retinal cultures exposed to various treatments. No CNTF, NT3 or GDNF was detected in the conditioned media from any of the treatment groups, but this may be due to insufficient concentrating of conditioned media (see text for details). n = 4 for all groups except NAZ wherein n = 3. Standards are recombinant versions of respective NTF protein supplied with respective ELISA kits and show that all reagents were working correctly allowing lack of signal for any treatment group to be reliably inferred as reflecting a lack of the appropriate NTF in the conditioned media assayed. The 'top standard' group shows the highest detected concentration of these recombinant protein standards.

4.2.11 Previous experiments detected NTF in the conditioned media from AG1478 treated primary retinal cultures

Although Figure 4.11 shows that no NTFs were detected in the conditioned media of primary retinal cultures exposed to AG1478 in the present experimental series, Drs Z. Ahmed and M. Douglas previously detected physiologically relevant levels of NGF, BDNF and NT-3 in similarly treated retinal cultures. Having obtained express permission, Figure 4.12 shows the levels of NTF they detected in conditioned media from AG1478 and non-AG1478 treated cultures. NT-3, BDNF and NGF were all present in AG1478 treated culture media but absent in non AG1478 treated control culture media.

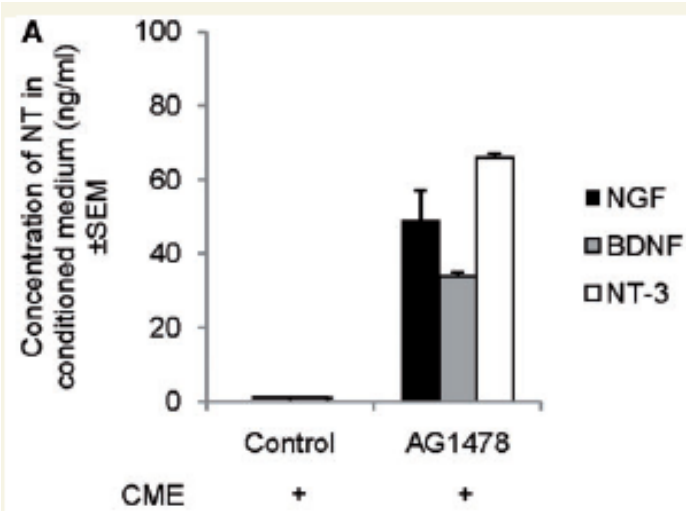

Figure 4.12. ELISA results for NGF, BDNF and NT-3 in conditioned media from AG1478+CNS Myelin Extract treated retinal cultures. NGF, BDNF and NT-3 were all found to be present at physiological concentrations in AG+Myelin treated cultures. Untreated control cultures were found not to contain NGF, BDNF or NT-3. Experimental result and figure courtesy of Dr Zubair Ahmed and Dr Mike Douglas, University of Birmingham.

4.2.12 PCR on control retinal culture lysate detected BDNF and NT-3

Following RT-PCR to obtain DNA, PCR was performed on lysate from the cells in untreated, control, retinal cultures, using forwards and backwards primers for BDNF, CNTF, NGF, NT-3, NT-4 and the housekeeping gene GAP-dh (Figure 4.13). Clear bands visualised at the correct size for BDNF and NT-3 indicated that the RNA for both these neurotrophins was expressed by cells within control retinal cultures, and thus strongly suggested that the proteins BDNF and NT-3 were expressed. No bands were detected for CNTF, NGF or NT-4. Although this result could suggest that these factors were not present in control retinal cultures, the fact that no band was detected in either AG1478 treated culture lysates (Figure 4.14) nor in whole rat brain lysate (Figure 4.15) strongly suggested that one or both of the primers for each of these failed to function.

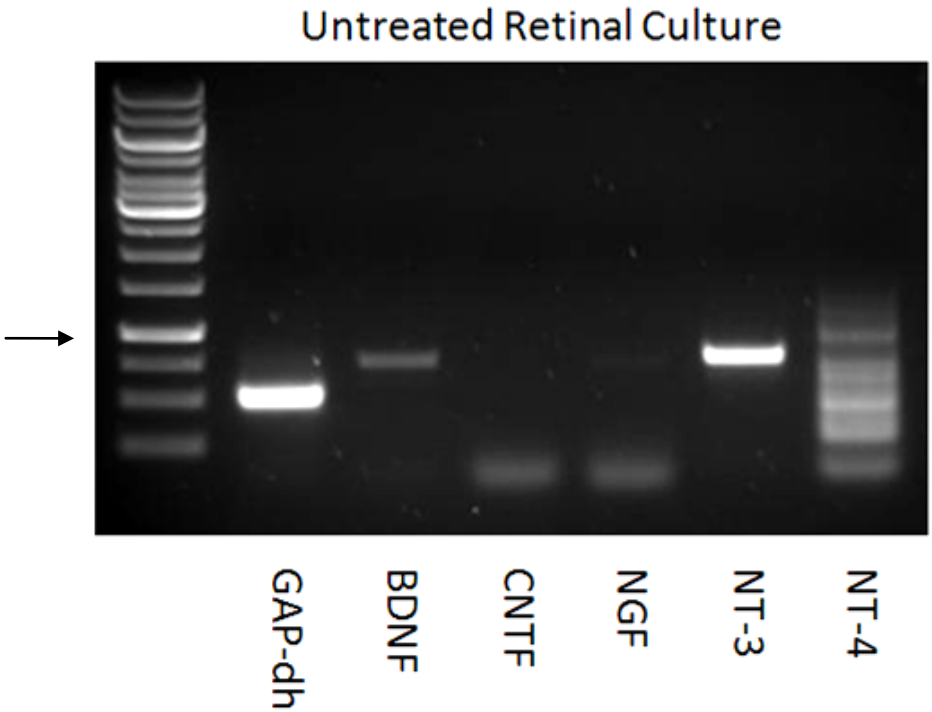

Figure 4.13. PCR results from untreated retinal culture lysate, using primers for BDNF, CNTF, NGF, NT-3, NT-4 and the house keeping gene GAP-dh. Bands for CNTF, NGF and NT-4 were not observed, whereas clear bands were observed for both NT-3 and BDNF as well as the housekeeping gene GAP-dh. Arrow indicates molecular weight band signifying 1000 base pairs.

4.2.13 PCR on AG1478 treated retinal culture lysate detected BDNF and NT-3

Following RT-PCR to obtain DNA, PCR was performed on lysate from AG1478 treated retinal cultures, using forwards and backwards primers for BDNF, CNTF, NGF, NT-3, NT-4 and the housekeeping gene GAP-dh (Figure 4.14). Clear bands at the correct size for BDNF and NT-3 indicated that the RNA for both these neurotrophins was expressed by cells within AG1478 treated retinal cultures, and thus strongly suggested that the proteins BDNF and NT-3 were expressed. Again, no bands were detected for CNTF, NGF or NT-4, suggesting that one or both of the primers for each of these failed to function.

.

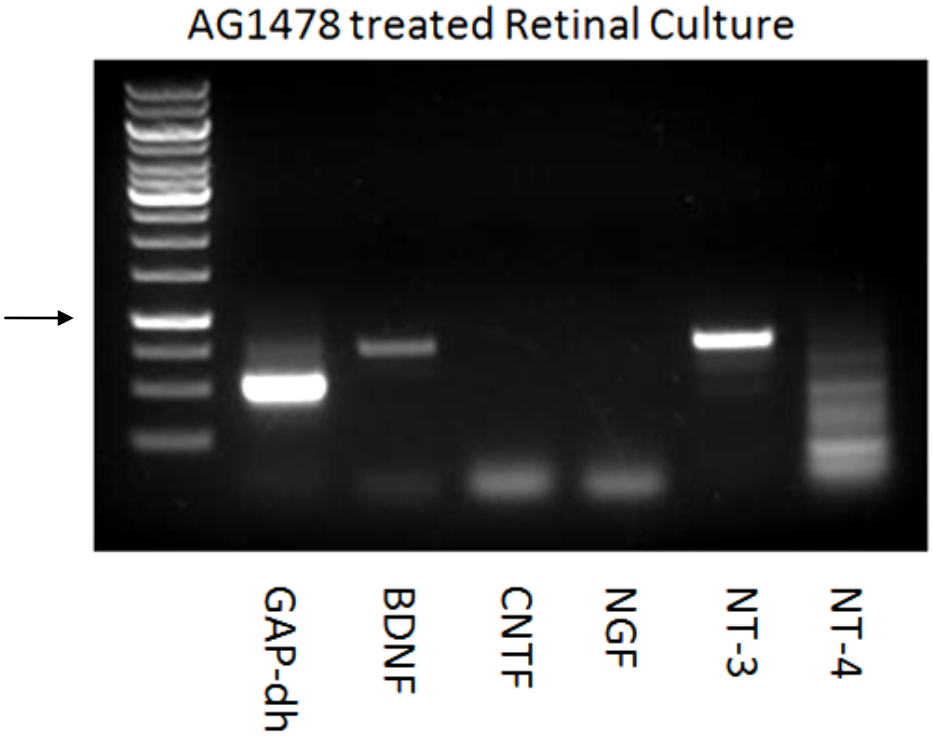

Figure 4.14. PCR results from AG1478 treated retinal culture lysate, using primers for BDNF, CNTF, NGF, NT-3, NT-4 and the house keeping gene GAP-dh. Bands for CNTF, NGF and NT-4 were not observed, whereas a clear band was observed for both NT-3 and BDNF as well as the housekeeping gene GAP-dh. Arrow indicates molecular weight band signifying 1000 base pairs.

4.2.14 PCR on whole rat brain lysate detected BDNF and NT-3

Following RT-PCR to obtain DNA, PCR was performed on whole rat brain lysate, using forwards and backwards primers for BDNF, CNTF, NGF, NT-3, NT-4 and the housekeeping gene GAP-dh (Figure 4.15). Clear bands at the correct size for BDNF and NT-3 indicated that the RNA for both these neurotrophins was expressed by cells in the rat brain, and again strongly suggested that the proteins BDNF and NT-3 were expressed. That, once again, no bands were detected for CNTF, NGF or NT-4 suggested that one or both of the primers for each of these failed to function, particularly as the rat brain is known to contain both NGF and NT-4. Note the increased brightness of the band signifying BDNF (red box) compared to that seen in the culture lysate groups.

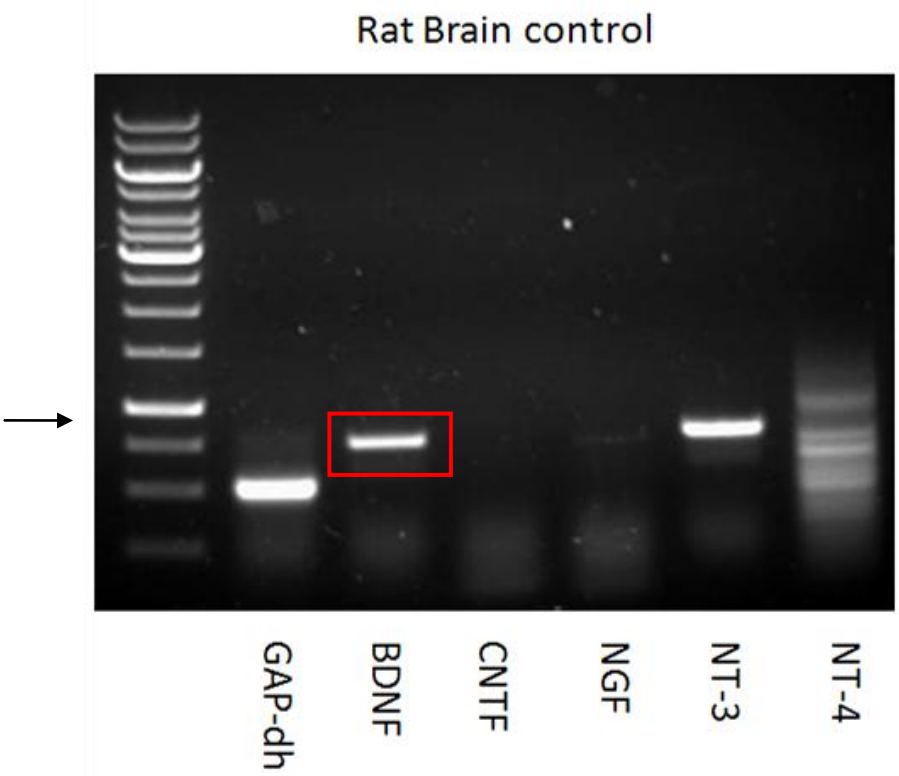

Figure 4.15. PCR results from control rat brain lysate, using primers for BDNF, CNTF, NGF, NT-3, NT-4 and the house keeping gene GAP-dh. Rat brain is known to contain each of the above proteins and as such absence of predicted bands for individual DNA stretches strongly suggested that the relevant primer did not function correctly. CNTF, NGF and NT-4 Primers appeared not to function correctly, whereas a clear band was obtained for BDNF, NT3 and the housekeeping gene GAP-dh. Arrow indicates band signifying 1000 base pairs.

4.2.15 Immunocytochemistry confirmed the presence of NGF in RGC

As NGF was not detected by PCR, yet was detected by ELISA by others (see figures 4.11-4.12) it was decided to attempt to visualise NGF immunocytochemically on RGC in AG-treated and non-AG treated retinal cultures using a well characterised antibody to NGF. NGF was detected on β-III-tubulin^{+} RGC somata and neurites both without (A) and with (B) 100nM AG1478, and no signal was observed in the no primary control (C) (Figure 4.16).

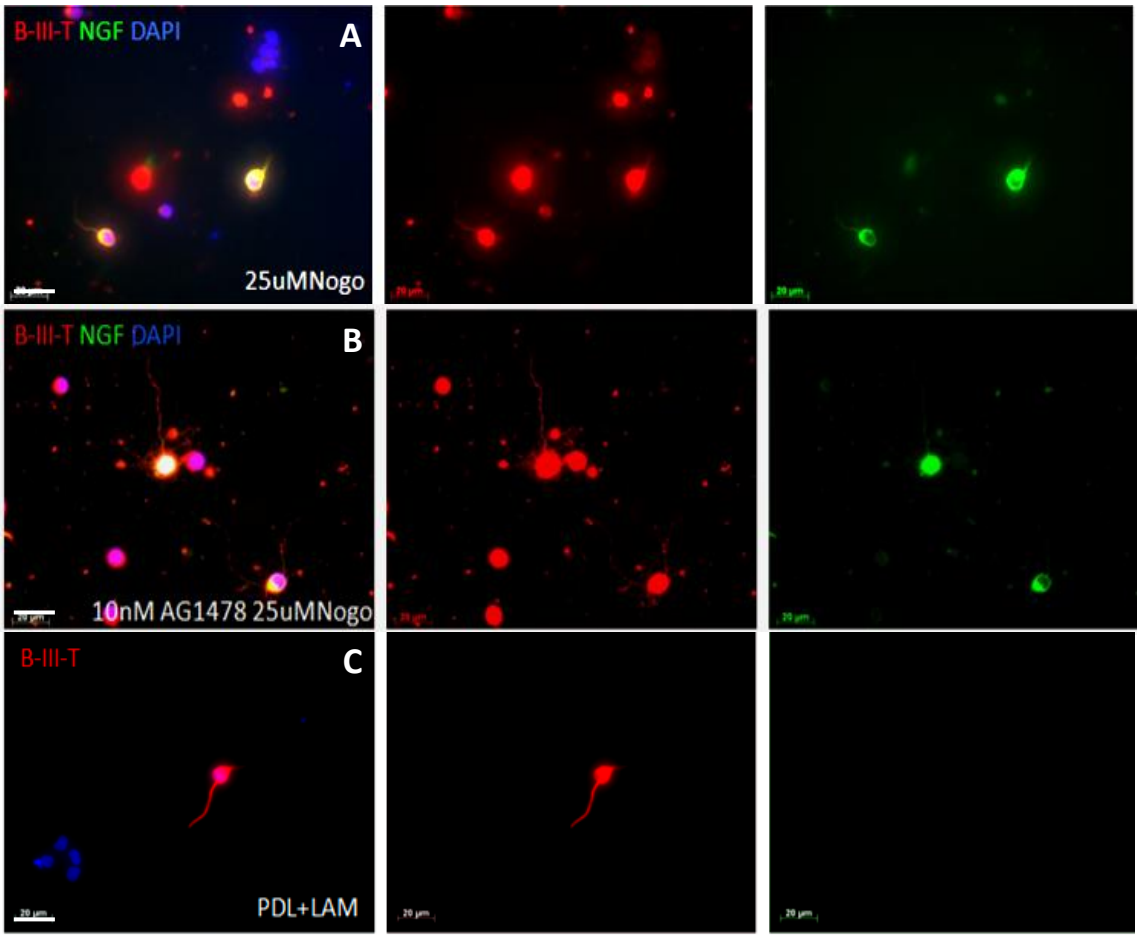

Figure 4.16. Immunocytochemistical staining for the RGC marker β-III-Tubulin (red) and NGF (green) in Nogo-P4 treated cultures without (A) and with (B) 100nM AG1478. (C) No primary antibody control for NGF antibody. NGF is present both before and after AG1478 exposure, in both somata and neurites. DAPI stained nuclei are blue. Scale bar = 20µm.

4.3 Discussion

4.3.1 Nogo-P4 dramatically inhibited RGC neuritogenesis

While Nogo-P4 significantly inhibited cultured primary RGC neurite outgrowth at concentrations of 25, 30 and 35µM, concentrations above 25µM proved cytotoxic, making it difficult to differentiate between genuine neurite growth inhibition and a lack of neurites due to ongoing apoptosis/necrosis. At 25µM Nogo P4 attenuated mean RGC neurite number as effectively as at 30µM and 35µM but without causing significant cell death (mean of 0.08 neurites per RGC compared to 0.63 neurites per RGC in the untreated control group). It appears that only one previous study (Wang and Zhu, 2008) has used recombinant Nogo-P4 to inhibit neurite outgrowth and, while this study also found Nogo-P4 to be antagonistic to neurite outgrowth at as little as 4µM, these neurons were derived from one day postnatal neuronal precursor cells taken from the rat spinal cord. Additionally the precursor cells were allowed to differentiate in the presence of Nogo P4 and/or differentiated neurons were exposed to the peptide at 3 days post plating; making these cells effectively postnatal day 3 neurons.

4.3.3 Nogo-P4 was cytotoxic to RGC at 30µM and 35µM but not at 25µM

Nogo-P4 caused significant RGC death at concentrations of 30 and 35µM, reducing mean number of RGC per field of view from 2.23 for the untreated control group to 1.58 and 1.70 respectively. The 25µM Nogo-P4 treated group exhibited mean number of RGC per field of view of 1.88; not significantly different from the untreated control. It is possible that at concentrations of above 25µM the Nogo peptide itself became cytotoxic to RGC, although there does not appear to be any direct link between NgR signalling and RGC cell death (in fact at least one study has suggested that NgR signalling can in fact be neuroprotective by sequestering $P75^{NTR}$ and rendering it unable to initiate apoptosis; Dupuis *et al.* 2008). It is also possible that severely restricting neurite outgrowth prevented dissociated RGC from establishing contact with adjacent glia, thus denying RGC contact-dependent NTF support and/or that Nogo-P4 above 25µM somehow affected glial survival or function (glial cell numbers were not investigated in any of these experiments). Nevertheless, it was found that 25µM Nogo-P4 strongly inhibited RGC neurite outgrowth and elongation without causing significant RGC death. This formed the basis of a RGC neurite outgrowth inhibitory assay which was subsequently used to examine the effects of the EGFRki, AG1478, on RGC neurite outgrowth.

4.3.4 Nogo-P4 drastically attenuated RGC neurite length

While 25, 30 and 35µM Nogo P4 inhibited RGC mean longest neurite length equally well (no significant difference was seen in mean longest neurite length between any of the three), only 25µM Nogo-P4 did so without causing significant RGC death - mean longest

neurite length of 2.2µm compared to 28.1µm for untreated control group. Along with the aforementioned non-cytotoxic blockade of neuritogenesis, this showed the potential of Nogo-P4 to form the basis of an excellent *in vitro* neurite outgrowth inhibition assay.

4.3.5 Nogo-P4 peptide did not affect RGC-5 cell survival

While primary RGC began to die in significant numbers at concentrations of Nogo-P4 above 25 µM, RGC-5 survival was entirely unaffected by Nogo-P4 peptide at concentrations of up to 40µM. This is not unexpected; while 1.07nM staurosporine is enough to cause significant RGC death i*n vivo* (Maass 2007), up to 316 nM staurosporine has been used to differentiate RGC-5 cells, with no reduction in cell number reported (J. o' Neill, unpublished data, Wood *et al.* 2010). That RGC-5 cells *in vitro* were impervious to a potent cytotoxin, present at levels 316 times higher than those required to kill primary RGC *in vivo*, highlights the fundamental difference between the two cell types and further illustrates the unsuitability of RGC-5 for use in a Nogo-P4 based assay.

4.3.6 Nogo-P4 peptide did not affect the mean number of RGC-5 neurites

In contrast to its effects on primary culture RGC, Nogo-P4 peptide failed to inhibit RGC-5 neuritogenesis, at concentrations of up to 40µM. That the mean neurite number per RGC-5 cell was not significantly affected by Nogo-P4, even at levels which proved cytotoxic for neurons in primary culture (see above), suggests that RGC-5 cells are an

unsuitable cell line for use in a Nogo-P4 based inhibitory assay. It is possible that, as an immortalised cell line, the potent growth inhibitory effects of Nogo-P4 seen with primary RGC are mediated by a signalling pathway which has been disrupted by the original transformation of the cells *via* the ψ2 E1A virus (Krishnamoorthy *et al.* 2001) and thus that the signalling cascade beginning with NgR and its coreceptors is interrupted before it reaches the actin cytoskeleton. Alternatively, if RGC-5 cells do not express NgR, the receptor through which Nogo-P4 signals, then Nogo-P4 would be impotent. Recent work within our lab, however, has repeatedly detected NgR on RGC-5 cells *via* immunocytochemistry (O'Neil, unpublished data), so this is unlikely. Another possibility is that the effects of Nogo-P4 are being countered by other factors; it is known that sufficient levels of NTF can overcome the neurite outgrowth inhibitory effects of myelin derived proteins *via* Regulated Intramembraneous Proteolysis (RIP) of the NgR coreceptor $p75^{NTR}$ (Ahmed *et al.* 2006b) so it is possible that RGC-5 cells, which grow continuously in the absence of glia or extraneous NTF support, generate their own NTF, which could potentially neutralise any neurite inhibitory and potentially cytotoxic effects.

4.3.7 Nogo-P4 peptide did not affect RGC-5 longest neurite length

Concentrations of Nogo-p4 up to 40μM did not affect the mean length of longest neurite per RGC-5 cell. As an immortalised cell line, it was perhaps unsurprising that almost all untreated control RGC-5 cells possessed multiple, extensive neurites in the absence of extraneous NTF. These cells, if not differentiated, divide continuously, and once differentiated, continuously extend neurites**.** The fact that neurites extended completely

unchecked for over 100µm, through an environment containing significant levels of an axon growth inhibitory peptide that is cytotoxic to putatively equivalent primary neurons, requires an explanation. As discussed above, it is possible that the immortalisation process altered signalling cascades impinged upon by NgR, such that signalling through NgR and its coreceptors do not effect changes on the cytoskeleton, and/or that RGC-5 produce their own NTFs which abrogate the effects of Nogo-P4 *via* RIP.

4.3.8 100nM AG1478 abolished the RGC neurite outgrowth inhibitory effects of Nogo-P4, and this effect was partially attenuated by 50 nM ZM21385

When exposed to 100nM AG1478 alone, the mean number of neurites per RGC was modestly but significantly higher than PDL-laminin control values; 0.61 to 0.49 respectively. That an EGFRki could elicit significant RGC neurite outgrowth in the absence of AGIM implied some sort of growth stimulatory mechanism of action for AG1478. The mean number of neurites per RGC for Nogo-P4 treated cultures was 0.23, showing the continued effectiveness of Nogo-P4 as a neurite inhibitory agent. Interestingly, AG1478 completely abrogated this effect: retinal cultures exposed to both 25µM Nogo-P4 and 100nM AG1478 exhibited neurite outgrowth at very similar levels to PDL – laminin control cultures, 0.53 neurites per RGC compared to control value of 0.49. This again suggested either a neurite outgrowth inhibitory role for EGFR, potentially as a required part of the inhibitory signalling cascade and/or, again, some novel mechainism of action for AG1478. Interestingly 50nM ZM21385 significantly abrogated AG1478-mediated rescue of Nogo-P4 mediated neurite outgrowth inhibition; mean number of neurites per RGC for the Nogo+AG+ZM21385 group was 0.36, not significantly different to

PDL-Laminin control, significantly lower than AG and Nogo+AG mean values and not significantly different from the 25µM Nogo-P4 treatment group. This synthetic compound, ZM21385, a potent, selective, Adenosine A2A receptor blocker, was included in these experiments to investigate whether the A2A receptor played a role in AG1478 mediated neurite outgrowth, following reports that the A2A receptor could strongly enhance neurite outgrowth and neuronal survival *via* transactivation of the Trk receptors (Jeanneteau and Chao 2006). That pharmacological blockade of a single receptor couldn significantly erode the neuritogenic capabilities of AG1478 implied that the adenosine A2A receptor played a part in whichever signalling pathway(s) AG1478 affected; either as an inhibitor of EGFR signalling or as part of some other off target signalling pathway, possibly involving Trk receptors.

4.3.9 100nM AG1478 abolished the neurite outgrowth inhibitory effects of Nogo-P4 and significantly enhanced longest neurite length

Mean longest neurite length per RGC for PDL – laminin control was 19.11µm. Mean longest neurite length per RGC for Nogo-P4 treated retinal cultures was significantly lower at 8.01µm, again highlighting the efficacy of Nogo-P4 as a neurite outgrowth inhibitory agent. AG1478 treated cultures exhibited mean longest neurite length per RGC of 28.92µm, significantly higher than PDL – laminin control cultures, demonstrating that AG1478 could elicit significant RGC neurite extension. Once again AG1478 completely ameliorated the neurite outgrowth inhibitory effects of Nogo P4 – mean longest neurite value for AG+ Nogo group was 21.21µm, near identical to PDL-laminin control values, implying that EGFR signalling was antagonistic to neurite elongation

and/or that AG1478 enhanced neurite extension *via* some other means. While the Nogo+AG+ZM treatment group showed a trend towards decreased mean longest neurite outgrowth, with a mean longest neurite length of 15.14µm, this was not significantly different from the AG+ Nogo group nor from control cultures. It should be noted that this value of 15.14µm is significantly lower than that of the AG1478 alone treatment group and, given that the SEM was notably larger for this group than for any other (due to an accidentally destroyed chamber slide, the n number for AG+Nogo+ZM group was one less (n = 3 instead of at least 4) it is possible that a real effect would be found if more experimental repeats were performed.

4.3.10 RGC survival was not affected by 25µMNogo-P4, 100nM AG1478 or 50 nM ZM21385

Neither 25µMNogo-P4, 100nM AG1478, 50 nM ZM21385 nor any combination of the three, significantly affected RGC survival, in the form of mean RGC number per field of view. This showed that any antagonistic effects on neuritogenesis and neurite elongation elicited by these compounds, either in concert or singly, were not a result of RGC death.

4.3.11 Conditioned media collected from primary retinal cultures did not contain detectable amounts of CNTF, NT-3 or GDNF

Once the retinal cultures used to obtain the above neurite outgrowth data were ready to be fixed and to undergo immunocytochemical staining, the conditioned media was carefully aspirated from the living cells and stored appropriately. Media was spun at for

10 minutes at 20,000 RPM and supernatant disgarded such that an approximate concentration factor of x 10 was achieved. This concentrated media was then probed using ELISAs designed to detect CNTF, NT-3 and GDNF. No trace of any of these three NTFs was found in any of the treatment or control groups. Absorbance readings from wells containing various dilutions of the standards provided with ELISAs (relevant concentrations of the recombinant NTF in question) proved that all ELISAs were performed correctly and that lack of signal did in fact reflect lack of NTF. In terms of relevance to *in vitro* RGC neurite outgrowth and survival, perhaps the most commonly used exogenous NTFs are CNTF and BDNF, the former for neurite outgrowth and the latter for RGC survival. Previous experiments performed by our group (see below) screened conditioned media from AG1478 treated retinal cultures for NGF, NT-3, and BDNF, finding physiological concentrations of each in the media from AG1478 treated cultures, and finding none in the media from control cultures (see Douglas *et al.* 2009 for data and discussion). For this reason it was assumed that the experiments described here should also have found similar levels of these NTFs so it was decided to ascertain if other NTFs, namely CNTF and GDNF, were present in conditioned media from AG1478 treated cells. When neither of these NTFs were detected, the ELISA for NT-3 was performed on samples of the same media. These too detected no NTF, suggesting that the conditioned media used latterly in the above experiments was not adequately concentrated (see section below).

4.3.12 Previous experiments detected NTFs in AG1478 treated retinal cultures

Although the above experiments detected no NTFs in the conditioned media of primary retinal cultures exposed to AG1478, previous experiments, specifically performed by Dr Z Ahmed and Dr M Douglas, detected physiologically relevant levels of NGF, BDNF and NT-3 in similarly treated retinal cultures. NT-3, BDNF and NGF were all present in AG1478 treated culture media but absent in non AG1478 treated control culture media (see Douglas *et al.* 2009). The concentration regime followed by Douglas *et al.* included the culturing of large numbers of whole retinal cultures, each split in half in two large petri dishes and treated with 5 hour pulses of AG1478, and the collection of up to 5 ml of media per experiment. These cultures were treated identically to the cultures used to generate neurite outgrowth data, except that larger populations of cells were used: the entire dissociated retina being split into two populations of around 1.5 million cells. After multiple repeats, upwards of 25 mls of media from each group were concentrated down to around 1 ml and ELISAs were performed on this concentrated medium. The experiments performed as part of this study, used only the conditioned media from the actual cultures of ~125,000 cells used to generate the *in vitro* data shown above, and as mentioned, involved concentrating these media by a factor of 10. Although the difference in concentration between the two sets of experiments is only x 2.5 (x 10 vs x 25) the relatively small volume of media collected by myself compared to that obtained by Ahmed and Douglas could have prevented me from detecting NTFs due to their relatively low abundance. However, each of the ELISAs used was sensitive enough to detect picograms of NTF; and the levels detected by Ahmed and Douglas were on the

order of tens of nanograms. This is a difference of around 3 orders of magnitude, which should have been easily enough to overcome these differences in volume and concentration of media.

4.3.13 RT-PCR on control retinal culture lysate detected BDNF and NT-3 mRNA

As ELISAs failed to detect NTF it was decided to attempt NTF mRNA detection in whole retinal culture lysate using RT-PCR. Following total RNA extraction and conversion to DNA, sets of NTF-specific forward and reverse primers (oligonucleotides) were used in an attempt to detect and amplify BDNF, NGF, NT-3 and NT-4 and the housekeeping gene GAP-dh . Clear bands at the correct size for BDNF and NT-3 mRNA indicated that the RNA for both these neurotrophins was expressed by cells within control retinal cultures, strongly suggestding that the proteins BDNF and NT-3 were expressed. No bands were detected for CNTF, NGF or NT-4 mRNA. Although this could suggest that these factors were not present in control retinal cultures, the fact that no band was detected in either AG1478 treated culture lysates nor in whole rat brain lysate strongly suggests that one or both of the primers for each of these failed to function. The detection by PCR of NT-3 mRNA in retinal lysates when no NT-3 was found *via* ELISA suggests either a) that NT-3 was present in amounts too small to detect with ELISA, b) that NTFs were being synthesized but not secreted or c) that the original RNA was transcribed but no protein was produced. By extension, it is possible that the other NTFs which were screened for and not detected by ELISA, namely CNTF and GDNF, were not detected for similar reasons. That NGF, another NTF detected with ELISAs on retinal culture conditioned

media by Ahmed and Douglas, was detected immunocytochemically in retinal cultures (see below,) lends credence to the idea that collected media contained insufficient amounts of NTF for detection by these methods.

4.3.14 RT PCR on AG1478 treated retinal culture lysate detected BDNF and NT-3 mRNA

As in the control group, clear bands at the correct size for BDNF and NT-3 mRNA indicated that the RNA for both these neurotrophins was expressed by cells within AG1478-treated retinal cultures, suggesting that the proteins BDNF and NT-3 were expressed. Once again, no bands were detected for CNTF, NGF or NT-4, implying that one or both of the primers for each of these failed to function. As in the control group, the detection by PCR of NT-3 mRNA in retinal lysates when no NT-3 was found *via* ELISA suggests that NT-3 may have been present in conditioned media in amounts too small to detect with ELISA.

4.3.15 RT PCR on whole rat brain lysate detected BDNF and NT-3 mRNA

The whole rat brain lysate group was included as a tissue control. As the brain contains large amounts of nearly every NTF known (with the possible exception of CNTF, but see Yang *et al.* 2008 for recent evidence of CNTF in the adult rat subventricular zone), any failure to detect the mRNA of a specific NTF in whole brain lysate could more reliably be said to be due to experimental error. As the predicted bands for CNTF, NGF and NT-4 mRNA were not obtained from rat brain lysate, whilst those bands representing BDNF and NT-3 mRNA were obtained, it is likely that the specific primers for CNTF, NGF and NT-

4 mRNA failed to function. There is then strong evidence that the lack of corresponding bands for both the AG-treated and the control retinal lysates reflect this primer failure.

4.3.16 Immunocytochemistry confirmed the presence of NGF in RGC

As ELISA and PCR failed to verify the presence of NGF in AG1478 treated RGC it was decided to attempt to visualise this NT immunocytochemically. NGF was observed on all RGC in both the control and the AG-treated primary retinal cultures. At least one other study has immunocytochemically detected NGF on RGC in primary culture (Agarwal *et al.* 2007), which suggests that either NGF was synthesised but not released by RGC or that NGF was released but was not detected *via* ELISA. As others have detected NGF in AG-treated-RGC conditioned media (Douglas *et al.* 2009) the latter explanation seems likely. It should be noted however that the aforementioned study did not detect NGF (nor BDNF, nor NT-3) in the conditioned media taken from non-AG-treated, control cultures. Although it is possible that AG1478 elicits the release of previously synthesised NGF from RGC, it is perhaps more likely that AG1478 stimulates NGF release from glia. To this end co-immunocytochemical staining using antibodies raised against retinal glial markers, such as GFAP, as well as anti-NGF antibodies, would confirm the presence or absence of glial NGF in such cultures.

4.3.17 Interim Conclusions

The purpose of this series of experiments was to investigate the actions of AG1478 *in vitro*, in an attempt to confirm the EGFRki-meditated neurite outgrowth disinhibition reported by Koprivica *et a* (2005). To this end a neurite outgrowth inhibitory assay was designed. Based on the synthetic Nogo-P4 peptide, this assay was intended to serve as an *in vitro* model of the inhibitory environment within the adult mammalian CNS. With this in place it was then possible to investigate the putative RGC neurite outgrowth disinhibitory effects of AG1478. Preliminary experiments with Nogo-P4 on primary retinal cultures and the RGC-5 cell line yielded interesting results. Primary RGC were significantly affected by concentrations of Nogo-P4 above 25µM, with neurite number and length being drastically attenuated. Unfortunately 30µM and 35µM Nogo-P4 caused moderate but significant RGC death, making it very difficult to confidently ascribe attenuated neurite number and/or length to outgrowth inhibition, as opposed to ongoing/impending RGC death. At a concentration of 25µM Nogo-P4 inhibited neurite number, longest neurite length and, importantly, did not cause significant RGC death. Accordingly, this concentration of Nogo-P4 was used in subsequent experiments involving AG1478, serving as a novel inhibitory assay.

In an attempt to create an inexpensive, reliable and easily replicated *in vitro* neurite outgrowth inhibitory assay, RGC-5 cells were exposed to varying concentrations of Nogo-P4, including the 25-35µM range which had dramatically affected primary RGC. RGC-5 cells were completely unaffected by the Nogo-P4 peptide up to and including concentrations of 40µM; no effect on survival, neurite number or neurite length was observed. For this reason RGC-5 cells were deemed unsuitable for a Nogo-P4 based

inhibitory assay and all subsequent experiments were performed on primary retinal cultures. Nevertheless, it should be noted that this easily replicable, non cytotoxic Nogo-P4 mediated RGC neurite outgrowth inhibition assay is, as far as can be seen, entirely novel and could prove very useful for future studies on inhibitory mechanisms.

Previously, conditioned media taken from AG1478 treated primary retinal cultures has been shown to promote considerable RGC neurite elongation and a concomitant increase in average neurite number when added to otherwise untreated primary retinal cultures (Douglas *et al.* 2009), although this is somewhat at odds with the findings of Koprivica *et al*(2005) ,who observed no effect of AG1478 on control cultures. One possible explanation for this is that the former study plated retinal cultures onto PDL + Laminin coated wells whereas Koprivica *et al(2005)* plated their cultures on PDL alone. It is possible that the modest but significant enhancement to neurite outgrowth in response to AG1478 is masked by the relatively less growth-permissive nature of PDL. In any case, the present study found that AG1478 effected a small but significant increase in RGC neurite outgrowth, both in terms of mean neurite length and mean number of neurites, on otherwise untreated cultures plated on PDL+ laminin. Crucially, AG1478 completely abrogated the effects of Nogo-P4; Nogo-P4 + AG1478 treated cultures exhibited mean neurite number and mean neurite length values which were near identical to those of control cultures. This result confirmed that AG1478, an EGFRki, was capable of rendering primary RGC invulnerable to the effects of Nogo-P4, an analogue of a potent myelin derived neurite outgrowth inhibitory factor, present and active in the CNS. Interestingly the addition of the adenosine A2A receptor antagonist ZM21385 to AG+ Nogo treated cultures was found to partially restore the neurite inhibitory actions of Nogo-P4. RGC in AG+Nogo+ZM treated cultures exhibited a small but significant decrease in mean neurite

number, and there was a similar trend for mean neurite length, although this trend did not reach statistical significance. This implies that the A2A receptor is involved in the events underlying AG1478-mediated neurite outgrowth. ZM21385 was included in these experiments to investigate the previously reported phenomenon of transactivation of Trk receptors, the receptors for the neurotrophins, by the A2A receptor (Lee *et al.* 2002, Chao *et al.* 2006). Douglas *et al.* (2009) showed that the pan-Trk blocker K252a and Trk-Fc proteins completely blocked the neuritogenic effects of AG1478, showing the neuritogenic effects of AG1478 to be Trk mediated. Similarly, it would follow that blockading the A2A receptor, which primarily transactivates only Trk-B, would produce a similar but smaller effect.

Having confirmed that AG1478 could elicit significant enhancement of otherwise untreated primary RGC neurite outgrowth and, more importantly, ameliorate the outgrowth inhibitory actions of Nogo-P4, it was decided to attempt to uncover the mechanisms by which it did so. Previous work had already shown the *in vitro* neuritogenic effects of AG1478 to be Trk dependent (Douglas *et al.* 2009) and had detected significant levels of the NT (BDNF, NGF and NT3) in AG-treated retinal culture media which was not present in untreated culture media. The present study used ELISA to assay conditioned media for GDNF, CNTF and NT-3. This media was collected from the cultures used to generate the *in vitro* neurite outgrowth data and stored separately by treatment group. No trace of GDNF, CNTF or NT-3 was found in the media from any treatment or control group. CNTF and GDNF were initially assayed for due to the Douglas *et al* (2009) study having performed ELISAs for, and finding the NTs BDNF, NGF and NT3. When neither CNTF nor GDNF were detected in conditioned media, the assay for NT-3, one of the NTs already confirmed to be released by retinal cultures in response to

AG11478 (Douglas *et al.* 2009), was performed. When no NT-3 was detected, where another study had detected it in substantial amounts, it was suspected that the apparent lack of CNTF and GDNF may not have reflected an actual lack of these NTFs and instead might represent either experimental error (unlikely as all standards returned perfect absorbance readings) or perhaps insufficient concentrating of media (unlikely as the sensitivity of each specific ELISA would have meant that even picogram levels of protein would be detected). For details on differences in media-concentrating methodology see above discussion of this result. The ultimate reasons for this discrepancy thus remain unknown, but it should be noted that the presence or absence of CNTF and GDNF in AG-treated retinal cultures is still to be determined due to the results obtained in the present study being inconclusive.

The failure to detect NTF release by ELISA led to an attempt to detect NT-3, NT-4, NGF, BDNF and CNTF mRNA in AG-treated retinal culture lysates *via* RT PCR. That NT-3 and BDNF were both strongly expressed by both control and AG-treated retinal cultures suggests that the negative results obtained from ELISAs were inaccurate and supports the NTF release described by Douglas *et al*(2005). Unfortunately NT-4, NGF and CNTF mRNA were not detected but this is almost certainly due to primer malfunction as the same absence of band or blurred multiple band was observed in the rat brain control group. Once again, it should be noted that CNTF has been described as being absent from the brain, or present in only a sub population of cells in the SVZ, so it remains a possibility that the lack of CNTF mRNA observed does in fact reflect a real lack of CNTF, as the tissue control (brain) may be inappropriate for this particular NTF. That NGF was detected immunocytochemically on both control and AG-treated primary RGC further reinforces the idea that the absence of NTF observed in ELISAs of conditioned media did not

accurately reflect actual NTF levels.

One of the overall goals of this study was to elucidate the mechanism of action by which AG1478 both promotes considerable axon regeneration *in vivo,* and elicits neurite outgrowth and neutralises the outgrowth inhibitory actions of compounds such as Nogo-P4 (as above), myelin (Douglas *et al.* 2009, Koprivica *et al.* 2005) and CSPG (Koprivica *et al.* 2005) *in vitro*. The authors of the original study using EGFRki to facilitate neurite outgrowth, Koprivica *et al* (2005), did not put forward a specific hypothesis as to the events underlying these effects other than to implicate the EGFR as being a vital component in the NgR mediated inhibitory signalling cascade, and implied that the effects of AG1478 were as a direct result of EGFR blockade. The authors also demonstrated that a calcium influx was required for the phosphorylation of EGFR, showing that calcium chelators prevented EGFR phosphorylation. It should be noted however that this paper did <u>not</u> directly show that calcium chelators neutralised the outgrowth-inhibitory actions of myelin, its derivative proteins, not CSPG. The authors concluded that EGFR transactivation was "required but not sufficient" for the transduction of NgR mediated outgrowth inhibitory signalling. Douglas *et al* (2009), having showed that AG1478 effects NTF release from primary retinal cultures, suggested that this NTF support could induce the destruction of the $p75^{NTR}$ coreceptor, a key signalling partner of NgR, *via* RIP. They further showed that AG1478 treated cultures to exhibit significantly raised levels of cAMP. Raised levels of this intracellular secondary messenger are known to enhance *in vivo* axonal regeneration and *in vitro* neurite outgrowth (see Hannilla and Filbin, 2007 for review) and have been shown to actually switch the effects of at least one myelin derived protein, MAG, from axon-growth antagonistic to growth promoting (Cai *et al.* 2001).

A search of the existing literature also revealed at least two additional potential

pathways through which AG1478 could also be exerting its beneficial effects. Regarding the first, a recent study demonstrated that AG1478 could strongly inhibit the activity of the calcium sensing receptor (CaR) (Tomlins *et al.* 2005), showing that the blockade of EGFR transactivation by AG1478 largely neutralised downstream CaR signalling. Another study, roughly contemporaneous with the first (Davies *et al.* 2006), reported that the CaR could signal through Rho and ROCK, causing actin stress fiber assembly and altered cellular morphology. These are processes which, in a growth cone, lead to filopodial retraction and growth cone collapse. It would thus seem that there is a possibility that AG1478 could actively prevent growth cone collapse. One caveat associated with this hypothesis is that both studies used non neuronal cells (primary rat fibroblasts and Human Embryonic Kidney (HEK 293) cells, respectively) which may not respond to EGFR, CaR or Rho/ROCK signalling in a manner identical to neurons – one obvious difference being that these cell types maintain an ability to respond to mitogenic signalling pathways whereas primary culture neurons are effectively terminally differentiated. Regarding the second potential pathway through which AG1478 could be exerting its neuritogenic effects, three drugs very similar to AG1478, genistein and the tyrphostins B44 and 51, were shown to strongly inhibit phosphodiesterase (PDE) activity. As cAMP is hydrolysed by certain PDE subtypes, this results in higher levels of intracellular cAMP (Ho and Chik 1995, Nichols and Morimoto, 1999). It is noteworthy that the latter study was concerned specifically with PDE4 – a subtype of PDE strongly associated with RGC. The supplementary material from Koprivica *et al.* (2005) contains a table listing the results of a high throughput study on the effects of over 400 compounds on *in vitro* neurite outgrowth in the presence of myelin, arranged by magnitude of effect on neuritogenesis. This table shows that this study tested both genistein and tyrphostin B44 and found the

former compound to exhibit no significant neurite outgrowth and the latter to elicit modest but apparently unremarkable outgrowth. This table also shows that alongside AG1478 and two other tyrphostins, A23 and A46, the PDE4 inhibitor etzolate hydrochloride elicited significant neurite outgrowth. It would appear then that this is another means by which AG1478 could elicit neurite outgrowth – by raising cAMP levels within RGC *via* the inhibition of PDE-mediated cAMP hydrolysis. This hypothesis is supported by the raised cAMP levels found in AG-treated primary retinal cultures reported by Douglas *et al.* (2009).

Having identified potential mechanisms by which AG1478 could be exerting its neuritogenic effects, and having ratified the *in vitro* findings of Koprivica *et al*(2005) and Douglas *et al* (2009), namely that the EGFRki AG1478 promotes and disinhibits primary RGC neurite outgrowth, it remained to confirm the effects of EGFRki *in vivo*. It was thus decided to investigate the effects of the irrereversible EGFRki PD168393 on the regeneration of RGC axons following ONC. Along with AG1478, Koprivica *et al*(2005) also tested the *in vitro* effects of the EGFRki PD168393, showing the two compounds to elicit comparable neurite outgrowth. PD168393 is an irreversible EGFRki (as opposed to AG1478 which is reversible and will dissociate in time) and, as i*n vivo* axonal regeneration is measured on the timescale of days or weeks, PD168393 was accordingly selected by Koprivica *et al*(2005) over AG1478 for their subsequent *in vivo* investigations of intra-optic nerve post-ONC axonal regeneration, due to this requirement for long term EGFR blockade. While Koprivica *et al* (2005)applied PD at the lesion site in the injured ON, it was decided to investigate the effects of *intravitreal (i.v.)* PD168393 on intra-optic nerve RGC axonal regeneration.

Chapter 5

Examining the effects of Intravitreal Injections of the EGFRki PD168393 on RGC axonal regeneration and survival

5.1 Introduction

The previous Chapter confirmed that the EGFRki AG1478 was capable of disinhibiting and actively driving RGC neurite outgrowth *in vitro.* The next step was to investigate the mechanisms of action of EGFRki *in vivo*. Subsequent to Koprivia *et al. (*2005) study, at least one paper has reported *in vivo* axonal regeneration in response to EGFRki; Erschbamer *et al.* (2007) delivered PD168393 intrathecally and reported significant recovery of locomotor function and enhanced performance in several other functional recovery paradigms in the weight drop-injured rat spinal cord. As it did not appear that any group had studied the effects of *ivit* EGFRki on axotomised RGC, it was decided to attempt to recapitulate the regeneration seen by Koprivica *et al* (2005) by delivering PD168393 directly to RGC somata within the retina itself.

If PD168393 were to be successful in eliciting RGC axonal regeneration in the ON whilst being present only in the retina this would refute any hypothesis that revolved around EGFRki acting directly on growth cones within the ON. Additionally, RGC regeneration in response to *ivit* PD would strongly suggest that the regenerative effects of intra-ON PD168393 reported by Koprivica *et al* (2005) were largely not a result of rendering the ON a less growth inhospitable environment. In other words, this would suggest that EGFRki do not achieve the greater part of their effects on axonal regeneration *via* the abrogation of various EGFR-dependent cellular processes/events. Conversely, if *ivit* PD168393 is found to have no effect on axotomised RGC this will constitute strong evidence that the effects of such EGFRki are mostly mediated by cells and structures in the ON - chiefly growth cones, glia and invading immune/inflammatory cells – making the retrograde transport of EGFRki to RGC somata, a potential hypothesis

outlined in Chapter 3, unlikely to be relevant.

In order to accurately compare and statistically analyse any differences in regeneration between treatment and control groups it was necessary to quantify the number of axons regenerating past the lesion site as well as the total distance regenerated by each axon. To this end, distance intervals of 250µm past the centre of the lesion site, up to 1.75 mm, were to be marked on composite photomicrographs of post experiment GAP-43 stained ON sections. The number of axons crossing each interval (represented by a line drawn across the photomicrograph, perpendicular to the long axis of the nerve) would be counted and the results tabulated. In this way numbers of axons regenerating increasing distances from the crush site could be quantified – i.e. if one treatment potentiated a small number of axons regenerating long distances whereas another treatment encouraged larger numbers of axons to cross the lesion site but not progress as far, this would be detected, measured statistically and represented on a bar graph as 'number of fibres crossing 0.25mm, 0.5mm etc". Were this to be applied to an intra-ON experiment this could potentially discriminate between strongly stimulated axonal elongation (potentially few fibres, advancing well into the distal segment of the ON) and a general abrogation of the inhibitory elements of the CNS environment (many fibres regenerating across the lesion but for relatively short distances).

Although the primary focus of this series of experiments was to examine the effects of *ivit* PD168393, it was also decided to investigate the effects of combined *ivit* PD168393 and Nogo-P4. As mentioned briefly in Chapter 2, Douglas *et al.* (2009) observed that AG1478 in the presence of CME actually results in a supra-normal growth stimulus to RGC in primary retinal cultures, i.e. AG+CME yields superior neurite outgrowth to AG1478 treatment alone. If this is a real phenomenon, one possible

explanation is that CNS myelin contains a compound which, along with the putative NTF release caused by AG1478, enhances axonal regeneration. One such candidate is Inosine, and this matter is discussed in the discussion section of this Chapter. Another possibility is that AG1478/PD168393 could effectively change the growth antagonistic properties of a myelin derived protein to growth promoting. Douglas *et al.* (2009) showed that AG1478 treated cultures exhibit significantly raised levels of cAMP, and raised levels of this intracellular secondary messenger have been shown to render MAG an actively growth promoting agent (Cai et al. 2001). As CNS myelin is absent from the rat retina, it was decided to investigate whether a similar synergistic effect could occur with *ivit* PD168393 and Nogo-P4. Additionally, as several previous studies by our group have generated accurate and reliable data as to the behaviour of axotomised RGC axons in sham-*ivit* injected, but otherwise untreated animals, and as the aforementioned treatment groups consisted of a) *ivit* PD alone and b) *ivit* PD+Nogo P4, it was thought sensible to have the third group receive *ivit* Nogo-P4 alone. Such a group would function as a control for the PD+Nogo-P4 group, as well as being a treatment group in its own right. As the literature does not appear to contain any examples of *ivit* delivered Nogo-P4, this group also represents a novel application of this peptide.

In order to have a positive control, ON sections from a regenerating ONC+PN group retina, from a previous set of experiments, were to be stained with GAP-43 and would undergo the same quantification procedure detailed above. As *ivit* PN grafts are known to result in significant numbers of fibres crossing the lesion site and penetrating into the distal ON, this will provide a benchmark level of axonal regeneration with which to compare any regeneration obtained with *ivit* PD, Nogo-P4 or both.

Koprivica *et al* (2005) demonstrated that intra-ON PD168393 did not affect RGC

survival, despite producing significant numbers of regenerating RGC axons. If EGFRki such as AG1478 and PD168393 do in fact cause NTF release from local glia, intra-ON PD could potentially have supplied an NTF gradient up which growth cones could grow, reminiscent of the original target seeking behaviour of these axons *in utero*, a process which would not necessarily directly influence survival. Additionally, any NTF released in the ON would have to be retrogradely transported through RGC axons to the somata if they are to have any effect on cell signalling cascades and transcription. As the present study will be injecting PD directly into the vitreal body, any NTF release by local retinal glia will be effectively juxtacrinally supplied to the RGC somata. Such direct delivery of multiple NTFs to RGC somata has been repeatedly demonstrated to promote RGC survival (see Berry *et al.* (2008) for review and references within) and it is thus possible that *ivit* PD168393 will significantly enhance RGC survival where intra-ON PD did not. To quantify this effect, the eyes from treated animals will be appropriately processed before being sectioned, stained with Haemotoxilin and Eosin (H & E), and the surviving RGC counted. In this way the mean number of surviving RGC per animal per group will be established and subsequently statistically analysed.

It is almost impossible to accurately measure the exact *in vivo* concentration of an injected drug, in terms of exposure of specific populations of cells. It is then important to have an indicator of a drugs efficacy, irrespective of whether or not the desired effects are observed. In the case of PD168393 the indicator will be EGFR phosphorylation levels in the GCL and the FL. pEGFR levels will be measured by staining retinal sections with an anti-pEGFR antibody and fluorescent secondary antibody and by analysing subsequent photomicrographs using the histogram function within the image analysis program ImagePro. By defining the GCL and the FL as an “area of interest”, Imagepro will measure

the mean pixel intensity of multiple stretches of retina, remove from this value the equivalent value for unstained control retina and calculate average pixel intensity per treatment group. In this way it will be possible to confirm whether or not PD168393 did in fact inhibit EGFR phosphorylation, preventing spurious conclusions being drawn regarding the efficacy of PD. If pEGFR levels are not shown to be significantly attenuated in retinae receiving PD, then it must be assumed that the EGFRki did not reach or did not affect ganglion cell and axonal EGFR. Conversely if pEGFR levels are shown to be significantly attenuated whilst no regeneration is observed, this will strongly suggest that retinal pEGFR alone is irrelevant to axonal regeneration. A third and final possibility is that PD168393 will be found not to inhibit RGC EGFR phosphorylation but nevertheless to promote significant axonal regeneration. This would strongly suggest that EGFR such as PD promote RGC axonal regeneration *via* entirely off-target effects, i.e. that despite their designation as EGFRki, PD and AG are exerting their effects on some other molecular target, and that the EGFR itself is largely irrelevant.

5.1.1 Specific Aims

- To attempt to elicit *in vivo* RGC axonal regeneration by injecting the vitreous body of ONC recipient rats with the EGFRki PD168393
- To ascertain if concomitant intravitreal injection of PD168393 and Nogo-P4 will elicit synergistic RGC axonal regeneration
- To examine the effects of *ivit* Nogo-P4 on RGC survival and regeneration after ONC

5.2 Results

5.2.1 Intravitreal PD168393 did not elicit RGC axonal regeneration

Ivit injection of 100nM PD168393 failed to enhance RGC axonal regeneration 14 days after ONC. GAP-43 staining showed that the vast majority of axons did not advance beyond the lesion site (Figure 5.1) and that the minority that did so failed to progress further than 0.25 mm (Figure 5.5, red-brown column). In terms of the mean number of axons crossing the lesion site, no significant difference was found between the PD treated group and the Nogo-P4 and Nogo+PD treatment groups (figure 5.5).

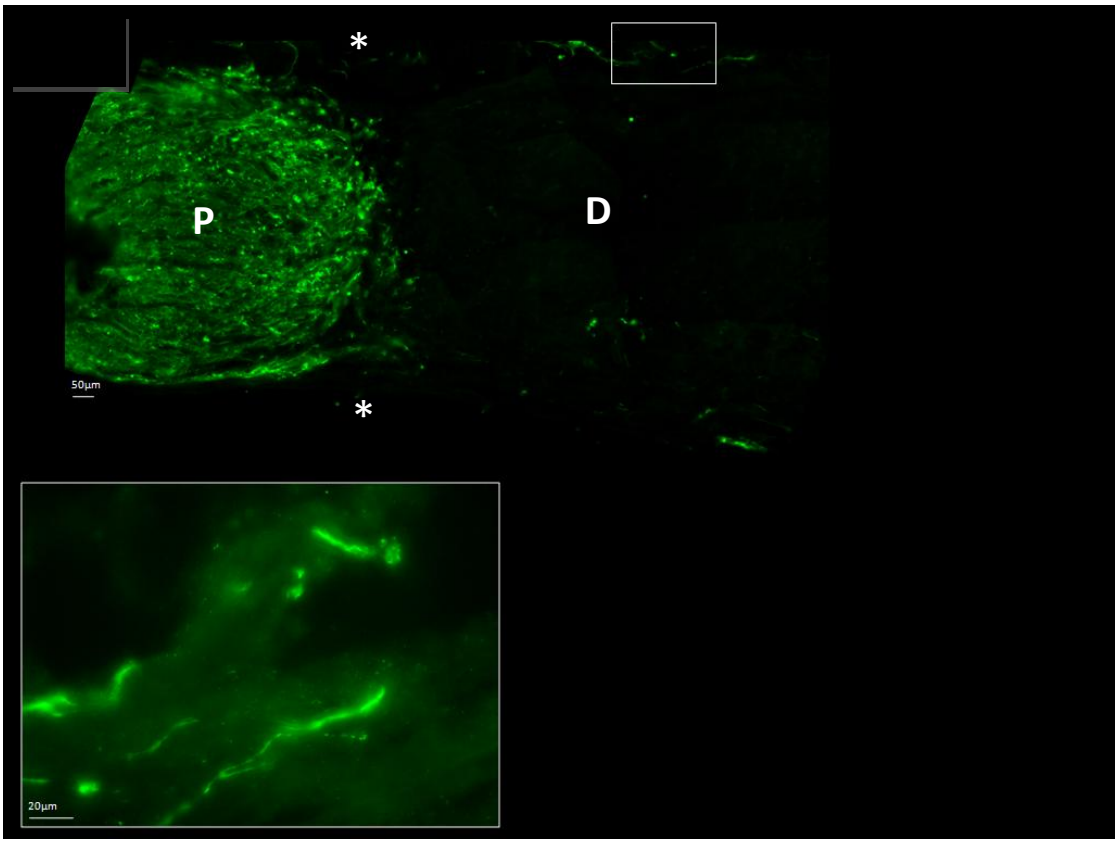

Figure 5.1. GAP-43 staining showed the absence of significant RGC axon regeneration beyond the crush site following *ivit* PD168393 treatment. * denotes centre of crush site. Inset shows high power (x400) image of the single furthest regenerating/spared axon. P= Proximal section D= Distal section.

5.2.2 Intravitreal Nogo-P4 peptide did not affect RGC axonal regeneration

Ivit injection of 25µM Nogo-P4 peptide failed to influence RGC axonal regeneration after 14 days after ONC. GAP-43 staining again showed that the vast majority of axons did not advance beyond the lesion site (Figure 5.2) and that the minority that did so failed (with one exception) to progress further than 0.25 mm (Figure 5.5, purple column). In terms of the mean number of axons crossing the lesion site, no significant difference was found between the Nogo-P4 treated group and the PD168393 and Nogo+PD treatment groups (figure 5.5).

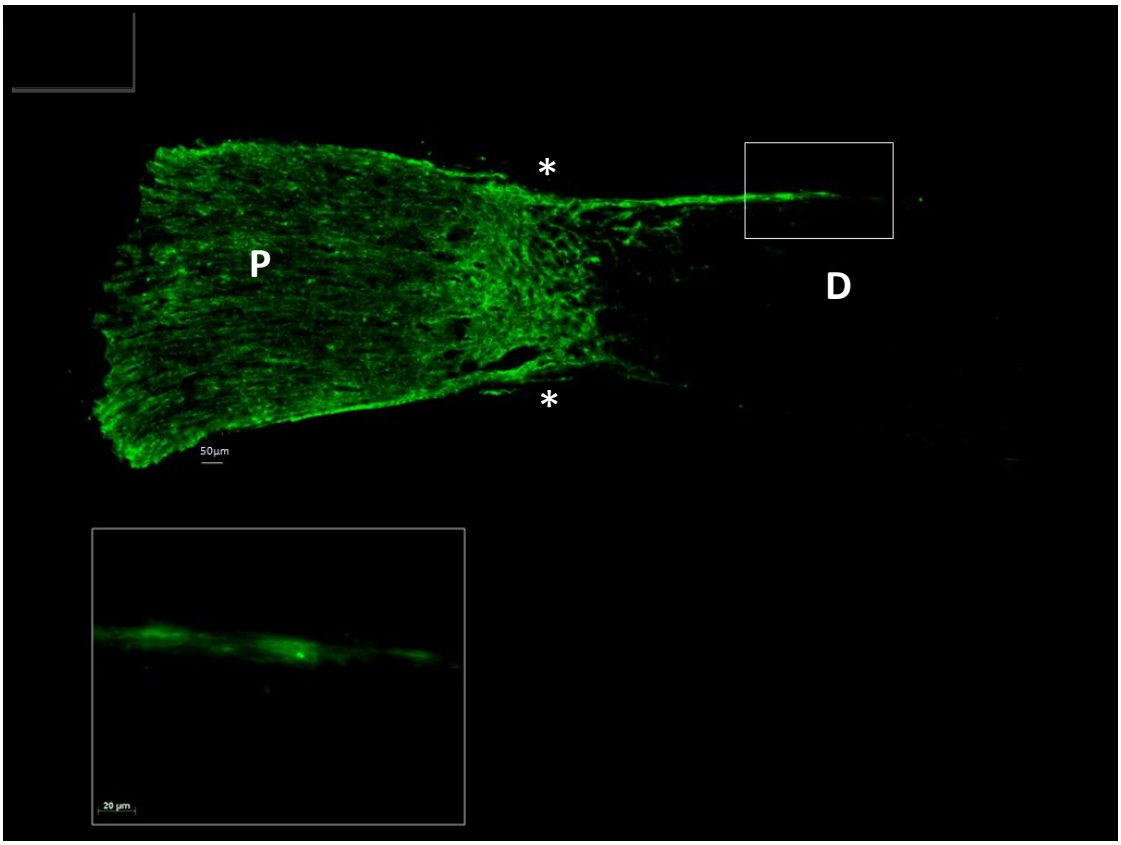

Figure 5.2. GAP-43 staining showed the absence of significant RGC axon regeneration beyond the crush site following *ivit* Nogo P4 treatment. * denotes centre of crush site. Inset shows high power (x400) image of the single furthest regenerating/spared axon. P= Proximal section D= Distal section.

5.2.3 Intravitreal PD168393 + Nogo-P4 peptide did not affect RGC axonal regeneration

Ivit injection of 100µM PD168393 + 25µM Nogo-P4 peptide failed to influence RGC axonal regeneration 14 days after ONC. GAP-43 staining showed that the vast majority of axons did not extend beyond the lesion site (Figure 5.3) and that the minority that did so failed (with few exceptions) to progress further than 0.25 mm (Figure 5.5, green column). In terms of the mean number of axons crossing the lesion site, no significant difference was found between the PD+Nogo treated group and the PD168393 and Nogo-P4 treatment groups (figure 5.5).

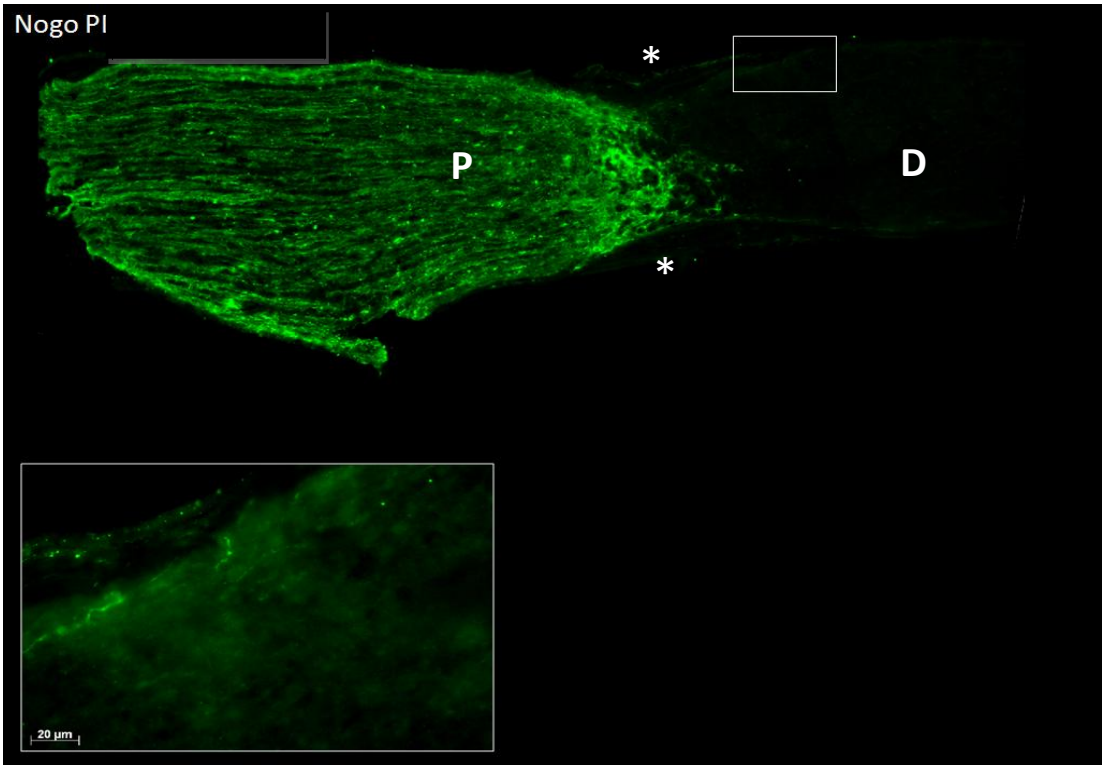

Figure 5.3. GAP-43 staining showed the absence of significant RGC axon regeneration beyond the crush site following *ivit* PD168393 +Nogo P4 treatment. * denotes centre of crush site. Inset shows high power (x400) image of single furthest regenerating/spared axon. P= Proximal section D= Distal section.

5.2.4 No treatment group elicited significant axonal regeneration

Figures 5.1 - 5.3 show that neither PD, Nogo-P4 nor PD+Nogo-P4 treatment promoted axonal regeneration, as qualified by GAP-43 staining. Figure 5.4 shows an example of significant axonal regeneration achieved with an *ivit* PN graft, as shown by GAP-43 staining, with large numbers of axons crossing the lesion site and extending up to ~2 mm into the distal section of the nerve.

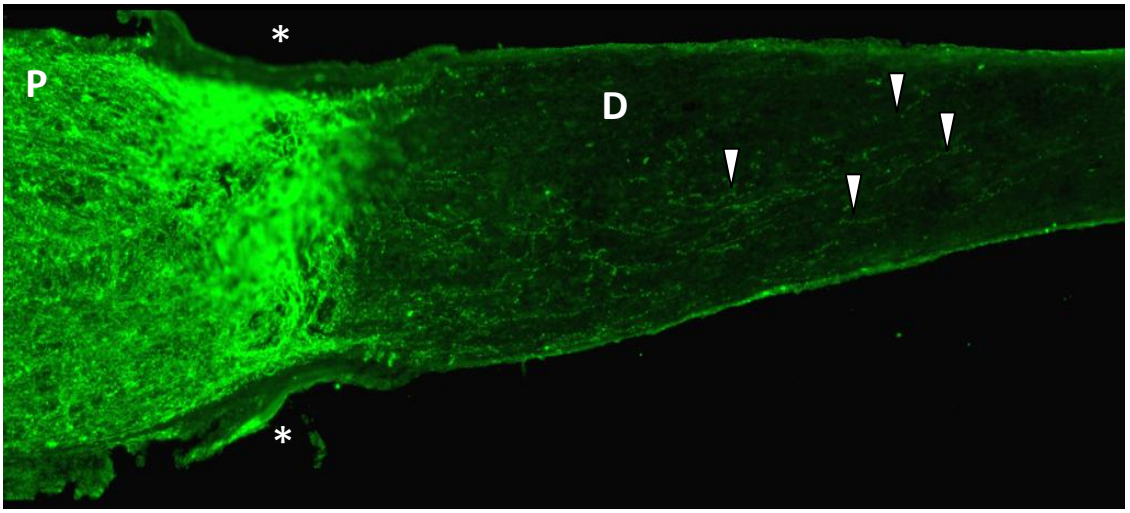

Figure 5.4. Example of axonal regeneration seen in response to *ivit* PN graft. Axons regenerated up to ~2mm past crush site 14 days after ONC + PN implant. Note large number of axons crossing lesion site (white box) and extending up to ~ 2mm distally (white arrows). * denotes centre of crush site. P= Proximal section D= Distal section.

Quantification of the mean number of axons extending up to 1.25 mm beyond the crush site for each treatment group, followed by statistical analyses, showed that neither PD, Nogo-P4 nor PD+Nogo-P4 treatment significantly differed from one another (Figure 5.5). In contrast, ONC + PN treatment was shown to yield statistically significant increases in mean numbers of axons extending up to and well beyond 1.25 mm distally. Figure 5.5 shows the mean number of axons extending 0.25, 0.5, 0.75, 1 and 1.25 mm past the

lesion site, with means and statistical analyses for number of axons crossing each of these distances. No statistically significant difference was found between PD168393, Nogo-P4 nor PD+Nogo-P4 treatment groups for any of these distances, while each distance interval contained statistically significantly more PN-treatment group axons crossing it (figure 5.5, blue column).

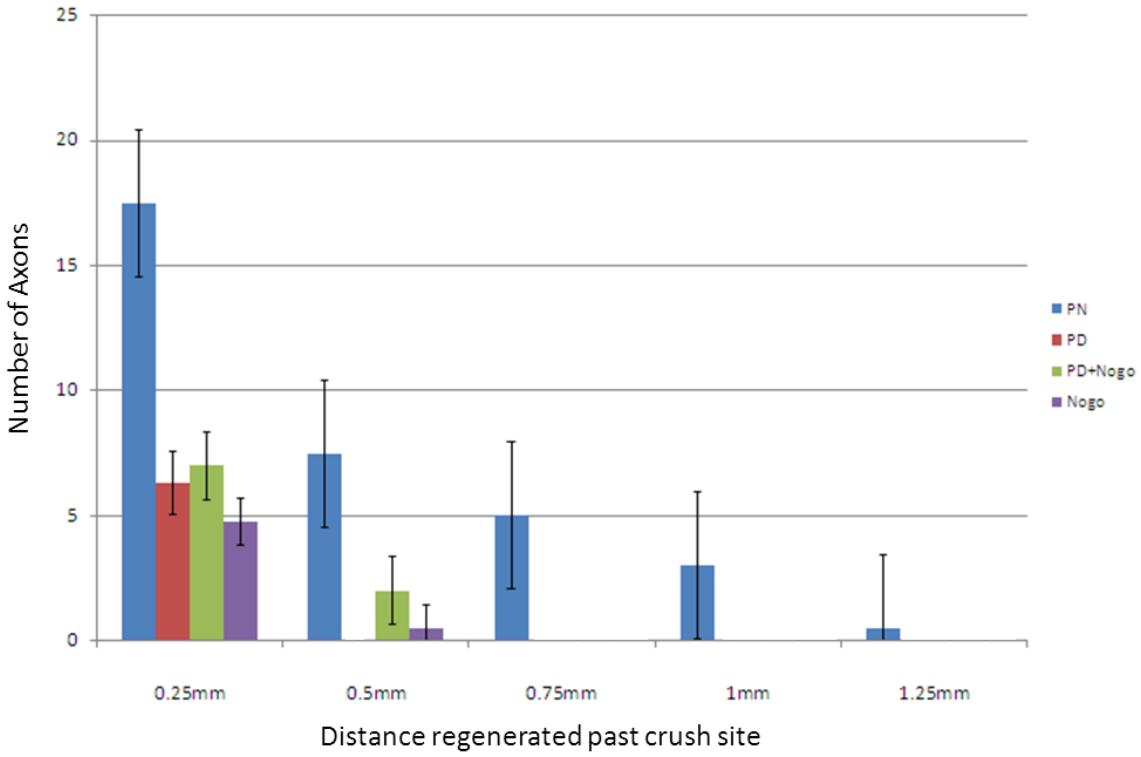

Figure 5.5. *Ivit* PD168393 did not elicit significant RGC axon regeneration. Number of axons regenerating up to 1.25 mm past the crush site were not significantly different between PD alone, Nogo-P4 alone and Nogo-P4+PD treatment groups. In each group numbers of regenerating axons were negligible compared to the number of axons seen to regenerate in response to *ivit* PN graft. n = 4 for each group. ***= p value of <0.001. Error bars signify 95% Confidence Intervals.

5.2.5 Intravitreal PD168393 significantly attenuated retinal pEGFR staining

In order to confirm that the injected PD168393 was in fact bioactive, retinal sections from each treatment group were immunohistochemically probed for pEGFR and, using the histogram function within the image analysis program ImagePro, relative pEGFR staining intensity was measured in the FL, GCL and IPL. Subtracting the mean background pixel intensity for unstained retina, obtained from control tissue exposed to secondary but not primary antibodies, the relative mean pixel intensity was calculated for each treatment group (Figure 5.6). Both the PD168393 and the PD168393+Nogo treated groups exhibited significantly lower pEGFR staining intensity compared to the Nogo treated group.

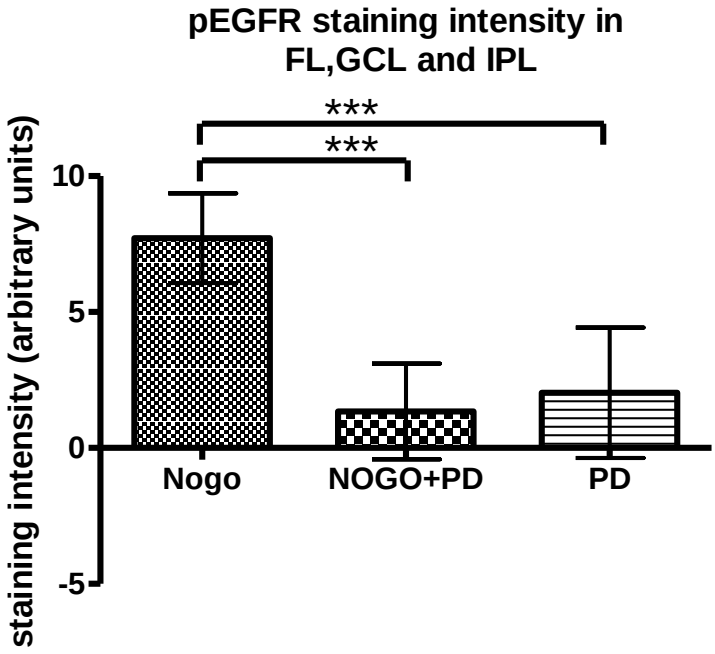

Figure 5.6. PD168393 reduced pEGFR staining intensity in the FL, GCL and IPL layers of the retinae. Units are mean pixel brightness values as measured with image anaylsis software histogram function. n = 4 for all groups Error bars are 95% confidence intervals.

5.26 Intravitreal PD168393 did not enhance RGC survival 14 days post ONC

Ivit PD168393 did not promote RGC survival 14 days after ONC. No significant difference was found in mean surviving RGC number between PD168393, Nogo-P4, PD+Nogo-P4 or ONC-alone treatment groups (Figure 5.7). Mean number of RGC per field of view for uninjured control was 56 ± 4.3, compared to between 31 ± 7.6 and 35 ± 4.5 for the treatment groups and previously collated ONC alone data (inter-treatment group differences were not statistically significant).

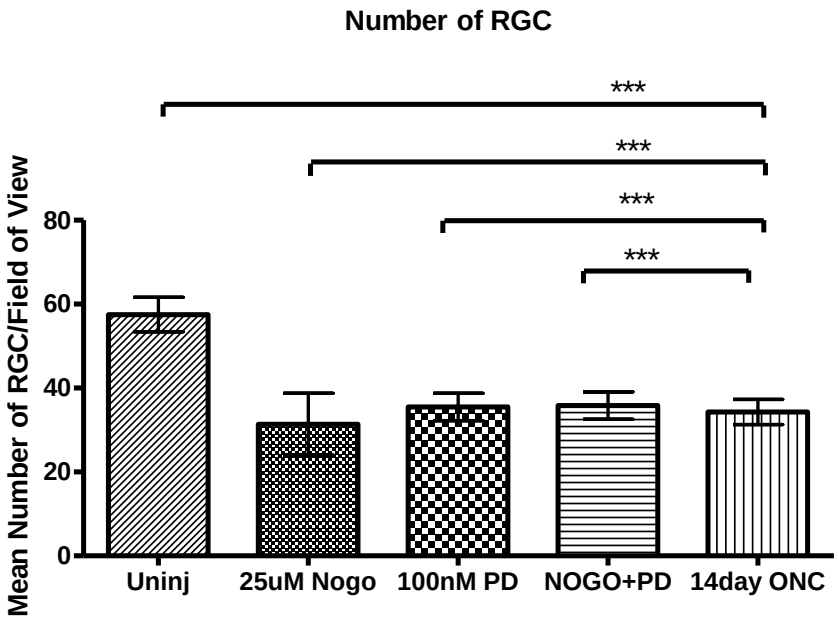

Figure 5.7. PD168393 did not affect RGC survival 14 days after ONC. Mean numbers 14 days after ONC were unaffected by *ivit* application of PD168393, Nogo-P4 or PD+Nogo-P4. Mean was calculated by averaging retinal ganglion cell counts over multiple fields of view of GCL. n = 4 for all groups ***= p value of <0.001. Error bars = 95% confidence intervals.

5.3 Discussion

5.3.1 Intravitreal PD168393 did not elicit RGC axonal regeneration

Chapter 3 showed all RGC axons in both the retina and the ON to be $pEGFR^{-}$, with only a subpopulation of RGC somata being $pEGFR^{+}$. By contrast the majority of glia in both the retina and ON were shown to be predominantly $pEGFR^{+}$ and to exhibit enhanced pEGFR levels following ONC. That *ivit* injections of the EGFRki PD168393 failed to elicit RGC axonal regeneration suggests that its primary mechanism of action is <u>not</u> the blockade of neuronal EGFR, as hypothesised by Koprivica *et al (2005)*. Although there is always the possibility with any *in vivo* drug application that the compound did not reach the target area, (or having done so, failed to impact on target cells), the significant attenuation of pEGFR staining intensity in the GCL and other layers of the retina (discussed in detail below) strongly suggests that RGC EGFR phosphorylation was indeed inhibited. As *ivit* application of PD168393 yielded no significant RGC axonal regeneration whatsoever, while Koprivica *et al(2005)* observed considerable regeneration in response to intra-ON PD168393, it would appear that the events underlying this regeneration occur in the ON and not in the retina. The results and discussion sections from Chapters 3 and 4 provide evidence for multiple different potentially beneficial actions of EGFRki specifically within the ON. First and foremost are the myriad of EGFR-dependent cellular processes which are antagonistic to axonal growth, including astrogliosis, astrocytic CSPG deposition, fibroblast-astrocyte interactions leading to scar formation and the astrocytic and microglially mediated recruitment of immune cells into the lesion site, which debride and further damage axons (see Chapter 3 discussion for details). If the abrogation or attenuation of these intra ON processes even partially underlies EGFRki-mediated

regeneration, then this would absolutely require EGFRki within the ON – the presence of *ivit* EGFRki would be largely irrelevant.

Secondly, there is considerable evidence to suggest that some glia may respond to EGFRki by releasing NTFs (Chapter 4, results and discussion). While this has been shown to be true in AG1478 treated mixed retinal cultures *in vitro* (Chapter 4, results and discussion, Douglas *et al.* 2009), it is likely that this effect would be more pronounced in the ON *in vivo*, due to the larger numbers of glia involved (including oligodendrocytes which are absent from the retina), the irreversible nature of PD168393 (as opposed to the reversible EGFR blockade instigated by AG1478), and the juxtaposition of ON glia and axonal growth cones. It is important to note that this is based on the assumption that the actions of PD168393, both on and off target, are identical to that of AG1478, which is by no means certain – the latter is a Tyrphostin, a reversible kinase inhibitor which achieves its EGFR blockade by competing locally for ATP, whereas the former binds directly and irreversibly to EGFR at Cys 773. Nevertheless, Koprivica *et al* (2005) reported that PD and AG both elicited similar neurite outgrowth *in vitro* and Douglas *et al (2009)* demonstrated NT3 upregulation in RGC somata following *ivit* PD injection, suggesting that both EGFRki are having similar effects.

Thirdly, it is possible that the immunohistochemical investigation of ON pEGFR localisation shown in Chapter 3 failed to localise pEGFR on axonal growth cones, as the axonal antigen, NF-200, detected by the anti-axonal antibody used, is expressed only by consolidated section of the growing axon and not by the growth cone itself. This is considered unlikely as no $pEGFR^{-}$ NF colocalisation was observed at all, requiring all pEGFR to be in the growth cone itself, signifying a complete lack of retrograde and anterograde transport of pEGFR to and from the somata, making it impossible for EGFR

to interact with the nucleus and thus affect protein synthesis/transcription. While considered unlikely, it should be noted that it is still technically possible that EGFR transactivation could be taking place within the growth cone, and that subsequently the putative role for EGFR in the NgR signalling cascade put forward by Koprivica *et al* (2005) could still hold true, providing that all interactions took place within the growth cone.

5.3.2 Intravitreal PD168393 + Nogo-P4 peptide did not affect RGC axonal regeneration

It has been observed that, while RGC axon outgrowth *in vitro* is inhibited by the presence of CME, RGC exposed to both CME and AG1478 exhibit synergistic neurite outgrowth, above and beyond PDL-Laminin controls (Douglas *et al.* 2009). Taking into account the evidence that AG1478 causes raised levels of intra-RGC cAMP (Douglas *et al.* 2009), and that high levels of cAMP can cause MAG to switch from being neurite outgrowth inhibitory to being actively growth promoting (Cai *et al.* 2001), it was decided to investigate whether dual *ivit* injections of the CNS myelin derivative Nogo-P4 peptide and PD168393 could elicit this synergistic axonal outgrowth *in vivo*, there being no CNS myelin within the rat retina. That no regeneration was observed in this study might have suggested that Nogo-P4 peptide does not provide the same synergistic boost to RGC outgrowth as CME, but being that *ivit* PD168393 injections alone failed to promote axonal regeneration, this cannot be asserted. It is probable that some other, as yet unidentified, factor in CME is responsible for this counter-intuitive growth stimulatory *in vitro* effect, and this factor may be required for the unprecedented *in vivo* RGC regeneration originally reported with EGFRki by Koprivica et al. in 2005.

5.3.3 Intravitreal Nogo-P4 peptide did not affect RGC axonal regeneration

Numerous previous *in vivo* experiments performed by our group featured control groups which received *ivit* saline/appropriate vehicle, meaning the levels of RGC axonal regeneration associated with such controls were well documented after large numbers of experimental replicates. Additionally, as one treatment group consisted of PD+ Nogo-P4, a Nogo alone group allowed the ascription of any observed effects of RGC regeneration in the dual treatment group to either PD or the combination of PD+Nogo, as opposed to the Nogo peptide itself. This group therefore functioned both as a negative control and as a treatment group, examining the effects of *ivit* injected Nogo-P4 peptide on RGC axonal regeneration. Taking into account Nogo-P4's growth antagonistic effects, the lack of significant difference in mean number of regenerating axons between both of the PD treated groups and this Nogo-P4 group demonstrates that no regeneration took place in any treatment group.

5.3.4 No treatment group elicited significant axonal regeneration

When compared to a ONC + *ivit* PN graft treated ON, all three treatment groups exhibited statistically significantly less axonal regeneration at measured checkpoints of 0.25, 0.5, 0.75, 1.0 and 1.25 mm distal to the crush site, with PD treated RGC regenerating no better than those exposed to Nogo-P4. The best ON regeneration reported to date, in terms of total percentage of all RGC axons regenerating beyond the lesion site is, as mentioned previously, 0.6-10% at 3 weeks after intravitreal peripheral nerve graft implant (Berry *et al.* 1996) and 7.5% at 4 weeks after a triple combination of c3-transferase

mediated Rho inactivation, application of exogenous, cell-permeable cAMP and simultaneous peripheral nerve autografting onto the cut end of optic nerve (Hu *et al.* 2007). In comparison, the intra-ON, PD168393-mediated, *in vivo* axonal regeneration reported by Koprivica *et al* (2005). was estimated by the authors as being ~0.5% of the total population of RGC, and the number of fibres regenerating in each of the three treatment groups in the present study was effectively zero. It is thus apparent that, even where effective, *in vivo* delivery of EGFRki does not elicit as effective an RGC regenerative response as an *ivit* PN graft.

5.3.5 Intravitreal PD168393 significantly attenuated retinal pEGFR staining

Levels of pEGFR immunofluorescence in the FL, GCL and IPL were significantly lower in *Ivit* PD – treated groups, demonstrating that PD168393 both reached the target cells and acted upon EGFR in those layers. This is a critical result, providing strong evidence that PD168393 was bioactive within the PD treated retina and hence that the observed ineffectiveness of *ivit* PD as an *in vivo* RGC regenerative agent was a valid result and not a consequence of failed drug-delivery. Although there are numerous, more direct, and more reliably quantitative methods of determining phosphoprotein levels (SDS-PAGE with densitometry for example) these would have required the partial or total destruction of the retinae being analysed, which would have made it impossible to perform RGC survival counts. Had *in vivo* regeneration been observed then there would have been justification for experimental repeats followed by one or more of these techniques for directly quantifying protein levels. As no such regeneration occurred, and because the above indirect method using immunofluorescence pre-empted the likely results of any such

study, additional experiments to this end were deemed to be superfluous and an unjustifiable use of further animals.

5.3.6 Intravitreal PD168393 did not enhance RGC survival 14 days post ONC

RGC survival was unaffected by *ivit* delivery of PD168393, Nogo-P4 or PD+Nogo. This agrees with the findings of Korpivica *et al (2005),* who found PD to have no effect on RGC survival despite its reported regenerative effects. In contrast, *ivit* injections of even single NTFs have been shown to promote significant RGC survival. *Ivit* BDNF and CNTF were shown to promote 2-3 fold increase in RGC survival up to 4 weeks post ONC (Mey and Thanos 1993), *ivit* BDNF and, to a lesser extent, NT-4 (but not NT-3) were reported to delay RGC death by up to 3 days and significantly increase RGC survival rates up to 14 days post ONC, and *ivit* CNTF was shown to encourage RGC axonal regeneration into an implanted segment of PN (Cui *et al.* 1999). That intra-ON application of PD168393 (as performed by Koprivica *et al.(2005)* did not enhance RGC survival does not necessarily rule out the previously mentioned hypothesis that EGFRki such as PD and AG elicit local (i.e. intra ON) NTF release; it is possible that levels of NTF released are insufficient to significantly promote survival once retrogradely transported back to the RGC somata. More difficult to account for, working under the assumption that PD provokes local release of NTF, is the fact that *ivit* PD, which was shown to significantly reduce pEGFR levels in and around RGC somata, still failed to promote RGC survival. Douglas *et al.* (2009) showed that RGC in retinae receiving *ivit* PD but not vehicle, upregulated NT-3, but, as discussed above, NT-3 appears to be ineffective at promoting RGC survival/axonal

extension. It is then very likely that the *in vivo* effects of PD168393 are not exclusively mediated by NTF release, as such a pathway would almost certainly affect RGC survival.

5.37 Interim conclusions

Chapter 3 of this study showed that all RGC axons in both the retina and the ON were pEGFR^{-}. Chapter 4 and Douglas *et al.* (2009) both show the EGFRki PD168393 and AG1478 to have a demonstrable neuriteogenic effect and to effect the release of NTF *in vitro*. Koprivica *et al.* (2005) demonstrated significant *in vivo* RGC regeneration using only intra-ON PD168393. The present study (specifically this Chapter) also found that *ivit* PD168393, whilst effectively reducing EGFR phosphorylation, had no effect on *in vivo* RGC survival or axonal regeneration.

Taken together these results strongly suggest that the blockade of neuronal EGFR is not the primary means by which EGFRki exert their axogenic/neuritogenic effects, and points towards EGFR not being an integral part of the inhibitory signalling cascade. The original *in vivo* post-ONC regeneration reported by Koprivica *et al* (2005) cannot be explained in terms of intra-RGC pEGFR, as all intra ON axons were pEGFR^{-} and any pEGFR^{+} RGC somata, being in the retina, were almost certainly too far away from the area of ON exposed to PD168393 to be directly affected by the treatment, particularly as PD168393 in that case was largely contained within a gelfoam cuff placed around the injury site on the ON itself. Additionally, as shown above, *ivit* PD168393, whilst demonstrably affecting RGC EGFR phosphorylation, elicited no RGC survival or axonal regeneration whatsoever.

As mentioned previously, there are numerous processes antagonistic to axonal growth associated with almost every cell type found in the ON, glial or otherwise, (including invading inflammatory/immune cells) which depend either partially or wholly on EGFR signalling (for details see Chapters 3 and 4 discussion). The abrogation of any one of these processes, e.g. astrocytic CSPG secretion, would render the ON a less growth inhibitory environment for regenerating axons, so it is immediately apparent that the inhibition or reduction of EGFR phosphorylation on almost the entire non-neuronal cell population could indirectly enhance axonal regeneration, even in the absence of extraneous NTF support. There is also reason to believe that EGFRki may provoke the release of NTF from local glia (Douglas *et al.* 2009), which, in concert with the aforementioned reduction in axon growth antagonistic stimuli, could potentially explain the intra-ON regeneration obtained with PD168393 (Koprivica *et al.,* 2005). Unfortunately there are at least two caveats associated with this hypothesis. Firstly many of the same cell types within the ON are also present within the retina (with the important exception of oligodendrocytes), so paracrine/juxtacrine release of NTF by retinal glia in response to EGFRki should <u>also</u> stimulate growth, when in fact it does not. Secondly, while *ivit* PD168393 yielded no *in vivo* axonal regeneration through the growth inhibitory environment of the ON, dissociated primary retinal cultures , in which the exact same population of cells were exposed to AG1478 and to levels of Nogo-P4 peptide proven to inhibit RGC neurite outgrowth, <u>did</u> exhibit disinhibited neurite outgrowth. This difference is likely to be at least partially a result of the difference in growth substrates between the two models: retinal cultures were plated on PDL + Laminin coated chamber slides, a surface known to be permissive to neurite outgrowth, whereas axons *in vivo* have no option but to grow in, around and through various growth inhibitory proteins and

cellular debris, in the presence of numerous other noxious influences such as inflammatory and immune interference. Although the difference in growth substrate almost certainly plays a part, it is unlikely that the failure of *in vivo* axons to respond to *ivit* PD is entirely a consequence of this: the fact remains that Intra-ON PD elicits axonal regeneration, whereas intra-retinal PD does not.

One hypothesis put forward to explain both these phenomena is that a factor present in CNS myelin is capable of acting in concert with EGFRki such as PD and AG and provoking a supra-disinhibitory stimulus, i.e. PD/AG, in concert with this unknown factor, provokes levels of outgrowth above and beyond that associated with the mere abrogation of inhibitory stimuli - the interplay between EGFRki and unknown agent actively *driving* axonal regeneration as opposed to simply disinhibiting it. This hypothesis is based on the observations that 1) retinal cultures exposed to both CME and AG1478 exhibited supra-disinhibtory levels of neurite outgrowth – the combination of CME and AG appeared to actively drive growth in a manner reminiscent of that seen in response to exogenously delivered NTF (Douglas *et al.* 2009), 2) neither the mouse nor the rat (nor the human) retina contains CNS myelin and 3) this effect was not seen with recombinant Nogo-P4 peptide (see Chapter 4). It should be noted that while Koprivica *et al* (2005) also used CME as an inhibitory agent and did not report any such synergistic effects, this study did not include details about the nature of the CME used and it is unlikely that the CME contained the exact complement of compounds at exactly the same relative concentrations as the CME used by Logan *et al* (2006) to outline the above hypothesis. It is therefore possible that a factor present in myelin *in vivo* and in the CME used by Douglas *et al.* (2009) could act in concert with EGFRki to promote synergistic neuritogenesis and axonal regeneration, potentially including NTFs. One potential

candidate for this unknown factor is Inosine. This purine nucleoside is a breakdown product of Adenosine and has been implicated as being involved in at least two different pathways which could potentially aid axonal regeneration. Firstly, inosine has been shown to activate MST3b, a protein kinase critical to axonal outgrowth (Irwin *et al.* 2006) and secondly, Inosine has been reported to serve as a ligand for the adenosine A2A receptor (Nascimento, 2010) which in turn has been shown to transactivate Trk receptors, resulting in growth and axogenic responses similar to that obtained with conventional NTF-therapy (Jeanneteau and Chao, 2006). Chapter 4 of the present study showed how the A2A receptor antagonist ZM21385 partially inhibited the growth promoting effects of AG1478 on primary retinal cultures, an effect potentially attributable to either (or both) of these two pathways, and recent work from within our laboratory has shown that CME contains physiologically relevant levels of Inosine (Ahmed *et al.* unpublished data). If Inosine and/or other compounds contained within CNS myelin are in fact necessary for EGFRki-mediated axonal regeneration, this would explain why intra-ON but not *ivit* PD168393 promoted growth because, again, neither rat nor mouse retinae contain CNS myelin.

Whether or not the presence of CNS myelin is required for EGFRki to elicit *in vivo* axonal regeneration, the fact remains that *ivit* PD168393 failed to produce such an effect. Having confirmed that AG1478 stimulated neuritogenesis and disinhibited RGC growth *in vitro* (see Chapter 4) and having shown *ivit* PD168393 to be ineffective, it was decided to investigate the effects of intra-ON PD168393, in an attempt to confirm the original *in vivo* findings of Koprivica *et al* (2005)

Chapter 6

Examination of the effects of *Intra*-ON implantation of collagen matrix implanted with the EGFRki PD168393 on RGC survival and axonal regeneration

6.0 Introduction

Chapter 3 of this study showed that activated EGFR was not present in RGC axons, either before or after injury. This contradicts the hypothesis of a purely intra-axonal role of pEGFR in abortive intra-ON axonal regeneration. Chapter 4 confirmed that at least one EGFRki, AG1478, could stimulate RGC neurite outgrowth in the presence of otherwise outgrowth-precluding conditions *in vitro* - concentrations of Nogo-P4 peptide sufficient to largely abolish neurite outgrowth were rendered impotent following administration of AG1478. Chapter 5 showed that *ivit* injections of the EGFRki PD168393 suppressed retinal pEGFR levels but neither promoted RGC axonal regeneration nor enhanced RGC survival. Taken together these results showed that while *ivit* application of an EGFRki did not elicit *in vivo* RGC axonal regeneration, *in vitro* models did indeed show a significant growth promoting effect on previously inhibited RGC. Furthermore, while the mechanisms underlying these *in vitro* effects were at least partially uncovered - including the release of putatively glially derived NTFs - the mechanisms underlying the *in vivo* regeneration reported by Koprivica *et al.*(2005) as well as those underlying the regenerative failure seen in *ivit* experiments, remained to be elucidated. The observation by Koprivica *et al* (2005) that considerable *in vivo* RGC axonal regeneration resulted from the intra-ON application of PD immediately suggested that EGFRki were exerting their axonal regenerative effects in or around the ON lesion site itself. It was therefore decided to chronically expose the ON lesion site of ONC-recipient rats to the EGFRki PD168393 in an attempt to a) confirm the efficacy of intra-ON EGFRki therapy and b) elucidate the means by which PD, and putatively by extension other EGFRki, achieve such regeneration. In planning this experiment the primary goal was to expose the axons and cells in and

around the ON lesion site to relevant concentrations of PD168393 for the duration of the experiment, 14 days. To deliver intra-ON PD for 14days, Koprivica *et al* (2005) wrapped sections of soluble-PD-saturated gelfoam around the ON lesion site, replacing sections with fresh PD-saturated sections every 3 days. Each gelfoam replacement required surgery to expose and then reseal the lesion site, as well as the associated anaesthesia and recuperation of animals. When planning the *in vivo* experiments described in this Chapter it was decided that this level of invasive surgery was unacceptable, in terms of surgical logistics, potential distress to animals and, crucially, the potentially experiment-confounding inflammatory and immune responses to each and every surgical intervention. Although various long-term *in vivo* drug-delivery techniques were appraised, the chosen method of intra-ON PD168393 delivery was that of collagen matrix implantation.

Collagen matrices have been used for decades to enhance wound healing in tissues as varied as skin and muscle (Carlson and Longaker, 2004), bone (Bonadio, 1999) and, crucially, in the mammalian CNS (Berry *et al.* 2001, Gonzalez *et al.* 2009, Yang *et al.* 2010). In many circumstances collagen matrices (referred to in the literature as, variously, scaffolds, matrices, lattices or frameworks) are seeded with cells such as Schwann cells or fibroblasts (see Carlson and Longaker 2004 for review) which secrete desired factors, or with genes encoding desired proteins (Berry *et al.* 2001) or with replication deficient viruses containing such genes (Gonzalez *et al.* 2009). The latter two studies reported successful implantation of collagen matrices into the rat ON lesion site which promoted significant axonal and cellular invasion, resulting in the uptake of genes/virions by RGC and relevant glia. The dual advantages of such a structure is that it provides a positive growth substrate along which axons can advance whilst allowing

compounds required to affect invading cells/axons to be effectively immobilised within its structure. This immobilisation of factors/viruses/plasmids has itself three key advantages. The immobilisation of bioactive agents prevents both their active clearance and their passive diffusion, which ensures the maintenance of a relatively fixed concentration of compound within the matrix whilst conserving the stock of compound, allowing long-term bioactivity. This immobilisation also effectively renders the compound in question accessible only to cells/axons abutting or invading the matrix itself, a particularly desirable effect when seeking target-cell specific actions. Finally, when implanted as a lyophilised, dry bolus such collagen matrices expand as they absorb tissue fluids, swelling to fill the lesion site. In the case of ON lesions, this ensures that the matrix is in physical contact with both the proximal and the distal ends of the severed ON, ensuring a continuous growth substrate for axons across the entirety of the lesion site (Berry *et al.* 2001). The 14dpi timepoint was selected for several reasons. Firstly, by 14 dpi sufficient numbers of control group RGC will have died (~70%) to make any effects on RGC survival more salient in treatment groups. Secondly, 14 days is sufficient time for any regenerating axons to invade and cross the lesion site, allowing for the verification of long tract regeneration. Thirdly, for exactly these two reasons, all IHC results from Chapter 3 are from 14dpi animals thus setting all subsequent *in vivo* experiments to end at the same time period allows a more valid comparison of results. Finally, the *in vivo* intra-ON experiments performed by Koprivica *et al* (2005)were concluded at 14dpi, thus by using the same time point in the present study all experimental results could be compared and contrasted with those of the former.

In order to allow close comparison of the effects of intra-ON PD168393 on RGC survival and axonal regeneration with those of the *ivit* PD therapy detailed in Chapter 5, identical analytical methodology was followed. Full details for each of these are given in the introduction to Chapter 5. Briefly:,to establish extent of axonal regeneration, distance intervals of 250µm past the centre of the lesion site, up to 1.75 mm, were marked on composite photomicrographs of post experiment GAP-43 stained ON sections. The number of axons crossing each interval (represented by a line drawn across the photomicrograph, perpendicular to the long axis of the nerve) were counted and the results tabulated. To quantify RGC survival, eyes from treated animals were appropriately processed before being sectioned, H & E stained, and the surviving RGC counted. In this way the mean number of surviving RGC per animal per group were established. To confirm that PD effected EGFR phosphorylation blockade, the immunofluorescence of each pEGFR immunostained lesion site of each animal was compared to that of the adjoining proximal and distal sections of ON, with the prediction that the lesion site/matrix would exhibit significantly less pEGFR staining, reflecting an abrogation of EGFR phosphoylation. This was done under the assumption that PD would not affect pEGFR levels in any areas outside the immediate surrounds of the matrix. Finally, to provide a useful comparison in terms of numbers of axons surviving and regenerating, sections of ON from PN-graft recipient rats from previous experiments were stained for GAP-43 and the extend of regeneration ascertained, while the respective retinae were sectioned, H & E stained and counted to provide RGC survival values. As the mean numbers of axons regenerating and the mean numbers of surviving RGC at 14dpi in this model have long been established by repeated experiments performed by our research group, the values obtained in the present study could immediately be checked against

these figures, lending extra validity to comparisons of the extent of regeneration and RGC survival between PN graft and PD-matrix models.

Taking into account the provenance of previous collagen matrix implantation studies, the effects of intra-ON PD168393 reported by Koprivica *et al* (2005), including significant axonal regeneration without increase in RGC survival, and the results of *ivit* PD injection, it was predicted that considerable axonal regeneration would be observed in the PD-matrix group, that pEGFR levels would be attenuated in the lesion site of PD-matrix group animals, and that no effect would be found on RGC survival. It was not known to what extent, if any, the collagen matrix alone would promote axonal regeneration.

6.1.1 Specific Aims

- To promote *in vivo* RGC axonal regeneration using the EGFRki PD168393 (contained within a collagen matrix) and so confirm the *in vivo* results of Koprivica *et al* (2005).

.

- To obtain more robust RGC axonal regeneration than reported by Koprivica *et al.*(2005) due to the combination of permissive growth substrate and constant source of PD168393 provided by the implanted collagen matrix

6.1.2 Specific Hypotheses

1) RGC axons will regenerate into and through the implanted PD-impregnated collagen matrix

2) RGC survival will likely not be affected by the presence of PD168393

6.2 Results

Due to time constraints and accidental tissue destruction during tissue processing for IHC, several of the analyses comprising this final results section are less complete than intended. Specifically, several of the below results relying on ON tissue sections were not fully obtained in triplicate – the minimum required for statistical analysis. Where this was the case it has been stated explicitly so as not to mislead. Unless stated otherwise, *n* = 3 or more, as in all previous experiments. Additionally, several results refer to and show data derived from, *ivit* PN graft treated animals. These data were included to serve as an example of substantial RGC survival and axonal regeneration with which to compare any EGFRki-initiated regeneration, but, as these experiments were performed prior to all other experiments listed below, using a different strain of rat and did not involve any experimental manipulation of the ON beyond ONC, the results should <u>not</u> be directly compared.

6.2.1 RGC axons invaded lesion sites containing PD-matrix

GAP-43 staining showed that in PD-matrix implanted ON, many RGC axons advanced into, and often beyond, the lesion site (Figures 6.1-6.3). Many axons entered the PD-matrix and regenerated until they abutted the distal section of the ON, although most failed to exit the matrix and enter the distal ON segment. In terms of the mean number of axons crossing the lesion site, statistical analysis was impossible due to the results for the control matrix group consisting of only 2 animals (n = 2). Nevertheless, it can be seen that

all 3 PD-matrix-implanted ON exhibited considerable regeneration (Figures 6.1-6.3 and 6.6). Figure 6.6 shows the number of axons crossing various distances distal to the centre of the lesion site. The *ivit* PN group data were taken from a previous experiment and was included as an example of definite *in vivo* regeneration. This group did not receive any intra-ON treatment whatsoever beyond ONC.

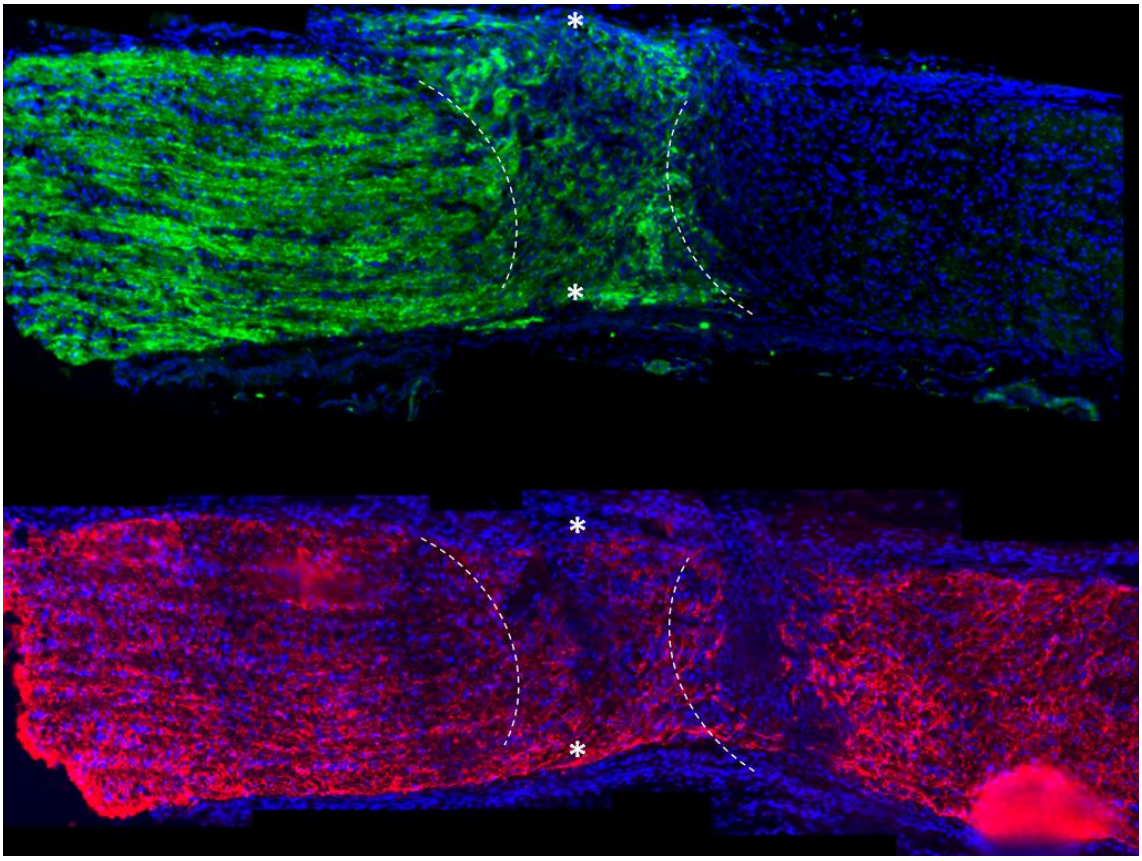

Figure 6.1. PD-matrix was invaded by axons which crossed the lesion site and progressed through the matrix and its border abutting the distal ON segment. Upper image shows GAP-43^{+} axons (green), lower image shows GFAP^{+} Astrocytes (red). ON sections are consecutive. Note the extent of axonal and astrocytic invasion of the matrix/lesion site. The collagen matrix has expanded such that it contacts both ends of the ON. The boundaries of the lesion site are traced in white. *=Approximate centre line of lesion. P= Proximal segment, D= Distal segment.

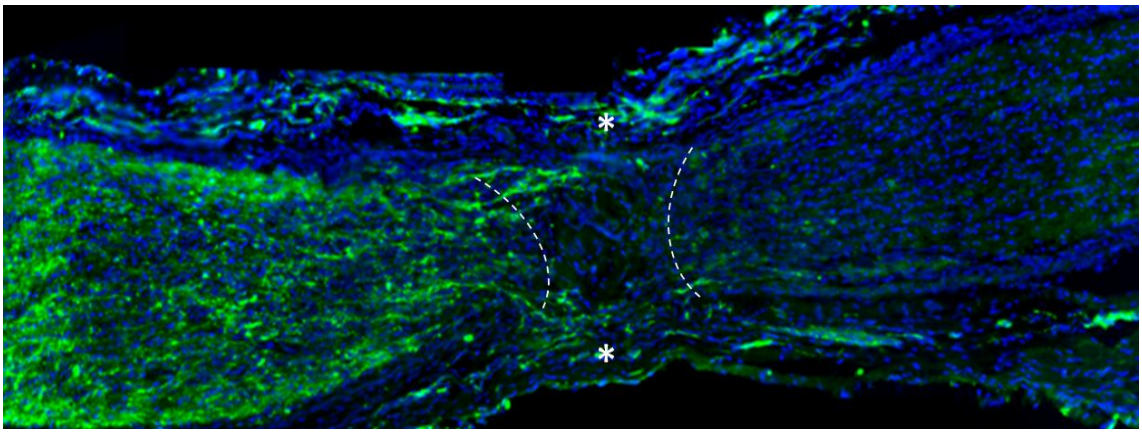

Figure 6.2. GAP-43^{+} axons (green) entering the lesion/PD-matrix of second PD-matrix implanted ON. No GFAP staining available due to the accidental destruction of tissue. The Collagen matrix has expanded such that it contacts both cut ends of the ON. The boundaries of the lesion site are traced in white. *=Approximate centre line of lesion**.** P= Proximal segment, D= Distal segment.

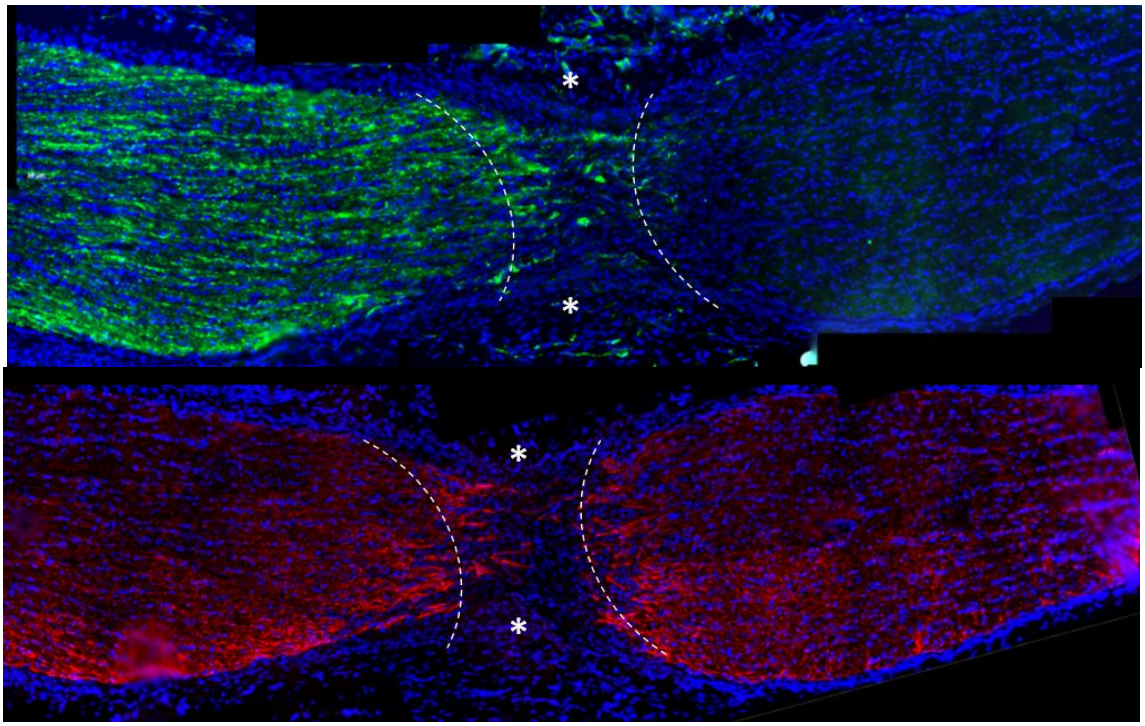

Figure 6.3. Third replicate of PD-matrix implanted ON. GAP-43^{+} axons (green, upper image) and GFAP^{+} astrocytes (red, lower image) have partially invaded the lesion site/PD-matrix . ON sections are consecutive. The collagen matrix has expanded such that it contacts both cut ends of the ON. The boundaries of the lesion site are traced in white. *=Approximate centre line of lesion**.** P= Proximal segment, D= Distal segment.

6.2.2 RGC axons did not invade lesion sites containing control-matrix

GAP-43 staining showed that almost no axons entered the control-matrices, with very few axons crossing into the matrix/lesion site and no axons whatsoever progressing further than the centre of the lesion (figures 6.4, 6.5, 6.6). As mentioned above, time constraints and experimental error resulted in only 2 complete control-matrix results, which precludes the use of statistics to determine the significance of differences in regenerating axon numbers. Despite this, a qualitative comparison of the number of axons entering and subsequently traversing the lesion site in the PD- and control-matrix groups (figures 6.1 – 6.3) strongly suggests that intra ON PD168393 promoted RGC axon regeneration.

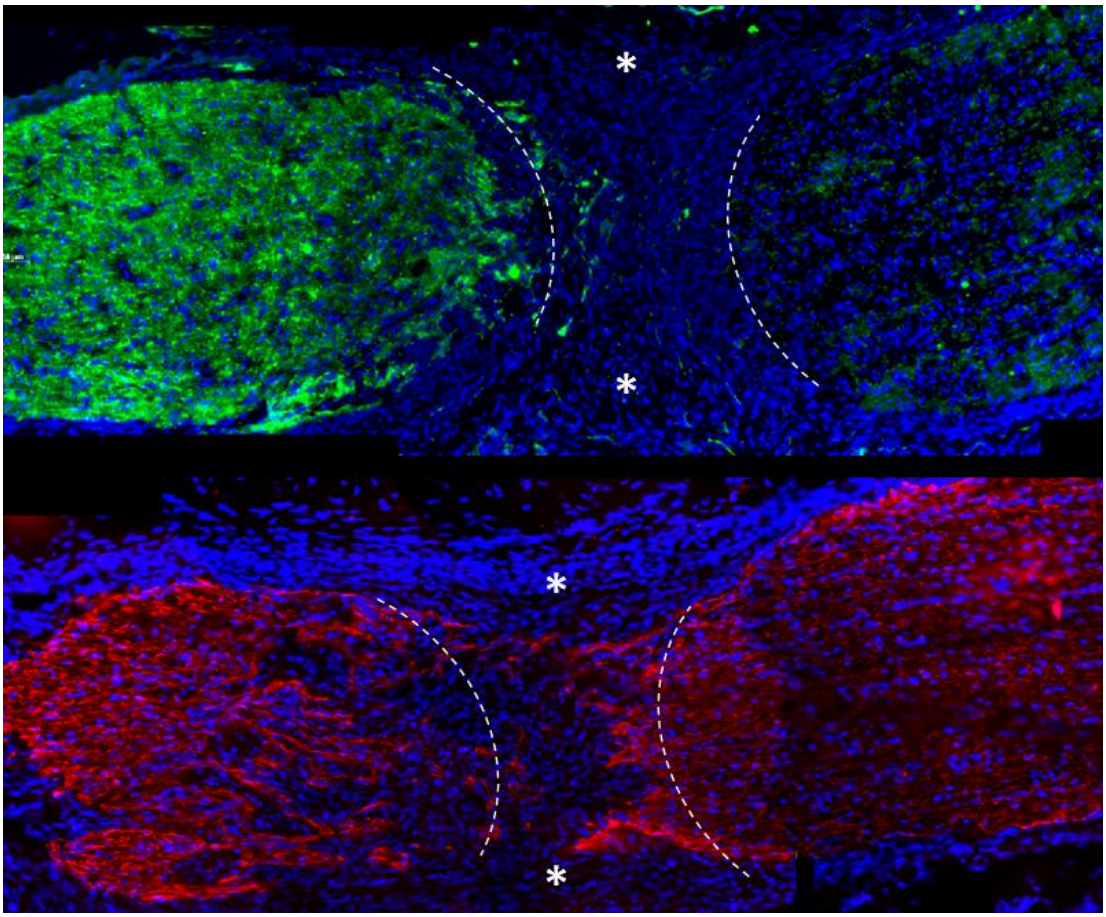

Figure 6.4. Control matrix implantation elicited no regeneration into or beyond the lesion site. Upper image shows GAP-43^{+} axons (green) failing to enter lesion site. Lower image shows GFAP^{+} astrocytes (red) showing the approximate boundaries of the lesion site (traced on upper image in white). Few astrocytes can be seen invading the lesion site. ON sections are consecutive. The collagen matrix has expanded such that it contacts both cut ends of the ON. The boundaries of the lesion site are traced in white. *=Approximate centre line of lesion**.** P= Proximal segment, D= Distal segment.

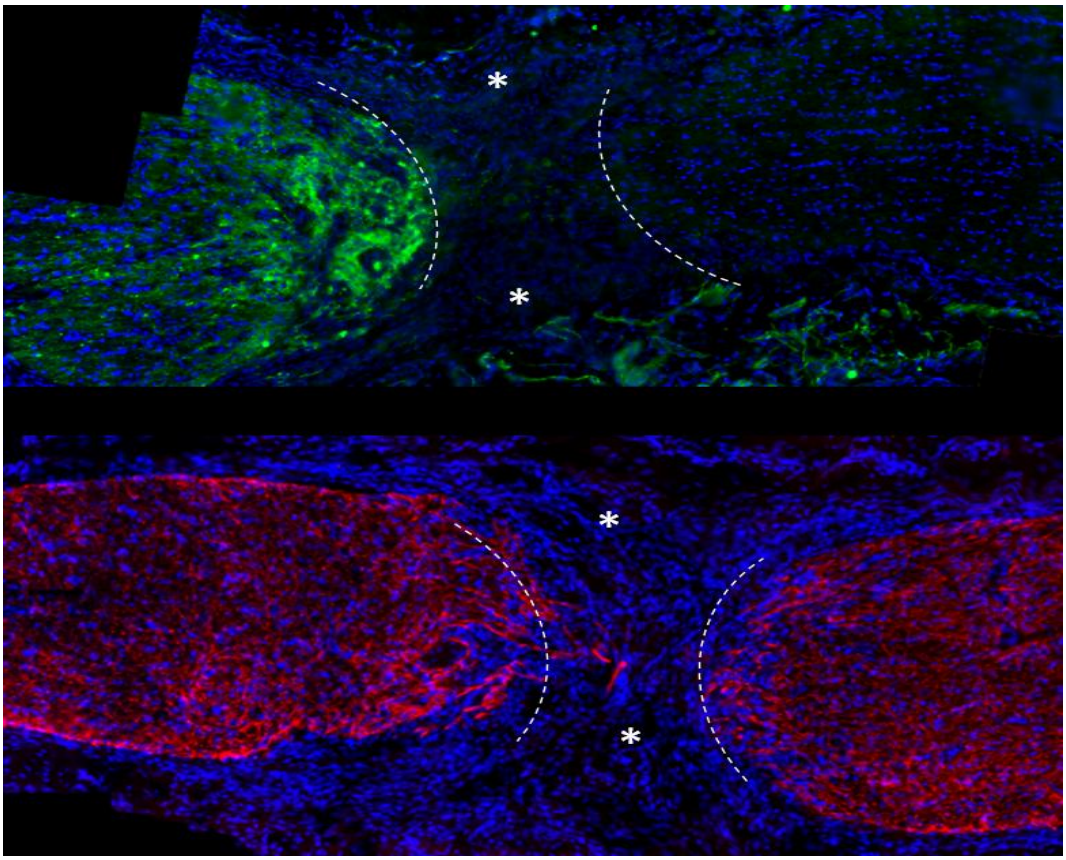

Figure 6.5. Control matrix implantation elicited no regeneration into or beyond the lesion site. Upper image shows GAP-43^{+} axons (green) failing to enter lesion site. Partial GFAP^{+} astrocyte influx/sparing within the lesion site is visible (red, lower image). ON sections are consecutive. The collagen matrix has expanded such that it contacts both cut ends of the ON. The boundaries of the lesion site are traced in white. *=Approximate centre line of lesion**.** P= Proximal segment, D= Distal segment.

6.2.3 PD-matrix promoted axonal regeneration, albeit less than ivit PN graft

Figure 6.6 shows the mean number of axons that regenerated increasing distances from the centre of the lesion site. PD-matrix (blue) and *ivit* PN graft (green) groups regenerated axons up to and including 1.25mm distal to the centre of the lesion site. Several PD-matrix group axons were also observed to have exited the lesion site and to have entered the distal ON section (Fig 6.2, 6.3). Although a small number of axons were seen to cross the proximal boundary of the lesion site and enter the control-matrix, no

axons were observed to extend further than 0.25mm distal to the proximal boundary of the lesion (Figures 6.4 and 6.5).

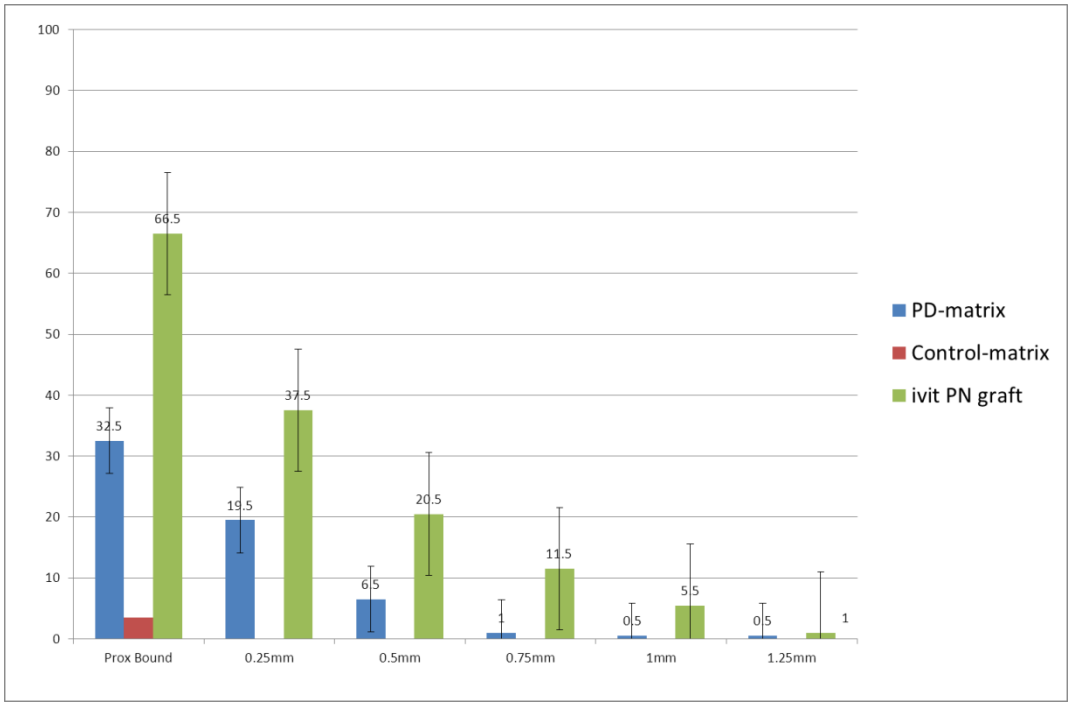

Figure 6.6. Mean number of axons regenerating past the proximal boundary of the lesion site and distances of 0.25 – 1.25 mm distally. i*vit* PN graft (green) and intra-ON PD-matrix (blue) implantation resulted in considerable axonal regeneration. Intra-ON control matrix implantation (brown) did not promote axon regeneration.

The following rationale were used to translate the values for regenerating axon numbers shown in Figure 6.6 into the percentages of total axonal population regenerating per treatment group shown in figure 6.7:

Average diameter of adult albino rat ON = 504.8µm (Melo *et al.* 2006)

Average diameter of adult albino rat ON axon = 0.77µm (Foster *et al.* 1982)

So in any ON section taken at or around midline of ON, number of axons in section = Diameter of ON/Diameter of axon = 504.8/0.77 = 655.6.

Therefore any one section of uninjured ON taken near ON midline should contain ~650 axons.

Regenerating axons are defined as being GAP-43^{+} and extending beyond the proximal boundary of the lesion site.

Thus:

Percentage of total RGC axon population regenerating in each 15µm-thick ON section=

(No. regenerating GAP-43^{+} axons/650) x 100

Using this formula, the approximate mean percentages of total RGC population regenerating in each 15µm-thick ON section were calculated for control matrix, PD-matrix and *ivit* PN groups (Figure 6.7).

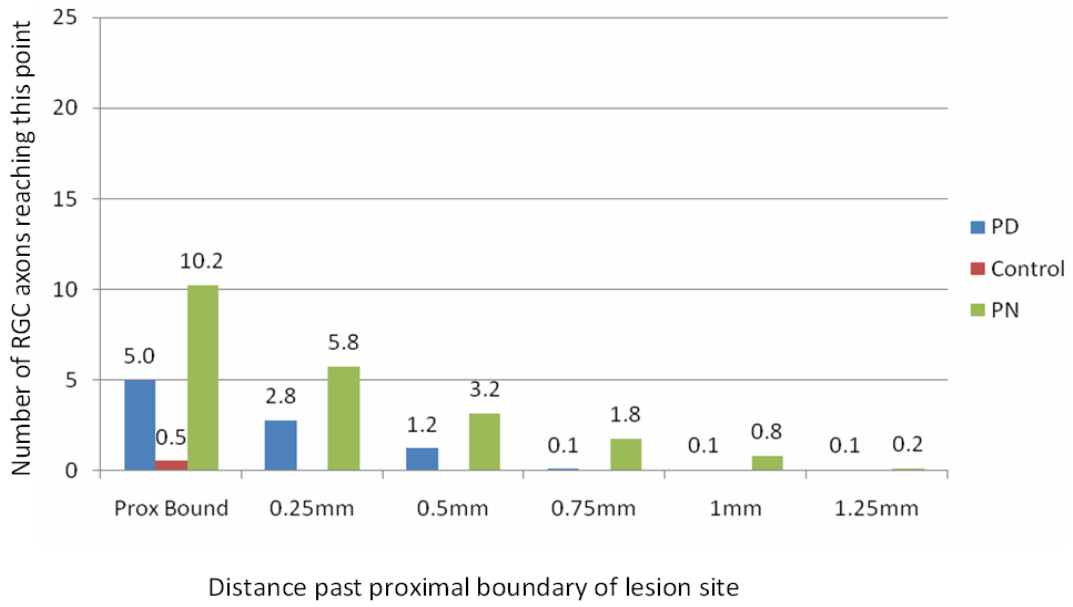

Figure 6.7. Estimated percentage of total axonal population (per 15µm-thick ON section) regenerating past the proximal boundary of the lesion site and distances of 0.25 – 1.25 mm distally. *ivit* PN graft (green) and intra-ON PD-matrix (blue) implantation resulted in considerable axonal regeneration. Intra-ON control matrix implantation (brown) did not promote axon regeneration.

6.2.4 PD-matrix implantation did not enhance RGC survival

PD-matrix implantation did not significantly affect RGC survival as compared to control-matrix (Figure 6.8). The mean number of RGC per field of view, as counted in the GCL in H&E stained retinal sections, did not alter significantly between the two groups, being 15.0 ± 1.2 and 17.2 ± 0.8 for control and PD groups respectively. *Ivit* PN group was not included as these animals were of a different strain – Sprague Dawley as opposed to Wistar – and the two strains are known to exhibit average different RGC density (see discussion for details and analysis).

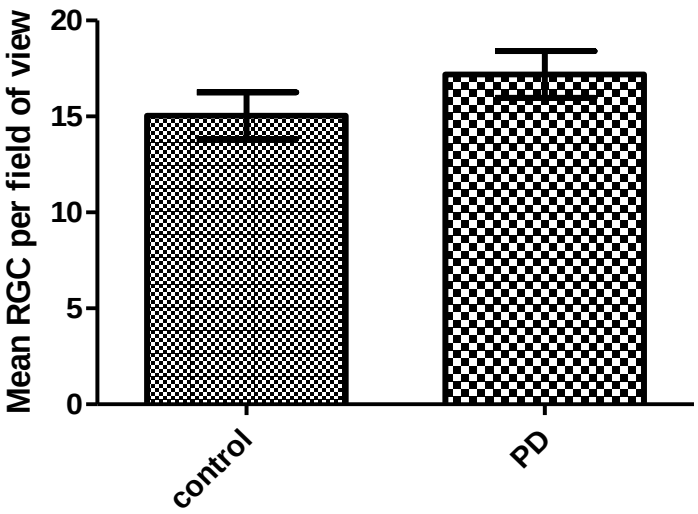

Figure 6.8. No difference in RGC survival was found between PD-matrix and control-matrix treatment groups. n = 4 for each group. Error bars represent 95% confidence intervals.

6.2.5 Lesion site pEGFR levels were unaffected by intra-ON PD-matrix implantation

In order to confirm the bioactivity of PD168393, pEGFR immunofluorescence levels were measured (in terms of pixel intensity) in the lesion site and the proximal and distal sections of each ON (see Chapter 5 introduction for further details). The mean immunofluorescence values for each of these ON areas, for each group, are shown below (Figure 6.9), expressed as arbitrary units. Control-matrix (blue bar) and PD-matrix (red bar) lesion sites exhibited no apparent differences in pEGFR staining, and lesion site pEGFR staining did not appear reduced, when compared to proximal/distal sections, in either group. As n = 2 for each group in these immunofluorescence studies, statistical analysis was not possible.

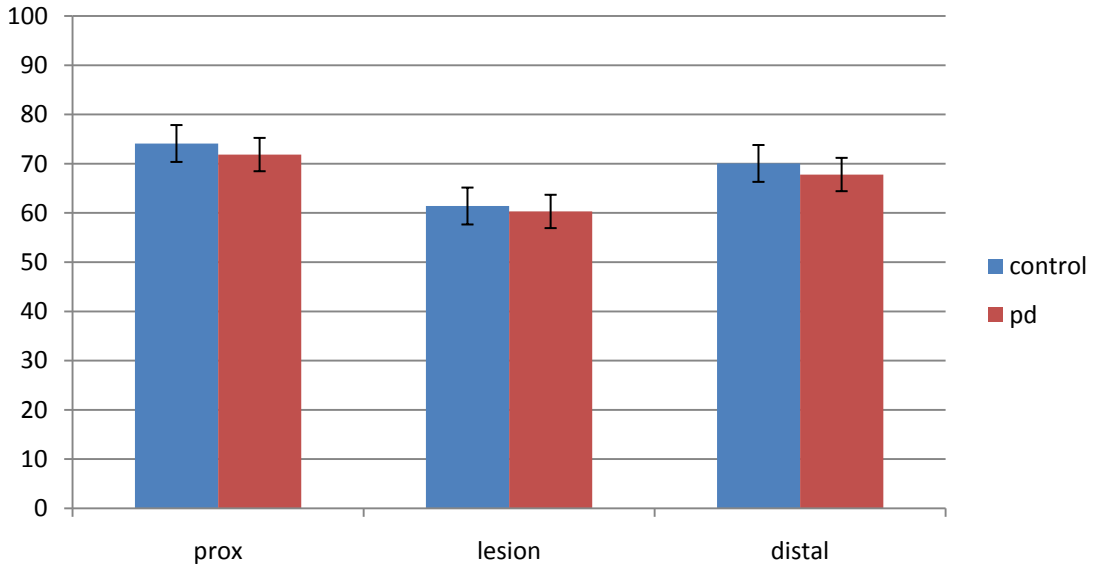

Figure 6.9 pEGFR levels in the proximal sections, lesion sites and distal sections of PD-matrix and control-matrix implanted ON, as inferred by pEGFR immunostaining intensity. No difference was observed between PD-matrix (blue) and control-matrix (red) intra-lesion site pEGFR staining intensity. Also, pEGFR staining levels in the lesion sites of both groups were not notably lower than the respective proximal and distal sections of the same ON. Units are mean pixel brightness values, as measured with histogram function within image analysis software, and are expressed as arbitrary units (a.u).

6.3 Discussion

6.3.1 RGC axons invaded lesion sites containing PD-matrix

That significant numbers of RGC axons invaded PD-matrices but not control-matrices (see below) strongly suggests that PD168393 promoted axonal regeneration; the first intra-ON confirmation of the original experiment by Koprivica *et al.* (2005). A population of axons regenerated across each PD-matrix-implanted lesion site, with a small number even penetrating into the distal segment of the ON. Having showed in Chapter 5 that delivering PD to the RGC somata and surrounding glia *via ivit* injection elicited no RGC axonal regeneration, the subsequent efficacy of intra-ON PD effectively narrows the potential target(s) of EGFRki such as PD to the cells, structures and molecules in and around the ON lesion site itself. Various hypotheses as to the nature of these intra-ON interactions are discussed in detail below.

6.3.2 RGC axons did not invade lesion sites containing control-matrix

The failure of axons to invade implanted control collagen matrices may be due to the lack of an active growth stimulus. It is has been shown that RGC axons fail to enter freeze-thawed PN grafts in which all cells are dead, whilst readily invading non-freeze thawed, living, but otherwise identical grafts (Berry *et al.* 1988), and that even PN axons will not invade such acellular PN tissue (Anderson *et al.* 1983, Nadim *et al.* 1990). This effect is

due to the secretion of survival and growth promoting NTF by Schwann cells contained within the graft, which drives axonal growth along the enhanced growth substrate of Schwann cell derived basal laminal tubes. Interestingly, Nadim *et al.* (1990) showed that axons from the rat tibial nerve tended not to extend into sections of freeze-thawed, acellular tibial nerve, and those few axons which did enter the acellular graft progressed no further than a maximum of 1mm. The almost complete failure of RGC axons to enter implanted control-collagen matrices echoes this effect; and it is hypothesised that just as the lack of Schwann-cell derived NTFs prevent both CNS and PNS axons from invading an otherwise permissive growth environment, RGC axons invading implanted PD-matrices do so in response to NTFs released by PD-conditioned ON glia such as astrocytes, which readily invade such collagen matrices soon after implantation (Gonzalez *et al.* 2009, Chapter 4, results section). As collagen matrices have been reported to reliably retain molecules of DNA (Berry *et al.* 2001) it is likely that very little PD would escape the matrix, but that subsequently released NTF could diffuse out, perhaps creating neurotrophic gradient "up" which RGC axons could grow, causing them to enter the PD-matrix. In the absence of this putative PD-provoked, glially secreted NTF support, control group axons would not have the stimulus to invade implanted control collagen matrices. Once again it must be pointed out that the small *n* number for control animals, in this case *n* = 2, is a potential caveat, and it is possible that larger numbers of control matrix results may have exhibited more significant axon regeneration.

6.3.3 RGC Axonal regeneration is promoted by implanted PD-matrix

Koprivica *et al.*(2005), using the quantification method used by Lehmann *et al.* (1999), estimated that approximately 0.5% of the total RGC population regenerated more that 0.5mm beyond the lesion site in response to intra-ON PD168393. The former study equated this level of axon regeneration to that seen in response to the Rho activity-blocking enzyme C3 transferase(<1%), which was the primary focus of the latter study. In comparison, PD-matrix and *ivit* PN graft groups regenerated approximately 1.2% and 3.2% of the total RGC population up to or beyond 0.5 mm past the lesion site. If accurate, the numbers of axons regenerating in the present study, in response to intra-ON PD-collagen matrices, is over twice that reported by Koprivica *et al*(2005). in response to PD introduced *via a* gelfoam cuff around the ONC site. The implanted collagen matrix itself served as a positive growth substrate for the (putatively indirectly) PD-stimulated advancing growth cones. In support of this, a*xo*ns of primary CNS neurons have been shown to grow faster in collagen gels than on flat monolayers of growth substrates such as laminin (Harris *et al.* 1985). It should be noted at this point that while both this study and that of Lehman *et al*(1999). used rats (Rattus norvegicus) for all *in vivo* experiments, Koprivica *et al*(2005). performed their experiments on mice (Mus musculus). This species difference makes it difficult to define real differences in percentage RGC regeneration and it is possible that PD-matrix implantation experiments as described here would have yielded different results in a mouse model.

6.3.4 PD-matrix did not enhance RGC survival

Statistical analysis of retinal RGC counts showed that levels of RGC survival were not significantly different between intra-ON PD-matrix and control-matrix implanted groups, despite the apparent enhanced axon regeneration exhibited by the PD-matrix implanted group. This agrees with the findings of Koprivica *et al.*(2005) who also found PD to have no effect on RGC survival, despite promoting significant axonal regeneration. Neuronal survival and axonal regenerative signalling pathways often overlap to the extent that any factor promoting one will promote the other, both processes being primarily mediated by the JAK/STAT, ERK and PI3K pathways (see general introduction), although which of these pathways is of primary importance appears to depend on circumstance. For example, the PI3K/Akt pathway has been shown to determine RGC survival following increased intra-orbital pressure, but to be irrelevant to RGC survival in control animals (Huang *et al.* 2008). Many neuroprotective therapies can enhance RGC survival without directly promoting *in vitro* neurite outgrowth or *in vivo* axon regeneration, primarily by activating or blocking pro- and anti-apoptotic members of the BCL-2 family of mitochondrial permeability regulating proteins (for review see Chao and Korsmeyer, 1998). Conversely, for any factor to elicit considerable *in vivo* axonal regeneration whilst not enhancing neuronal survival is unusual, but not unprecedented: Li *et al.* (2009) showed certain synthetic FGF analogues to differentially promote either *in vitro* neurite outgrowth or neuronal survival but not both and both Cui *et al.* (1999) and Cho *et al.* (1999) separately reported that CNTF promoted significant regeneration of axotomized hamster RGC axons, despite comprehensively failing to enhance RGC survival rates. The latter study suggested that CNTF may exert its regenerative effects *via* stimulating GAP-43 which is

known to act both directly and indirectly on the actin cytoskeleton, as well as influencing microtubule dynamics (Nguyen *et al.* 2009). This picture is complicated somewhat by the findings of Gupta *et al.* (2009), who show the neuroprotective effects of BDNF to be GAP-43 dependent, linking GAP-43 directly to neuronal survival. Nevertheless, that PD168393 promoted *in vivo* RGC axonal regeneration whilst having no effect on RGC survival suggests that the as yet unknown mechanism of action of such EGFRki does not directly involve the JAK/STAT, ERK or PI3K signalling pathways, as these growth promoting pathways usually simultaneously promote neuronal survival.

6.3.5 Lesion site pEGFR levels were unaffected by PD-matrix

Despite effecting measurable axonal regeneration, implanted PD-matrices did not render the lesion site less $pEGFR^{+}$ compared to the proximal and distal areas of the respective ON, and pEGFR immunofluorescence levels were not significantly different between PD- and control- matrix group lesion sites. Had no axonal regeneration been obtained with PD-matrices, this result would have likely have been interpreted as a failure in drug delivery, i.e. it would have been surmised that the concentration of PD within the matrices was too low to effect significant pEGFR blockade, or that incorporation of PD into the matrices had somehow inactivated it or prevented it from being uptaken by cells and axons. As significant regeneration was observed in response to PD- , but not control-matrix implantation, it must be assumed that PD168393 was accessible to the necessary cells and/or axons as well as being present at sufficient concentration to elicit this effect. There are three possible explanations for this result. Firstly, it is possible that PD was

present and accessible to an extent which allowed the putative, as-yet unknown signalling pathways to promote axonal regeneration but *not* to an extent which produced verifiable pEGFR blockade. This is possible when the potential promiscuity of many EGFRki, as reported by Fabian *et al.* (2005), is taken into account (see interim conclusions section below), i.e. it is possible that PD168393 may exert its beneficial effects on as yet unknown targets, at concentrations below that at which EGFR is affected. This would mean EGFR blockade was not the primary means by which PD, and by extension, perhaps other EGFRki, exert their axonal regenerative effects. Secondly, as collagen matrices are known to be almost fully degraded by around the time point used in the present study (Gonzalez *et al.* 2009), it is possible that the cells originally exposed to PD, and their subsequent abrogated pEGFR immunofluorescence, were obscured or diluted by the subsequent waves of invading $pEGFR^{+}$ inflammatory and immune cells (as confirmed by ED-1 and OX-42 staining, results section, Chapter 3). This possibility highlights the inadequacy of attempting to ascertain EGFR phosphorylation levels *via* the indirect, at best semi quantitative methods used here. Due to this combination of cellular events and less than ideal methodology, the level of ON pEGFR attenuation in response to PD-matrix implantation cannot be reliably ascertained from the results shown here. Further evidence that the inflammatory and immune cellular invasion may have played a key role in masking a reduction in pEGFR immunofluorescence is the clear and significant attenuation of retinal EGFR phosphorylation obtained as a result of *ivit* PD injections (Chapter 5, results) – despite the well documented macrophage influx in response to *ivit* injections, the associated small injury to the eye and the presence of retinal cellular debris following RGC apoptosis in response to distal ONC. The GCL, INL and IPL were all free from the large scale invasive cellular obfuscation seen in the injury site of the ON

allowing any changes in local pEGFR levels to be more readily detected. Finally, it is possible that a proportion of the PD contained within the matrices somehow diffused into the surrounding tissue, attenuating pEGFR immunofluorescence in the proximal and distal ON sections, leading to a lack of significant difference in fluorescence levels between the lesion site and the proximal and distal sections.

6.3.6 Interim Conclusions

Several hypotheses or models present themselves as to why intra-ON but not *ivit* PD would promote RGC axonal regeneration. These are based on the proposed models for EGFRki mechanism of action described in the discussion sections of Chapters 3 – 5.

In the first model, PD is thought to act directly on intra-ON RGC growth cones by inhibiting EGFR phosphorylation on the surface of the growth cone itself, as suggested by Koprivica *et al (2005*. The *in vitro* findings of this study, which showed evidence that pEGFR was associated with growth cone collapse, and those of Schachtrupp *et al.* (2007), which postulated that this signalling was mediated by the blood protein fibrinogen and subsequent intraneuronal β-3-integrin/EGFR interaction, would support such an intra-axonal model. This arrangement would mean that the primary mechanism of action of EGFRki such as PD and AG is to blockade the EGFR phosphorylation which occurs as a direct result of axons encountering fibrinogen, preventing the putative subsequent growth cone collapsing signalling cascade. If this hypothesis were correct, it would explain why intra-ON, but not *ivit* EGFRki, promoted axon regeneration: fibrinogen is present within the ON lesion site but not the retina, thus *ivit* PD would <u>not</u> prevent the

putative fibrinogen-EGFR interactions reported to trigger growth cone collapse. There are, however, several problems with this model. RGC axons do not contain pEGFR (Chapter 3 results) and, although growth cones were not directly visualised, it is unlikely that pEGFR was exclusively confined to growth cones without any retro- or antero-grade axonal signalling to/from the cell body, which would almost certainly have been visible following IHC analysis. It should be noted at this point that a Pubmed search of the literature failed to find a single study reporting the visualisation of EGFR on growth cones *in vivo*. Furthermore, Douglas *et al.* (2009) showed that RGC in primary retinal cultures treated did not exhibit enhanced neurite outgrowth when treated with siRNA such that EGFR was knocked down by over 90%, and further showed that these RGC still responded to subsequent AG1478 treatment with enhanced neuritogenesis. The present study also showed that *ivit* PD168393 successfully attenuated pEGFR levels in the GCL, yet this had no effect on axonal regeneration (Chapter 5), and it has been observed that all $pEGFR^{-}$ RGC, when dissociated *in vitro,* become highly pEGFR immunoreactive irrespective of subsequent neuriteogenesis (Douglas *et al.* 2009). Thus it would appear that the balance of current evidence suggests a purely on-target, axonal/growth cone-specific role for PD168393 to be very unlikely.

In the second proposed model PD acts intraneuronally, but not specifically on EGFR – i.e. off target. Many protein kinases and receptor tyrosine kinases have similar tyrosine phosphorylation domains and it is possible that PD168393 affected other, as yet unknown, kinases. Fabian *et al.* (2005) created a small molecule-kinase interaction map for 20 clinically aimed kinase inhibitors and examined their effects of 120 kinases. They showed several EGFRki to affect numerous other kinases distinct from EGFR, concluding that: “specificity varies widely and is not strongly correlated with chemical structure or

the identity of the intended target". PD has been shown, for example, to inhibit the activity of stat3 and ERK (Chen *et al.* 2005), albeit it at 10x the concentration needed to inhibit EGFR kinase activity (values were described in terms of IC50 measurements). Also supporting this idea of off-target effect is the fact that Koprivica *et al*(2005) compiled a list of the effects of over 400 compounds on the disinhibition of CGN neurite outgrowth, including several EGFRki (Koprivica *et al.* (2005), supplementary material)), and while some EGFRki promoted considerable neurite outgrowth, (e.g. the tyrphostins A23, A46, A47, B44, and AG1478), other EGFRki had absolutely no effect on neuritogenesis (tyrphostin B42, PD153035). It is possible that the putative unknown target or targets of EGFRki is/are present in the growth cones or intra-ON axons of RGC but <u>not</u> present in the retina, hence the failure of *ivit* PD to elicit regeneration. In this model, EGFR is not directly involved in growth-inhibitory signalling at all and its identity as the original target of EGFRki such as PD168393 is irrelevant.

The third proposed model has EGFRki such as PD168393 and AG1478 achieving their beneficial effects on RGC axonal regeneration indirectly, through influences on ON glia. Here, EGFRki is proposed to perform a dual on-target/off-target role; inhibiting the various previously discussed growth antagonistic cellular events linked to non-neuronal EGFR signalling (described in detail in the discussion section of Chapter 3), whilst simultaneously effecting the release of NTFs local to axons within the ON, encouraging regeneration. The fact that RGC axons severed inside the retina regenerate spontaneously up to the optic disc (McConell and Berry 1982), while RGC axons severed at any point beyond the optic disc emphatically do not has been at least partially attributed to the lack and presence of growth inhibitory CNS myelin before and after the optic disc respectively. It is possible instead/additionally that this difference is due to the

aforementioned actions of several cell types in the ON which are not present in the retina, including oligodendrocytes, symamtocytes, and numerous inflammatory/immune cells invading the ON after injury and subsequent disruption of the BBB. If these cell types and t heir associated EGFR-dependent processes are in fact a major source of axonal growth antagonism this would explain why intra-ON, but not *ivit*, PD effected regeneration - locally applied EGFRki would abrogate the putatively responsible EGFR signalling whereas *ivit* PD would not. It should be noted however that glial NTF release in response to EGFRki has only been directly confirmed *in vitro*, and even then, only in primary retinal cultures (Douglas *et al.* 2009). One potential problem with this NTF release hypothesis is the absence of increased RGC survival in PD treated ON, as reported by Koprivica *et al*(2005). and confirmed in this present study. Numerous papers have been published on the effectiveness of both single and combinatorial NTF therapy in promoting significant RGC survival *in vivo* (see Berry *et al.* 2008, section 3, for review) and the lack of such increased RGC survival in PD treated ON is difficult to explain if local NTF release is part of such EGFRki's mechanism of action.

The fourth and final proposed model proposes, as mentioned previously, that the effects of PD168393 (and by extension, potentially other EGFRki such as AG1478) on RGC are a result of their interaction with one or more compounds found within CNS myelin - a hypothesis based on the observations of Douglas *et al. (*2009) who reported that CME+EGFRki treated retinal cultures exhibited synergistic growth. A short description of one such possible candidate, inosine, is described in the discussion section of Chapter 3 (also, see Douglas *et al.* 2009). If components of CNS myelin are required for EGFRki-mediated regeneration then this could also explain why *ivit* PD failed to elicit RGC axonal regeneration; there being no myelin in the rat/mouse eye. As mentioned previously, at

least one myelin derived protein, MAG, has been shown to switch from being growth antagonistic to being growth promoting, given sufficiently high levels of the intracellular secondary messenger cAMP (Cai *et al.* 2001) and the EGFRki AG1478 has been shown to elevate cAMP levels in primary retinal cultures *in vitro* (Douglas *et al.* 2009). It is thus possible that some other component of CNS myelin is acting analogously and synergistically boosting the effects of EGFRki. It should be noted that this model makes the assumption that EGFRki must be delivered intra-ON, as *ivit* PD treated RGC are still technically exposed to PD as well as CME (at the lesion site). Thus this model suggests that EGFRki, working in concert with some component of CME, act synergistically on growth cones/ON glia.

A recently published study has provided evidence compatible with the third, glia-centred model. In a paper published in 2007, Schachtrupp *et al.* provided *in vivo* evidence that, following spinal cord injury, the blood protein fibrinogen can induce EGFR phosphorylation and transactivation *via* the β-3 integrin receptor, resulting in the abolition of neurite outgrowth. This study showed that fibrinogen deposition coincided extremely closely with pEGFR staining and with local axonal regenerative failure. In this final model, ONC allows blood, containing fibrinogen, to come into contact with axons and glial cells in the damaged ON, whereupon fibrinogen sets in motion various EGFR dependent growth antagonistic events known to hinder *in vivo* axonal regeneration, including CSPG deposition and increased myelin production. In this model, the efficacy of intra-ON as compared to *ivit* application of PD is explained as a local effect on glial cells which would otherwise be affected by fibrinogen. As fibrinogen is concentrated in the ON, *ivit* PD would not ameliorate its effects. Interestingly, the success of intra ON but not *ivit* PD application suggests that at least two of these proposed mechanisms-of-action for

EGFRki are mutually compatible, and may be occurring simultaneously. EGFRki such as PD could be simultaneously effecting NTF release from ON glia, blockading the harmful effects of putatively fibrinogen-mediated glial EGFR signalling, and exerting outgrowth-enhancing, as yet unknown off-target effects on axons and/or growth cones.

Irrespective of the underlying signalling mechanisms, it appears that PD168393, immobilised within collagen matrices implanted into the crush site of rat ON, promoted substantial and statistically significant RGC axonal regeneration. This regeneration appears to represent around 1.2% of the total RGC population, over a twofold increase of the estimated 0.5% RGC which Koprivica *et al*(2005) reported regenerating in response to PD-saturated gelfoam cuffs placed around the lesion site. In further agreement with the findings of this study, no effect on RGC survival was observed.

Chapter 7

Summary and Final Conclusions

7.1 Summary

This study had two interconnected goals. Firstly, to determine whether or not the Epidermal Growth Factor Receptor is involved in the failure of RGC axons to regenerate, and secondly, to elucidate the means by which certain EGFRki exert their previously demonstrated *in vitro* and *in vivo* neuritogenic and axogenic effects. The four preceding Chapters provide evidence sufficient to construct several models which simultaneously describe the putative roles of EGFR and those of the EGFRki investigated. These models have been described in each accompanying discussion section, and what follows is a brief discussion of the evidence for each, taking into account all relevant recently published literature, including potential/additional mechanisms of action for EGFRki that are based on the findings of studies outside the field of CNS repair. This analysis will culminate with the propounding of a final model of the involvement of EGFR and EGFRki in RGC axon regeneration, based on all known experimental evidence to date.

The first model is the intra-axonal model proposed by Koprivica *et al.* in 2005, which places the EGFR somewhere within the signalling cascade which links the NgR/LINGO/$p75^{NTR}$ (or TROY) receptor complex to the Rho A/ROCK-mediated cytoskeletal changes known underlying growth cone collapse and abortive regeneration. Koprivica *et al.*(2005) showed evidence that blocking EGFR with EGFRki such as AG1478 and PD168393 allowed *in vitro* neurite outgrowth in otherwise growth-antagonistic conditions, and promoted *in vivo* RGC axonal regeneration. By contrast Schachtrupp *et al.* (2007) showed that fibrinogen, signalling through β-3 integrin receptors, inhibited neurite outgrowth, and suggested that it is this process which is attenuated by EGFRki such as PD168393. Both studies concluded that the neuritogenic actions of EGFRki were a result

of their abrogation of EGFR signalling. However, Chapter 3 of the present study showed all RGC axons to be pEGFR^{-}, both in the the retina and in the ON, both before and after ONC and that only a ~30% subpopulation of RGC express pEGFR at the somata – a precentage far greater than the population of regenerating axons seen in response to intra-ON EGFRki therapy. It should also be noted that at the time of writing (2010) no study had demonstrated the presence of pEGFR on RGC axons. Further, it has been demonstrated that AG1478 can enhance RGC neurite outgrowth *in vitro* even in primary retinal cultures which have had had EGFR levels reduced to < 10% with siRNA, and conversely, that this siRNA therapy alone does <u>not</u> promote neurite outgrowth. Finally, it has been shown on numerous occasions that the blockade of any single outgrowth-antagonistic signalling pathway alone will not result in neurite outgrowth or axonal regeneration (see Berry *et al.* 2008 for review), and even blocking critical intracellular effector proteins such as ROCK, which serve as nexus points for numerous outgrowth antagonistic pathways, will only promote modest outgrowth at best (Fischer *et al.* 2004). As such, intra-axonal EGFR signalling alone cannot explain the EGFRki-mediated *in vitro* and *in vivo* outgrowth of any study published to date and subsequently, of all the proposed models to explain the actions of EGFRki discussed in the present study, this is the only model which can be confidently discarded.

The second proposed model, illustrated in Figure 7.1 below, still has the axon/growth cone/RGC somata as the primary target of EGFRki therapy, but hypothesises that EGFRki are not exerting their effects through EGFR blockade but instead are acting on other, unrelated, signalling pathways, including other kinases. Recall that Fabian *et al.* (2005) created a small molecule-kinase interaction map for 20 clinically aimed kinase inhibitors, including several EGFRki, and examined their effects on 120 intracellular

kinases. They showed several EGFRki to affect numerous other kinases distinct from EGFR, concluding that: "specificity varies widely and is not strongly correlated with chemical structure or the identity of the intended target". PD168393, for example, has shown to partially inhibit the activity of stat3 and ERK (Chen *et al.* 2005), and while koprivica *et al.* showed that several EGFRki promoted considerable neurite outgrowth, (tyrphostins A23, A46, A47, B44, and AG1478), other EGFRki had absolutely no effect on neuritogenesis (tyrphostin B42, PD153035).

As well as these potential interactions with other kinases, there are two additional pathways through which EGFRki be acting. Firstly, it was reported that AG1478 could strongly inhibit the activity of the calcium sensing receptor (CaR) (Tomlins *et al.* 2005), and that the CaR could signal through Rho and ROCK, causing actin stress fiber assembly and altered cellular morphology (Davies *et al.* 2006) - processes which could potentially lead to filopodial retraction and growth cone collapse. Secondly, several EGFRki, including genistein and the tyrphostins B44 and tyrphostin 51, were also shown to strongly inhibit *in vitro* neuronal phosphodiesterase (PDE) activity (Ho *et al.* 1995), and to decrease phosphodiesterase activity 80-85% in a neural cell line (Stringfield and Morimoto 1997), while the PDE4 inhibitor etazolate hydrochloride was shown to elicit *in vitro* neurite outgrowth levels equivalent to that seen in response to AG1478 (Koprivica *et al.* 2005, supplementary material). As cAMP is hydrolysed by certain PDE subtypes (particularly the aforementioned PDE4 in neurons) this PDE blockade results in increased levels of intracellular cAMP (Ho *et al.* 1995, Nichols and Morimoto, 1999), an event known to enhance (or perhaps even be required for) *in vivo* axonal regeneration (Cai *et al.* 2001, and see Hanilla and Filbin 2006 for review). Such elevated cAMP levels were found in AG 1478-treated primary retinal cultures reported by Douglas *et al.* (2009). The

ramifications of these studies is immediately apparent; EGFRki such as AG1478 and PD168393 could potentially drive axonal regeneration *via* elevated cAMP levels resulting from PDE inhibition, while simultaneously opposing (putatively) CaR-Rho-A mediated growth cone collapse, entirely independently of EGFR signalling.

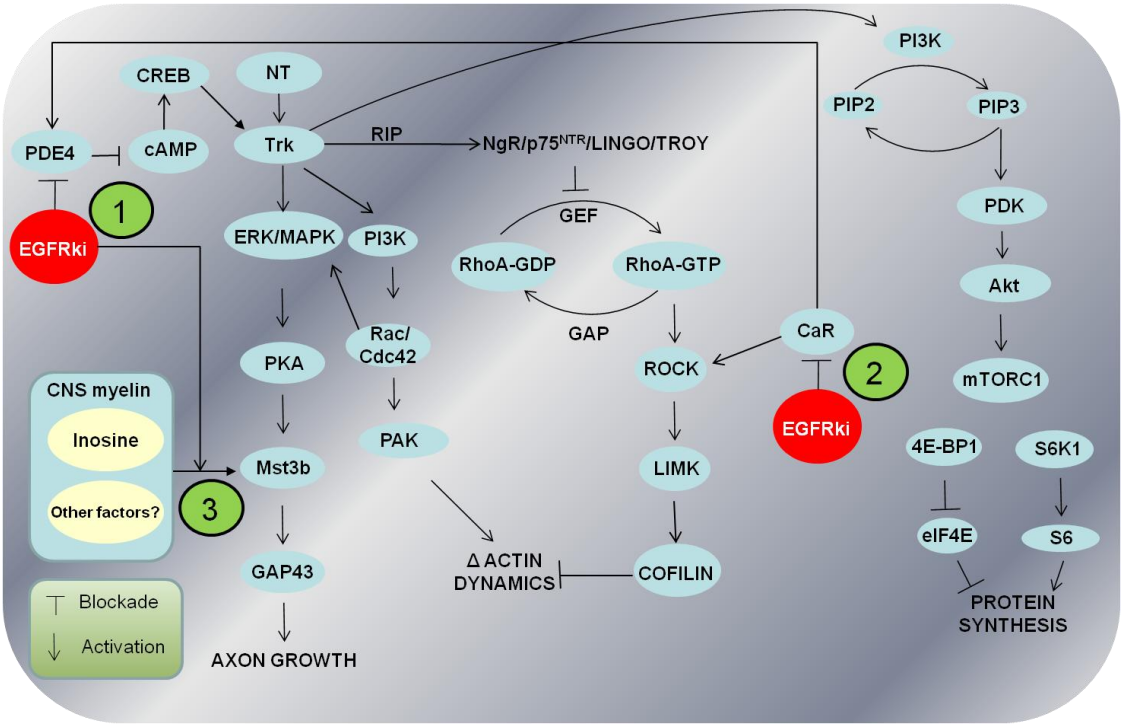

Figure 7.1. Proposed means by which EGFRki may exert intra-neuronal axonal-regenerative effects independently of EGFR signalling. 1. Blockade of phosphodiesterase 4 (PDE4) causes elevated intraneuronal cAMP levels, leading to Trk activation and axonal outgrowth. 2. Inactivation of the calcium sensing receptor (CaR) prevents its signalling for growth cone collapse through ROCK and its activation of PDE4. 3. EGFRki may also act synergistically with components of CNS myelin such as inosine to facilitate axonal regeneration.

The third model proposes that EGFRki primarily promote RGC axonal regeneration *in vivo,* and neurite outgrowth *in vitro*, through their effects on glia, firstly *via* the amelioration of the myriad of glially mediated, EGFR signalling-dependent, regeneration antagonistic processes known to occur in the injured CNS, and secondly by eliciting glial NTF release. These growth antagonistic processes are summarised and illustrated in Figure 7.2 below.

In this model it is surmised that the axonal regenerative effects of intra-ON PD168393 stem from rendering the lesion site a less hostile axon-growth environment, and by concomitantly stimulating the release of NTFs from local glia. This model benefits from having considerable evidence for each proposed glia-EGFR-axon interaction and it is very likely that a large part of any successful intra-ON anti-EGFR therapy will be as a direct result of blocking these processes. There is less evidence for the suggested accompanying glial NTF release, being as it is an extrapolation of an *in vitro* effect seen in primary retinal cultures exposed to AG1478 (Douglas *et al.* 2009).

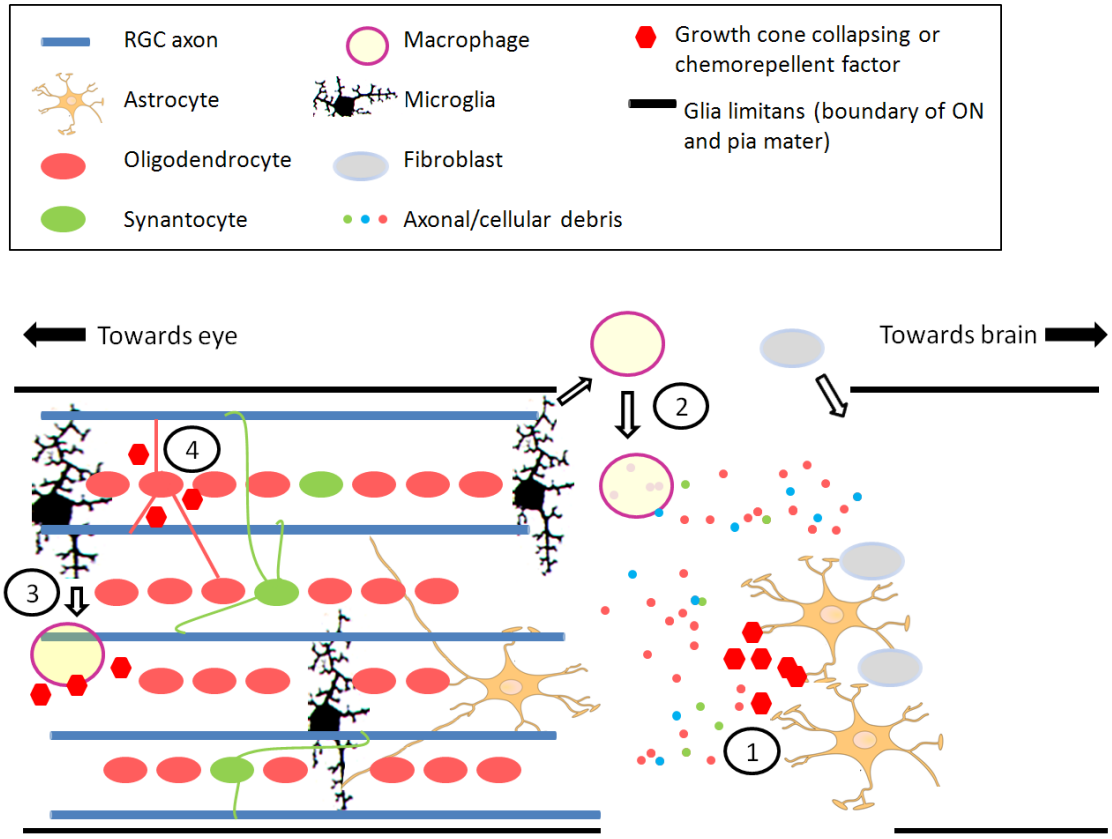

Figure 7.2. Schematic of the post-crush optic nerve, illustrating the various regeneration-antagonistic processes resulting from glial EGFR signalling. 1. Astrocytes activate, hypertrophy and migrate to lesion site, where they begin to simultaneously secrete growth cone-repulsive factors including semaphorins, ephrins, SLITS and CSPG, and along with fibroblasts, begin construction of the glial scar. 2. Haematogenous monocytes enter the CNS through the compromised BBB and differentiate into phagocytic macrophages, debriding damaged axons and damaging them further. This influx is in part a response to various macrophage attractant factors secreted by astrocytes and microglia. 3. Microglia activate, take on a macrophage-like phenotype, attacking and debriding myelinated axons, whilst secreting cytotoxic substances including various ROS, and releasing various chemokines and cytokines which initiate lymphocyte and neutrophil influx, leading to futher cytotoxicity and axonal damage. 4. Oligodendrocytes increase production of CNS myelin as part of an attempt to remyelinate debrided axons. Although there is no extant literature concerning synantocyte EGFR signalling, these cells were included in this diagram for completeness.

The fourth model suggests that some factor 'x' in CNS myelin, acting in conjunction with EGFRki such as PD168393, actively promotes RGC axonal regeneration (illustrated above in Figure 7.1). This hypothesis is based on the fact that AG1478 elicited far greater *in vitro* RGC neuritogenesis when in the presence of CME (Douglas *et al.* 2009) and that intra-ON, but not *ivit* PD168393, promoted axonal regeneration (Chapters 5 and 6, this study) - the lack of CNS myelin in the rat retina precluding any such synergistic

axonal growth in the *ivit* PD168393 experiments. The initial candidate suggested to be this factor 'x' was inosine, identified for its previously described roles in axonal outgrowth. Inosine has been shown to activate MST3b, a protein kinase critical to axonal outgrowth (Irwin et al. 2006) as well as serving as a ligand for the adenosine A2A receptor (Nascimento, 2010) which in turn can transactivate Trk receptors, resulting in growth and axogenic responses similar to that obtained with conventional NTF-therapy (Jeanneteau and Chao, 2006). In support of this, Chapter 4 of the present study showed how the A2A receptor antagonist ZM21385 partially inhibited the growth promoting effects of AG1478 on primary retinal cultures, an effect potentially attributable to either (or both) of these two pathways. It is also possible that the elevated cAMP levels resulting from EGFRki therapy could be potentiating this effect – as seen with the switch of MAG from growth-antagonistic to growth promoting (Cai *et al.* 2001).

With the exception of the first model, which has been rendered all but untenable by the results of the present study (as well as those of others in our research group), all of the models proposed above are in principle mutually compatible: the events described in each could potentially occur simultaneously. As such, the final model illustrated in Figure 7.3 is an amalgamation of these models and, this author believes, represents the most complete picture to date of how the EGFR and EGFRki are involved in the prevention and restoration of RGC axonal regeneration. This model takes into account EGFR distribution and signalling, on- and off- target effects of EGFRki, neuronal and glial influences and is based on evidence from scores of studies, including the data comprising the present study.

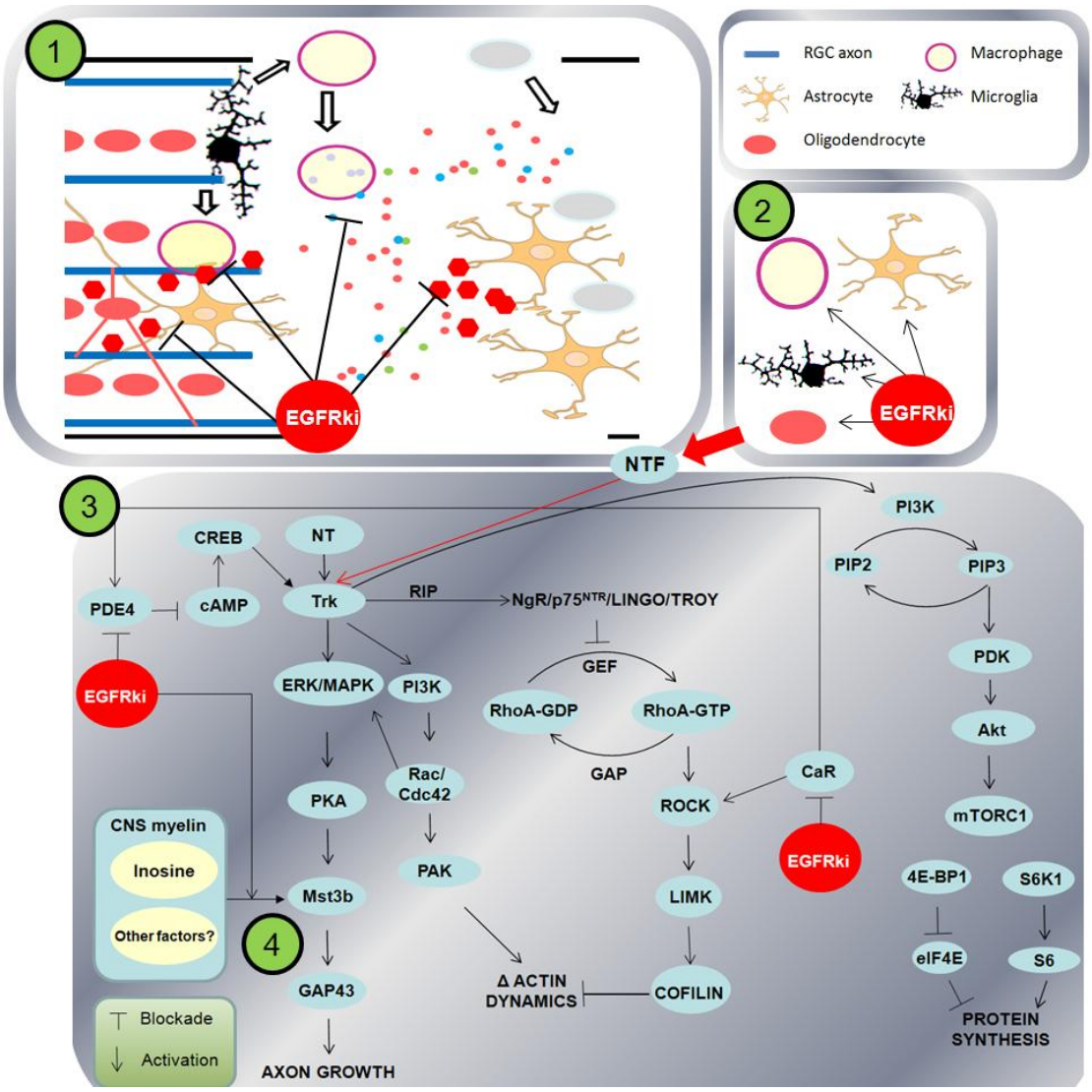

Figure 7.3. The final proposed model of the actions of EGFR and EGFRki in the injured optic nerve. 1. EGFRki abrogate various glially mediated growth-antagonistic EGFR-signalling dependent cellular events, reducing secondary axonal damage and truncating intra-ON levels of growth-cone collapsing factors. 2. In response to EGFRki, ON glia produce and secrete various growth-promoting NTFs. 3. Acting intraneuronally, EGFRki simultaneously a) inhibit the function of the CaR, preventing it from signalling for growth cone collapse through ROCK, and b) inactivate PDE4, raising intraneuronal levels of cAMP, which in tandem with the NTFs released from ON glia activate the Trk receptors leading to further enhanced axon growth. 4. EGFRki mediated effects may also include the actions of some factor present in CNS myelin - such as inosine - the synergistic effects of which may also facilitate axonal outgrowth.

7.2 Final conclusions

In summary, the role of the EGFR in RGC axonal regenerative failure appears to be chiefly a glial one, with EGFR governing a variety of growth antagonistic processes which render the CNS a more growth-hostile environment. There is no compelling evidence for, and considerable evidence against, a direct, intra-axonal role for EGFR, effectively excluding the possibility that EGFR itself is part of the NgR/LINGO/$p75^{NTR}$ signalling pathway converging on RhoA/ROCK which leads to growth cone collapse. Mirroring this, there is a wealth of data to suggest that EGFRki almost certainly do not achieve their RGC axonal regenerative effects through the blockade of neuronal EGFR. They likely do so instead *via* the abrogation of the various aforementioned harmful EGFR-dependent glial signalling processes, the stimulation of glial NTF release, the inhibition of PDE4, resulting in the elevation of intra-neuronal/axonal cAMP levels, and, potentially, by blockading the putative growth cone collapse-initiating CaR-RhoA signalling pathway and by interacting with an as yet unknown component of CNS myelin.

Thus EGFR is almost certainly not directly involved in RGC axonal growth cone collapse, but plays an important if indirect role *via* its impact on glial events, while EGFRki such as AG1478 and PD168393 promote axonal regeneration through off-target intra-/neuronal and both on- and off-target effects on glia, but do not do so by blockading axonal EGFR signalling.

7.3 Futher studies

This study has variously demonstrated the distribution of pEGFR in the rat visual system, constructed a novel *in vitro* inhibitory and disinhibitory assay for primary retinal cultures using the Nogo-P4 peptide and EFGRki, demonstrated the inefficacy of *ivit* PD168393 on post ONC axonal regeneration and shown *in vivo* axonal regeneration using PD-impregnated collagen matrices implanted into the ON lesion site. Arguably the lattermost is the most important result, (despite the limitations of the experiment and the need for its repetition – discussed below) the axonal regeneration obtained from PD168393-impregnated collagen matrices being approximately double that of that reported by Koprivica *et al.*(2005) in response to PD-soaked gelfoam placed around the crushed mouse ON (~1.2% to ~0.5% respectively). Although EGFRki are a modestly promising potential therapeutic tool, the use of EGFRki-implanted collagen matrices would perhaps achieve greater regeneration if used in some form of combinatorial therapy. Almost as remarkable as the regeneration obtained by both this approach and that of Koprivica *et al.*(2005) is the complete lack of enhanced RGC survival which normally accompanies such regrowth. While the reasons for this apparent paradox remain unclear, it suggests that if collagen matrices were impregnated not only with EGFRki, but with other factors conducive to RGC survival, such as BDNF, greater levels of regeneration might be obtained. Previous studies have shown that collagen matrices can be successfully impregnated with viruses or naked-plasmids containing the genes for growth promoting agents, or can be made to contain such factors themselves, and that such agents remain almost entirely with the matrix whilst being readily endocytosed by invading cells/axons

and as such a combinatorial cocktail of such factors or genes, along with EGFRki such as PD168393 could potentially promote RGC survival, as well as providing a regenerative drive and a strong growth substrate through which to progress. It should also be recalled that the axonal regeneration in response to intra-ON PD-matrix implantation reported here is considerably less robust than that observed to occur in response to several other previously described therapies, such as *ivit* PN graft implantation or multiple NTF therapy, and that almost all previously reported regeneration-promoting therapies also promoted significant RGC survival, which PD-matrix implantation did not.

While this study has provided substantial evidence as to the actions of EGFR and EGFRki in the injured visual system, several of the results obtained need to be confirmed through extra experiments, and many of the constituent pathways and interactions in the proposed final model require experimental confirmation.

Although absolutely no axon pEGFR was observed in the axonal/pEGFR colocalisation studies comprising Chapter 3, and despite the lack of any reports of axonal pEGFR in the literature, to finally exclude intra-RGC growth cone EGFR signalling, an IHC colocalisation study should be performed in the post ONC ON using antibodies to both growth-cone specific proteins such as the actin-associated protein 2G13p and to pEGFR.

Due to loss of considerable control-matrix group ON tissue, the intra-ON PD-matrix experiments detailed in Chapter 6 suffered from insufficient *n* numbers in the control-matrix group, and barely sufficient numbers ($n = 3$) in the PD-matrix treatment group. As such these experiments should be repeated such that $n = 4$ (at least) for each treatment and control group, each accompanied by retinal RGC survival counts. Until this is accomplished the results shown in Chapter 6 cannot be fully trusted or published in a peer reviewed journal. Although the primary result - that PD-matrix implantation led to

RGC axonal regeneration - was confirmed in triplicate, and only the relative contribution of the collagen matrix itself, illustrated by the presence/absence of control-matrix group axonal regeneration, is technically in question, *n* = 3 is the minimum number which allows statistical analysis, and thus additional *n* numbers for each group would reduce error margins and is thus desirable. These two studies could potentially be combined into a single experiment, allowing for both the confirmation of the effects of intra-ON PD-matrix implantation and edification as to the existence of growth cone pEGFR *in vivo* in both regenerating and non-regenerating models.

The various potentially axon growth-arresting actions of the neuronal calcium sensing receptor (CaR) is perhaps the most potentially rewarding area of futher research. This receptor appears to be able to signal through ROCK while lowering the levels of intraneuronal cAMP through activation of PDE4, and it has been reported that the CaR can be inactivated by AG1478 . This suggests that not only could CaR inactivation underlie much of the effects of EGFRki, this receptor could potentially be another key activator of the inhibitory signalling cascade which leads to growth cone arrest and collapse. To investigate this, the effects of CaR inactivation should be investigated, initially *in vitro*, *via* such methods as siRNA knockdown combined with pharmacological blockade of the CaR itself using CaR-specific antagonists such as SB-423562 and SB-423557 (taken from Kumar *et al.* 2010) or agents similar to those described by Arey *et al.* (2005). The latter study describes a factor designated “Compound 1” which is a potent, selective CaR antagonist with a relatively long half life (systemically measured to be greater than 1 hour in adult rats), the longevity of which would likely be extended by its immobilisation within a collagen matrix *in vivo*, however this compound may not be generally available. Were CaR antagonism to prove neuritogenic *in vitro*, CaR blocking

agents or CaR specific siRNA sequences could constitute part of a ‘cocktail’ to be immobilised within collagen matrices for subsequent intra-ON implantation , with the hope of promoting RGC survival and axonal regeneration.

Reference Section

Abe K, Saito H. (1992)

Selective enhancement by basic fibroblast growth factor of NMDA receptor-mediated increase of intracellular Ca2+ concentration in hippocampal neurons

Brain Research. 1992 Nov 6;595(1):128-32.

Aguayo AJ, Dickson R, Trecarten J, Attiwell M, Bray GM, Richardson P (1978)

Ensheathment and myelination of regenerating PNS fibres by transplanted optic nerve glia

Neuroscience Letters, 1978 Sep;9 (2-3):97-104

Aguayo AJ, David S, Bray GM (1981)

Influences of the glial environment on the elongation of axons after injury: transplantation studies in adult rodents

The Journal of Experimental Biology, 1981 Dec;95:231-40

Aguirre A, Dupree JL, Mangin JM, Gallo V. (2007)

A functional role for EGFR signaling in myelination and remyelination

Nature Neuroscience. 2007 Aug;10(8):990-1002.

Ahmed Z, Dent RG, Leadbeater WE, Smith C, Berry M, Logan A. (2005)

Matrix metalloproteases: degradation of the inhibitory environment of the transected optic nerve and the scar by regenerating axons

Molecular and Cellular Neuroscience. 2005 Jan;28(1):64-78.

Ahmed Z, Suggate EL, Brown ER, Dent RG, Armstrong SJ, Barrett LB, Berry M, Logan A. (2006a)

Schwann cell-derived factor-induced modulation of the NgR/p75NTR/EGFR axis disinhibits axon growth through CNS myelin in vivo and in vitro

Brain. 2006 Jun;129(Pt 6):1517-33.

Ahmed Z, Mazibrada G, Seabright RJ, Dent RG, Berry M, Logan A. (2006b)

TACE-induced cleavage of NgR and p75NTR in dorsal root ganglion cultures disinhibits outgrowth and promotes branching of neurites in the presence of inhibitory CNS myelin

FASEB Journal. 2006 Sep;20(11):1939-41.

Ahmed Z, Berry M, Logan A. (2009)

ROCK inhibition promotes adult retinal ganglion cell neurite outgrowth only in the presence of growth promoting factors

Molecular and Cellular Neuroscience. 2009 Oct;42(2):128-33.

Ahmed Z, Mazibrada G, Seabright RJ, Dent RG, Berry M, Logan A. (2006b)

TACE-induced cleavage of NgR and p75NTR in dorsal root ganglion cultures disinhibits outgrowth and promotes branching of neurites in the presence of inhibitory CNS myelin

FASEB Journal. 2006 Sep;20(11):1939-41.

Allan SM, Rothwell NJ (2001)

Cytokines and acute neurodegeneration

Nature Reviews Neuroscience. 2001 Oct;2(10):734-44.

Anchan RM, Reh TA, Angello J, Balliet A, Walker M. (1991)

EGF and TGF-alpha stimulate retinal neuroepithelial cell proliferation in vitro

Neuron. 1991 Jun;6(6):923-36.

Andl CD, Rustgi AK. (2005)

No one-way street: cross-talk between e-cadherin and receptor tyrosine kinase (RTK) signaling: a mechanism to regulate RTK activity

Cancer Biology and Therapy. 2005 Jan;4(1):28-31.

Ankeny DP, Popovich PG. (2009)

Mechanisms and implications of adaptive immune responses after traumatic spinal cord injury

Neuroscience. 2009 Feb 6;158(3):1112-21

Appleton CT, Usmani SE, Mort JS, Beier F. (2010)

Rho/ROCK and MEK/ERK activation by transforming growth factor-alpha induces articular cartilage degradation

Laboratory Investigation. 2010 Jan;90(1):20-30.

Anderson PN, Mitchell J, Mayor D, Stauber VV. (1983)

An ultrastructural study of the early stages of axonal regeneration through rat nerve grafts

Neuropathology and Applied Neurobiology. 1983 Nov-Dec;9(6):455-66.

Arey BJ, Seethala R, Ma Z, Fura A, Morin J, Swartz J, Vyas V, Yang W, Dickson JK Jr, Feyen JH. (2005)

A novel calcium-sensing receptor antagonist transiently stimulates parathyroid hormone secretion in vivo

Endocrinology. 2005 Apr;146(4):2015-22.

Barres BA, Jacobson MD, Schmid R, Sendtner M, Raff MC. (1993)

Does oligodendrocyte survival depend on axons?

Current Biology. 1993 Aug 1;3(8):489-97

Bazley LA, Gullick WJ. (2005)

The epidermal growth factor receptor family

Endocrine Related Cancer. 2005 Jul;12 Suppl 1:S17-27.

Berry M, Rees L, Hall S, Yiu P, Sievers J. (1988)

Optic axons regenerate into sciatic nerve isografts only in the presence of Schwann cells

Brain Research Bulletins. 1988 Feb;20(2):223-31.

Berry, Carlile and Hunter (1996)

Peripheral nerve explants grafted into the vitreous body of the eye promote the regeneration of retinal ganglion cell axons severed in the optic nerve

Journal of Neurocytology. Volume 25, Number 1, 147-170, 1996

Berry M, Ahmed Z, Douglas MR, Logan A. (2010)

Epidermal growth factor receptor antagonists and CNS axon regeneration: Mechanisms and controversies

Brain Research Bulletin. E-Pub 2010 Aug 13.

Berry M, Hunter AS, Duncan A, Lordan J, Kirvell S, Tsang WL, Butt AM. (1999a)

Axon-glial relations during regeneration of axons in the adult rat anterior medullary velum

Journal of Neurocytology. 1998 Dec;27(12):915-37.

Berry M, Carlile J, Hunter A, Tsang W, Rosenstiel P, Sievers J. (1999b)

Optic nerve regeneration after intravitreal peripheral nerve implants: trajectories of axons regrowing through the optic chiasm into the optic tracts

Journal of Neurocytology. 1999 Sep;28(9):721-41

Berry M, Gonzalez AM, Clarke W, Greenlees L, Barrett L, Tsang W, Seymour L, Bonadio J, Logan A, Baird A (2001)

Sustained effects of gene-activated matrices after CNS injury

Molecular and Cellular Neuroscience. 2001 Apr;17(4):706-16.

Berry M, Rees L, Hall S, Yiu P, Sievers J. (1988a)

Optic axons regenerate into sciatic nerve isografts only in the presence of Schwann cells

Brain Research Bulletins. 1988 Feb;20(2):223-31

Berry M, Ahmed Z, Lorber B, Douglas M, Logan A. (2008)

Regeneration of axons in the visual system

Restorative Neurology and Neuroscience. 2008;26(2-3):147-7

Bertrand J, Winton MJ, Rodriguez-Hernandez N, Campenot RB, McKerracher L. (2005)

Application of Rho antagonist to neuronal cell bodies promotes neurite growth in compartmented cultures and regeneration of retinal ganglion cell axons in the optic nerve of adult rats

Journal of Neuroscience. 2005 Feb 2;25(5):1113-2

Bertrand J, Di Polo A, McKerracher L. (2007)

Enhanced survival and regeneration of axotomized retinal neurons by repeated delivery of cell-permeable C3-like Rho antagonists

Neurobiology of Disease. 2007 Jan;25(1):65-72. Epub 2006 Sep 28

Blackmore M, Letourneau PC. (2006)

Changes within maturing neurons limit axonal regeneration in the developing spinal cord

Journal of Neurobiology. 2006 Mar;66(4):348-60.

Blight AR. (1983)

Cellular morphology of chronic spinal cord injury in the cat: analysis of myelinated axons by line-sampling

Neuroscience. 1983 Oct;10(2):521-43

Blight AR, Decrescito V. (1986)

Morphometric analysis of experimental spinal cord injury in the cat: the relation of injury intensity to survival of myelinated axons

Neuroscience. 1986 Sep;19(1):321-41.

Bomze HM, Bulsara KR, Iskandar BJ, Caroni P, Skene JH. (2001)

Spinal axon regeneration evoked by replacing two growth cone proteins in adult neurons

Nature Neuroscience. 2001 Jan;4(1):38-43.

Bonilla IE, Tanabe K, Strittmatter SM. (2002)

Small proline-rich repeat protein 1A is expressed by axotomized neurons and promotes axonal outgrowth

Journal of Neuroscience. 2002 Feb 15;22(4):1303-15

Bringmann A, Iandiev I, Pannicke T, Wurm A, Hollborn M, Wiedemann P, Osborne NN, Reichenbach A. (2009)

Cellular signaling and factors involved in Müller cell gliosis: neuroprotective and detrimental effects

Progress in Retinal Eye Research. 2009 Nov;28(6):423-51. Epub 2009 Aug 4. Review.

Bundesen LQ, Scheel TA, Bregman BS, Kromer LF. (2003)

Ephrin-B2 and EphB2 regulation of astrocyte-meningeal fibroblast interactions in response to spinal cord lesions in adult rats

Journal of Neuroscience. 2003 Aug 27;23(21):7789-800.

Burke JM, Smith JM. (1981)

Retinal proliferation in response to vitreous hemoglobin or iron

Investigative Ophthalmology and Visual Science. 1981 May;20(5):582-92.

Cabodi S, Moro L, Bergatto E, Boeri Erba E, Di Stefano P, Turco E, Tarone G, Defilippi P. (2004)

Integrin regulation of epidermal growth factor (EGF) receptor and of EGF-dependent responses

Biochemical Society Transactions. 2004 Jun;32(Pt3):438-42.

Cai D, Qiu J, Cao Z, McAtee M, Bregman BS, Filbin MT. (2001)

Neuronal cyclic AMP controls the developmental loss in ability of axons to regenerate

Journal of Neuroscience. 2001 Jul 1;21(13):4731

Carlson MA, Longaker MT. (2004)

The fibroblast-populated collagen matrix as a model of wound healing: a review of the evidence

Wound Repair and Regeneration. 2004 Mar-Apr;12(2):134-47. Review.

Caroni P, Schwab ME. (1988a)

Antibody against myelin-associated inhibitor of neurite growth neutralizes nonpermissive substrate properties of CNS white matter

Neuron. 1988 Mar;1(1):85-96.

Chao DT, Korsmeyer SJ. (1998)

BCL-2 family: regulators of cell death

Annual Reviews in Immunology. 1998;16:395-419. Review

Chao MV, (2003)

Neurotrophins and their receptors: a convergence point for many signalling pathways

Nature Reviews Neuroscience. 2003 Apr;4(4):299-309.

Chao MV, Rajagopal R, Lee FS, (2006)

Neurotrophin signalling in health and disease

Clinical Science (London). 2006 Feb;110(2):167-73

Chaturvedi D, Gao X, Cohen MS, Taunton J, Patel TB. (2009)

Rapamycin induces transactivation of the EGFR and increases cell survival

Oncogene. 2009 Mar 5;28(9):1187-96. Epub 2009 Jan 19.

Chen MS, Huber AB, van der Haar ME, Frank M, Schnell L, Spillmann AA, Christ F, Schwab ME, (2000)

Nogo-A is a myelin-associated neurite outgrowth inhibitor and an antigen for monoclonal antibody IN-1

Nature. 2000 Jan 27;403(6768):434-9

Chen H, Kovar J, Sissons S, Cox K, Matter W, Chadwell F, Luan P, Vlahos CJ, Schutz-Geschwender A, Olive DM. (2005)

A cell-based immunocytochemical assay for monitoring kinase signaling pathways and drug efficacy

Analytical Biochemistry. 2005 Mar 1;338(1):136-42.

Chen H, Liu B, Neufeld AH. (2007)

Epidermal growth factor receptor in adult retinal neurons of rat, mouse, and human

Journal of Comparitive Neurology. 2007 Jan 10;500(2):299-310.

Chi JH. (2010)

Scar-busting chondroitinase with peripheral nerve grafting promotes axonal regeneration in chronic spinal cord injury

Neurosurgery. 2010 Feb;66(2):N12.

Chierzi S, Ratto GM, Verma P, Fawcett JW. (2005)

The ability of axons to regenerate their growth cones depends on axonal type and age, and is regulated by calcium, cAMP and ERK

European Journal of Neuroscience. 2005 Apr;21(8):2051-62

Chierzi S, Fawcett JW. (2001)

Regeneration in the mammalian optic nerve

Restorative Neurology and Neuroscience. 2001;19(1-2):109-18.

Cho KS, Chan PM, So KF, Yip HK, Chung SK (1999)

Ciliary neurotrophic factor promotes the regrowth capacity but not the survival of intraorbitally axotomized retinal ganglion cells in adult hamsters

Neuroscience, 1999;94(2):623-8

Close JL, Liu J, Gumuscu B, Reh TA. (2006)

Epidermal growth factor receptor expression regulates proliferation in the postnatal rat retina

Glia. 2006 Aug 1;54(2):94-104.

Cohen J, Johnson AR. (1991)

Differential effects of laminin and merosin on neurite outgrowth by developing retinal ganglion cells

Journal of Cell Science Supplement. 1991;15:1-7.

Crocker SJ, Whitmire JK, Frausto RF, Chertboonmuang P, Soloway PD, Whitton JL, Campbell IL. (2006)

Persistent macrophage/microglial activation and myelin disruption after experimental autoimmune encephalomyelitis in tissue inhibitor of metalloproteinase-1-deficient mice

American Journal of Pathology. 2006 Dec;169(6):2104-16.

Crowe MJ, Bresnahan JC, Shuman SL, Masters JN, Beattie MS. (1997)

Apoptosis and delayed degeneration after spinal cord injury in rats and monkeys

Nature Medicine. 1997 Jan;3(1):73-6.

Csordás G, Santra M, Reed CC, Eichstetter I, McQuillan DJ, Gross D, Nugent MA, Hajnóczky G, Iozzo RV. (2000)

Sustained down-regulation of the epidermal growth factor receptor by decorin. A mechanism for controlling tumor growth in vivo

Journal of Biological Chemistry. 2000 Oct 20;275(42):32879-87

Cui Q, Lu Q, So KF, Yip HK. (1999)

CNTF, not other trophic factors, promotes axonal regeneration of axotomized retinal ganglion cells in adult hamsters

Investigative Ophthalmology and Visual Science. 1999 Mar;40(3):760-6

Cui Q, Yin Y, Benowitz LI. (2009)

The role of macrophages in optic nerve regeneration

Neuroscience. 2009 Feb 6;158(3):1039-48. Epub 2008 Jul 25.

David S, Aguayo AJ (1985)

Axonal regeneration after crush injury of rat central nervous system fibres innervating peripheral nerve grafts

Journal of Neurocytology, 1985 Feb;14(1):1-12

Davies JE, Tang X, Denning JW, Archibald SJ, Davies SJ. (2004)

Decorin suppresses neurocan, brevican, phosphacan and NG2 expression and promotes axon growth across adult rat spinal cord injuries

European Journal of Neuroscience. 2004 Mar;19(5):1226-42.

Davies JE, Tang X, Bournat JC, Davies SJ. (2006)

Decorin promotes plasminogen/plasmin expression within acute spinal cord injuries and by adult microglia in vitro

Journal of Neurotrauma. 2006 Mar-Apr;23(3-4):397-408.

Davies SL, Gibbons CE, Vizard T, Ward DT (2006).

Ca2+-sensing receptor induces Rho kinase-mediated actin stress fiber assembly and altered cell morphology, but not in response to aromatic amino acids

American Journal of Physiology Cellular Physiology. 2006 Jun;290(6):C1543-51.

Danton GH, Dietrich WD (2003)

Inflammatory mechanisms after ischemia and stroke

Journal of Neuropathology and Experimental Neurology. 2003 Feb;62(2):127-36.

Dinarello CA. (1994)

The interleukin-1 family: 10 years of discovery

FASEB Journal. 1994 Dec;8(15):1314-25.

Donnelly DJ, Popovich PG. (2008)

Inflammation and its role in neuroprotection, axonal regeneration and functional recovery after spinal cord injury

Experimental Neurology. 2008 Feb;209(2):378-88. Epub 2007 Jun 30.

Douglas MR, Morrison KC, Jacques SJ, Leadbeater WE, Gonzalez AM, Berry M, Logan A, Ahmed Z. (2009)

Off-target effects of epidermal growth factor receptor antagonists mediate retinal ganglion cell disinhibited axon growth

Brain. 2009 Nov;132(Pt 11):3102-21. Epub 2009 Sep 25

Dupuis L, Pehar M, Cassina P, Rene F, Castellanos R, Rouaux C, Gandelman M, Dimou L, Schwab ME, Loeffler JP, Barbeito L, Gonzalez de Aguilar JL. (2008)

Nogo receptor antagonizes p75^{NTR}-dependent motor neuron death

Proceeds of the National Acadademy of Science USA. 2008 Jan 15;105(2):740-5.

Edwin Smith Papyrus (1930)

Full article is in public domain at: http://www.touregypt.net/edwinsmithsurgical.htm

Elkabes S, DiCicco-Bloom EM, Black IB. (1996)

Brain microglia/macrophages express neurotrophins that selectively regulate microglial proliferation and function

Journal of Neuroscience. 1996 Apr 15;16(8):2508-21.

Erschbamer M, Pernold K, Olson L. (2007)

Inhibiting epidermal growth factor receptor improves structural, locomotor, sensory, and bladder recovery from experimental spinal cord injury

Journal of Neuroscience. 2007 Jun 13;27(24):6428-35.

Fabes J, Anderson P, Brennan C, Bolsover S. (2007)

Regeneration-enhancing effects of EphA4 blocking peptide following corticospinal tract injury in adult rat spinal cord

European Journal Neuroscience. 2007 Nov;26(9):2496-505. Epub 2007 Oct 26.

Fabian MA, Biggs WH 3rd, Treiber DK, Atteridge CE, Azimioara MD, Benedetti MG, Carter TA, Ciceri P, Edeen PT, Floyd M, Ford JM, Galvin M, Gerlach JL, Grotzfeld RM, Herrgard S, Insko DE, Insko MA, Lai AG, Lélias JM, Mehta SA, Milanov ZV, Velasco AM, Wodicka LM, Patel HK, Zarrinkar PP, Lockhart DJ. (2005)

A small molecule-kinase interaction map for clinical kinase inhibitors

Nature Biotechnology. 2005 Mar;23(3):329-36. Epub 2005 Feb 13.

Faden, AI (1996)

Pharmacologic treatment of acute traumatic brain injury

Journal of the American Medical Association. 1996 Aug 21;276(7):569-70.

Fawcett JW, Keynes RJ. (1990)

Peripheral nerve regeneration

Annual Reviews in Neuroscience. 1990;13:43-60

Ferguson KM. (2008)

Structure-based view of epidermal growth factor receptor regulation

Annual Review Biophysics. 2008;37:353-73.

Filbin MT. (2003)

Myelin-associated inhibitors of axonal regeneration in the adult mammalian CNS

Nature Reviews Neuroscience. 2003 Sep;4(9):703-13. Review. No abstract available.

Fischer D, Petkova V, Thanos S, Benowitz LI. (2004b)

Switching mature retinal ganglion cells to a robust growth state in vivo: gene expression and synergy with RhoA inactivation

Journal of Neuroscience. 2004 Oct 6;24(40):8726-40.

Fischer D, Heiduschka P, Thanos S. (2001)

Lens-injury-stimulated axonal regeneration throughout the optic pathway of adult rats

Experimental Neurology. 2001 Dec;172(2):257-72.

Fischer D, He Z, Benowitz LI. (2004a)

Counteracting the Nogo receptor enhances optic nerve regeneration if retinal ganglion cells are in an active growth state

Journal of Neuroscience. 2004 Feb 18;24(7):1646-51.

Fournier AE, GrandPre T, Strittmatter SM (2001)

Identification of a receptor mediating Nogo-66 inhibition of axonal regeneration

Nature. 2001 Jan 18;409(6818):341-6

Gaete J, Kameid G, Alvarez J. (1998)

Regenerating axons of the rat require a local source of proteins

Neuroscience Letters. 1998 Jul 31;251(3):197-200.

Gallo G, Letourneau PC, (2004)

Regulation of growth cone actin filaments by guidance cues

Journal of Neurobiology. 2004 Jan;58(1):92-102

Gao Y, Deng K, Hou J, Bryson JB, Barco A, Nikulina E, Spencer T, Mellado W, Kandel ER, Filbin MT. (2004)

Activated CREB is sufficient to overcome inhibitors in myelin and promote spinal axon regeneration in vivo

Neuron. 2004 Nov 18;44(4):609-21

Garden GA, Möller T. (2006)

Microglia biology in health and disease

Journal of Neuroimmune Pharmacology. 2006 Jun;1(2):127-37

Goldberg JL, Espinosa JS, Xu Y, Davidson N, Kovacs GT, Barres BA. (2002b)

Retinal ganglion cells do not extend axons by default: promotion by neurotrophic signaling and electrical activity

Neuron. 2002 Feb 28;33(5):689-702.

Goldberg JL. (2004)

Intrinsic neuronal regulation of axon and dendrite growth

Current Opinion Neurobiology. 2004 Oct;14(5):551-7.

Goldshmit Y, McLenachan S, Turnley A (2006)

Roles of Eph receptors and ephrins in the normal and damaged adult CNS

Brain Research Reviews. 2006 Sep;52(2):327-45. Epub 2006 Jun 13.

Gómez-Pinilla F, Knauer DJ, Nieto-Sampedro M. (1988)

Epidermal growth factor receptor immunoreactivity in rat brain. Development and cellular localization

Brain Research. 1988 Jan 12;438(1-2):385-90.

Gonzalez AM, Berlanga O, Leadbeater WE, Cooper-Charles L, Sims K, Logan A, Eliceiri B, Berry M, Baird A. (2009)

The deployment of adenovirus-containing gene activated matrices onto severed axons after central nervous system injury leads to transgene expression in target neuronal cell bodies

Journal of Gene Medicine. 2009 Aug;11(8):679-88.

GrandPré T, Nakamura F, Vartanian T, Strittmatter SM. (2000)

Identification of the Nogo inhibitor of axon regeneration as a Reticulon protein

Nature. 2000 Jan 27;403(6768):439-44

GrandPré T, Li S, Strittmatter SM. (2002)

Nogo-66 receptor antagonist peptide promotes axonal regeneration

Nature. 2002 May 30;417(6888):547-51.

Gross RE, Mei Q, Gutekunst CA, Torre E (2007)

The pivotal role of RhoA GTPase in the molecular signaling of axon growth inhibition after CNS injury and targeted therapeutic strategies

Cell Transplantation. 2007;16(3):245-62.

Gschwind A, Zwick E, Prenzel N, Leserer M, Ullrich A. (2001)

Cell communication networks: epidermal growth factor receptor transactivation as the paradigm for interreceptor signal transmission

Oncogene. 2001 Mar 26;20(13):1594-600.

Gumy LF, Tan CL, Fawcett JW. (2010)

The role of local protein synthesis and degradation in axon regeneration

Experimental Neurology. 2010, May;223(1):28-3

Gupta SK, Mishra R, Kusum S, Spedding M, Meiri KF, Gressens P, Mani S. (2009)

GAP-43 is essential for the neurotrophic effects of BDNF and positive AMPA receptor modulator S18986

Cell Death and Differentiation. 2009 Apr;16(4):624-37. Epub 2009 Jan 9.

Hagino S, Iseki K, Mori T, Zhang Y, Hikake T, Yokoya S, Takeuchi M, Hasimoto H, Kikuchi S, Wanaka A. (2003)

Slit and glypican-1 mRNAs are coexpressed in the reactive astrocytes of the injured adult brain

Glia. 2003 Apr 15;42(2):130-8.

Hannila SS, Filbin MT. (2008)

The role of cyclic AMP signaling in promoting axonal regeneration after spinal cord injury

Experimental Neurology. 2008 Feb;209(2):321-32. Epub 2007 Aug 27. Review.

Harris WA, Holt CE, Smith TA, Gallenson N. (1985)

Growth cones of developing retinal cells in vivo, on culture surfaces, and in collagen matrices

Journal of Neuroscience Research. 1985;13(1-2):101-22.

Higashiyama S, Iwabuki H, Morimoto C, Hieda M, Inoue H, Matsushita N. (2008)

Membrane-anchored growth factors, the epidermal growth factor family: beyond receptor ligands

Cancer Science. 2008 Feb;99(2):214-20.

Ho AK, Chik CL. (1995)

Phosphatase inhibitors potentiate adrenergic-stimulated cAMP and cGMP production in rat pinealocytes

American Journal of Physiology. 1995 Mar;268(3 Pt 1):E458-66.

Hocking AM, Shinomura T, McQuillan DJ. (1998)

Leucine-rich repeat glycoproteins of the extracellular matrix

Matrix Biology. 1998 Apr;17(1):1-19.

Honda S, Nakajima K, Nakamura Y, Imai Y, Kohsaka S. (1999)

Rat primary cultured microglia express glial cell line-derived neurotrophic factor receptors

Neuroscience Letters. 1999 Nov 19;275(3):203-6.

Hu Y, Cui Q, Harvey AR. (2007)

Interactive effects of C3, cyclic AMP and ciliary neurotrophic factor on adult retinal ganglion cell survival and axonal regeneration

Molecular and Cellular Neuroscience. 2007 Jan;34(1):88-98. Epub 2006 Nov 27.

Huang Y, Cen LP, Luo JM, Wang N, Zhang MZ, van Rooijen N, Pang CP, Cui Q. (2008)

Differential roles of phosphatidylinositol 3-kinase/akt pathway in retinal ganglion cell survival in rats with or without acute ocular hypertension

Neuroscience. 2008 Apr 22;153(1):214-25. Epub 2008 Feb 19.

Hynes RO. (2002)

Integrins: bidirectional, allosteric signaling machines

Cell. 2002 Sep 20;110(6):673-87.

Inoue, K. (2006)

ATP receptors of microglia involved in pain

Novartis Foundation Symposium. 2006;276:263-72; discussion 273-81.

Irving EA, Vinson M, Rosin C, Roberts JC, Chapman DM, Facci L, Virley DJ, Skaper SD, Burbidge SA, Walsh FS, Hunter AJ, Parsons AA. (2005)

Identification of neuroprotective properties of anti-MAG antibody: a novel approach for the treatment of stroke?

Journal of Cereberal Blood Flow and Metabolism. 2005 Jan;25(1):98-107.

Ivins JK, Yurchenco PD, Lander AD. (2000)

Regulation of neurite outgrowth by integrin activation

Journal of Neuroscience. 2000 Sep 1;20(17):6551-60.

Jadhav AP, Roesch K, Cepko CL. (2009)

Development and neurogenic potential of Müller glial cells in the vertebrate retina

Progress in Retinal Eye Research. 2009 Jul;28(4):249-62

Jain A, Brady-Kalnay SM, Bellamkonda RV (2004)

Modulation of Rho GTPase activity alleviates chondroitin sulfate proteoglycan-dependent inhibition of neurite extension

Journal of Neuroscience Research. 2004 Jul 15;77(2):299-307.

Jeanneteau F, Chao MV. (2006)

Promoting neurotrophic effects by GPCR ligands

Novartis Foundation Symposium. 2006;276:181-9; discussion 189-92, 233-7, 275-81.

Jin K, Mao XO, Sun Y, Xie L, Jin L, Nishi E, Klagsbrun M, Greenberg DA. (2002)

Heparin-binding epidermal growth factor-like growth factor: hypoxia-inducible expression in vitro and stimulation of neurogenesis in vitro and in vivo

Journal of Neuroscience. 2002 Jul 1;22(13):5365-73.

Jorissen RN, Walker F, Pouliot N, Garrett TP, Ward CW, Burgess AW. (2003)

Epidermal growth factor receptor: mechanisms of activation and signalling

Experimental Cell Research. 2003 Mar 10;284(1):31-53. Review.

Kaneko S, Iwanami A, Nakamura M, Kishino A, Kikuchi K, Shibata S, Okano HJ, Ikegami T, Moriya A, Konishi O, Nakayama C, Kumagai K, Kimura T, Sato Y, Goshima Y, Taniguchi M, Ito M, He Z, Toyama Y, Okano H. (2006)

A selective Sema3A inhibitor enhances regenerative responses and functional recovery of the injured spinal cord

Nature Medicine. 2006 Dec;12(12):1380-9. Epub 2006

Kasina S, Scherle PA, Hall CL, Macoska JA. (2009)

ADAM-mediated amphiregulin shedding and EGFR transactivation

Cell Proliferation. 2009 Dec;42(6):799-812. Epub 2009 Sep

Keely SJ, Calandrella SO, Barrett KE. (2000)

Carbachol-stimulated transactivation of epidermal growth factor receptor and mitogen-activated protein kinase in T(84) cells is mediated by intracellular ca(2+), PYK-2, and p60(src)

Journal of Biological Chemistry. 2000 Apr 28;275(17):12619-25.

Kim BS, Nikolovski J, Bonadio J, Smiley E, Mooney DJ. (1999)

Engineered smooth muscle tissues: regulating cell phenotype with the scaffold

Experimental Cell Research. 1999 Sep 15;251(2):318-28.

Klöcker N, Jung M, Stuermer CA, Bähr M. (2001)

BDNF increases the number of axotomized rat retinal ganglion cells expressing GAP-43, L1, and TAG-1 mRNA--a supportive role for nitric oxide?

Neurobiology of Disease. 2001 Feb;8(1):103-13.

Knall C, Young S, Nick JA, Buhl AM, Worthen GS, Johnson GL. (1996)

Journal of Biological Chemistry. 1996 Feb 2;271(5):2832-8.

Interleukin-8 regulation of the Ras/Raf/mitogen-activated protein kinase pathway in human neutrophils

Koh CG. (2006)

Rho GTPases and their regulators in neuronal functions and development

Neurosignals. 2006-2007;15(5):228-37.

Koprivica V, Cho KS, Park JB, Yiu G, Atwal J, Gore B, Kim JA, Lin E, Tessier-Lavigne M, Chen DF, He Z. (2005)

EGFR activation mediates inhibition of axon regeneration by myelin and chondroitin sulfate proteoglycans

Science. 2005 Oct 7;310(5745):106-10.

Kornblum HI, Zurcher SD, Werb Z, Derynck R, Seroogy KB. (1999)

Multiple trophic actions of heparin-binding epidermal growth factor (HB-EGF) in the central nervous system

European Journal of Neuroscience. 1999 Sep;11(9):3236-46.

Kottis V, Thibault P, Mikol D, Xiao ZC, Zhang R, Dergham P, Braun PE. (2002)

Oligodendrocyte-myelin glycoprotein (OMgp) is an inhibitor of neurite outgrowth

Journal of Neurochemistry. 2002 Sep;82(6):1566-9.

Kramer A, Yang FC, Snodgrass P, Li X, Scammell TE, Davis FC, Weitz CJ. (2001)

Regulation of daily locomotor activity and sleep by hypothalamic EGF receptor signaling

Science. 2001 Dec 21;294(5551):2511-5.

Kreibich TA, Chalasani SH, Raper JA (2004)

The neurotransmitter glutamate reduces axonal responsiveness to multiple repellents through the activation of metabotropic glutamate receptor 1

Journal of Neuroscience. 2004 Aug 11;24(32):7085-95.

Krishnamoorthy RR, Agarwal P, Prasanna G, Vopat K, Lambert W, Sheedlo HJ, Pang IH, Shade D, Wordinger RJ, Yorio T, Clark AF, Agarwal N. (2001)

Characterization of a transformed rat retinal ganglion cell line

Brain Research Molecular Brain Research. 2001 Jan 31;86(1-2):1-12.

Kubo T, Yamashita T, (2007)

Rho-ROCK inhibitors for the treatment of CNS injury

Recently Patents on CNS Drug Discovery. 2007 Nov;2(3):173-9

Kumar S, Matheny CJ, Hoffman SJ, Marquis RW, Schultz M, Liang X, Vasko JA, Stroup GB, Vaden VR, Haley H, Fox J, DelMar EG, Nemeth EF, Lago AM, Callahan JF, Bhatnagar P, Huffman WF, Gowen M, Yi B, Danoff TM, Fitzpatrick LA. (2010)

An orally active calcium-sensing receptor antagonist that transiently increases plasma concentrations of PTH and stimulates bone formation

Bone. 2010 Feb;46(2):534-42. Epub 2009 Sep 26

Lamb DJ, Modjtahedi H, Plant NJ, Ferns GA. (2004)

EGF mediates monocyte chemotaxis and macrophage proliferation and EGF receptor is expressed in atherosclerotic plaques

Atherosclerosis. 2004 Sep;176(1):21-6.

Lang DM, Warren JT Jr, Klisa C, Stuermer CA. (2001)

Topographic restriction of TAG-1 expression in the developing retinotectal pathway and target dependent reexpression during axon regeneration

Molecular and Cellular Neuroscience. 2001 Feb;17(2):398-414.

Lee FS, Rajagopal R, Chao MV. (2002)

Distinctive features of Trk neurotrophin receptor transactivation by G protein-coupled receptors

Cytokine Growth Factor Review. 2002 Feb;13(1):11-7.

Lehmann M, Fournier A, Selles-Navarro I, Dergham P, Sebok A, Leclerc N, Tigyi G, McKerracher L. (1999)

Inactivation of Rho signaling pathway promotes CNS axon regeneration

Journal of Neuroscience. 1999 Sep 1;19(17):7537-47.

Leist M, Jäättelä M, (2001)

Four deaths and a funeral: from caspases to alternative mechanisms

Nature Reviews in Molecular and Cellular Biology. 2001 Aug;2(8):589-98

Leon S, Yin Y, Nguyen J, Irwin N, Benowitz LI. (2000)

Lens injury stimulates axon regeneration in the mature rat optic nerve

Journal of Neuroscience. 2000 Jun 15;20(12):4615-26.

Lemons ML, Condic ML. (2008)

Integrin signaling is integral to regeneration

Experimental Neurology. 2008 Feb;209(2):343-52. Epub 2007 Jun 14.

Leu ST, Jacques SA, Wingerd KL, Hikita ST, Tolhurst EC, Pring JL, Wiswell D, Kinney L, Goodman NL, Jackson DY, Clegg DO. (2004)

Integrin alpha4beta1 function is required for cell survival in developing retina

Developmental Biology. 2004 Dec 15;276(2):416-30.

Lillien L. (1995)

Changes in retinal cell fate induced by overexpression of EGF receptor

Nature. 1995 Sep 14;377(6545):158-62.

Li S, Christensen C, Køhler LB, Kiselyov VV, Berezin V, Bock E. (2009)

Agonists of fibroblast growth factor receptor induce neurite outgrowth and survival of cerebellar granule neurons

Developmental Neurobiology. 2009 Nov;69(13):837-54

Liu B, Chen H, Johns TG, Neufeld AH. (2006)

Epidermal growth factor receptor activation: an upstream signal for transition of quiescent astrocytes into reactive astrocytes after neural injury

Journal of Neuroscience. 2006 Jul 12;26(28):7532-40.

Liu B, Neufeld AH. (2004)

Activation of epidermal growth factor receptor causes astrocytes to form cribriform structures

Glia. 2004 Apr 15;46(2):153-68.

Liu B, Neufeld AH. (2007)

Activation of epidermal growth factor receptors in astrocytes: from development to neural injury

Journal of Neuroscience Research. 2007 Dec;85(16):3523-9. Review.

Liu B, Neufeld AH. (2003)

Activation of epidermal growth factor receptor signals induction of nitric oxide synthase-2 in human optic nerve head astrocytes in glaucomatous optic neuropathy

Neurobiology of Disease. 2003 Jul;13(2):109-23.

Liu Q, Londraville RL, Azodi E, Babb SG, Chiappini-Williamson C, Marrs JA, Raymond PA. (2002)

Up-regulation of cadherin-2 and cadherin-4 in regenerating visual structures of adult zebrafish

Experimental Neurology. 2002 Oct;177(2):396-406.

Logan A, Ahmed Z, Baird A, Gonzalez AM, Berry M. (2006)

Neurotrophic factor synergy is required for neuronal survival and disinhibited axon regeneration after CNS injury

Brain. 2006 Feb;129(Pt 2):490-502. Epub 2005 Dec 9.

Lorber B, Berry M, Logan A. (2008)

Different factors promote axonal regeneration of adult rat retinal ganglion cells after lens injury and intravitreal peripheral nerve grafting

Journal of Neuroscience Research. 2008 Mar;86(4):894-90

Lorber B, Hendriks WJ, Van der Zee CE, Berry M, Logan A (2005)

Effects of LAR and PTP-BL phosphatase deficiency on adult mouse retinal cells activated by lens injury

European Journal of Neuroscience. 2005 May;21(9):2375-83.

Lorber B, Howe ML, Benowitz LI, Irwin N. (2009)

Mst3b, an Ste20-like kinase, regulates axon regeneration in mature CNS and PNS pathways

Nature Neuroscience. 2009 Nov;12(11):1407-14. Epub 2009 Oct 2

Lowery LA, Van Van Vactor D (2009)

The trip of the tip: understanding the growth cone machinery

Nature Reviews Molecular Cellular Biology. 2009 May;10(5):332-43. Epub 2009 Apr 17.

Lucas R, Warner TD, Vojnovic I, Mitchell JA. (2005)

Cellular mechanisms of acetaminophen: role of cyclo-oxygenase

FASEB Journal. 2005 Apr;19(6):635-7

Maass A, von Leithner PL, Luong V, Guo L, Salt TE, Fitzke FW, Cordeiro MF. (2007)

Assessment of rat and mouse RGC apoptosis imaging in vivo with different scanning laser ophthalmoscopes

Current Eye Research. 2007 Oct;32(10):851-61.

Majdan M, Miller FD, (1999)

Neuronal life and death decisions functional antagonism between the Trk and p75 neurotrophin receptors

International Journal of Developmental Neuroscience. 1999 Jun;17(3):153-61

Maness PF, Schachner M. (2007)

Neural recognition molecules of the immunoglobulin superfamily: signaling transducers of axon guidance and neuronal migration

Nature Neuroscience. 2007 Jan;10(1):19-26.

McConnell P, Berry M. (1982)

Regeneration of ganglion cell axons in the adult mouse retina

Brain Research. 1982 Jun 10;241(2):362-5.

McKerracher L, Higuchi H. (2006)

Targeting Rho to stimulate repair after spinal cord injury

Journal of Neurotrauma 2006 Mar-Apr;23(3-4):309-17

McKerracher L, David S, Jackson DL, Kottis V, Dunn RJ, Braun PE (1994)

Identification of myelin-associated glycoprotein as a major myelin-derived inhibitor of neurite growth

Neuron. 1994 Oct;13(4):805-11.

Mey J, Thanos S. (1993)

Intravitreal injections of neurotrophic factors support the survival of axotomized retinal ganglion cells in adult rats in vivo

Brain Research. 1993 Feb 5;602(2):304-17.

Mi S, Lee X, Shao Z, Thill G, Ji B, Relton J, Levesque M, Allaire N, Perrin S, Sands B, Crowell T, Cate RL, McCoy JM, Pepinsky RB. (2004)

LINGO-1 is a component of the Nogo-66 receptor/p75 signaling complex

Nature Neuroscience. 2004 Mar;7(3):221-8. Epub 2004 Feb 15

Milenkovic I, Weick M, Wiedemann P, Reichenbach A, Bringmann A. (2003)

P2Y receptor-mediated stimulation of Müller glial cell DNA synthesis: dependence on EGF and PDGF receptor transactivation

Investigative Ophthalmology and Visual Science. 2003 Mar;44(3):1211-20.

Minor K, Tang X, Kahrilas G, Archibald SJ, Davies JE, Davies SJ. (2008)

Decorin promotes robust axon growth on inhibitory CSPGs and myelin via a direct effect on neurons

Neurobiology of Disease. 2008 Oct;32(1):88-95. Epub 2008 Jun 26.

Murphy JA, Franklin TB, Rafuse VF, Clarke DB. (2007b)

The neural cell adhesion molecule is necessary for normal adult retinal ganglion cell number and survival

Molecular and Cellular Neuroscience. 2007 Oct;36(2):280-92. Epub 2007 Jul 24.

Murphy JA, Hartwick AT, Rutishauser U, Clarke DB. (2009)

Endogenous polysialylated neural cell adhesion molecule enhances the survival of retinal ganglion cells

Investigative Ophthalmology and Visual Science. 2009 Feb;50(2):861-9.

Nadim W, Anderson PN, Turmaine M. (1990)

The role of Schwann cells and basal lamina tubes in the regeneration of axons through long lengths of freeze-killed nerve grafts

Neuropathology and Applied Neurobiology. 1990 Oct;16(5):411-21.

Nascimento FP, Figueredo SM, Marcon R, Martins DF, Macedo SJ Jr, Lima DA, Almeida RC, Ostroski RM, Rodrigues AL, Santos AR. (2010)

Inosine reduces pain-related behavior in mice: involvement of adenosine A1 and A2A receptor subtypes and protein kinase C pathways

Journal of Pharmacology and Experimental Therapeutics. 2010 Aug;334(2):590-8.

Nguyen QT, Sanes JR, Lichtman JW. (2002)

Pre-existing pathways promote precise projection patterns

Nature Neuroscience. 2002 Sep;5(9):861-7.

Nguyen L, He Q, Meiri KF. (2009)

Regulation of GAP-43 at serine 41 acts as a switch to modulate both intrinsic and extrinsic behaviors of growing neurons, via altered membrane distribution

Molecular and Cellular Neuroscience. 2009 May;41(1):62-73. Epub 2009 Feb 26.

Nichols MR, Morimoto BH. (1999)

Tyrosine kinase-independent inhibition of cyclic-AMP phosphodiesterase by genistein and tyrphostin 51

Archives of Biochemistry and Biophyics. 1999 Jun 15;366(2):224-30.

Nikulina E, Tidwell JL, Dai HN, Bregman BS, Filbin MT (2004).

The phosphodiesterase inhibitor rolipram delivered after a spinal cord lesion promotes axonal regeneration and functional recovery

Proceeds of the National Academy of Science U S A. 2004 Jun 8;101(23):8786-90.

Oda K, Matsuoka Y, Funahashi A, Kitano H. (2005)

A comprehensive pathway map of epidermal growth factor receptor signaling

Molecular Systems Biology. 2005;1:2005.0010. Epub 2005 May 25.

Park JB, Yiu G, Kaneko S, Wang J, Chang J, He XL, Garcia KC, He Z. (2005)

A TNF receptor family member, TROY, is a coreceptor with Nogo receptor in mediating the inhibitory activity of myelin inhibitors

Neuron. 2005 Feb 3;45(3):345-51. Erratum in: Neuron. 2005 Mar 3;45(5):81

Park KK, Liu K, Hu Y, Smith PD, Wang C, Cai B, Xu B, Connolly L, Kramvis I, Sahin M, He Z. (2008)

Promoting axon regeneration in the adult CNS by modulation of the PTEN/mTOR pathway

Science. 2008 Nov 7;322(5903):963-6.

Pasterkamp RJ, Verhaagen J. (2001)

Emerging roles for semaphorins in neural regeneration

Brain Research Reviews. 2001 Mar;35(1):36-54. Review.

Pernet V, Di Polo A. (2006)

Synergistic action of brain-derived neurotrophic factor and lens injury promotes retinal ganglion cell survival, but leads to optic nerve dystrophy in vivo

Brain. 2006 Apr;129(Pt 4):1014-26. Epub 2006 Jan 17.

Planas AM, Justicia C, Soriano MA, Ferrer I. (1998)

Epidermal growth factor receptor in proliferating reactive glia following transient focal ischemia in the rat brain

Glia. 1998 Jun;23(2):120-9

Popovich PG, Wei P, Stokes BT. (1997)

Cellular inflammatory response after spinal cord injury in Sprague-Dawley and Lewis rats

Journal of Comparitive Neurology. 1997 Jan 20;377(3):443-64

Prag S, Lepekhin EA, Kolkova K, Hartmann-Petersen R, Kawa A, Walmod PS, Belman V, Gallagher HC, Berezin V, Bock E, Pedersen N (2002)

NCAM regulates cell motility

Journal of Cell Science. 2002 Jan 15;115(Pt 2):283-92.

Presta M, Urbinati C, Dell'era P, Lauro GM, Sogos V, Balaci L, Ennas MG, Gremo F. (1995)

Expression of basic fibroblast growth factor and its receptors in human fetal microglia cells

International Journal of Developmental Neuroscience. 1995 Feb;13(1):29-39.

Prinjha R, Moore SE, Vinson M, Blake S, Morrow R, Christie G, Michalovich D, Simmons DL, Walsh FS. (2000)

Inhibitor of neurite outgrowth in humans

Nature. 2000 Jan 27;403(6768):383-4

Profyris C, Cheema SS, Zang D, Azari MF, Boyle K, Petratos S. (2004)

Degenerative and regenerative mechanisms governing spinal cord injury

Neurobiology of Disease. 2004 Apr;15(3):415-36.

Raff M, (1998)

Cell suicide for beginners

Nature. 1998 Nov 12;396(6707):119-22

Rhodes KE, Fawcett JW. (2004)

Chondroitin sulphate proteoglycans: preventing plasticity or protecting the CNS?

Journal of Anatomy. 2004 Jan;204(1):33-48.

Richardson PM, McGuinness UM, Aguayo AJ (1980)

Axons from CNS neurons regenerate into PNS grafts

Nature. 1980 Mar 20;284(5753):264-5

Roque RS, Caldwell RB, Behzadian MA. (1992)

Cultured Müller cells have high levels of epidermal growth factor receptors

Investigative Ophthalmology and Visual Science. 1992 Aug;33(9):2587-95.

Rossi F, Gianola S, Corvetti L. (2007)

Regulation of intrinsic neuronal properties for axon growth and regeneration

Progress in Neurobiology. 2007 Jan;81(1):1-28. Epub 2006 Dec 22

Rozengurt E. (2007)

Mitogenic signaling pathways induced by G protein-coupled receptors

Journal of Cellular Physiology. 2007 Dec;213(3):589-602.

Sahin U, Blobel CP. (2007)

Ectodomain shedding of the EGF-receptor ligand epigen is mediated by ADAM17

FEBS Letters. 2007 Jan 9;581(1):41-4. Epub 2006 Dec 6.

Sandvig A, Berry M, Barrett LB, Butt A, Logan A (2004)

Myelin-, reactive glia-, and scar-derived CNS axon growth inhibitors: expression, receptor signaling, and correlation with axon regeneration

Glia. 2004 May;46(3):225-51.

Sakisaka T, Takai Y, (2005)

Cell adhesion molecules in the CNS

Journal of Cell Science. 2005 Dec 1;118(Pt 23):5407-10

Sasaki T, Yamaguchi M, Kojima S. (2005)

Demonstration of hyperaccumulation of [18F]2-fluoro-2-deoxy-D-glucose under oxygen deprivation in living brain slices using bioradiograph

Synapse. 2005 Mar 15;55(4):252-61.

Sattler R, Tymianski M. (2001)

Molecular mechanisms of glutamate receptor-mediated excitotoxic neuronal cell death

Molecular Neurobiology. 2001 Aug-Dec;24(1-3):107-29.

Schecterson LC, Bothwell M, (2010)

Neurotrophin receptors: Old friends with new partners

Developmental Neurobiology. 2010 Apr;70(5):332-8

Scott EK, Reuter JE, Luo L (2003)

Small GTPase Cdc42 is required for multiple aspects of dendritic morphogenesis

Journal of Neuroscience. 2003 Apr 15;23(8):3118-23.

Schachtrup C, Lu P, Jones LL, Lee JK, Lu J, Sachs BD, Zheng B, Akassoglou K. (2007)

Fibrinogen inhibits neurite outgrowth via beta 3 integrin-mediated phosphorylation of the EGF receptor

Proceeds of the National Academy of Science U S A. 2007 Jul 10;104(28):11814-9.

Scherer J, Schnitzer J. (1994)

Growth factor effects on the proliferation of different retinal glial cells in vitro

Brain Research Developmental Brain Research. 1994 Jul 15;80(1-2):209-21

Scholes AG, Hagan S, Hiscott P, Damato BE, Grierson I. (2001)

Overexpression of epidermal growth factor receptor restricted to macrophages in uveal melanoma

Archives of Ophthalmology. 2001 Mar;119(3):373-7.

Schneider MR, Wolf E. (2009)

The epidermal growth factor receptor ligands at a glance

Journal of Cellular Physiology. 2009 Mar;218(3):460-6.

Shankaran H, Wiley HS, Resat H. (2006)

Modeling the effects of HER/ErbB1-3 coexpression on receptor dimerization and biological response

Biophysical Journal. 2006 Jun 1;90(11):3993-4009. Epub 2006 Mar 13.

Shewan D, Dwivedy A, Anderson R, Holt CE. (2002)

Age-related changes underlie switch in netrin-1 responsiveness as growth cones advance along visual pathway

Nature Neuroscience. 2002 Oct;5(10):955-62

Skaper SD, Facci L, Williams G, Williams EJ, Walsh FS, Doherty P. (2004)

A dimeric version of the short N-cadherin binding motif HAVDI promotes neuronal cell survival by activating an N-cadherin/fibroblast growth factor receptor signalling cascade

Molecular and Cellular Neuroscience. 2004 May;26(1):17-23.

Skaper SD. (2005)

Neuronal growth-promoting and inhibitory cues in neuroprotection and neuroregeneration

Annals of the New York Academy of Sciences. 2005 Aug;1053:376-85.

Smith GM, Strunz C.(2005)

Growth factor and cytokine regulation of chondroitin sulfate proteoglycans by astrocytes

Glia. 2005 Nov 15;52(3):209-18.

Spira ME, Dormann A, Ashery U, Gabso M, Gitler D, Benbassat D, Oren R, Ziv NE. (1996)

Use of Aplysia neurons for the study of cellular alterations and the resealing of transected axons in vitro

Journal of Neuroscience Methods. 1996 Oct 21;69(1):91-102.

Stefanová I, Dorfman JR, Germain RN. (2002)

Self-recognition promotes the foreign antigen sensitivity of naive T lymphocytes

Nature. 2002 Nov 28;420(6914):429-34

.

Syntichaki P, Xu K, Driscoll M, Tavernarakis N. (2002)

Specific aspartyl and calpain proteases are required for neurodegeneration in C. elegans.

Nature. 2002 Oct 31;419(6910):939-44

Tanaka EM, Ferretti P. (2009)

Considering the evolution of regeneration in the central nervous system

Nature Reviews Neuroscience. 2009 Oct;10(10):713-23.

Tanaka S, Koike T.(2002)

Selective inflammatory stimulations enhance release of microglial response factor (MRF)-1 from cultured microglia

Glia. 2002 Dec;40(3):360-71.

Tang X, Davies JE, Davies SJ. (2003)

Changes in distribution, cell associations, and protein expression levels of NG2, neurocan, phosphacan, brevican, versican V2, and tenascin-C during acute to chronic maturation of spinal cord scar tissue

Journal of Neuroscience Research. 2003 Feb 1;71(3):427-44.

Tanuma N, Sakuma H, Sasaki A, Matsumoto Y. (2006)

Chemokine expression by astrocytes plays a role in microglia/macrophage activation and subsequent neurodegeneration in secondary progressive multiple sclerosis

Acta Neuropathologica. 2006 Aug;112(2):195-204. Epub 2006 May 30.

Thallmair M, Metz GA, Z'Graggen WJ, Raineteau O, Kartje GL, Schwab ME. (1998)

Neurite growth inhibitors restrict plasticity and functional recovery following corticospinal tract lesions

Nature Neuroscience. 1998 Jun;1(2):124-31. Erratum in: Nat Neurosci 1998 Aug;1(4):329.

Thuen M, Singstad TE, Pedersen TB, Haraldseth O, Berry M, Sandvig A, Brekken C. (2005)

Manganese-enhanced MRI of the optic visual pathway and optic nerve injury in adult rats

Journal of Magnetic Resonance Imaging. 2005 Oct;22(4):492-500

Tom VJ, Kadakia R, Santi L, Houlé JD. (2009)

Administration of chondroitinase ABC rostral or caudal to a spinal cord injury site promotes anatomical but not functional plasticity

Journal of Neurotrauma. 2009 Dec;26(12):2323-33.

Tomlins SA, Bolllinger N, Creim J, Rodland KD. (2005)

Cross-talk between the calcium-sensing receptor and the epidermal growth factor receptor in Rat-1 fibroblasts

Experimental Cell Research. 2005 Aug 15;308(2):439-45.

Twiss JL, van Minnen J. (2006)

New insights into neuronal regeneration: the role of axonal protein synthesis in pathfinding and axonal extension

Journal of Neurotrauma. 2006 Mar-Apr;23(3-4):295-308.

Vargas ME, Barres BA. (2007)

Why is Wallerian degeneration in the CNS so slow?

Annual Reviews in Neuroscience. 2007;30:153-79.

Wagner B, Natarajan A, Grünaug S, Kroismayr R, Wagner EF, Sibilia M. (2006)

Neuronal survival depends on EGFR signaling in cortical but not midbrain astrocytes

The EMBO Journal. 2006 Feb 22;25(4):752-62. Epub 2006 Feb 9

Wang Q, Villeneuve G, Wang Z. (2005)

Control of epidermal growth factor receptor endocytosis by receptor dimerization, rather than receptor kinase activation

EMBO Reports. 2005 Oct;6(10):942-8.

Wang F, Zhu Y. (2008)

The interaction of Nogo-66 receptor with Nogo-p4 inhibits the neuronal differentiation of neural stem cells

Neuroscience. 2008 Jan 2;151(1):74-81. Epub 2007 Nov 12.

Wang KC, Koprivica V, Kim JA, Sivasankaran R, Guo Y, Neve RL, He Z, (2002)

Oligodendrocyte-myelin glycoprotein is a Nogo receptor ligand that inhibits neurite outgrowth

Nature. 2002 Jun 27;417(6892):941-4. Epub 2002 Jun 16

Weidner N, Ner A, Salimi N, Tuszynski MH. (2001)

Spontaneous corticospinal axonal plasticity and functional recovery after adult central nervous system injury

Proceeds of the National Academy of Science U S A. 2001 Mar 13;98(6):3513-8

Wells, A (1999)

EGF receptor

International Journal of Biochemistry and Cell Biology. 1999 Jun;31(6):637-43.

Wetzker R, Böhmer FD. (2003)

Transactivation joins multiple tracks to the ERK/MAPK cascade

Nature Reviews Molecular Cell Biology. 2003 Aug;4(8):651-7.

Wiley HS. (2003)

Trafficking of the ErbB receptors and its influence on signaling

Experimental Cell Research. 2003 Mar 10;284(1):78-88. Review.

Wolman MA, Sittaramane VK, Essner JJ, Yost HJ, Chandrasekhar A, Halloran MC. (2008)

Transient axonal glycoprotein-1 (TAG-1) and laminin-alpha1 regulate dynamic growth cone behaviors and initial axon direction in vivo

Neural Development. 2008 Feb 20;3:6.

Wong RW, Guillaud L. (2004)

The role of epidermal growth factor and its receptors in mammalian CNS

Cytokine Growth Factor Review. 2004 Apr-Jun;15(2-3):147-56.

Wood JP, Chidlow G, Tran T, Crowston JG, Casson RJ. (2010)

A comparison of differentiation protocols for RGC-5 cells

Investigative Ophthalmology and Visual Science. 2010 Jul;51(7):3774-83. Epub 2010 Feb 24.

Yakovlev AG, Faden AI. (2004)

Mechanisms of neural cell death: implications for development of neuroprotective treatment strategies.

American Society for Experimental NeuroTherapeutics 2004 Jan;1(1):5-16.

Yamada KM, Even-Ram S. (2002)

Integrin regulation of growth factor receptors

Nature Cell Biology. 2002 Apr;4(4):E75-6.

Yamada M, Ikeuchi T, Hatanaka H. (1997)

The neurotrophic action and signalling of epidermal growth factor

Progress in Neurobiology. 1997 Jan;51(1):19-37.

Yamashima T,(2000)

Implication of cysteine proteases calpain, cathepsin and caspase in ischemic neuronal death of primate.

Progress in Neurobiology. 2000 Oct;62(3):273-95.

Yang P, Arnold SA, Habas A, Hetman M, Hagg T. (2008)

Ciliary neurotrophic factor mediates dopamine D2 receptor-induced CNS neurogenesis in adult mice

Journal of Neuroscience. 2008 Feb 27;28(9):2231-41.

Yang Z, Qiao H, Li X. (2010)

Effects of the CNTF-collagen gel-controlled delivery system on rat neural stem/progenitor cells behavior

Science China Life Science. 2010 Apr;53(4):504-10. Epub 2010 May 7.

Yin Y, Cui Q, Li Y, Irwin N, Fischer D, Harvey AR, Benowitz LI. (2003)

Macrophage-derived factors stimulate optic nerve regeneration

Journal of Neuroscience. 2003 Mar 15;23(6):2284-93.

Yin Y, Henzl MT, Lorber B, Nakazawa T, Thomas TT, Jiang F, Langer R, Benowitz LI.(2006)

Oncomodulin is a macrophage-derived signal for axon regeneration in retinal ganglion cells

Nature Neuroscience. 2006 Jun;9(6):843-52. Epub 2006 May 14.

Xiang YY, Dong H, Wan Y, Li J, Yee A, Yang BB, Lu WY. (2006)

Versican G3 domain regulates neurite growth and synaptic transmission of hippocampal neurons by activation of epidermal growth factor receptor

Journal of Biological Chemistry. 2006 Jul 14;281(28):19358-68. Epub 2006 Apr 28.

Zhang X, Neufeld AH. (2005)

Activation of the epidermal growth factor receptor in optic nerve astrocytes leads to early and transient induction of cyclooxygenase-2

Investigative Ophthalmology and Visual Science. 2005 Jun;46(6):2035-41.

Zheng JQ, Kelly TK, Chang B, Ryazantsev S, Rajasekaran AK, Martin KC, Twiss JL. (2001)

A functional role for intra-axonal protein synthesis during axonal regeneration from adult sensory neurons

Journal of Neuroscience. 2001 Dec 1;21(23):9291-303.

Zhu JX, Goldoni S, Bix G, Owens RT, McQuillan DJ, Reed CC, Iozzo RV. (2005)

Decorin evokes protracted internalization and degradation of the epidermal growth factor receptor via caveolar endocytosis

Journal of Biological Chemistry. 2005 Sep 16;280(37):32468-79. Epub 2005 Jul 1.